

**INTERACTION BETWEEN HYDROGEN BROMIDE OR DIBROMINE AND SOLID
SUPPORTS**

**Thesis submitted to the University of Glasgow in fulfilment
of the requirement of the degree of Doctor of Philosophy.**

**by
PAUL ROBERT STEVENSON.**

**Department of Chemistry
The University of Glasgow
October, 1992**

P. R. STEVENSON.

ProQuest Number: 13818568

All rights reserved

INFORMATION TO ALL USERS

The quality of this reproduction is dependent upon the quality of the copy submitted.

In the unlikely event that the author did not send a complete manuscript and there are missing pages, these will be noted. Also, if material had to be removed, a note will indicate the deletion.



ProQuest 13818568

Published by ProQuest LLC (2018). Copyright of the Dissertation is held by the Author.

All rights reserved.

This work is protected against unauthorized copying under Title 17, United States Code
Microform Edition © ProQuest LLC.

ProQuest LLC.
789 East Eisenhower Parkway
P.O. Box 1346
Ann Arbor, MI 48106 – 1346

Thesis
9766
copy 1

GLASGOW
UNIVERSITY
LIBRARY

DEDICATION.

I would like to dedicate this work to my parents.

CONTENTS

ACKNOWLEDGEMENTS

SUMMARY i - iii

CHAPTER 1 - INTRODUCTION

1.1	Bromine.	1
1.2	Aim of This Work.	2
1.3	Radioactive Isotopes of Bromine.	4
1.4	Preparation of [⁸² Br]-Bromine Labelled Dibromine and Hydrogen Bromide.	6
1.5	Brønsted-Lowry Definition of Acids and Bases.	10
1.6	Lewis Acid-Base Concept.	11
1.7	Montmorillonite K10.	13
1.8	Phases of Alumina.	17
1.9	Fluorination and Chlorination of γ -Alumina and Montmorillonite K10.	18

CHAPTER 2 - EXPERIMENTAL

2.1	Experimental.	23
2.1.1	The vacuum system.	23
2.1.2	The inert atmosphere box.	24
2.2	Preparation and Purification of Reactants.	24
2.2.1	Preparation of [⁸² Br]-bromine labelled ammonium bromide.	24
2.2.2	Preparation of [⁸² Br]-bromine labelled hydrogen bromide.	25
2.2.3	Preparation of [⁸² Br]-bromine labelled dibromine.	26

2.2.4	Purification and storage of dibromine.	27
2.2.5	Preparation and storage of dibromomethane, bromochloromethane and tribromomethane.	28
2.2.6	Purification of pyridine and 2,6-dimethylpyridine.	28
2.2.7	Calcination of γ -alumina.	28
2.2.8	Calcination of montmorillonite K10.	29
2.2.9	Chlorination of γ -alumina.	29
2.2.10	Chlorination of montmorillonite K10.	30
2.2.11	Fluorination of γ -alumina.	30
2.3	Infrared Spectroscopy.	31
2.3.1	Transmission infrared spectroscopy in the vapour phase.	31
2.3.2	<u>Diffuse reflectance infrared fourier</u> <u>transformed spectroscopy (D.R.I.F.T.S.).</u>	31
2.3.3	<u>Photoacoustic spectroscopy (P.A.S.).</u>	33
2.4	Gas Chromatography.	34
2.5	Radiochemistry.	34
2.5.1	Statistical errors.	34
2.5.2	Scintillation counting.	35
2.5.3	Half-life and decay corrections.	36
2.5.4	[⁸² Br]-Bromine counting cells.	37
2.5.5	Determination of specific count rate of [⁸² Br]-bromine labelled hydrogen bromide.	38
2.5.6	Determination of specific count rate of [⁸² Br]-bromine labelled dibromine.	38
2.5.7	Neutron activation analysis.	39
2.6	²⁷ Al-MAS-NMR.	42

CHAPTER	3 - Reaction of Halomethanes with γ-Alumina and Montmorillonite K10.	
3.1	Introduction.	43
3.2	Experimental.	46
3.3	Results.	52
3.4	Discussion.	64
	3.4.1 Bromination of γ -alumina.	64
	3.4.2 Bromination of chlorinated γ -alumina.	67
	3.4.3 Halogenation of montmorillonite K10.	71
	3.4.4 Comparisons among the halogenating reagents.	75
	3.4.5 Comparisons among the halogenated solids.	76
CHAPTER	4 - Interaction of Hydrogen Bromide with Solid Supports and Their Effects on Hydrobromination Reactions.	
4.1	Introduction .	79
4.2	Experimental.	81
4.3	Results .	94
4.4	Discussion	114
	4.4.1 Interaction of [⁸² Br]-bromine labelled hydrogen bromide with solid supports.	114
	4.4.2 Reaction of hydrogen bromide with butenes in the presence of acidic solid supports.	117
	4.4.3 Reaction of hydrogen bromide with 1,9-decadiene in the presence of acidic solid supports.	121
	4.4.4 Alkene isomerisation in the presence of acidic supports.	126
CHAPTER	5 - Interaction of Dibromine with Solid Supports and the of Solid Supports in bromination Reactions.	
5.1	Introduction .	128
5.2	Experimental .	130

5.3	Results .	138
5.4	Discussion .	148
5.4.1	Interaction of [⁸² Br]-bromine labelled dibromine with solid supports.	148
5.4.2	Interaction of dibromine with anisole in the presence of calcined Degussa 'C' γ -alumina.	152
5.4.3	Interaction of dibromine with hexanoic acid in the presence of acidic solid supports.	153
CHAPTER	6 - Infrared Analysis of Pyridine and 2,6-Dimethylpyridine Adsorption onto Solid Supports.	
6.1	Introduction .	158
6.2	Experimental .	160
6.3	Results .	164
6.4	Discussion .	169
6.4.1	The adsorption of pyridine onto modified solid supports.	169
6.4.2	The adsorption of 2,6-dimethylpyridine onto modified solid supports.	174
CHAPTER	7 - Conclusions : The Nature of Brominated Oxides and Their Catalytic Functions.	176
REFERENCES		183

Acknowledgements.

I would like to express my sincere thanks to my supervisor, Dr J.M.Winfield and industrial supervisors, Dr H.Marsden and Dr K.Tattershall, for all their guidance, encouragement and patience shown throughout this work. I would also like to express my thanks to the Associated Octel Company Ltd and the SERC, without whoms support this work could not have been undertaken.

Thanks are also due to my colleagues in the department, Mr L.McGhee, Dr J.Thomson, Dr I.Fallis, Miss J.Rowden, Mrs I.Nicol, Miss V.Yeats and Miss F.McMonagle for their discussion, assistance and friendship thought my period of study. I would also like to thank Mr W.McCormack for the glass blowing assistance, Mr A.Wilson for his invaluable assistance at the SURRC and also Mr M.Littlewood of Nicolet Instruments for allowing me the use of their latest spectrometers.

Summary

Organobromine compounds have a wide range of uses in the chemical industry, which vary from petrol additives and drilling fluids to dyestuffs and pharmaceuticals. The production of these compounds under more environmentally and industrially friendly conditions is desirable.

In this work the ability of γ -alumina and montmorillonite K10 to adsorb bromine onto the surface, and the ability of these adsorbed species to enhance bromination reactions, are investigated. These investigations include the bromination of the supports using, dibromomethane, hydrogen bromide and dibromine. The action of each of these individual reagents upon the supports results in its own distinct adsorbed bromine species on the surface. These investigations also include the hydrobromination of alkenes and the Hell Volhard Zelinsky reaction (bromination of the carbon α to the carboxylic acid group). The alkenes chosen for this work include 1,9-decadiene and butenes, as these give rise to both liquid and gas phase interactions with the solid supports. For the Hell Volhard Zelinsky reaction hexanoic acid was used.

The techniques employed to analyse these reactions include:-

- I) Transmission FTIR spectroscopy: to identify the volatile products of the reactions.
- II) DRIFTS and PAS: to investigate the surface of the supports after the reactions had occurred.
- III) ^{27}Al -MAS-NMR: for analysis of the supports after reactions.
- IV) Neutron activation analysis: for determination of the halogen content of the supports.
- V) [^{82}Br]-Bromine labelled hydrogen bromide and dibromine: for *in situ* studies of the bromination reactions.

A major part of this work involves developing the necessary methods for the preparation, handling and counting of radiolabelled bromine compounds in heterogeneous systems.

The interaction of dibromomethane and tribromomethane (bromoform) results in the formation of at least two types of bromine species on the surface of the supports. One arises from the direct interaction of the halomethane with the support the other from the dissociative adsorption of hydrogen bromide, which forms during the reaction. These interactions do not occur to any appreciable extent below 523K. An indication as to the possible reason for this high temperature is provided by the formation of carbon monoxide. This suggests that the bromination process involves the substitution of surface oxygen species with bromine, a process which requires a high activation energy. Determination of the bromine content after these interactions indicates contents of between 0.5 and 1.2 mg atom Br g⁻¹. There is no indication, however, that the bromination of the supports with halomethanes enhances the Lewis acidity of the supports to any great extent.

The [⁸²Br]-bromine labelled hydrogen bromide tracer studies indicate that the room temperature interaction of hydrogen bromide with the supports is rapid, resulting in a bromine content of approximately 1.0 mg atom g⁻¹. The bromine uptake values increase in the presence of unsaturated hydrocarbons. These radiotracer experiments also indicate that the adsorption of hydrogen bromide onto montmorillonite K10 results in at least two types of bromine species. One of these species is labile to room temperature exchange with unlabelled hydrogen bromide, the other inert. The effectiveness of acidic supports in enhancing hydrobromination of alkenes, appears to be related to the uptake of hydrogen bromide onto the supports. The regioselectivity of hydrobromination is greater where the overall reaction process occurs to a less extent.

Results from the [⁸²Br]-bromine labelled dibromine interactions with the supports show these interactions to be much slower than those observed for hydrogen bromide. These interactions, like those of the previous halogenating reagents, result in more than one type of bromine species. The [⁸²Br]-bromine radiotracer experiments indicate a bromine content much greater than observed for the other brominating reagents. Most of the bromine is removed, however, if the support is degassed. This results in a bromine content similar to that observed for the previous reagents, 1.0 mg atom Br g⁻¹. A consequence of this ability of dibromine to adsorb onto the surface, in such large

quantities, is that if dibromine is added to the support first then no surface mediated reactions occur due to the swamping of these sites by bromine, and the order of addition of reagents, therefore, determines the reaction products obtained. The Hell Volhard Zelinsky reaction is not enhanced by either calcined γ -alumina or montmorillonite K10. There are indications however that chlorinated montmorillonite K10 and chlorinated γ -alumina may enhance this reaction to some degree.

The acidic nature of the surface of the solid support is investigated by the adsorption of vapour phase basic probe molecules (pyridine and 2,6-dimethylpyridine) onto these sites. The pyridine adsorption studies indicate that halogenation of the supports alters surface features to such an extent that the spectra of pyridine adsorbed onto calcined supports are completely different from the spectra of pyridine adsorbed on halogenated support. These studies show the complexity of the interaction of hydrogen bromide with pyridine adsorbed onto the supports. In contrast, the 2,6-dimethylpyridine adsorption studies indicate that the surface features of montmorillonite K10, montmorillonite K10 treated with carbonyl chloride and γ -alumina treated with carbonyl chloride, are very similar.

CHAPTER 1

Introduction.

1.1 Bromine

Bromine, in its elemental form, is a dense, mobile, dark red liquid at room temperature. It was isolated by A.J.Balard in 1825 whilst experimenting with an end-liquor, from salt manufacture using waters of the Montpellier salt marshes [1], a liquor rich in $MgBr_2$. J.von Liebig failed to discover the element several years earlier by incorrectly identifying it as iodine monochloride [2]. Balard reported his discovery to the French Academy of Science suggesting the name 'muride'. The committee, nominated by the academy, confirmed Balards findings. They suggested that the new element be called 'brome' from the Greek 'bromos', meaning stink, in recognition of its unpleasant odour.

Bromine was the third of the halogen family to be discovered and separated, after chlorine (1774) and iodine (1811). The atomic weight was reported in 1833 [3] as 78.392 (based on $H=1$). In 1841 the first mineral containing bromine (bromyrite, $AgBr$) was discovered. The light sensitive properties of $AgBr$ led to the major use of bromine in the photographic industry [4]. In 1857 bromine, in the form of KBr , was used in the medical world as a sedative and anti-convulsant in the treatment of epilepsy [4].

Bromine, the third in the halogen group, occurs principally as bromide salts of the alkalis and alkaline earths. It is substantially less abundant in crustal rocks (2.5ppm) than either fluorine (544ppm) or chlorine (126ppm) and is forty-sixth in order of abundance. The largest natural source of bromine, like chlorine, is in the oceans, but the bromine concentration of 65ppm is still significantly less than the chlorine content

which makes up more than half the total average salinity of the oceans (3.4 wt%).

Industries' main sources of bromine are the Arkansas brines (4000-5000ppm), the Dead sea (4000-5000ppm) and the Michigan brines (~2000ppm) [5].

Industrial production of bromine involves the oxidation of the bromide ion in the brine with Cl_2 . Bromine is removed from the solution by either 'steaming out' with a passage of steam or 'blowing out' with air, condensed then purified. The total world production of bromine, at 270000 tonnes p.a., is only one-hundredth the scale of the chlorine industry, the main producers being USA, USSR, UK, Israel, France and Japan [6].

The industrial usage of bromine had been dominated by the compound ethylene dibromide, which acts as a scavenger for lead from the petroleum anti-knock additive PbEt_4 . In 1975, 53% of all manufactured bromine was used as a fuel additive [7]. The agricultural industry, with 17.9%, was the next largest user. Here the bromine was used, notably in the form of methyl bromide, as a general pesticide (insecticide, fungicide and herbicide). 25000 Tonnes of bromine (8.9%) was used in fire retardant fibres and plastics, with the remaining 19.6% of bromine involved in a variety of uses including cleaning agents, water sanitation, dyestuffs, drilling fluids, photography, pharmaceuticals and organic and inorganic synthesis. Environmental legislation reducing the amount of PbEt_4 allowed to be used in fuel has resulted in a world wide reduction in the market for ethylene dibromide. Fortunately for the bromine producers, however, bromine is now being used on a larger scale by many other industries.

1.2 Aim of This Work.

Electrophilic bromination of organic compounds is an important reaction and of considerable relevance to the Associated Octel Company who are the Co-operating Body in the work, since many synthetic intermediates concerning bromine have

potential commercial value. The requirement for selective bromination of simple organic compounds, often in unfavourable positions, presents a synthetic challenge and recent work in this area includes the use of powerful electrophiles, for example BrF [8], Br₂ adsorbed on zeolites [9] and polymer-supported reagents [10].

The objective of the present work was to explore the potential and hence develop new routes for the controlled introduction of bromine into organic compounds under electrophilic conditions. Most synthetic procedures have employed homogeneous conditions but the case for heterogeneous conditions has considerable attractions. For example, selectivity is potentially achievable from constraints imposed by the surface. The initial strategy was to direct attention to two areas; firstly vapour phase bromination using Br₂ on a strongly acidic, brominated γ -alumina surface and secondly, bromination using bromine containing cations supported on materials such as γ -alumina or KSbF₆. In practice the first area required considerable development. It quickly became apparent that bromination of oxides such as γ -alumina was significantly different from chlorination. The work has been based on bromination and hydrobromination reactions involving γ -alumina and the clay montmorillonite K10.

The study of bromine containing compounds under heterogeneous conditions requires experimental methods for identifying products and in particular for monitoring the behaviour of bromine containing species on a gas/solid or liquid/solid interface. Analytical methods, for studying the bromine on a solid support, that were discounted included:- I) Infrared spectroscopy, including DRIFTS and PAS. The finger print region of bromine contained too much background noise from the solid support. II) Mass spectroscopy. The samples were non-volatile. III) NMR. Although bromine is NMR active it has a large quadrupole, broadening out any signals. NMR of the solid supports was possible using the ²⁷Al isotope as discussed in chapter 2.

A major consideration is the requirement for the detection of small quantities of bromine containing species on an inorganic surface. Radiolabelling offers the necessary sensitivity (0.1mmol). Radiolabelled bromine is a very useful tool as it has several gamma emitting isotopes, of varying half-lives, described later in the chapter (section

1.3). The isotope ^{80}Br , with a half-life of 18 minutes, is very useful for neutron activation analysis (section 2.5.7), whilst the ^{82}Br , with a half-life of 35.5h, is useful for *in situ* measurement of bromine uptake.

Although the University of Glasgow has considerable experience in the use of the radio-isotopes of fluorine, chlorine and iodine, no previous work in these laboratories has used radio-isotopes of bromine. For this reason a major part of this work involved developing the necessary methods for the preparation, handling and counting of radiolabelled bromine compounds in heterogeneous systems.

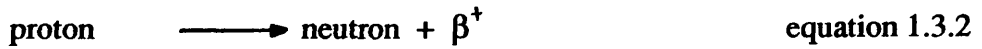
1.3 Radioactive Isotopes of Bromine.

Bromine has a number of radioactive isotopes which have been obtained using a variety of nuclear processes. These isotopes have been used in exchange reactions and other tracer studies of chemical reactions, in chemical analysis, biology and other fields of science, technology and industry [11-13]. Bromine isotopes formed as a result of the fission of heavier elements are of considerable interest and importance to nuclear reactor technology. Radiative neutron capture by bromine isotopes has played an important part in the development of a branch of radiochemistry, referred to as 'hot-atom' chemistry, and was the process by which radioactive bromine was produced in this work [14].

Naturally occurring bromine consists of a mixture of two isotopes, ^{79}Br and ^{81}Br . The relative abundances of these are 50.5% and 49.5% respectively. Radioactive bromine isotopes have masses 74 to 90 inclusive; these isotopes are only available in sufficient quantities for study when prepared by synthetic or degradative methods.

Bromine isotopes which have a smaller mass than a stable isotope of the element have a lower neutron to proton ratio than is required for nuclear stability. The ratio can be corrected by converting a proton into a neutron by means of either β^+ emission, orbital electron capture or both processes in competition, equations 1.3.1 & 1.3.2. In all

cases the atomic number is reduced. Isotopes of mass greater than a stable isotope have a neutron excess and the decay is by β^- emission, converting a neutron into a proton, equation 1.3.3, thus increasing the atomic number.



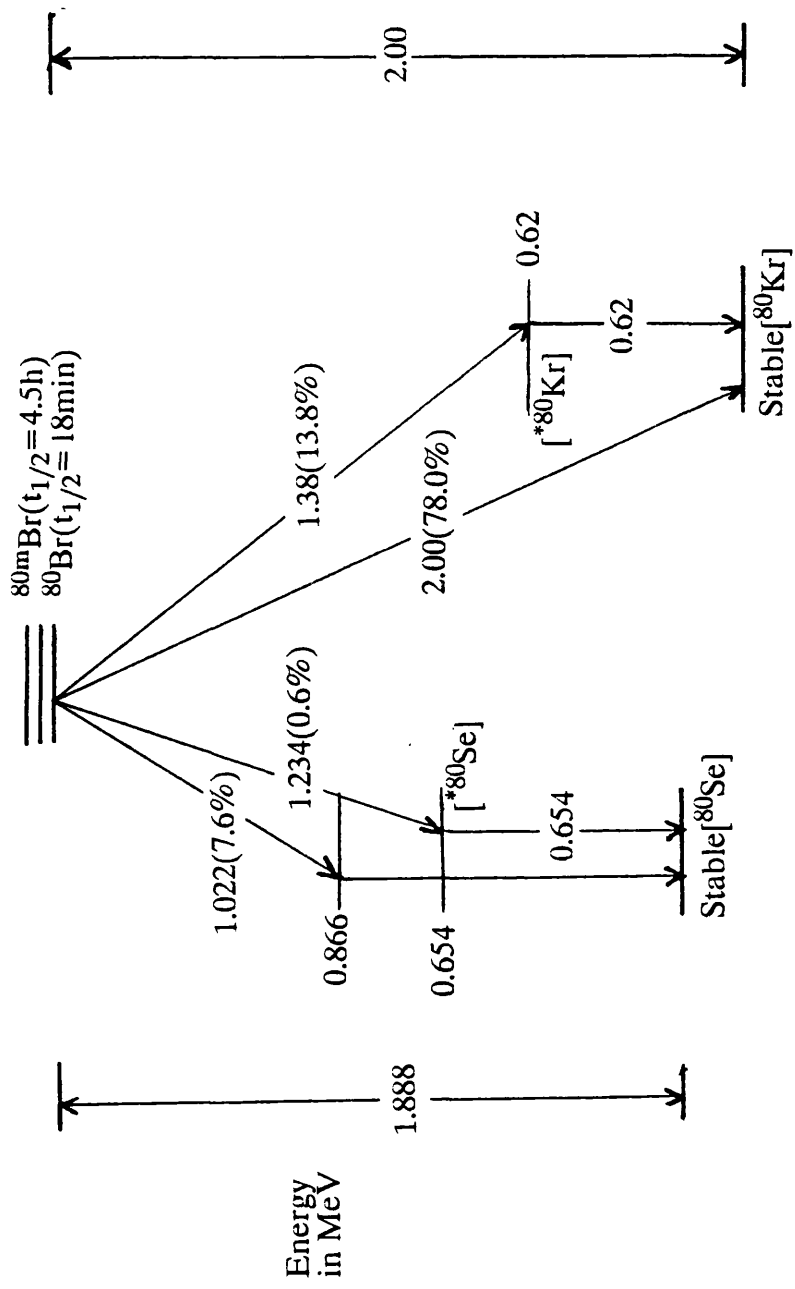
It is not uncommon for the daughter product to be formed in an excited state, making the decay schemes of the isotopes (parents and daughters) quite complicated.

Fortunately the decay schemes of the [^{80m}Br], [^{80}Br] and [^{82}Br] isotopes, that were used in this work, are known in some detail [15-17].

The [^{80m}Br] and [^{80}Br] isotopes are in the unusual situation of having mass numbers which lie between those of two stable isotopes, [^{79}Br] and [^{81}Br]. When compared with the stable [^{79}Br] isotope, the [^{80m}Br] and [^{80}Br] isotopes have a lower neutron to proton ratio than is required for nuclear stability, and will undergo the rearrangements shown in equations 1.3.1 and 1.3.2, to form [^{80}Se]. When these isotopes are compared with the stable [^{81}Br] isotope, they have a higher neutron to proton ratio than is required for nuclear stability, and will therefore undergo the rearrangement shown in equation 1.3.3, to form [^{80}Kr].

The [^{80m}Br] isotope successively undergoes two low energy internal transitions to the ground state [^{80}Br], which in turn decays mainly by emitting β^- particles with a maximum energy (end point) of 2.00 MeV. A small but significant proportion of the decays proceed by β^+ emission or orbital electron capture to the ground state of stable [^{80}Se]. It is believed that a very small proportion, about 0.6%, of the total decays may go through a metastable state of [^{80}Se] of energy 0.654 MeV above the ground state. The remainder, 13.8%, of the decays go through a metastable [^{80}Kr], falling to the ground state by the emission of a γ -ray of energy 0.62 MeV, scheme 1.3.1.

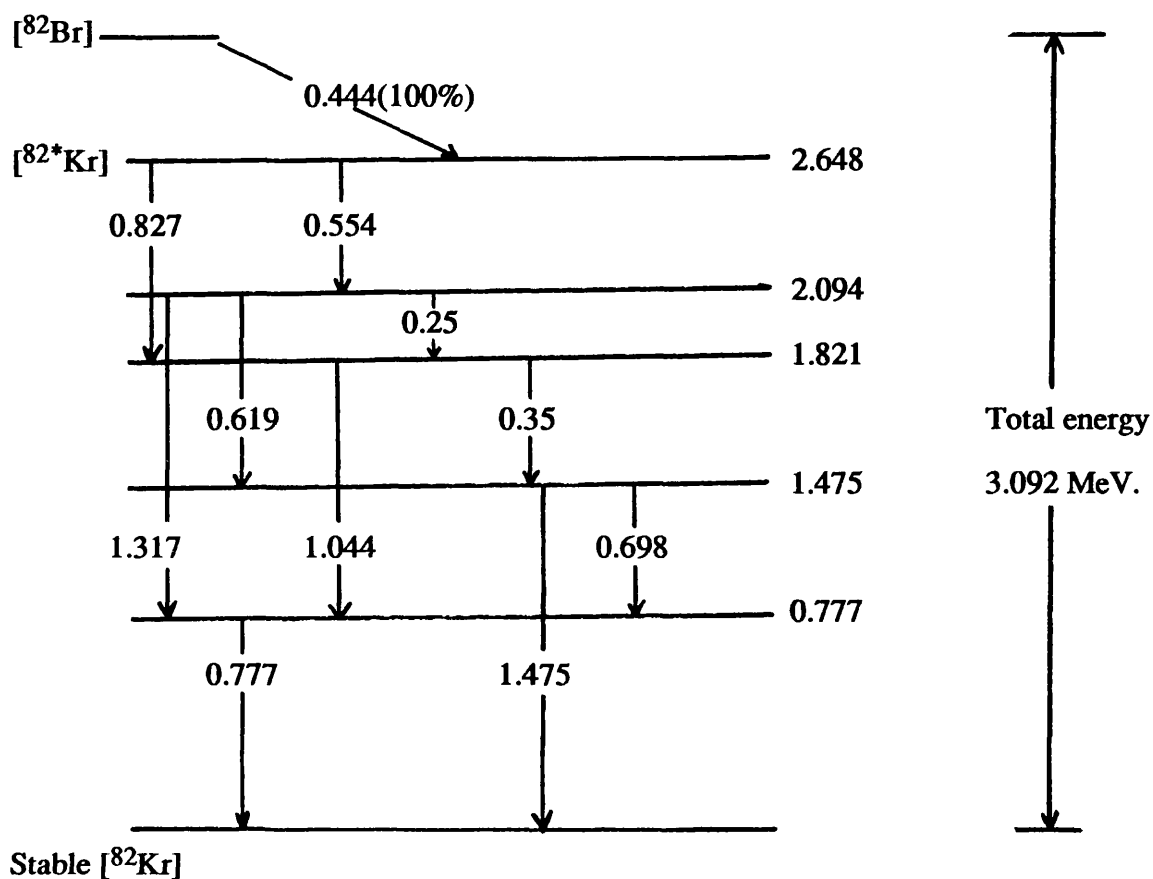
[^{82}Br] decays entirely by β^- emission (end point energy 0.444 MeV) to a high



* denotes excited state

Scheme 1.3.1. Radioactive decay of [$^{80\text{m}}\text{Br}$] and [^{80}Br]

energy metastable state of [^{82}Kr] which decays to the ground state by a series of internal transitions shown in scheme 1.3.2.



Scheme 1.3.2. Radioactive decay of [^{82}Br].

1.4 Preparation of [^{82}Br]-Bromine Labelled Dibromine and Hydrogen Bromide.

Nuclear reactor regulations state that, no liquids are permitted into the core of the reactor for irradiation purposes, hence it was not possible to irradiate dibromine to form [^{82}Br]-bromine labelled dibromine. The bromine salt, ammonium bromide, was

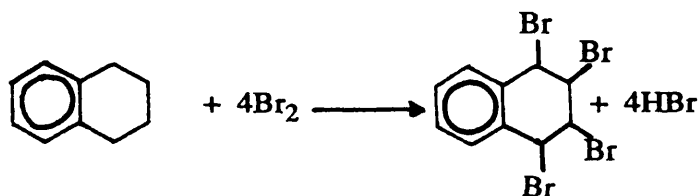
therefore placed into the core of the reactor for irradiation. After irradiation, the ammonium bromide could be converted into dibromine.

[⁸²Br]-Bromine labelled dibromine was prepared by the addition of 98% sulphuric acid to [⁸²Br]-bromine labelled ammonium bromide. A new route had to be postulated for [⁸²Br]-bromine labelled hydrogen bromide, as the standard routes for the formation of hydrogen bromide, shown in table 1.4.1, were found to be unsuitable.

Table 1.4.1. Methods for the preparation of hydrogen bromide	
Methods of preparation.	Comments.
Direct synthesis from the elements, without catalyst.	
	slow combination at 523K
	rapid combination at 773K
From inorganic bromides	
phosphoric acid	laboratory method
98% sulphuric acid	some decomposition through oxidation.
Reduction of dibromine	
Water vapour	rapid 773K, over charcoal
hydrocarbons	tetralin, rapid at 293K
red phosphorous	laboratory method

Both direct synthesis from the elements and reduction of dibromine involve making [⁸²Br]-bromine labelled dibromine before any attempt to make [⁸²Br]-bromine labelled hydrogen bromide can proceed. Since there is an inefficiency in converting NH₄⁸²Br into [⁸²Br]-bromine labelled dibromine, due to formation of H⁸²Br and the solubility of dibromine in 98% sulphuric acid, further inefficiencies resulting in the loss of more [⁸²Br] activity have to be minimised.

In the reaction of [⁸²Br]-bromine labelled dibromine with tetralin, equation 1.4.1, half of the active bromine is lost in brominating the hydrocarbon.

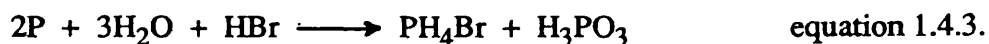


equation 1.4.1

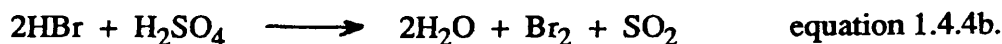
Formation of $^{82}\text{BrBr}$ has an approximate efficiency of 70% conversion of $\text{NH}_4^{82}\text{Br}$ to $^{82}\text{BrBr}$, so the activity of $[^{82}\text{Br}]$ in hydrogen bromide will be approx 35% of the starting activity. The reaction of dibromine with red phosphorous [20], equations 1.4.2a & 1.4.2b, may become violent and explosions have occurred.



The hydrogen bromide formed will react to some extent with phosphorus, equation 1.4.3.



Reaction of 98% sulphuric acid or phosphoric acid with ammonium bromide is a more direct method of hydrogen bromide preparation. Sulphuric acid readily oxidises hydrogen bromide to form dibromine [21], equations 1.4.4a and 1.4.4b, so this method is more suitable for $^{82}\text{BrBr}$ than for H^{82}Br .



Dibromine was formed even on the slow addition of sulphuric acid to the ammonium bromide. Sulphur dioxide formed during the oxidation of hydrogen bromide is an additional disadvantage and is difficult to separate from the hydrogen bromide in a fast and efficient manner.

Syrupy phosphoric acid gives a good yield of hydrogen bromide, without any significant by-products, equation 1.4.5.



The main disadvantages of this method are I) its high viscosity and II) the reaction mixture requires to be heated before reaction occurs.

The most successful method used to produce [⁸²Br]-bromine labelled hydrogen bromide, is to react ammonium bromide with trifluoromethanesulphonic acid (triflic acid), equation 1.4.6.



The advantages of this method are I) it can be carried out in the same apparatus as that used for the production of [⁸²Br]-bromine labelled dibromine, II) the reaction is rapid at room temperature, III) a very good yield is obtained; most of the [⁸²Br] activity (approx 100%) is found in the hydrogen bromide and IV) there are no observable by-products. Experimental details of the methods used for H⁸²Br and ⁸²BrBr synthesis are discussed in chapter 2.

1.5 Brønsted-Lowry Definition of Acids and Bases.

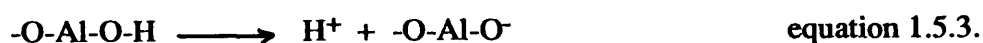
The Brønsted-Lowry definition of acids and bases was proposed independently in 1923 by the Danish chemist, J.N.Brønsted [22] and the British chemist, T.M.Lowry [23]. Their aim was to attempt to broaden the scope of acid/base systems to cover all protonic solvents. The advantage of the Brønsted-Lowry system was that a base need not contain hydroxyl ions, as is the requirement for the Arrhenius concept. Acids are defined as proton donors and bases as proton acceptors and every acid has a conjugate base, equation 1.5.1.



The ionization of hydrogen bromide in water is an example of a Brønsted acid/base system, since the hydrogen bromide donates protons to the water and the bromide ion is the conjugate base, equation 1.5.2.



In a solid acid, the conjugate base is a site which will accept a proton and the conjugate acid a protonated surface site. The catalytic activity of homogeneous and heterogeneous Brønsted acids is dependent on the ability of the Brønsted acid to lose a proton. This ability should be related, at least approximately, to the dissociation constant of the acid. Unfortunately the dissociation constants of Brønsted acids are measured in aqueous medium, and do not apply directly to heterogeneous systems. However, the dissociation constant is the equilibrium constant for the deprotonation of a conjugate acid into a proton and conjugate base. For a Brønsted acid site on γ -alumina ($-\text{OAl}-\text{OH}$) the ratio of the equilibrium constants, shown in equation 1.5.3, is equal to K_a , equation 1.5.4.



$$K_a = \frac{k}{k'} = \frac{\text{Specific rate of reaction of O-Al-O-H}}{\text{specific rate of reaction of H}^+ + \text{O-Al-O}^-}$$

equation 1.5.4.

The specific forward and reverse reaction rates k and k' are not separable, therefore Brønsted [24] suggested the approximate relationship :-

$$K_{HA} = GK_a^x \quad \text{equation 1.5.5}$$

where K_{HA} is the catalytic co-efficient of the Brønsted acid with dissociation constant K_a , and G and x are constants for a given reaction.

In homogeneous catalytic reactions [25], the stronger the acid the greater the catalytic activity. This property may be applied to solid acids which contain Brønsted acid sites. Therefore, enhancement of Brønsted acidity in a solid catalyst will enhance the catalytic activity towards reactions that require a protonation step in a catalytic process. The use of promoters to enhance the Brønsted acidity of a solid support, such as CCl_4 and HCl , will also promote the catalytic activity of the support.

1.6 Lewis Acid-Base Concept.

The role of the electron lone pair is the basis of the definition of acids and bases proposed by G.N.Lewis in 1923. The Lewis definition of an acid substance is a compound 'which can employ a lone pair of electrons from another molecule in completing the stable group of its own atoms', and a basic substance is a compound

'which has a lone pair of electrons which may be used to complete the stable group of another atom' [26]. Neutralisation of these acids and bases corresponds therefore to the formation of a co-ordinate bond. The forward acid base reaction is shown in equation 1.6.1, where A is the acid species and B the base :-



Lewis proposed that the main functional criterion of an acid is that a stronger acid will displace a weaker acid from its acid base complex. Equations 1.6.2 to 1.6.4 outline the related heterolytic processes which follow from the fundamental relationship outlined in equation 1.6.1. In the following equations the acidity relationship is $A' > A''$ and the basicity relationship is $B' > B''$.



The Lewis acid/base concept can be used for a typical Brønsted-Lowry acid/base definition, as outlined in equation 1.6.1, where the proton in equation 1.6.5 represents the Lewis acid.



The advantage of the Lewis acid/base concept is that it can classify aprotic molecules as acids or bases. The disadvantage of the concept is that it is not yet a quantitative approach; the Lewis acid/base is made variable by the dependence upon the reaction or method for their evaluation. To quantify Lewis acid/base reactions the

hard/soft, acid/base formalism of R.G.Pearson [27] has to be adopted.

Although the original Lewis acid/base concepts were based on homogeneous systems, they can be applied to gas/solid reactions if the acid-base definitions are restated as follows :-

A Lewis acid site on a solid surface is a site which has an unoccupied orbital with a high affinity for an electron pair. When such a site shares an electron pair donated by an adsorbed Lewis base molecule there is a decrease in the orbital energy of the system. Lewis base sites on the surface are those which have electron pairs available and a decrease in the orbital energy results if they share this electron pair with an adsorbed electron pair acceptor.

1.7 Montmorillonite K10.

Montmorillonite was the name given to a clay mineral found near Montmorillon, France in 1874. The name montmorillonite became associated with expanding clays and was for many years used generically to describe the group. The term expanding clay is due to the clays ability to swell in one dimension by the reversible uptake of water. To avoid confusion the group of expanding clays has now been renamed smectites, of which montmorillonites, bentonites and Fuller's earth are members. As a clay, montmorillonite, general formula $M_y^I[Al_{2-y}Mg_y(OH)_2Si_4O_{10}].xH_2O$, belongs to a family of layered silicate compounds which also includes talc, vermiculite, micas and pyrophyllite [28].

The structure of all layered silicate compounds is based upon an oxygen cubic close packed lattice. The idealised silicate structures are split into several categories, the first based on the number of interstitial layers present in the structure i.e. a 2 layered or 3 layered structure. The two layered structure, figure 1.7.1, is made up of 3 oxygen layers, ABC, and two interstitial layers consisting of silicon in tetrahedral environments

and a metal cation in octahedral environments.

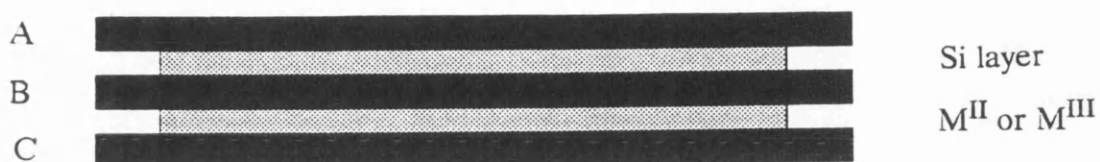


Figure 1.7.1. Two layered silicate structure.

The 3 layered structure, figure 1.7.2, is made up of 4 oxygen layers, ABCA, and three interstitial layers consisting of 2 layers of silicon in tetrahedral environments and one layer of metal cations in octahedral environments.

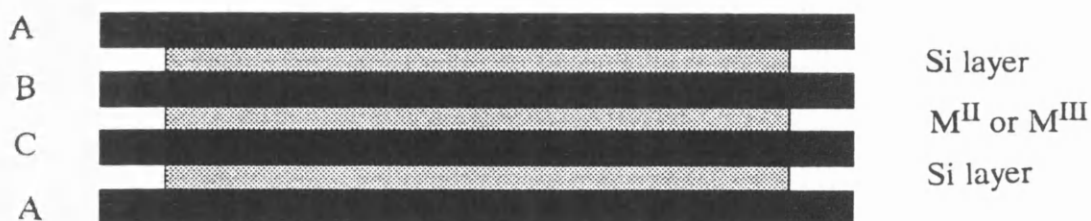
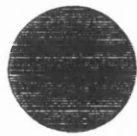
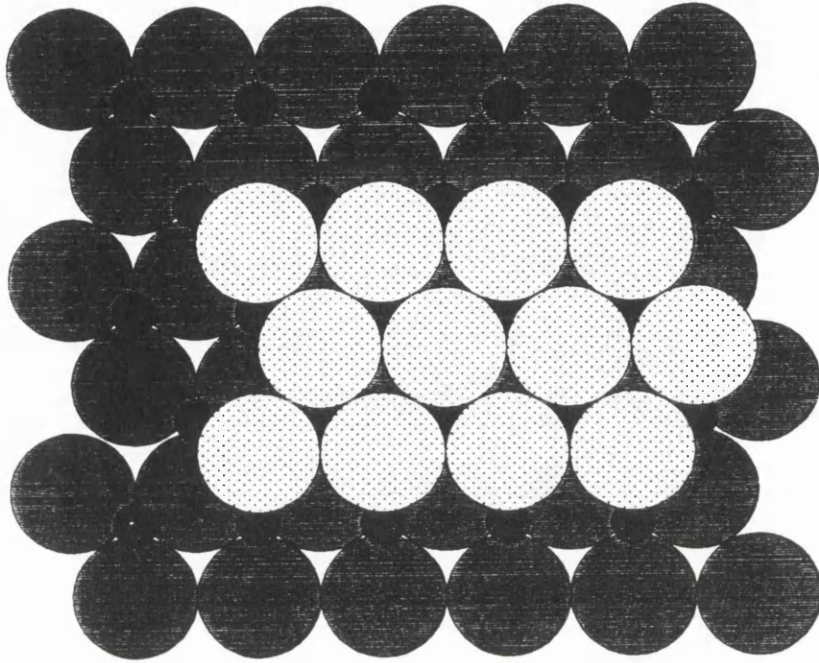


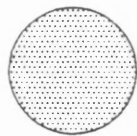
Figure 1.7.2. Three layered silicate structure.

The cationic interstitial layers are split into two categories, trioctahedral (brucite-type layers) and dioctahedral (gibbsite-type layers). The brucite-type layer, figure 1.7.3, which is based on $\text{Mg}(\text{OH})_2$, has the Mg^{II} cation in all the octahedral interstitial sites, an example of this being talc $[\text{Mg}_3(\text{OH})_2(\text{Si}_4\text{O}_{10})]$. The gibbsite type

Figure 1.7.3. Brucite type structure.



Lower layer oxygen



Top layer oxygen



Mg^{II}

structure, figure 1.7.5, is based on $\text{Al}(\text{OH})_3$ and has the Al^{III} cation in 2/3 of the octahedral sites available; pyrophyllite $[\text{Al}_2(\text{OH})_2(\text{Si}_4\text{O}_{10})]$ is an example of this. In the gibbsite type structure partial replacement of the Al^{III} by Mg^{II} , on a one to one basis, leads to a partial negative charge within the layers. To counter balance this negative charge, hydrated M^{I} or M^{II} cations can be incorporated between the plates, figure 1.7.4, to give an overall electrically neutral system. These hydrated cations are known as exchangeable cations and control, to a large extent, the hydration properties of expandable layer silicates [29-32].

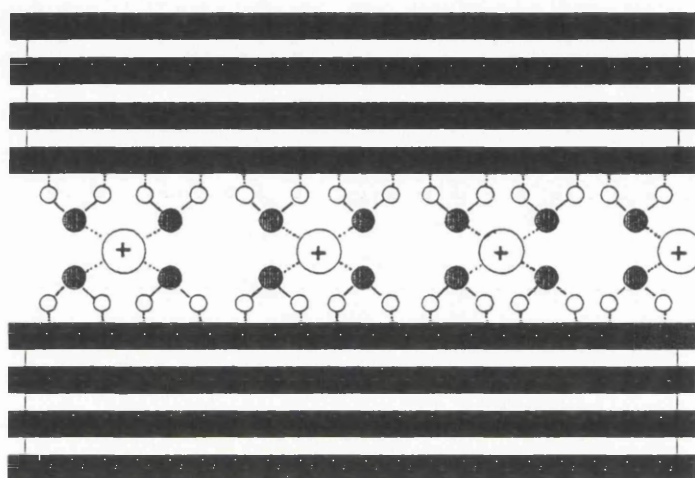
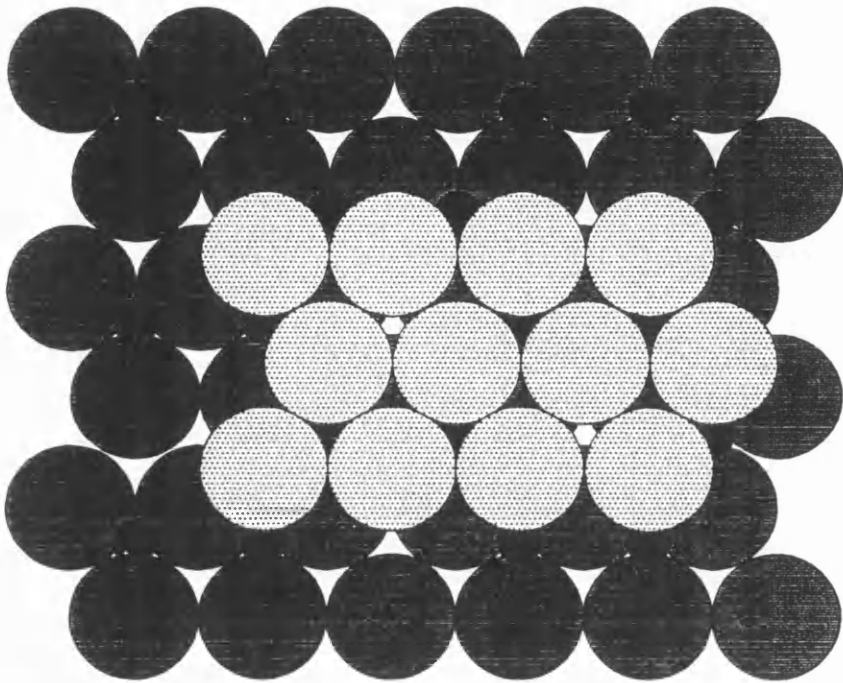


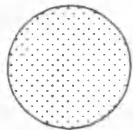
Figure 1.7.4. Incorporation of hydrated cations between the basal planes.

Montmorillonites with a trioctahedral (3 layered) system and a gibbsite type structure have the property of absorbing cations between the plates figure 1.7.4, and holding them strongly. As cations are positively charged, it can be assumed that the montmorillonite plates have a net negative charge, resulting from the replacement of Al^{III} with Mg^{II} . In the mineral montmorillonite Al^{III} is replaced by Mg^{II} in the approximate ratio of 6 to 1. This gives the montmorillonite plates a net negative charge (table 1.7.1), unlike talc and pyrophyllite which are both electrically neutral.

Figure 1.7.5. Gibbsite type structure.



Lower layer oxygen



Top layer oxygen



Al^{III}

Table 1.7.1. Electronic charges in smectites.

<i>Talc</i>		<i>Montmorillonite</i>		<i>Pyrophyllite</i>	
3O ²⁻	-6	3O ²⁻	-6	3O ²⁻	-6
2Si ⁴⁺	+8	2Si ⁴⁺	+8	2Si ⁴⁺	+8
2O ²⁻ +(OH) ⁻	-5	2O ²⁻ +(OH) ⁻	-5	2O ²⁻ +(OH) ⁻	-5
3Mg ²⁺	+6	1.67Al ³⁺ +0.33Mg ²⁺	+5.67	2Al ³⁺	+6
2O ²⁻ +(OH) ⁻	-5	2O ²⁻ +(OH) ⁻	-5	2O ²⁻ +(OH) ⁻	-5
2Si ⁴⁺	+8	2Si ⁴⁺	+8	2Si ⁴⁺	+8
3O ²⁻	-6	3O ²⁻	-6	3O ²⁻	-6
Net charge	0		-0.33		0

In montmorillonite the hydrated cations between the plates are most commonly Na^I and Ca^{II}. Fuller's earth is a montmorillonite in which the principal exchangeable cation is calcium. The pronounced cation exchange properties of Fuller's earth enable it to be converted, by exchanging the calcium with sodium, to sodium-montmorillonite.

Sodium-montmorillonite is commonly referred to as bentonite, but this is not strictly correct, as bentonite refers to a rock mineral which comprises mainly of sodium-montmorillonite; montmorillonite refers to a clay mineral. Since the stoichiometries of both bentonites and sodium-montmorillonites vary depending on where they originated, it is impossible to differentiate one from the other by chemical analysis.

The montmorillonite used in this work was montmorillonite K10, which is a montmorillonite which has been acidified [33]. The acidification process leads to the removal of aluminium from the gibbsite layer in the clay, figure 1.7.6, resulting in the collapse of the montmorillonite structure. This idealised model of montmorillonite contains only octahedral aluminium species but ²⁷Al-MAS-NMR studies have shown, chapter 3, that with montmorillonite K10 there are also tetrahedral aluminium species present. The use of pyridine as a probe molecule, chapter 6, has shown that there are both Lewis acid and Brønsted acid sites present in montmorillonite K10.

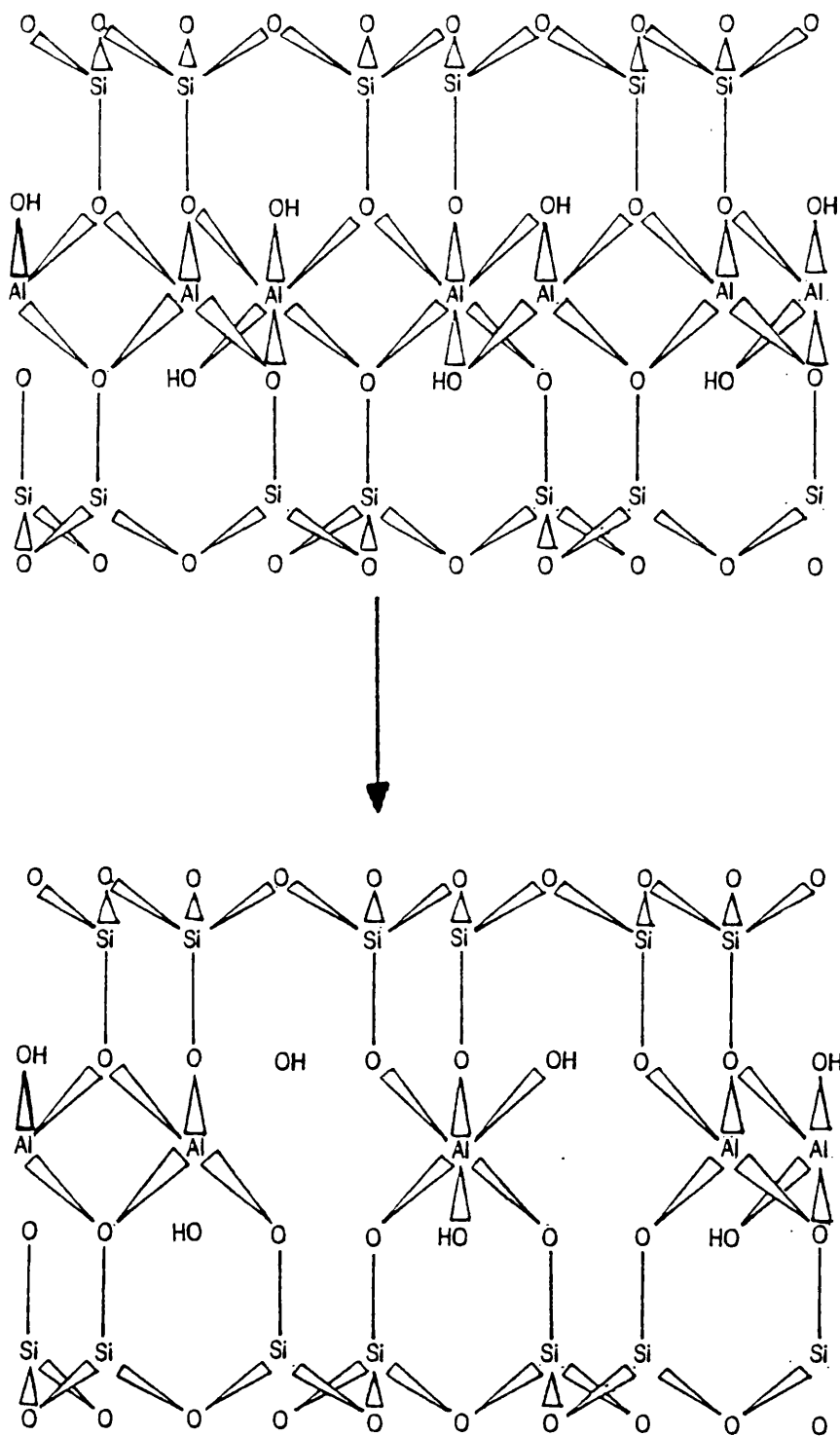


Figure 1.7.6. The structural collapse of montmorillonite after removal of aluminium.

1.8 Phases of Alumina.

Aluminium oxide has only one stoichiometric form [34], Al_2O_3 , but this simple form contains both polymorphs and several hydrated species [35]. These polymorphs and hydrated species are important as the catalytic behaviour of alumina is dependent upon the mode of preparation. Classification of the polymorphs based upon the crystallographic structures of the alumina has been implemented.

Alumina forms three distinguishable series (α , β , γ), based on the close packed oxygen lattices, with aluminium ions in octahedral and tetrahedral interstices. The α -series with hexagonally close packed lattices schematically ABAB..., the β -series with alternating close packed lattices, schematically ABAC-ABAC or ABAC-CABA, and the γ -series with cubic packed lattices schematically ABC ABC....

The sole representative of the α -series, α -alumina, is obtained in the form of stable corundum or as the decomposition product of diaspore [36]. The β -series is represented by alkali or alkaline earth oxides containing β -alumina and the decomposition products of gibbsite (χ and κ -alumina) which have related structures [37]. The γ -series is prepared from the decomposition products of the hydroxides bayerite, nordstandite and boehmite or by flame hydrolysis of aluminium(III) chloride. In this work the low temperature phase of γ -alumina was used [38].

The unit cell of a spinel (AB_2O_4) is formed by a cubic close packing of 32 oxygen atoms with 16 trivalent atoms in half of the octahedral interstices and 8 divalent atoms in tetrahedral holes [39]. Powder X-ray diffraction has established that γ -alumina crystallizes with a spinel-related structure [36] in which 32 oxygen atoms per unit cell are arranged exactly as in a spinel but with $21\frac{1}{3}$ aluminium atoms distributed over the 24 cation positions available [40], giving on average $2\frac{2}{3}$ vacant cation sites per unit cell. Electrical neutrality is partially achieved by the occurrence of these vacant sites. The crystallite surface containing hydroxyl groups, in place of oxygen ions, further contributes to the electrical neutrality of the γ -alumina crystallite.

The cleavage plane of boehmite is parallel to any array of parallel rows of oxygen atoms. The (110) face of boehmite is the cleavage plane, since γ -alumina maintains the spinel form of a cubic close-packed oxygen lattice. Cleavage of the (100) and (111) faces would result in a hexagonal close-packed stacking of oxygen atoms as in η -alumina [41]

During dehydration, the array of oxygen atoms remains in the spinel form, hence these parallel rows stack exclusively to form a cubic close-packed lattice resulting in the fairly well ordered oxygen lattice of γ -alumina. Two repeating types of layers can be derived from the (110) face of the spinel unit of γ -alumina (figure 1.8.1), and represented schematically as CDCD... The C-layer has equal numbers of tetrahedral and octahedral sites (figure 1.8.2), but the D-layer has only octahedral Al^{III} ions (figure 1.8.3). The occurrence of sharp diffuse lines in the X-ray pattern of γ -alumina indicated that the lattices are strongly disordered [42], a disorder caused strictly by the aluminium. The cation distribution of γ -alumina was determined by Fourier Synthesis of the electron diffraction patterns [43] and it was found that the octahedral aluminium sublattice is fully occupied and hence the necessary vacant sites must be distributed randomly over the tetrahedral interstices. Figures 1.8.1, 1.8.2 and 1.8.3 are, in the case of γ -alumina, idealised structures with all the tetrahedral aluminiums in place.

It is the surface of γ -alumina which is important in catalysis and since γ -alumina occurs in the form of lamellae, it is most probable that one type of surface plane is predominant. For the reasons discussed above the predominant surface plane is likely to be the (110) plane [36].

1.9 Fluorination and Chlorination of γ -Alumina and Montmorillonite K10.

The rapid hydrolysis of COF_2 at room temperature [44], on the surface of γ -alumina results in increased Brønsted acidity of the surface due to the hydrolysis

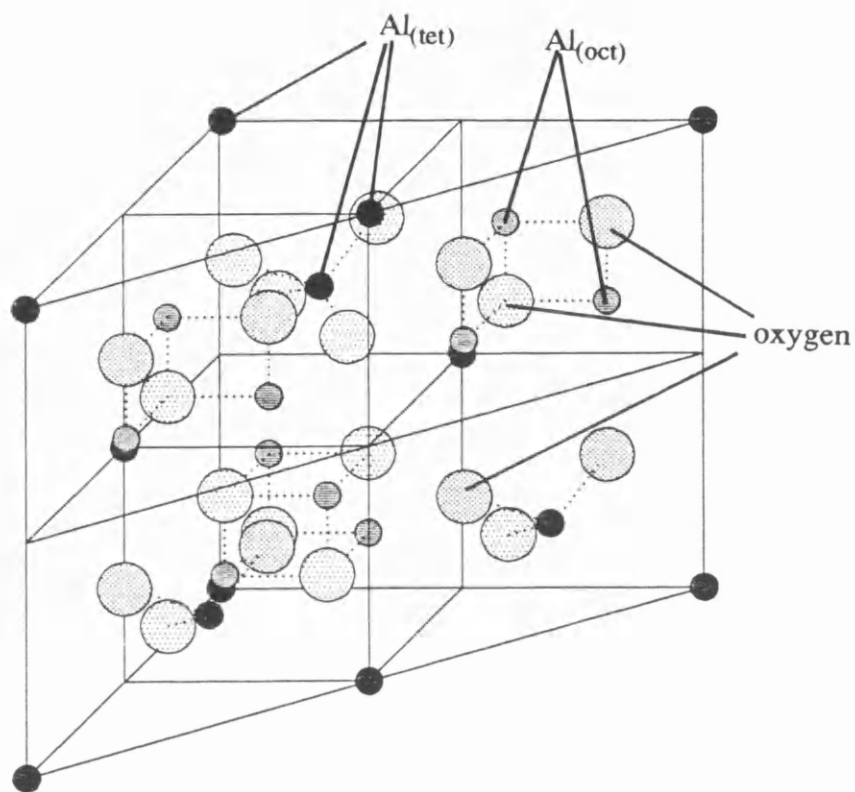


Figure 1.8.1. The (110) face of the spinel unit cell.

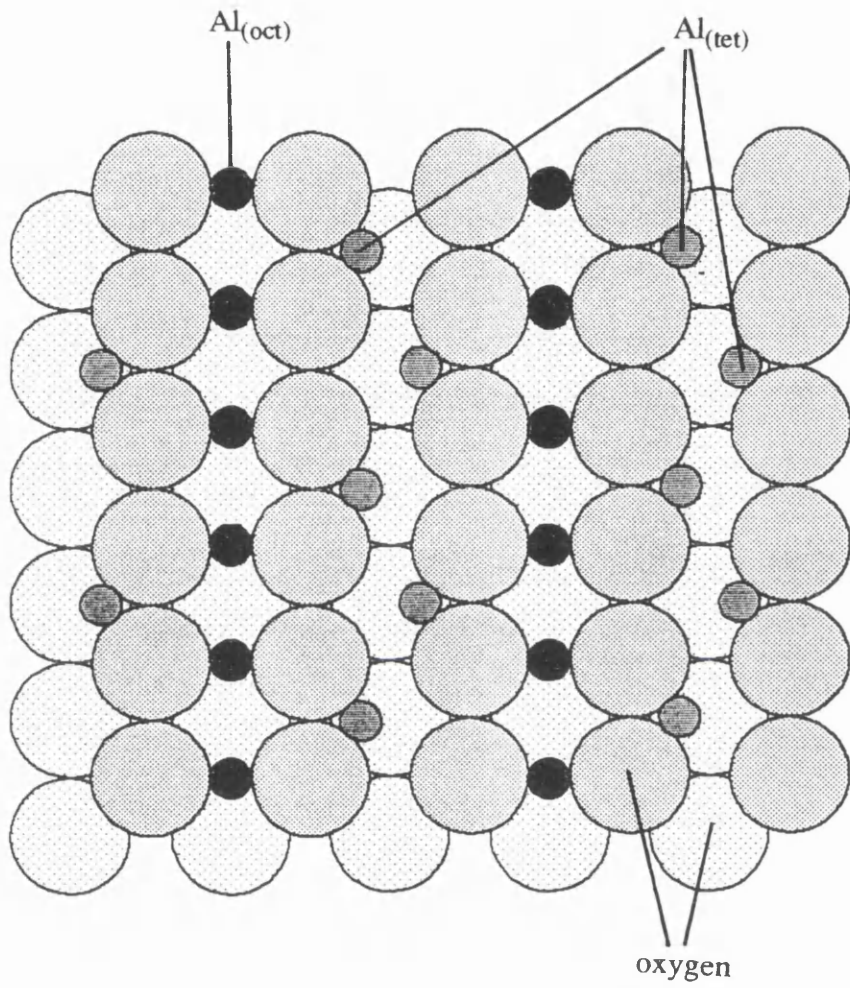


Figure 1.8.2. (110) Face of γ -alumina 'C-layer'

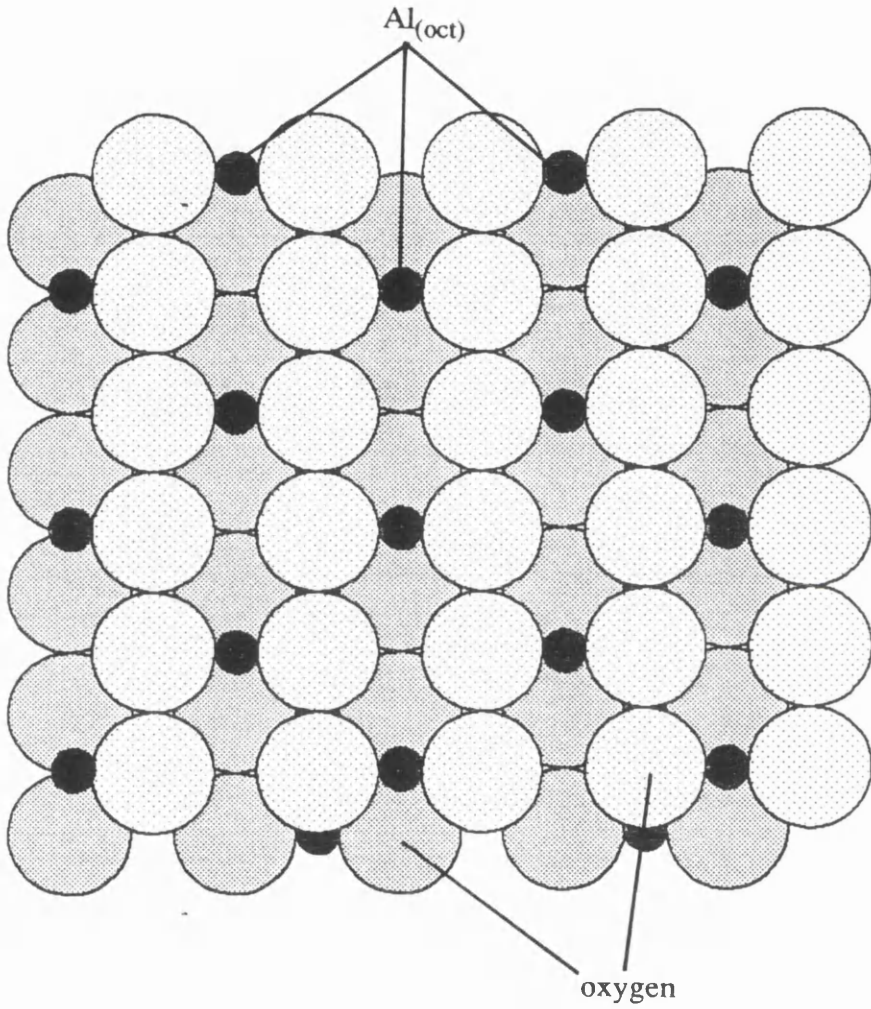


Figure 1.8.3. (110) Face of γ -alumina 'D-layer'

product HF. Promotion of Brønsted acidity by other fluorides, for example BF_3 and NH_4F has also been noted [45]. The room temperature interaction of SF_4 however results in the enhancement of Lewis acidity [44].

The chlorination of γ -alumina results in the enhancement of acidic sites on the surface of the alumina. The nature of this acidity depends on the chlorinating reagent used, chlorination of γ -alumina using anhydrous HCl leads to the enhancement of Brønsted acidity [46], whereas chlorination of γ -alumina using CCl_4 or OCCl_2 leads to enhanced Brønsted and Lewis acidity [47]. A study by A.G.Goble and P.A.Lawrance [48], indicated that the basic chlorination reaction involves an exchange of two chlorine atoms for each surface oxygen atom, resulting in the formation of Lewis acid sites. Isomerisation was considered to occur on a 'localised dual site' consisting of the Lewis acid site and an adjacent metal site. Goble and Lawrance [48] also discovered that hydrogen chloride and certain organic chlorine containing compounds gave rise to a catalyst that was inactive towards low temperature isomerisation, table 1.9.1.

Hydrogen Chloride	HCl
Methyl Chloride	CH_3Cl
Sym-tetrachloroethane	$\text{CHCl}_2\text{CHCl}_2$
1,2-Dichloroethane	$\text{CH}_2\text{ClCH}_2\text{Cl}$
Tetrachloroethylene	$\text{CCl}_2=\text{CCl}_2$
Acetyl Chloride	CH_3COCl

Table 1.9.1. Chlorine containing compounds which result in inactive low temperature isomerisation catalysts.

whilst other organic chlorine containing compounds gave catalysts active towards low temperature isomerisation, table 1.9.2.

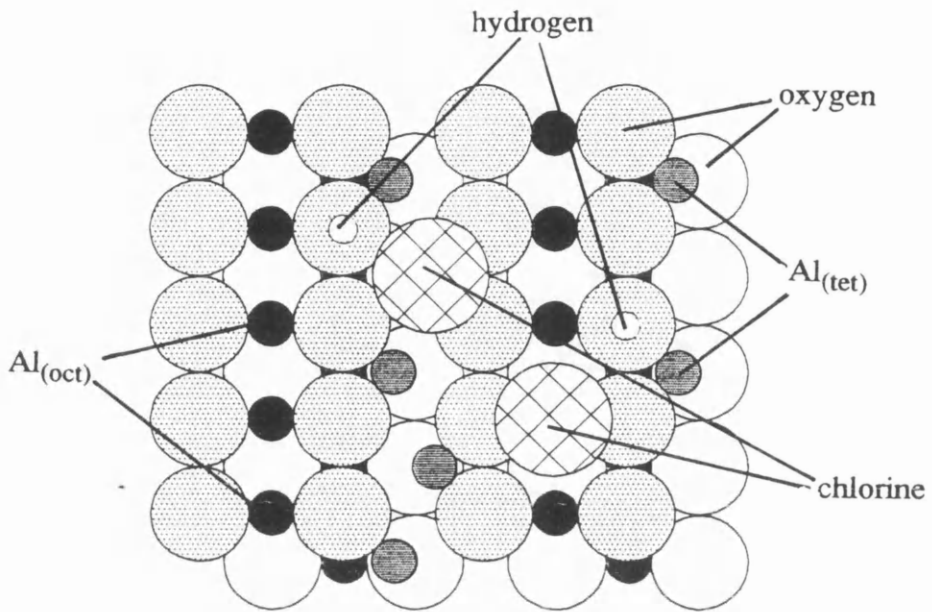


Figure 1.9.1. Chlorine species present on γ -alumina after the interaction of hydrogen chloride.

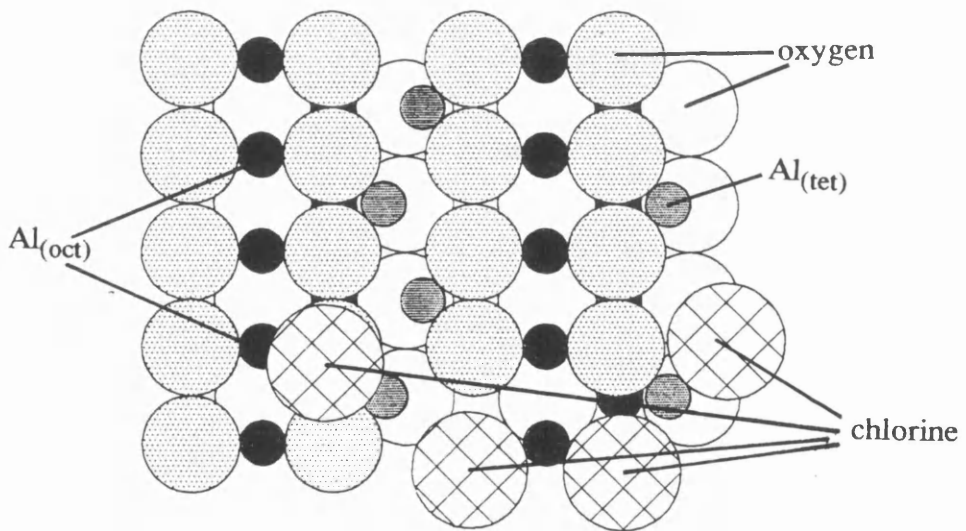


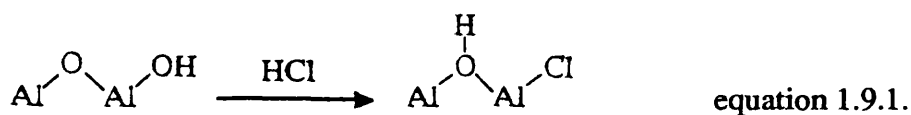
Figure 1.9.2. Chlorine species present on γ -alumina after the interaction of carbonyl chloride.

Carbon Tetrachloride	CCl_4
Chloroform	CHCl_3
Methylene Chloride	CH_2Cl_2
Difluorodichloromethane	CF_2Cl_2

Table 1.9.2. Chlorine containing compounds which result in active low temperature isomerisation catalysts.

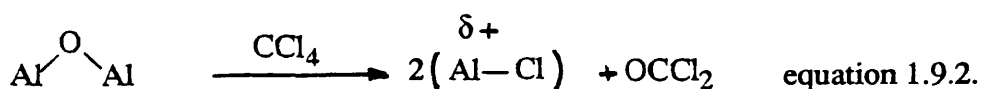
By using the radiotracer chlorine-36, it has been shown that the types of site can be differentiated. Chlorine associated with Brønsted sites is labile with respect to ^{36}Cl exchange with H^{36}Cl at room temperature, whereas chlorine associated with Lewis sites is inert to exchange with H^{36}Cl [45].

One explanation of the enhancement of Brønsted acidity observed after the treatment of calcined γ -alumina with anhydrous HCl is the formation, due to dissociative adsorption, of new acid sites. This involves the replacement of a terminal hydroxyl group by a chlorine atom and the protonation of a neighbouring bridged oxygen species [45].

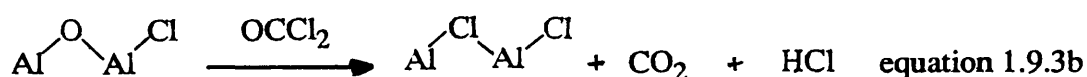
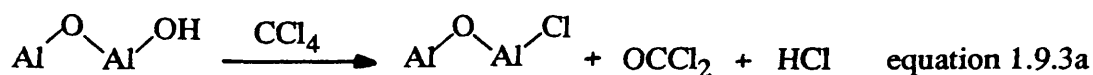


The replacement of the terminal hydroxyl group by the chlorine is possible for octahedral and tetrahedral Al^{III} environments, both of which are illustrated in figure 1.9.1. The enhancement of Brønsted acidity is due to the protonation of the bridged oxygen species. Since the chlorine atom is larger than the OH, the coordinately unsaturated $\text{Al}^{\text{III}}_{\text{oct}}$ surface species is effectively saturated and is thus not expected to exhibit Lewis acidity.

Reactions involving CCl_4 and OCCl_2 with γ -alumina are similar. This is not surprising as OCCl_2 is a reaction intermediate in the CCl_4 chlorination process, equation 1.9.2.



Whereas the interaction of HCl with γ -alumina takes place at room temperature, the interaction of CCl_4 with γ -alumina is minimal below 473K [49]. The initial reaction is believed to involve the replacement of terminal hydroxyl groups by chlorine, with the formation of OCCl_2 and HCl , equation 1.9.3a, the carbonyl chloride then reacts further to give CO_2 and HCl , equation 1.9.3b.



The hydrogen chloride formed in these reactions can then react with the surface as described previously. The chlorination reactions at this point involving both the anhydrous HCl and CCl_4 , appear to be very similar, but the Cl exchange reactions [49] show the chlorine species on the two surfaces to be very different. It has been postulated that the chlorination process involving CCl_4 and OCCl_2 , involves both terminal hydroxyl groups and inplane oxygens that bridge three Al^{III} atoms; two of these are surface atoms, and one lies immediately below the surface, figure 1.9.2.

It must be pointed out that figures 1.9.1 and 1.9.2 are based on the assumption of a perfect (110) spinel surface, and that γ -alumina is in fact a defect spinel. Figure 1.9.2,

does emphasise that the replacement of an inplane oxygen bridge by two chlorines, one terminal and one bridging, has a considerable disruptive effect on the lattice and hence requires a greater expenditure of energy than is required for chlorination using HCl.

The chlorination of montmorillonite K10, described in section 2.2.10, has not been as well documented as that of γ -alumina. Results obtained in this work have shown both similarities and differences between chlorinated montmorillonite K10 and chlorinated γ -alumina. Chlorination of montmorillonite K10 was carried out under the same conditions as that for γ -alumina. Infrared analysis of the vapour phase after the chlorination process has shown that CO_2 and HCl are present, as with γ -alumina, but results from neutron activation analysis (chapter 2) show a chlorine content of $7\text{mg atom Cl g}^{-1}$, double that of γ -alumina. The nature of the acidity of the chlorinated montmorillonite K10 was investigated (Chapter 6) using pyridine as a probe molecule. The chlorinated montmorillonite exhibited both Lewis and Brønsted acidity. The chlorinated montmorillonite is air sensitive (experiment 6.2.9), evolving hydrogen chloride when exposed to air. ^{27}Al MAS-NMR investigations, Chapter 3, provided evidence for both octahedral and tetrahedral aluminium environments.

At the outset of this work it was assumed that bromination of γ -alumina would lead to analogous situations as those encountered in the chlorination study carried out previously [46-49]. However this assumption proved to be unjustified; these findings were to influence greatly the work that was undertaken.

CHAPTER 2

2.1 Experimental.

The experimental work involving air sensitive materials was carried out in a Pyrex vacuum line, and involatile reactants transferred into the reaction vessels in a nitrogen atmosphere glove box. This ensured anhydrous and oxygen free conditions.

2.1.1 The vacuum system.

The vacuum line (figure 2.1.1) was an enclosed Pyrex glass structure consisting of a manifold, a constant volume manometer and a Vacustat, all of which were individually isolable. A rotary oil pump (Edwards high vacuum or Genevac) in series with a mercury diffusion pump (Jencons) provided a vacuum of 10^{-4} Torr. The pumps were protected from volatile material by a series of waste traps, before and after the mercury diffusion pump, which were cooled in liquid nitrogen. The Vacustat was used to measure the vacuum achieved by the pumps.

The constant volume manometer was used to measure pressures of gases in the manifold, with a precision of ± 0.5 Torr. The manifold had various B14 ground glass sockets, isolable from the line using high vacuum stopcocks (J.Young). Vacuum vessels (figure 2.1.2) and ampoules (figure 2.1.3), equipped with high vacuum stopcocks (J.Young) and B14 cones, were attached to the manifold sockets using Kel-F grease. The line and the vessels were flamed out, while the system was pumping, using a gas/oxygen flame.

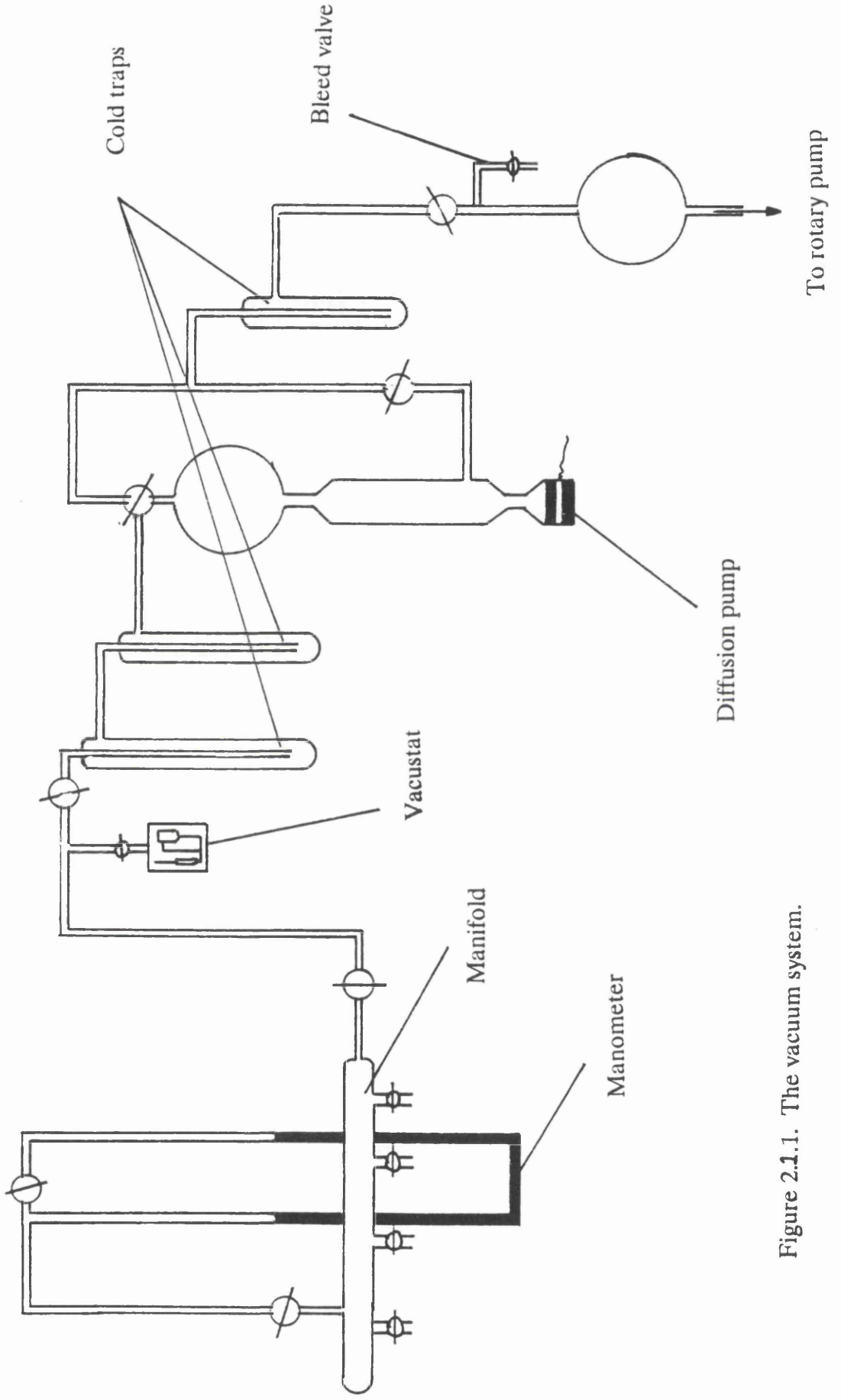
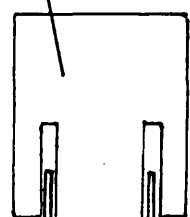


Figure 2.1.1. The vacuum system.

High vacuum stopcock (J. Young)



B14 Cone

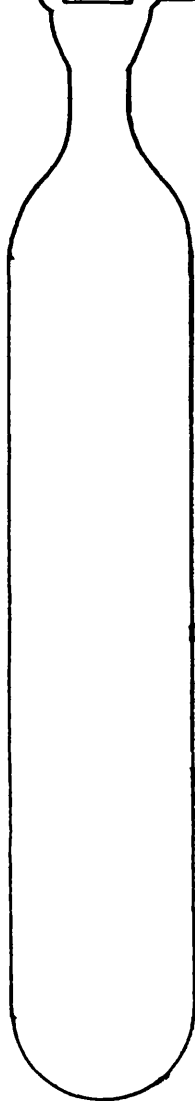
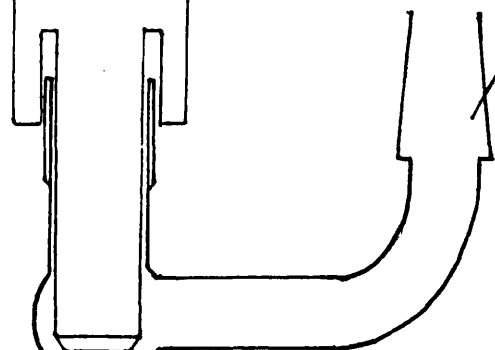
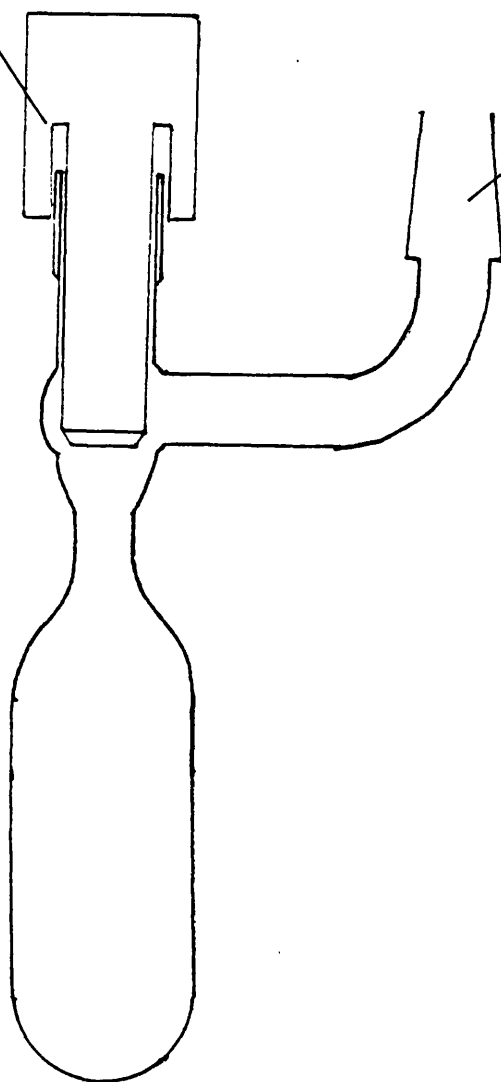


Figure 2.1.2. Pyrex Reaction Vessel.

High vacuum stopcock (J.Young)



B14 Cone

Figure 2.1.3. Pyrex Ampoule.

2.1.2 The inert atmosphere box.

A nitrogen atmosphere glove box ($H_2O < 4\text{ppm}$) was used when handling and storing all samples. The box contained an analytical balance, allowing the samples to be weighed precisely in a dry atmosphere.

2.2 Preparation and Purification of Reactants.

2.2.1 Preparation of [^{82}Br]-bromine labelled ammonium bromide.

The ^{82}Br isotope was prepared using the SURRC reactor facility at East Kilbride. Ammonium bromide (NH_4Br , 2mg) was placed in a polythene ampoule (figure 2.2.1), which was then wrapped in aluminium foil. The ampoule was transported to the Reactor Centre, where it was irradiated. Typical irradiation conditions were 3 hours, at a flux of 3.6×10^{12} neutron $\text{cm}^{-2}\text{s}^{-1}$, giving an activity of $100\mu\text{Ci}$.

The irradiation process produced 3 major radioactive isotopes, $^{80}\text{Br}(t_{1/2} 18\text{m})$, $^{80\text{m}}\text{Br}(t_{1/2} 4.5\text{h})$ and $^{82}\text{Br}(t_{1/2} 35.5\text{h})$. The isotopes [^{80}Br] and [$^{80\text{m}}\text{Br}$] have relatively short half-lives in comparison with the [^{82}Br], and could be discounted, since the irradiated sample was collected 48h after the irradiation process, leaving the one major radioisotope [^{82}Br].

Safety precautions when handling radioactive bromine involved; I) wearing latex gloves and a finger monitor, II) conducting all experiments in a fumehood, III) handling [^{82}Br]-bromine labelled ammonium bromide over a spill tray and IV) conducting all experiments behind a 10cm lead shield.

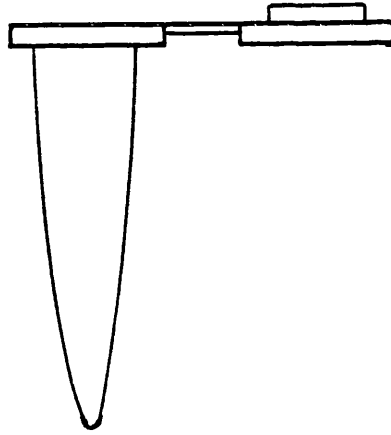


Figure 2.2.1. Polythene ampoule.

2.2.2 Preparation of [^{82}Br]-bromine labelled hydrogen bromide.

[^{82}Br]-Bromine labelled hydrogen bromide was prepared by the addition of trifluoromethanesulphonic acid (triflic acid) $\text{CF}_3\text{SO}_3\text{H}$ (Fluorochem Ltd) to [^{82}Br]-bromine labelled ammonium bromide.

Vessel A (figure 2.2.2) was attached to the vacuum line, via a right angled adaptor. The manifold and vessel were checked for leaks, by closing tap A on the vessel and opening taps B and C. The vessel was then evacuated, by opening tap D on the manifold, until the pressure gauge, attached to the manifold, returned to its original setting; at this point the pressure gauge was set to zero. The manifold was isolated from the vacuum line, but not from the pressure gauge. After 20min the pressure was read; if the pressure in the manifold had increased by more than 3-4 Torr then the usual procedure for finding leaks was undertaken until the change in pressure in the manifold was < 3-4 Torr over 20 minutes. Vessel A was isolated from the manifold by closing tap C, air was allowed into the vessel by opening tap A, then tap B was replaced by a glass funnel. Vessel B, the collection vessel (figure 2.1.2), was attached to the manifold and evacuated.

Ammonium bromide (Analar, BDH, 1.0g) was loaded into vessel A using the glass funnel. The radiolabelled ammonium bromide (2mg) was removed from the lead castle, with the aid of tweezers, and placed on a tray covered with a paper towel. The aluminium foil surrounding the ampoule was then removed. The ampoule was opened carefully and the radiolabelled ammonium bromide loaded into vessel A. A mini-monitor was used to check for any spillages of radioactive material and for contamination of the tweezers.

Once all the ammonium bromide had been loaded, tap B was replaced and closed. Triflic acid (approx 3cm^3) was added to the vessel through tap A. The vessel was evacuated by closing tap A and opening tap C, with the manifold open to the vacuum line. A Dewar flask containing liquid nitrogen was placed around vessel B. The manifold was then isolated from the vacuum line and tap B opened, allowing triflic acid to react with ammonium bromide. The hydrogen bromide evolved was condensed, using liquid nitrogen, into vessel B. After 20min tap C was closed and the manifold opened to the vacuum line.

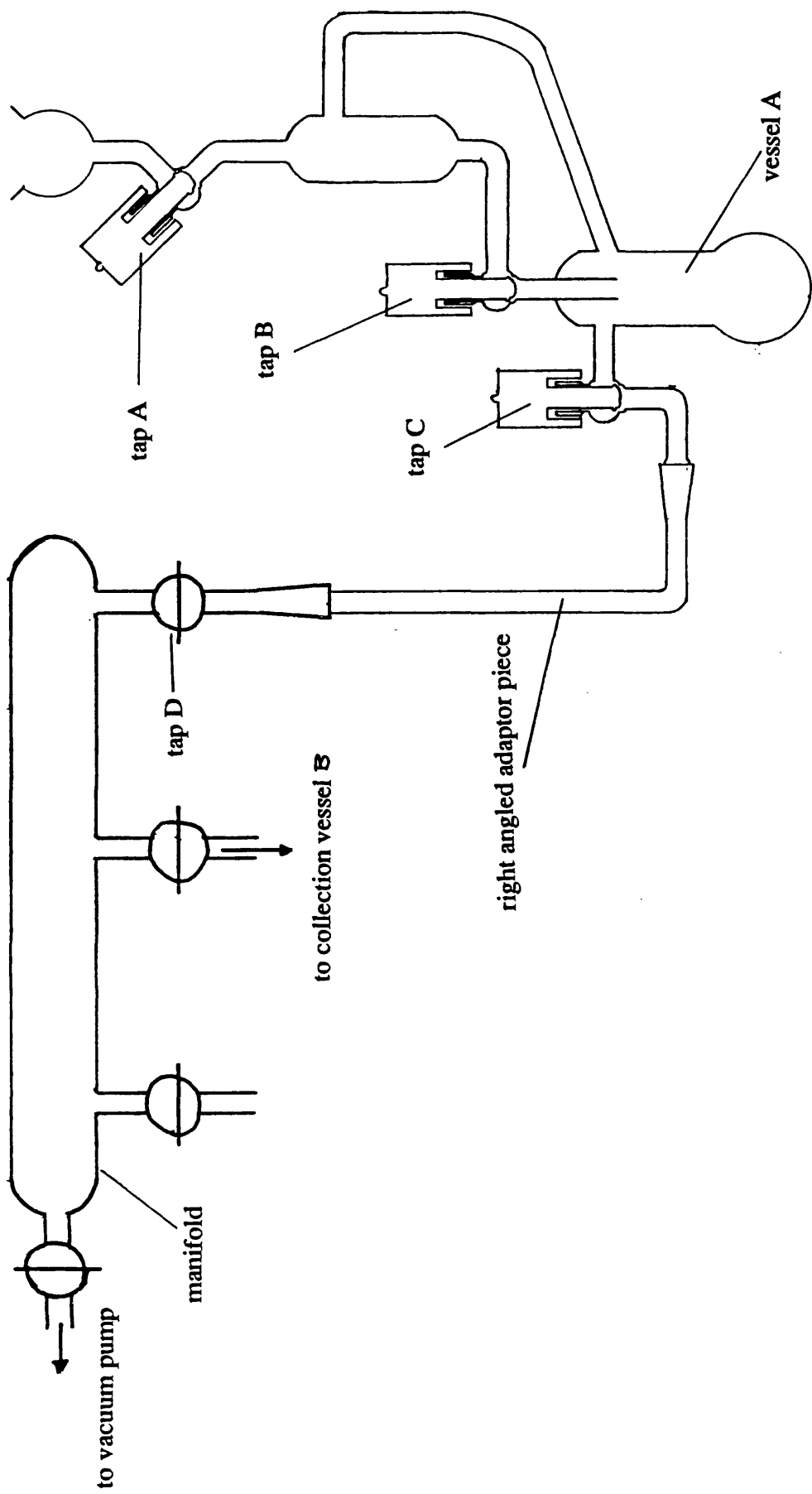


Figure 2.2.2. Apparatus used for the generation of H^{82}Br and Br^{82}Br .

Vessel B (containing the [^{82}Br]-bromine labelled hydrogen bromide) was then closed and the contents stored at 77K.

When the mini-monitor was placed next to the triflic acid in vessel A, after the reaction, only a background count was detected (10 count s^{-1}). Counting vessel B with the mini-monitor gave counts $> 2000 \text{ count s}^{-1}$.

2.2.3 Preparation of [^{82}Br]-bromine labelled dibromine.

[^{82}Br]-bromine labelled dibromine was prepared by the addition of 98% sulphuric acid (H_2SO_4), to [^{82}Br]-bromine labelled ammonium bromide.

In preliminary experiments undertaken in the formation of dibromine, from ammonium bromide, the solubility of dibromine in 98% sulphuric acid was such that the dibromine could not be distilled out of the solution at standard temperature and pressure. There were two options available; either increase the temperature or decrease the pressure, the latter being chosen as a safer option. The apparatus used to prepare the [^{82}Br]-bromine labelled dibromine was similar to that used to prepare [^{82}Br]-bromine labelled hydrogen bromide. The preparation of the apparatus, for example checking for leaks, was identical for both preparations.

Ammonium bromide (0.75g) was loaded into vessel A using the glass funnel. The radiolabelled ammonium bromide (2mg) was removed from the lead castle, with the aid of tweezers, and placed on a tray covered with a paper towel. The aluminium foil surrounding the ampoule was then removed. The ampoule was opened carefully and the radiolabelled ammonium bromide loaded into vessel A. A mini-monitor was used to check for any spillages of radioactive material and contamination of tweezers.

Once all the ammonium bromide had been loaded, tap B was replaced and closed. 98% Sulphuric acid (3cm^3) was added to the vessel through tap A. The vessel was evacuated by closing tap A and opening tap C, with the manifold open to the vacuum line.

A Dewar flask containing liquid nitrogen was placed around vessel B. The manifold was then isolated from the vacuum line and tap C closed. The sulphuric acid was added to the ammonium bromide by opening tap B. After 2min tap C was opened and the [^{82}Br]-bromine labelled dibromine evolved was condensed into vessel B. After 20min, vessel B and tap C were closed, and the manifold opened to the vacuum line. Vessel C (storage vessel) containing P_2O_5 was attached to the manifold and evacuated. A Dewar flask containing dichloromethane and dry ice, at 236K, was placed around vessel B before opening the vessel to the vacuum line to remove HBr and SO_2 formed during the reaction. The manifold was then isolated from the vacuum line and a Dewar flask containing liquid nitrogen placed around vessel C. Vessel C was opened and the [^{82}Br]-bromine labelled dibromine condensed into vessel C.

2.2.4 Purification and storage of dibromine.

98% Sulphuric acid (5cm^3) was loaded into a glass reaction vessel (figure 2.1.2), which was then transferred to a vacuum line and the contents degassed. An aliquot of dibromine was loaded into a separate glass reaction vessel and the contents degassed; this dibromine was then condensed into the vessel containing sulphuric acid and allowed to warm to room temperature. After 30min the dibromine was condensed into a storage vessel containing P_2O_5 . The contents of the storage vessel were degassed at 236K to remove any trace amounts of hydrogen bromide and hydrogen chloride that may have been present.

2.2.5 Preparation and storage of dibromomethane, bromochloromethane and tribromomethane.

The halogenating reagents dibromomethane, bromochloromethane and tribromomethane were all prepared and stored in the same manner.

An aliquot of dibromomethane (Analar, Aldrich, approx 5cm³) was loaded into a glass reaction vessel (figure 2.1.2), transferred to a vacuum line, and the contents of the vessel degassed. A separate glass reaction vessel containing activated 3A molecular sieves was attached to the vacuum line. The dibromomethane was condensed into this second reaction vessel and stored under vacuum.

2.2.6 Purification of pyridine and 2,6-dimethylpyridine.

The purification process used for pyridine (Analar, BDH) and 2,6-dimethylpyridine (Analar, Aldrich) was identical. An aliquot of pyridine (5cm³) was loaded into a glass reaction vessel, transferred to a vacuum line, and the contents of the vessel degassed. A second vessel, containing KOH pellets, was attached to the vacuum line and the contents degassed. The pyridine was condensed, at 77K, into the second vessel and stored under vacuum.

2.2.7 Calcination of γ -alumina

The γ -alumina used in this work was high purity Degussa 'C'. The standard pretreatment involved loading the γ -alumina to be calcined (generally 10g) into a glass vessel and attaching to the vacuum line. An electrical heater fitted with a vertical thermo-

couple was fixed around the vessel. The γ -alumina was pretreated by calcining *in vacuo* at 523K for 6 hours under dynamic vacuum. After the pretreatment was complete, the calcined γ -alumina was transferred to a dry box and stored under nitrogen.

2.2.8 Calcination of montmorillonite K10.

Montmorillonite K10, produced by Sud-Chemie A.G, Munich, Germany is a sulphuric acid-leached montmorillonite [35] and was supplied by the Aldrich Chemical Company Ltd. The standard pretreatment involved loading the montmorillonite K10 to be calcined (generally 5g) into a glass vessel, and attaching to the vacuum line. Due to the physical nature of the montmorillonite K10, special precautions were taken to avoid drawing the powder into the vacuum manifold. Precautions included fitting a specially designed piece of apparatus, figure 2.2.3, onto the calcination vessel, in order to trap any montmorillonite K10, before slowly degassing the vessel over a period of 2h. The montmorillonite K10 was pretreated by calcining at 523K for 6h under dynamic vacuum. After the pretreatment was complete the calcined montmorillonite K10 was transferred to a dry box and stored under nitrogen.

2.2.9 Chlorination of γ -alumina

The calcined γ -alumina sample (generally 1g) was loaded into a Monel bomb, under a nitrogen atmosphere in the glove box. The bomb was attached to the vacuum line and pumped for 10min to remove all nitrogen. The bomb was cooled to 77K, using liquid nitrogen, before an aliquot of COCl_2 was condensed into the bomb by vacuum distillation. An electrical heater was fitted around the bomb, and the bomb heated at 523K for 6h.

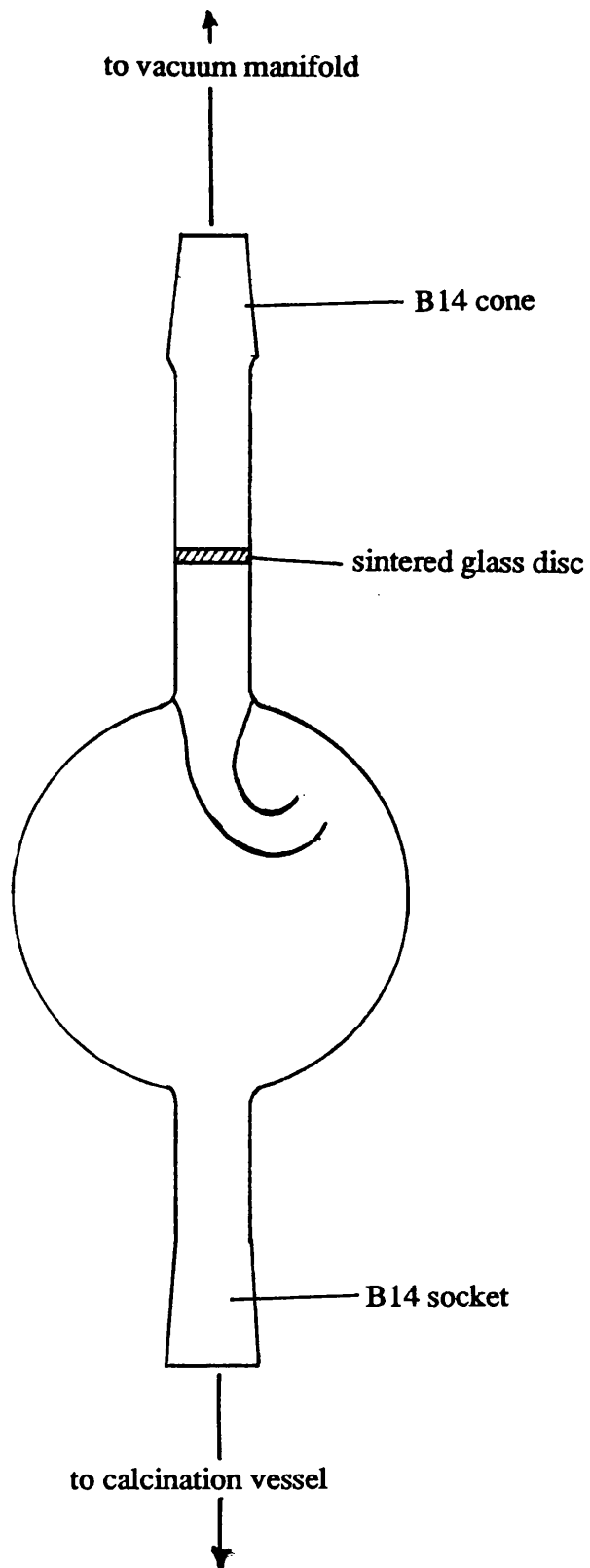


Figure 2.2.3. Apparatus used to avoid the carriage of montorillonite K10 into the vacuum manifold during calcination.

After the pretreatment was complete, the contents of the bomb were degassed before the chlorinated γ -alumina was transferred to a dry box and stored under nitrogen.

2.2.10 Chlorination of montmorillonite K10.

The calcined montmorillonite K10 sample (generally 1g) was loaded into a Monel bomb, under a nitrogen atmosphere in the glove box. The bomb was attached to the vacuum line and pumped for 10min to remove all nitrogen. The bomb was cooled to 77K, using liquid nitrogen, before an aliquot of COCl_2 was condensed into it by vacuum distillation. An electrical heater was then fitted around the bomb, and the bomb heated at 523K for 6h. After the pretreatment was complete, the contents of the bomb were degassed before the chlorinated montmorillonite K10 was transferred to a dry box and stored under nitrogen.

2.2.11 Fluorination of γ -alumina.

The calcined γ -alumina sample (approximately 1g) was loaded into a Monel bomb, under a nitrogen atmosphere in the glove box. The bomb was transferred to a Monel vacuum line and pumped for 10min to remove all nitrogen. One aliquot of SF_4 (1 mmol) was condensed onto the γ -alumina and allowed to warm to room temperature for 30min, after which time the contents of the bomb were pumped for 60secs to remove any volatile products. Another aliquot of SF_4 (1 mmol) was condensed into the bomb and the process repeated. This sequence was repeated a total of five times.

2.3 Infrared Spectroscopy

2.3.1 Transmission infrared spectroscopy in the vapour phase.

To obtain a vapour phase spectrum, the gas cell, figure 2.3.1, with KBr windows and a pathlength of 7cm, was evacuated and a background spectrum accumulated, usually 10 scans. Vapour phase infrared spectra of reaction products were obtained by attaching the reaction vessel and the gas cell to a vacuum line manifold and evacuating both. Vapour was expanded into the manifold to the desired pressure, usually 50 Torr. The cell was isolated from the manifold and the manifold evacuated, allowing the cell to be removed. A spectrum was then accumulated, usually for 10 scans.

Two spectrometers were used to obtain these vapour phase spectra; I) Philips PU 9800 FT-IR Spectrometer, with a DELL SYSTEM 200 computer and II) Perkin Elmer 16PC FT-IR with an EPSON EL3s computer.

2.3.2 Diffuse reflectance infrared fourier transformed spectroscopy (D.R.I.F.T.S.).

Reflectance spectroscopy differs from absorbance spectroscopy in that using reflectance spectroscopy, the radiation being analysed is reflected off the surface of the analyte, figure 2.3.2. In absorbance spectroscopy the radiation is passed completely through the sample.

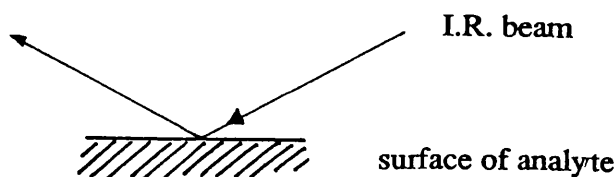


Figure 2.3.2. Reflectance spectroscopy.

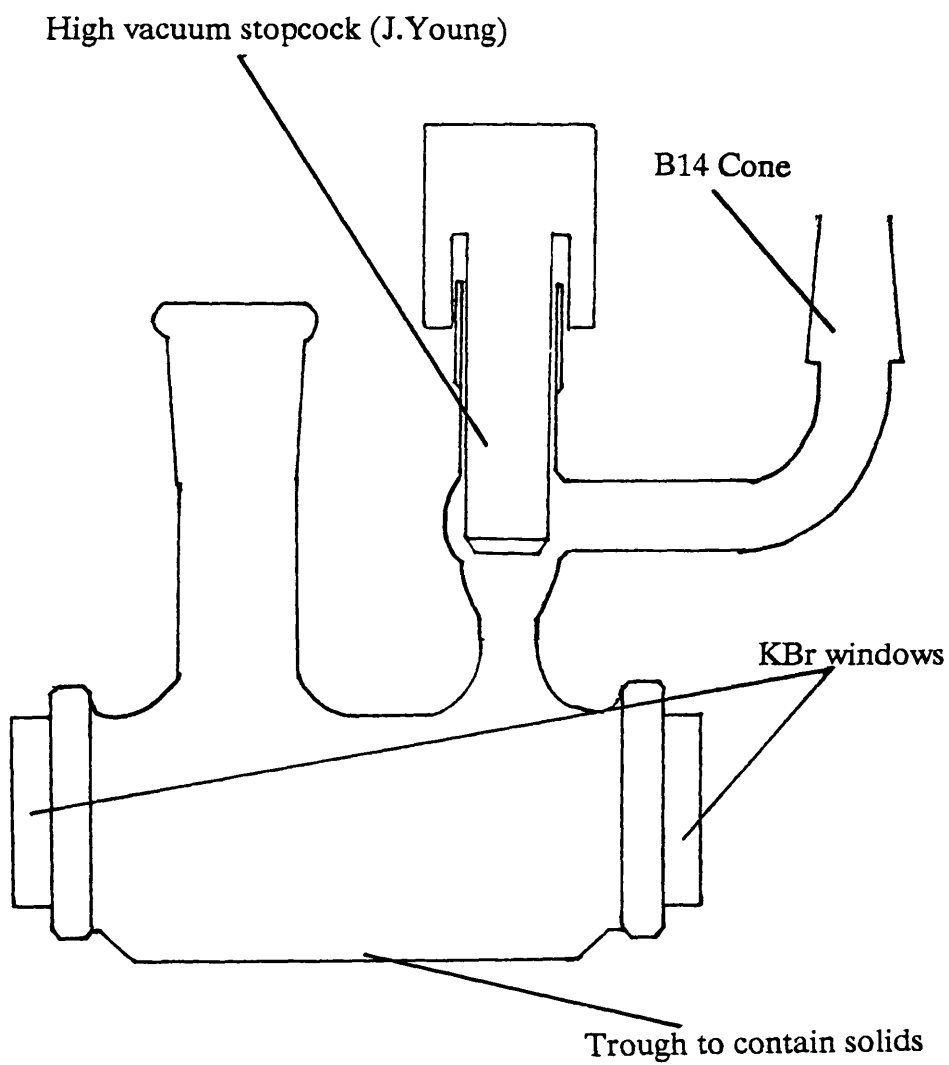


Figure 2.3.1. Gas Cell.

Diffuse reflectance spectroscopy reflects the infrared beam off an ellipsoid mirror, figure 2.3.3, and onto the sample. A blocker device (A) prevents radiation reflected without penetrating the sample from reaching the collection mirror. The diffusely reflected radiation (B) penetrates into the sample and is able to reach the collection mirror.

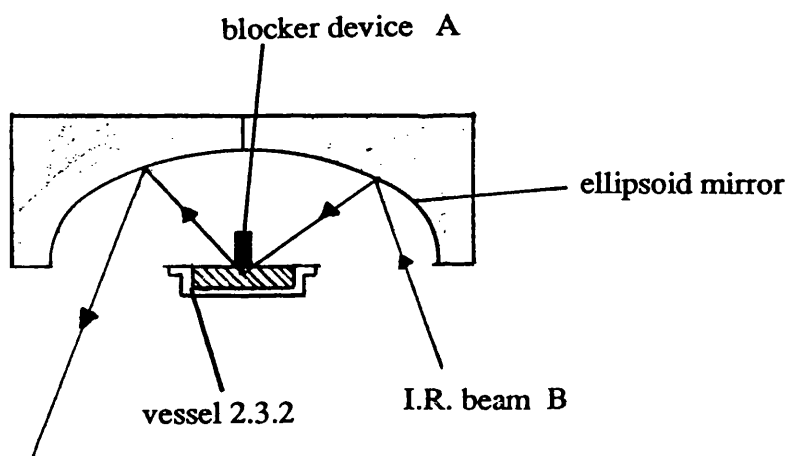


Figure 2.3.3. Diffuse reflectance cell.

Diffuse reflectance measurements provided a very simple method of obtaining infrared spectra of solids. To obtain a DRIFT spectrum, vessel 2.3.2 was loaded with KBr to give a 'flat' surface and a background spectrum was accumulated. The KBr was removed and the powder under investigation was loaded into the vessel. The vessel was placed into the spectrometer and several scans (usually 50) were obtained. The powders investigated were generally moisture sensitive, so handling and scanning times were kept to a minimum. Attempts at using an inert atmosphere shroud failed to produce acceptable spectra; noise levels were very high with respect to signals, even after 10000 scans. The spectrometer used for the DRIFTS analysis was a Nicolet 5DXC FT-IR Spectrometer with a Nicolet Auxiliary Experiment Module attached.

2.3.3 Photoacoustic spectroscopy (P.A.S.).

Photoacoustic spectroscopy, like DRIFTS, is a technique used for obtaining infrared spectra from the surface of solid materials. The photoacoustic technique involves placing the powder under investigation into the photoacoustic cell, figure 2.3.4, then purging the cell with helium for 10-20sec to remove all air from the system. The signal obtained from the powder is amplified through the helium medium before being picked up by the microphone. The signal is then processed by the computer and a spectrum obtained.

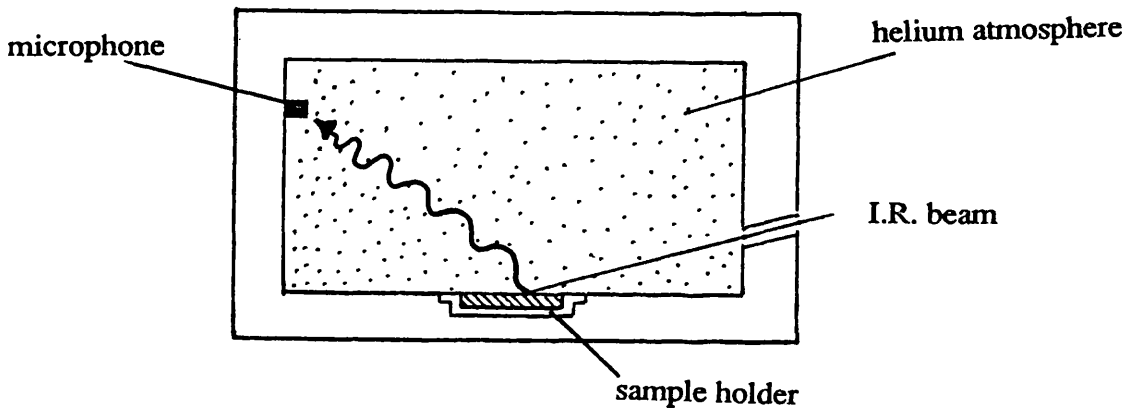


Figure 2.3.4. Photoacoustic cell.

Spectra were obtained by loading a carbon black disc into the photoacoustic cell, purging the cell with dry helium gas for 10secs and a background spectrum accumulated. The carbon black disc was removed and the powder under investigation loaded into the vessel, figure 2.3.2. The vessel was transferred to the PAS cell, and the cell purged with helium for 10secs. After purging, several scans (usually 20) were obtained.

The PAS analysis was carried out, with the help of Malcolm Littlewood, at Nicolet Instruments limited, Warwick and also at Strathclyde Police Headquarters, Glasgow, using a Nicolet 510 spectrometer.

2.4 Gas Chromatography.

All analysis involving gas chromatography and gas chromatographic mass spectroscopy was carried out at The Associated Octel Company Ltd, Ellesmere Port. An HPS crosslinked 5% Ph-Me-Silicone (5m x 0.32mm x 0.52micrometres) column was used for these analyses. Typical run conditions were; Initial Temp: 373K, Final Temp: 653K, Initial Time: 0min, Final Time : 20min, Rate: 10K/min and Injection Temp: 623K.

2.5 Radiochemistry.

2.5.1 Statistical errors.

Decay of a radioisotope is a random process and is therefore subject to fluctuations due to the statistical nature of the process. If a source of radioactivity is measured several times, the number of disintegrations observed during a fixed time will not remain constant, even allowing for half-life decay. The probability $W(m)$ of obtaining m disintegrations in time t from N_0 original radioactive atoms is given by the binomial expression (equation 2.5.1) :

$$W_m = \frac{N_0!}{(N_0-m)!m!} p^m(1-p)^{N_0-m}$$

equation 2.5.1.

where p is the probability of a disintegration occurring within the time of observation [51]. From this expression it can be shown [52,53,54,] that the expected standard deviation for radioactive disintegration θ is given by equation 2.5.2.

$$\theta = \sqrt{me^{-\lambda t}} \quad \text{equation 2.5.2.}$$

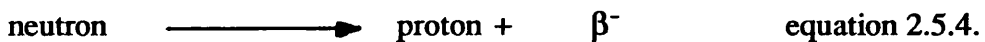
In practice the observation time t is short in comparison to the half-life so that t is small, reducing equation 2.5.3 to :

$$\theta = \sqrt{m} \quad \text{equation 2.5.3,}$$

where m is the number of counts obtained. In this work all errors quoted on radiochemical measurements are the combination of the uncertainty in the physical measurement, such as weight of sample and pressure of gas, and the uncertainty in the count obtained.

2.5.2 Scintillation counting.

[⁸²Br]-Bromine decays (100%) by the emission of a β^- particle (end-point energy 0.444MeV). This decay adjusts the amount of neutrons and protons present, in the nucleus by converting a neutron to a proton, equation 2.5.4.



The emission of β^- leaves the mass number of the isotope unchanged, but the atomic number increased by one, therefore [⁸²Br] decays to a high energy metastable state of [⁸²Kr], equation 2.5.5.



[⁸²*Kr] decays to the ground state [⁸²Kr] by internal transitions (figure 1.3.2), with the emission of a range of high energy γ -radiation. The γ -rays produced in the internal

transitions were counted using a Tl/NaI scintillation counter, attached to an SR7 scaler ratemeter. The most widely used inorganic scintillator is NaI activated with 0.1-0.2% thallium. The high density (3.7gcm^{-3}) of NaI and the high Z value of iodine make this a very efficient γ -ray detector. To produce one photon from the NaI scintillation crystal requires approximately 30eV. On average 10 photons are required to release one photoelectron at the photo-cathode of the multiplier. These photoelectrons are then accelerated, by an electrical potential gradient, to the first electrode, where each photoelectron produces approximately 4 more photoelectrons. These secondary electrons are similarly accelerated, so that in a 10 stage photomultiplier tube there is a gain of 10^4 . The resulting pulse is then fed into an amplifier and then to a scaler, where it is recorded.

To achieve a maximum pulse the scintillator crystal is surrounded by a reflector. The space between the crystal and the photomultiplier is filled with high viscosity paraffin or silicone oil, to improve the light transmission. The scintillation counter and scaler were calibrated before use, using a [^{60}Co] source which emits γ -rays of energy 1.33MeV. A γ -ray spectrum of [^{82}Br] was obtained by monitoring the counts from the source while varying the applied threshold, figure 2.5.1. γ -Ray spectra were also obtained for [^{82}Br], [$^{80\text{m}}\text{Br}$] and [^{80}Br] using the GeLi counter at SURRC, figure 2.5.2. The GeLi counter has a higher efficiency and a greater resolution than the NaI counter.

2.5.3 Half-life and decay corrections.

The half-life, $t_{1/2}$, is the time interval required for a measured activity A to decrease by one half of its original value. The half-life was conveniently determined from a plot of $\ln A$ versus t (time) and is related to the decay constant by equation 2.5.6. The half-life of [^{82}Br] was determined, from figure 2.5.3, to be 35.0h (literature value 35.3h [55]).

Figure 2.5.1. ^{82}Br Gamma ray spectrum recorded with a NaI detector.

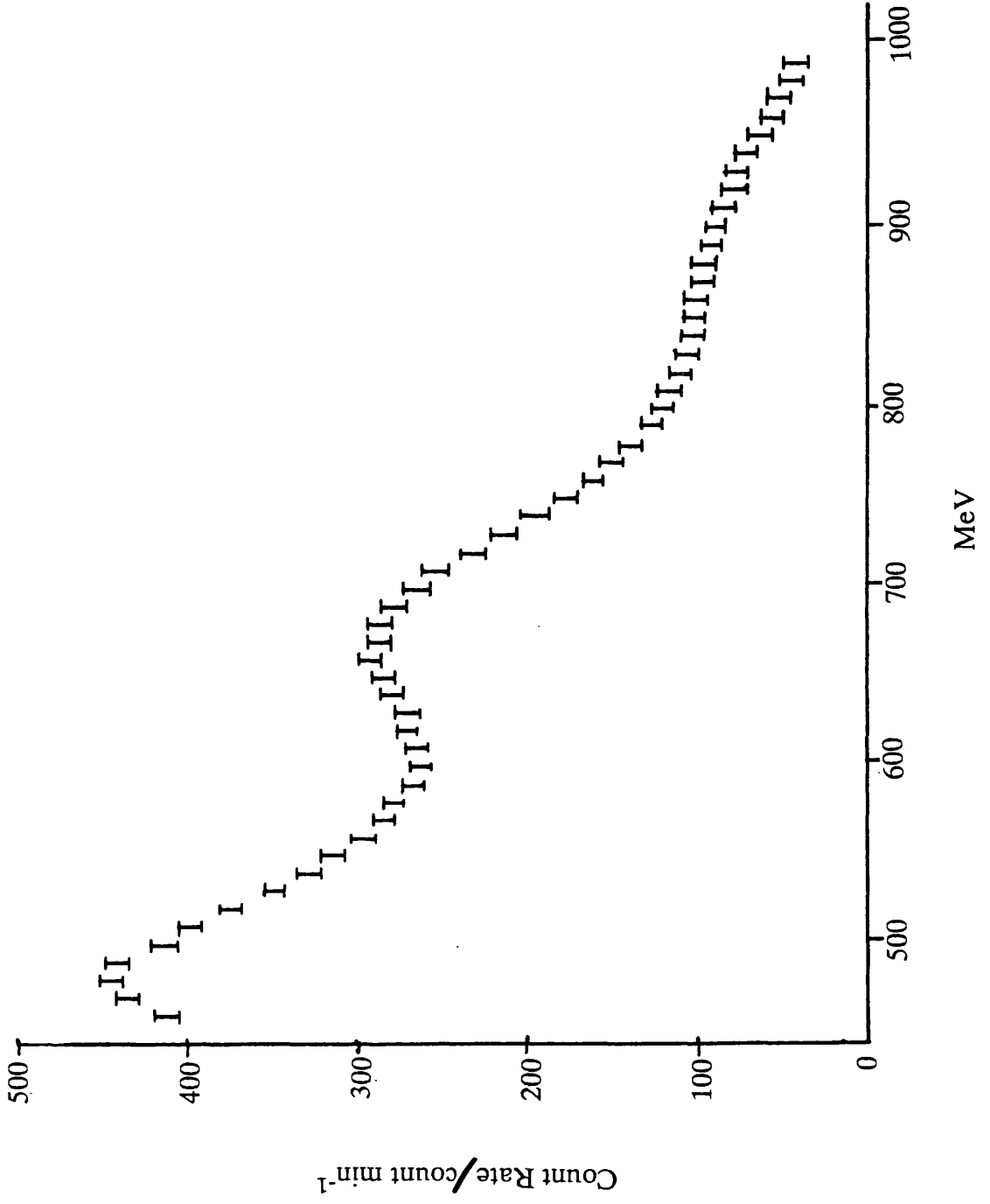


Figure 2.5.2. ^{82}Br Gamma ray spectrum recorded with a GeLi detector.

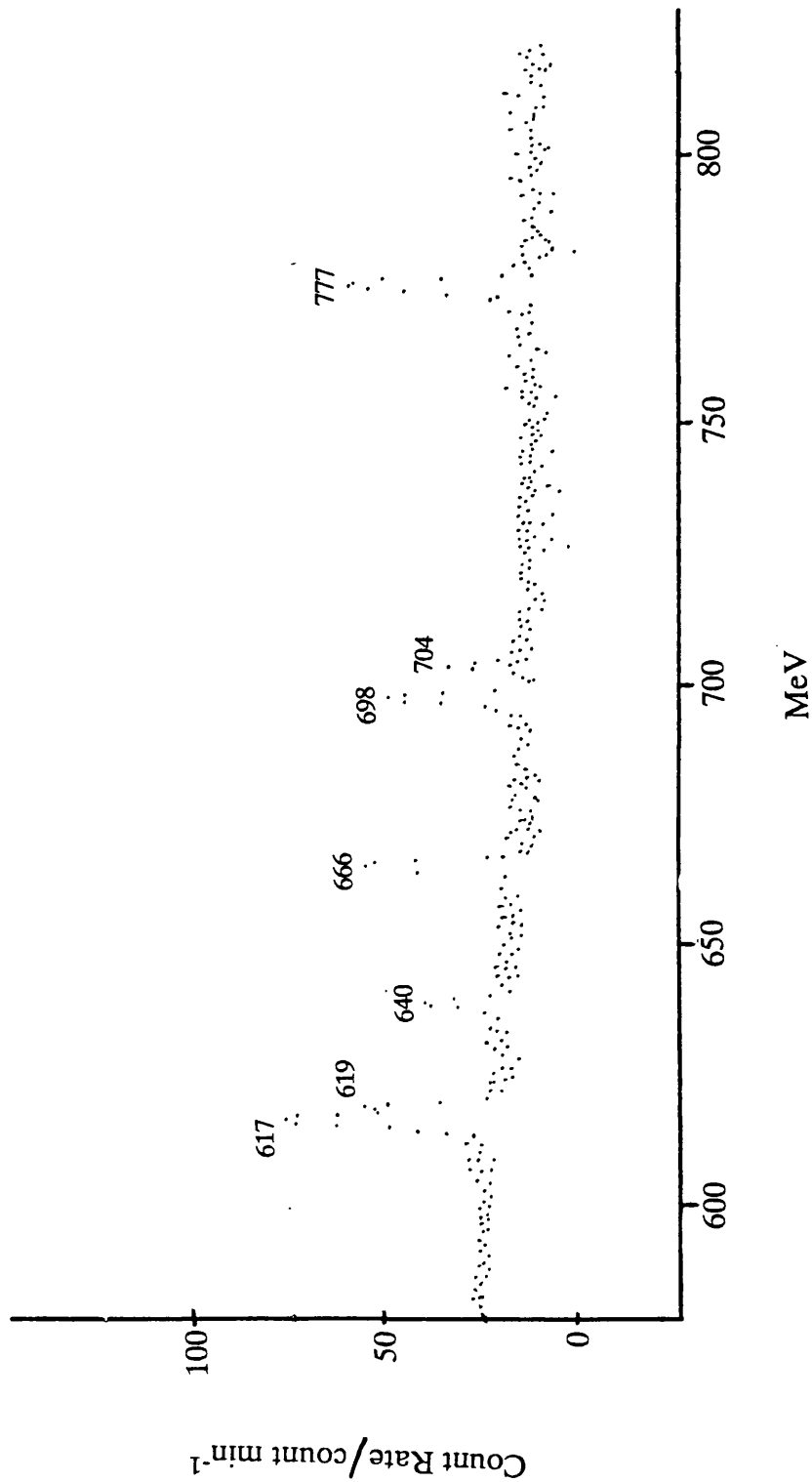
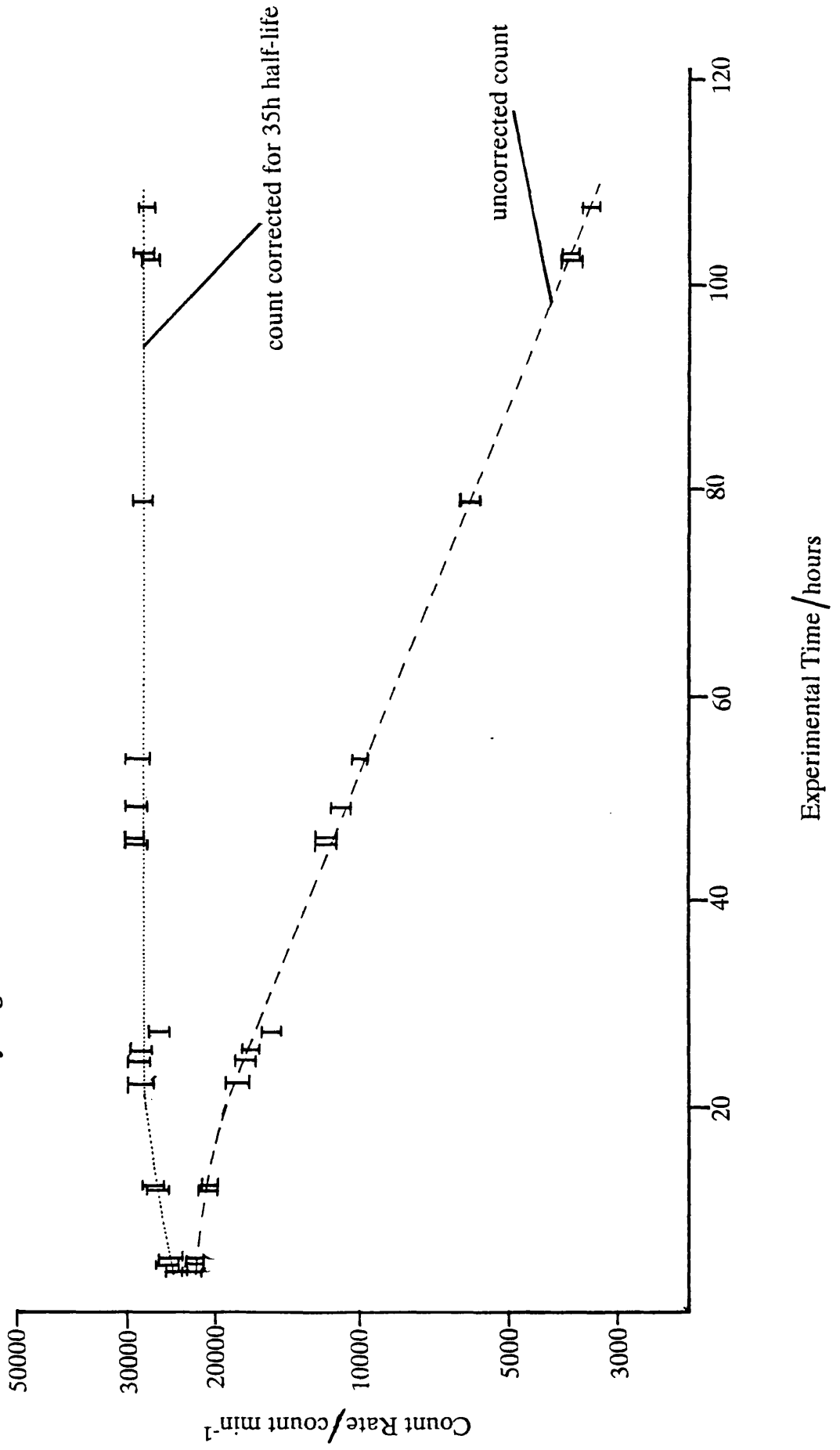


Figure 2.5.3. Surface count rate for the interaction of [^{82}Br]-bromine labelled hydrogen bromide with NaOH.



$$t_{1/2} = \frac{\ln 2}{\lambda} \quad \text{equation 2.5.6.}$$

The activity of a radioactive species decays according to equation 2.5.7. Since significant decay occurred in the time taken to carry out an experiment, all data obtained were corrected to zero time before being analysed.

$$A_t = A_0 e^{-\lambda t} \quad \text{equation 2.5.7.}$$

where; λ = decay constant in h^{-1}
 A_t = count rate of sample at time t
 A_0 = count rate of sample at time $t=0$.

2.5.4 [^{82}Br]-Bromine counting cells.

Reactions involving [^{82}Br]-bromine labelled Br_2 and HBr were monitored using single limbed counting vessel, figure 2.5.4, to measure the specific activity of the samples. A double limbed counting vessel, figure 4.2.1, was used to follow uptakes of [^{82}Br] at room temperature and a round bottomed reaction vessel, figure 4.2.3, was used to follow bromine uptakes at temperatures up to 353K.

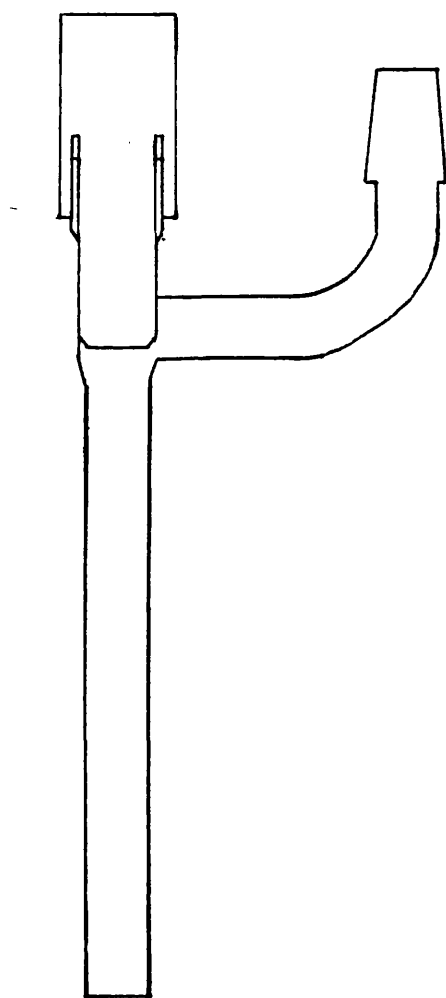


Figure 2.5.4. Single limbed counting vessel.

2.5.5 Determination of specific count rate of [⁸²Br]-bromine labelled hydrogen bromide.

The specific count rate of [⁸²Br]-bromine labelled hydrogen bromide was determined by reacting a measured quantity of hydrogen bromide with sodium hydroxide and counting the sodium bromide salt.

Solid sodium hydroxide (1.0g) was placed in a single limbed counting vessel, figure 2.5.4, and a few drops of water added. The counting vessel was transferred to a vacuum line and degassed for 5secs. The vessel was closed then cooled using liquid nitrogen. The manifold and pressure gauge were isolated from the vacuum pump. An aliquot of [⁸²Br]-bromine labelled hydrogen bromide was then released into the manifold, and the pressure noted. The single limbed vessel was opened to the manifold, and the hydrogen bromide condensed into it. The single limbed vessel was closed after 30 seconds, and the pressure noted. From the known pressure, i.e. difference between the 2 readings, the amount of [⁸²Br]-bromine labelled hydrogen bromide condensed into the limb could be calculated. The single limbed vessel was then placed into the NaI counter and a minimum of 10 individual counts taken, each in excess of 100000 counts. From the count rate and the known amount of hydrogen bromide present, a specific count rate could then be calculated, i.e. counts per mmol. Representative data for the calculation of the specific count rate of [⁸²Br]-bromine labelled hydrogen bromide shown in section 4.3.6.

2.5.6 Determination of specific count rate of [⁸²Br]-bromine labelled dibromine.

The specific count rate of [⁸²Br]-bromine labelled dibromine was determined by condensing dibromine into chloroform, then counting the solution.

Analar chloroform (2cm³) was decanted into a single limbed counting vessel. The vessel was transferred to a vacuum line manifold and a Dewar flask containing liquid

nitrogen placed around it. When the chloroform had frozen, the vessel was opened to the vacuum line and degassed. The chloroform was degassed a further 3 times. The manifold was isolated from the vacuum line but not the pressure gauge, and the pressure gauge set to zero. An amount of [^{82}Br]-bromine labelled dibromine vapour was then introduced into the manifold and the pressure noted. The single limbed counting vessel, in a liquid nitrogen bath, was opened and the [^{82}Br]-bromine labelled dibromine allowed to condense. After 60secs the vessel was closed and the pressure in the manifold noted again. The known amount of [^{82}Br]-bromine labelled dibromine was then placed in the NaI counter and a minimum of 10 individual counts taken, each in excess of 100000 counts. From the count rate and the known amount of [^{82}Br]-bromine labelled dibromine, a specific count rate could be calculated. Data for the calculation of the specific count rate of [^{82}Br]-bromine labelled dibromine are similar to that shown in section 4.3.6.

2.5.7 Neutron activation analysis.

Bromine and chlorine uptakes on both γ -alumina and montmorillonite K10 were determined using neutron activation analysis, (N.A.A.). N.A.A. is a non-destructive analytical technique based on the activation of stable isotopes to radioactive isotopes in a beam of neutrons. The identities of the isotopes formed are deduced from the energy of gamma-rays emitted from the sample. By observing the intensity of the gamma emissions with time, a count is obtained for the isotopes of interest. Since the gamma-emission spectrum was observed, self absorption was not a problem and uptakes of bromine and chlorine on γ -alumina and K10 were obtained directly from the count rate data.

If unknown samples are irradiated with samples of known bromine and chlorine content using identical flux, the quantity of bromine or chlorine present in an unknown sample can be obtained by proportion, equation 2.5.8.

$$\frac{\text{X in sample}}{\text{X in standard}} = \frac{\text{Counts from X in sample}}{\text{Counts from X in standard}} \quad \text{equation 2.5.8.}$$

(where X = Br or Cl)

Standards were selected (NH_4Br for bromine and $\text{MgCl}_2 \cdot 6\text{H}_2\text{O}$ for chlorine) to obtain an approximate quantity of bromide and chloride content, that would compare with the estimated bromide or chloride content of the sample.

The formation of the radioisotopes is governed by the first order rate laws:-

$$\text{Rate of formation} = n\sigma\phi$$

where n = number of nuclei of stable isotope
 σ = neutron capture cross section (barn)
 ϕ = irradiation flux (neutrons $\text{cm}^{-2}\text{s}^{-1}$)

$$\text{Rate of decay} = N\lambda$$

where N = number of nuclei formed
 λ = decay constant of product
 $\lambda = \ln 2/t_{1/2}$
 $t_{1/2}$ = half life of isotope formed

Overall

$$\frac{\delta N}{\delta t} = n\sigma\phi - N\lambda$$

$$N = \frac{n\sigma\phi}{(1 - e^{-\lambda t})}$$

$$\text{similarly } A = n\sigma\phi(1 - e^{-\lambda t})$$

where A = activity at the end of irradiation (Bq)

Samples were irradiated in the Scottish Universities Research Reactor, East Kilbride using the 'rabbit loop'. Weighed samples were contained in sealed plastic vials (figure 2.2.1) which were placed in the rabbit. The rabbit, shown in figure 2.5.5, consists of a cylindrical plastic container which may be transferred between the laboratory and the reactor by means of an evacuated loop. Care was taken to ensure that each were subject to an identical flux.

Typical irradiation conditions for the N.A.A. of bromine were 10secs at 300kW power (approximate neutron flux 3.6×10^{12} neutrons $\text{cm}^{-2}\text{s}^{-1}$). During irradiation ^{80}Br ($t_{1/2} = 17.4$ min), $^{80\text{m}}\text{Br}$ ($t_{1/2} = 4.4\text{h}$) and ^{82}Br ($t_{1/2} = 35.4\text{h}$) were produced by the process $^{79}\text{Br}(\text{n},\gamma)^{80}\text{Br}$, $^{79}\text{Br}(\text{n},\text{X-ray})$ and $^{81}\text{Br}(\text{n},\gamma)^{82}\text{Br}$. The [^{80}Br] and [^{82}Br] gamma-emission peaks (Table 2.5.1) of the irradiated samples were counted on a germanium-lithium counting system (ORTEC 7030) and compared with a known quantity of NH_4Br (typically 0.1mmol) as a standard at the same time.

Table 2.5.1. % Emission from radioisotopes of bromine.

<u>Energy (keV)</u>	<u>Isotope</u>	<u>% emission</u>
554	[^{82}Br]	80
617	[^{80}Br]	-
619	[^{82}Br]	50
666	[^{80}Br]	-
698	[^{82}Br]	33
776	[^{82}Br]	100
827	[^{82}Br]	30

Typical irradiation conditions for the N.A.A. of chlorine were 25secs at 300kW power. During irradiation ^{38}Cl ($t_{1/2} = 37.3$ min) was produced by the process $^{37}\text{Cl}(\text{n},\gamma)^{38}\text{Cl}$. The ^{38}Cl gamma-emission peak (1642 keV) of irradiated samples was counted on the ORTEC 7030 and compared with a known quantity of $\text{MgCl}_2 \cdot 6\text{H}_2\text{O}$ (typically 0.1mmol) as a standard at the same time.

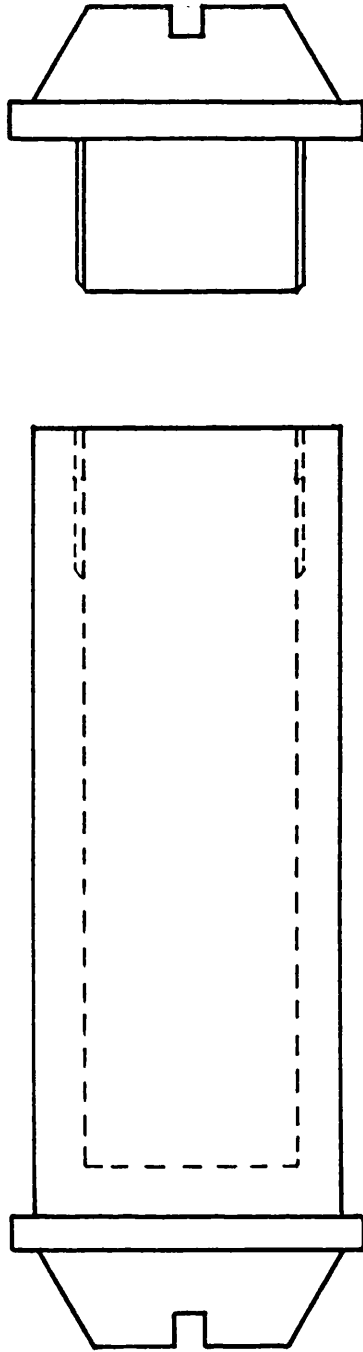


Figure 2.5.5. 'Rabbit' used in neutron activation analysis.

2.6 ^{27}Al -MAS-NMR.

The ^{27}Al magic angle spinning nuclear magnetic resonance spectroscopy investigation was carried out at the Industrial Research Laboratories of the University of Durham, using a Varian UXR-300/89 NMR spectrometer. This instrument is dedicated to solid-state NMR work and is equipped with a 7.0 Tesla superconducting magnet with 89mm vertical bore. It operates at 300 MHz for ^1H and at 78.152 MHz for ^{27}Al nuclei. The MAS-NMR spectrum was obtained using a pulse width of 15 degrees and decoupling the protons. Typically 1 μsec pulses were used with between 2000-4000 repetitions. The spectra were obtained using a probe which was aluminium free and gave no background signal. Chemical shifts were recorded, with aluminium(III) chloride serving as the external standard. Samples were contained in a 300 microlitre(μl) zirconia tube. The response of the samples under a single-pulse excitation combined with magic-angle spinning at between 10.8-12.8 KHz was used to obtain time domain data which were Fourier transformed for frequency domain information.

CHAPTER 3

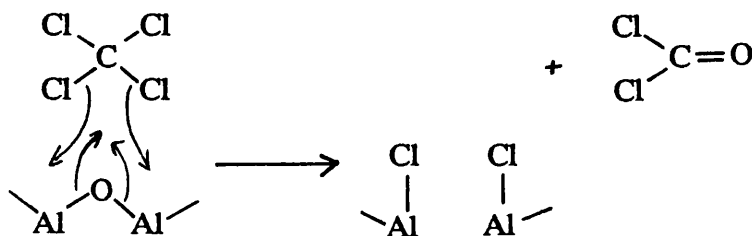
Reaction of Halomethanes with γ -Alumina and Montmorillonite K10.

3.1 Introduction.

As discussed in chapter 1, fluorination or chlorination of γ -alumina results in the promotion of acidity on the surface. In both cases the nature of the surface obtained depends on the reagent used. Fluorination of γ -alumina using SF_4 leads to the formation of strong Lewis acid sites which are capable of dehydrochlorinating CH_3CCl_3 at room temperature [44]; other covalent fluorides, for example BF_3 [45] or F_2CO [56] result in the enhanced Brønsted acidity as judged by the type of reactions catalysed. Chlorination of γ -alumina with anhydrous HCl at room temperature produces enhanced Brønsted acidity, whereas reactions between γ -alumina and CCl_4 or Cl_2CO at 523K [47,49] result in the formation of both Brønsted and Lewis sites, the latter catalysing CH_3CCl_3 dehydrochlorination [47]. Using the radiotracer chlorine-36, it has been shown that the type of site can be differentiated, since chlorine associated with Brønsted sites is labile with respect to ^{36}Cl exchange with H^{36}Cl at room temperature, whereas chlorine associated with Lewis sites is inert to exchange with H^{36}Cl [49].

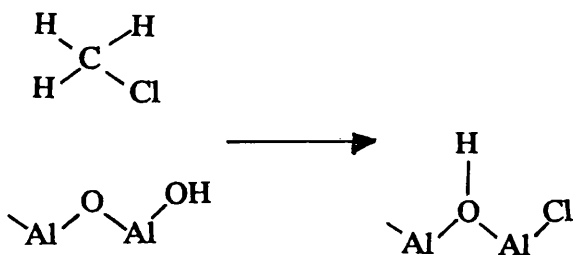
The original objective of the work described in this chapter was to prepare brominated γ -alumina with enhanced surface Lewis acidity. As bromine is less electronegative than both fluorine and chlorine little, or no work appears to have been reported concerning the effects of bromination on a γ -alumina surface. However, such a study affords the opportunity of testing postulates made about the nature of surface halogenated sites. The previous studies made of γ -alumina suggest that chlorinating

reagents bearing an even number of Cl atoms enhance Lewis acidity, so replacement of an in-plane O atom of γ -alumina (figure 1.9.2) requires a concerted reaction, scheme 3.1.1.



Scheme 3.1.1. Replacement of an in-plane O atom of γ -alumina with chlorine.

Reactions involving reagents with an odd number of Cl atoms leads to replacement of Al-OH(ter) groups and dissociative addition of HCl, with the formation of Brønsted sites scheme 3.1.2.



Scheme 3.1.2. Interaction of halomethane, with an odd number of halogen atoms, with γ -alumina.

It should be noted, however, that this apparently clear cut situation does not apply to F_2CO which appears to behave simply as an HF precursor.

The reagent chosen for bromination was CH_2Br_2 since it contains two bromine atoms and is a reagent manufactured by the collaborating body (The Associated Octel Company Ltd). The substrates were Degussa 'C' γ -alumina, chlorinated γ -alumina and acidified montmorillonite; the latter material was chosen because it is established that γ -alumina chlorinated with Cl_2CO is more acidic than γ -alumina and montmorillonite K10 has been widely used in recent work where an acidic surface is required [57-69]. It would be expected therefore that the three materials would behave differently.

The products obtained from reactions that were performed initially suggested that dismutation of CH_2Br_2 might occur, therefore another potential brominating agent CHBr_3 and the potential bromochlorinating agent CH_2BrCl were also examined. It has been shown, chapter 5, that chlorine present at the impurity level in Degussa 'C' γ -alumina is displaced when dibromine is allowed to react with the material. The possibility therefore exists that similar behaviour may occur when chlorinated oxides, γ -alumina and montmorillonite K10 are brominated using other reagents. The use of CH_2ClBr offers the possibility of examining chlorination and bromination of γ -alumina under competitive conditions, in order to throw further light on what appears at first sight to be an unexpected 'reverse' halogen exchange process.

3.2 Experimental.

3.2.1 Reaction of dibromomethane with Degussa 'C' γ -alumina.

Calcined Degussa 'C' γ -alumina (0.8g) was loaded, in the dry box, into a Monel bomb. The bomb was transferred to a vacuum line and the contents degassed. The bomb was cooled to 77K and dibromomethane (60mmol) was condensed into the bomb, which was placed in an electrical furnace. The contents of the bomb were then heated at 523K for 120h. The bomb was allowed to cool to room temperature. The gaseous material from the bomb was expanded into a manifold containing a gas cell to give a pressure of 50 Torr, and a gas phase FTIR spectrum obtained. The contents of the bomb were degassed and transferred to the dry box, where the alumina was transferred to a storage vessel. A sample of brominated alumina (0.0159g) was loaded, in the dry box, into a polythene ampoule which was then sealed. The ampoule was transferred to the SURRC at East Kilbride for neutron activation analysis (section 2.5.7).

Calcined γ -alumina (approx 0.2g) treated with dibromomethane at 523K for 120h was loaded into a holder (figure 2.3.3) and transferred into the DRIFTS cell; a spectrum was obtained, under atmospheric conditions, using 50 scans. The procedure for the investigation of the Lewis acidity of γ -alumina treated with dibromomethane was to load 1,1,1-trichloroethane (50 Torr) into a gas IR cell (figure 2.3.1) attached to a degassed vessel containing brominated alumina. An FTIR spectrum was then obtained for the 1,1,1-trichloroethane. The brominated alumina was introduced to the gas cell and a spectrum of the reaction mixture taken immediately. Spectra were recorded every 10 minutes for the next hour.

3.2.2 Reaction of bromochloromethane with Degussa 'C' γ -alumina.

The experimental procedure for the interaction of bromochloromethane with calcined γ -alumina at 523K is the same as that described for the interaction of dibromomethane with calcined γ -alumina (section 3.2.1). Two samples of the halogenated alumina (0.0113g for bromine analysis and 0.0299g for chlorine analysis) were loaded, in the dry box, into polythene ampoules for neutron activation analysis.

3.2.3 Reaction of bromoform with Degussa 'C' γ -alumina.

Calcined Degussa 'C' γ -alumina (0.8g) was loaded into the Monel reaction vessel. The vessel was transferred to a vacuum line manifold, containing the bromoform storage vessel, and the contents degassed. A Dewar flask containing liquid nitrogen was then placed around the reaction vessel, cooling the vessel to 77K. The manifold was isolated from the vacuum pump and the bromoform storage vessel opened. The bromoform was allowed to condense into the reaction vessel for 10min after which time the reaction vessel was closed. An electrical furnace was then placed around the reaction vessel and the contents heated at 523K for 120h. Identification of the reaction product vapour phase and the subsequent handling and storage of the solid was the same as that described in section 3.2.1. A sample of brominated alumina (0.0274g) was loaded, in the dry box, into a polythene ampoule for neutron activation analysis.

3.2.4 Reaction of dibromomethane with Degussa 'C' γ -alumina treated carbonyl chloride.

The experimental procedure for the reaction of dibromomethane with calcined γ -alumina treated with carbonyl chloride at 523K for 12h is the same as that for the reaction of dibromomethane with γ -alumina, section 3.2.1. Two samples of the brominated/chlorinated γ -alumina (0.0400g for bromine analysis and 0.0314g for chlorine analysis) were loaded, in the dry box, into polythene ampoules for neutron activation analysis.

3.2.5 Reaction of bromochloromethane with Degussa 'C' γ -alumina treated carbonyl chloride.

The investigation involving the reaction of bromochloromethane with calcined γ -alumina, treated with carbonyl chloride at 523K for 12h, was the same as that described in section 3.2.1. Two samples of the halogenated γ -alumina were taken for neutron activation analysis (0.0279g for bromine analysis and 0.0206g for chlorine analysis).

3.2.6 Reaction of bromoform with Degussa 'C' γ -alumina treated carbonyl chloride.

The experimental procedure for the reaction of bromoform with calcined γ -alumina treated with carbonyl chloride at 523K for 12h, was the same as that for the interaction of bromoform with calcined γ -alumina, section 3.2.3. Two samples of the halogenated γ -alumina were taken for neutron activation analysis (0.0312g for bromine analysis and 0.0334g for chlorine analysis). Another sample (approx 0.4g) was loaded into a polythene

ampoule for ^{27}Al -MAS-NMR analysis.

3.2.7 Reaction of dibromomethane with calcined montmorillonite K10.

Calcined montmorillonite K10 (1.0g) was loaded into a Monel bomb in the dry box. The bomb was transferred to a vacuum line manifold containing the dibromomethane storage vessel, and the contents degassed. The bomb was then cooled to 77K allowing dibromomethane (75mmol) to be condensed in. An electrical furnace was placed around the bomb and the contents heated at 523K for 120h. On allowing to cool to room temperature, gaseous material from the bomb was expanded into a manifold containing a gas cell to give a pressure of 50 Torr, and a gas phase FTIR spectrum obtained. The contents of the bomb were then degassed and transferred to the dry box, where the montmorillonite K10 was transferred to a storage vessel. A sample of brominated montmorillonite K10 (0.0265g) was taken for neutron activation analysis (chapter 2.5.7).

3.2.8 Reaction of bromochloromethane with montmorillonite K10.

The experimental procedure for the above investigation is the same as that described for the reaction of dibromomethane with calcined montmorillonite K10, section 3.2.7. Two samples of the halogenated montmorillonite K10 were taken for neutron activation analysis (0.0445g for bromine analysis and 0.0396g for chlorine analysis).

3.2.9 Reaction of bromoform with montmorillonite K10.

Calcined montmorillonite K10 (1.0g) was loaded into the Monel reaction vessel. The vessel was transferred to a vacuum line manifold, containing the bromoform storage vessel, and the contents degassed. A Dewar flask containing liquid nitrogen was then placed around the reaction vessel, cooling the vessel to 77K. The manifold was isolated from the vacuum pump and the bromoform storage vessel opened. The bromoform was allowed to condense into the reaction vessel for 10min after which time the reaction vessel was closed. An electrical furnace was then placed around the reaction vessel and the contents heated at 523K for 120h. The identification of the reaction product vapour phase and subsequent storage and handling of the halogenated solid was the same as that for the reaction of bromoform with calcined montmorillonite K10. A sample of the halogenated montmorillonite K10 (0.0292g) was loaded, in the dry box, into a polythene ampoule for neutron activation analysis.

3.2.10 Reaction of dibromomethane with montmorillonite K10 treated carbonyl chloride.

The investigation involving the reaction of dibromomethane with calcined montmorillonite K10 treated with carbonyl chloride at 523K for 12h, was the same as that described in section 3.2.7. Two samples of the brominated/chlorinated montmorillonite K10 were taken for neutron activation analysis (0.0250g for bromine analysis and 0.0280g for chlorine analysis).

3.2.11 Reaction of bromochloromethane with montmorillonite K10 treated carbonyl chloride..

The experimental procedure for the reaction of bromochloromethane with calcined montmorillonite K10 treated with carbonyl chloride at 523K for 12h, is the same as that described in section 3.2.7. Two samples of the halogenated montmorillonite K10 were taken for neutron activation analysis (0.0341g for bromine analysis and 0.0237g for chlorine analysis).

3.2.12 Reaction of bromoform with montmorillonite K10 treated carbonyl chloride.

The experimental procedure for the reaction of bromoform with calcined montmorillonite K10 treated with carbonyl chloride at 523K for 12h, is the same as that for the reaction of bromoform with calcined montmorillonite K10, section 3.2.9. Two samples of the halogenated montmorillonite K10 were taken for neutron activation analysis (0.0339g for bromine analysis and 0.0472g for chlorine analysis). Another sample (approx 0.4g) was loaded into a polythene ampoule for ^{27}Al -MAS-NMR analysis.

3.3 Results.

3.3.1 Reaction of dibromomethane with Degussa 'C' γ -alumina.

The products from the reaction of dibromomethane with calcined γ -alumina were identified using an FTIR spectrometer. The experiments were carried out at 523K for between 48 and 120h. The infrared peak assignments for the products identified are tabulated below (table 3.3.1(a)).

Table 3.3.1(a) Peak assignments for the volatile reaction products from the interaction of dibromomethane with calcined γ -alumina.

Band (cm ⁻¹)	Assignment	Compound
2986-2960	C-H(str)	CH ₃ Br & CH ₂ Br ₂
2700-2400	H-Br(str)	HBr
2240-2040	C-O(str)	CO
1320-1294	C-H(def)	CH ₃ Br
1200	C-H(def)	CH ₂ Br ₂ (*)
650	C-Br(str)	CH ₂ Br ₂ (*)
620	C-Br(str)	CH ₃ Br

(* starting material)

The relative intensities of the peaks in table 3.3.1(b) were estimated from % transmittance. All spectra were measured in the gas phase at a pressure of 50 Torr.

Table 3.3.1(b) A comparison of relative peak intensities observed in the vapour phase products.

Bands	48 hours	96 hours	120 hours
2700-2400cm ⁻¹	6	9	14
2240-2040cm ⁻¹	5	11	16
1320-1294cm ⁻¹	24	41	49
1200cm ⁻¹	60	72	58
650cm ⁻¹	87	88	72
620cm ⁻¹	36	36	48

Neutron activation analysis carried out on the γ -alumina after the 120 hour reaction indicated the quantity of bromine present to be 0.8mg atom Br g⁻¹ (table 3.3.1(c)). The DRIFT spectrum obtained of the γ -alumina after the interaction with dibromomethane, at 523K for 120h, showed an absorption band at 1625cm⁻¹ corresponding to γ -alumina. Bands were also observed at 3000-2875cm⁻¹, 1460cm⁻¹ and 1380cm⁻¹ corresponding to a carbonaceous laydown on the surface of the solid (figure 3.3.1). On the introduction of 1,1,1 trichloroethane to the brominated γ -alumina the IR spectrum of the volatile materials showed only bands due to the presence of 1,1,1 trichloroethane. After 90min no evidence was observed for the formation of 1,1 dichloroethene (dehydrochlorination product of 1,1,1 trichloroethane), indicating that no strong Lewis acid sites had been generated on the γ -alumina surface.

Table 33.1(c) Halogen contents of solid supports, obtained by neutron activation analysis.

Support	Halogenating reagent	Element analysed	ppm	mg atom g⁻¹	% Error
γ -alumina	dibromomethane	Br	6.2	0.8	6.8
γ -alumina	tribromomethane	Br	4.3	0.5	5.7
γ -alumina	bromochloromethane	Br	0.8	0.1	9.0
γ -alumina	bromochloromethane	Cl	2.9	0.8	5.8
γ -alumina	hydrogen bromide	Br	2.4	0.3	6.7
γ -alumina	HBr + but-1-ene	Br	6.3	0.8	5.6
Cl-alumina	dibromomethane	Br	8.0	1.0	5.2
Cl-alumina	dibromomethane	Cl	5.4	1.5	3.2
Cl-alumina	tribromomethane	Br	2.2	0.3	10.5
Cl-alumina	tribromomethane	Cl	14.7	4.1	2.3
Cl-alumina	bromochloromethane	Br	3.0	0.4	8.1
Cl-alumina	bromochloromethane	Cl	2.6	0.7	4.9
K10	carbonyl chloride	Cl	25.0	7.1	2.0
K10	dibromomethane	Br	9.9	1.2	5.3
K10	tribromomethane	Br	2.3	0.3	5.2
K10	bromochloromethane	Br	4.3	0.5	7.1
K10	bromochloromethane	Cl	1.8	0.5	5.4
Cl-K10	dibromomethane	Br	10.0	1.2	5.2
Cl-K10	dibromomethane	Cl	2.5	0.7	4.9
Cl-K10	tribromomethane	Br	11.0	1.4	4.9
Cl-K10	tribromomethane	Cl	16.8	4.8	2.2
Cl-K10	bromochloromethane	Br	4.6	0.6	9.0
Cl-K10	bromochloromethane	Cl	8.4	2.4	2.7

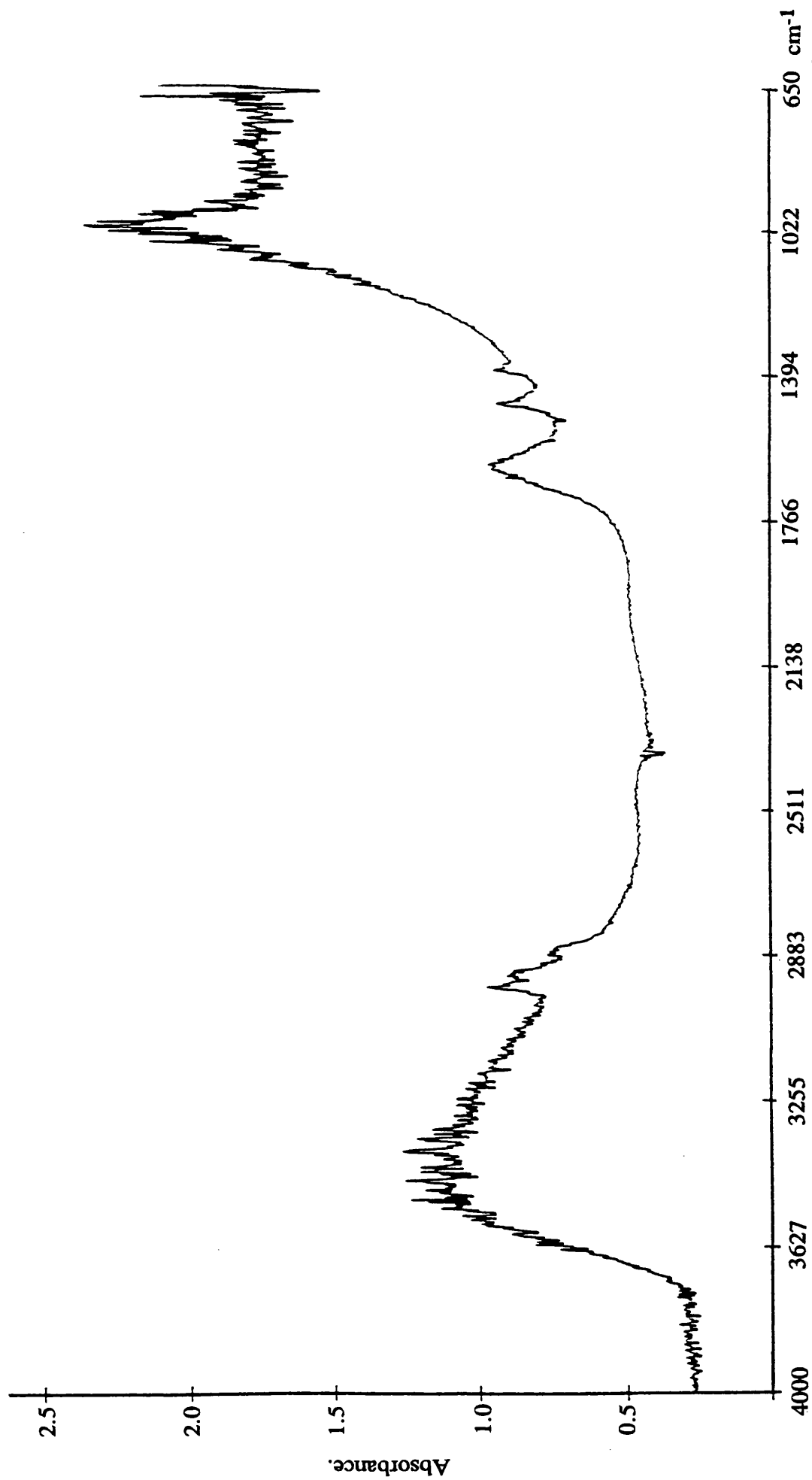


Figure 3.3.1. DRIFT spectrum of calcined γ -alumina treated with dibromomethane.

3.3.2 Reaction of bromochloromethane with Degussa 'C' γ -alumina.

Bromochloromethane was allowed to heat at 523K in the presence of γ -alumina for 5 days, after which time it was allowed to cool to room temperature. An infrared spectrum was obtained of the vapour phase reaction product mixture and the results are tabulated below (table 3.3.2).

Table 3.3.2. Peak assignments for the volatile reaction products from the interaction of bromochloromethane with calcined γ -alumina.

Band (cm^{-1})	Assignment	Compound
3100-2700	HCl(str)	HCl
2700-2400	HBr(str)	HBr
2240-2040	CO(str)	CO
1294	C-H(def)	CH ₃ Br
1239	C-H(def)	CH ₂ ClBr (*)
1225	C-H(def)	CH ₂ ClBr (*)
1200	C-H(def)	CH ₂ Br ₂
740	C-Cl(str)	CH ₂ ClBr (*)
650	C-Br(str)	CH ₂ Br ₂
621	C-Br(str)	CH ₃ Br
610	C-Br(str)	CH ₂ ClBr (*)

(* starting material)

These results reveal the formation of dibromomethane and methyl bromide from the chlorobromomethane but not their chlorine analogues, dichloromethane and methyl chloride. The formation of the other reaction products; carbon monoxide, hydrogen bromide and hydrogen chloride was expected, as similar reaction products were observed after the interaction of dibromomethane with calcined γ -alumina. Neutron activation analysis of the halogenated γ -alumina indicated the quantity of bromine present to be 0.1mg atom Br g⁻¹ and of chlorine to be 0.8mg atom Cl g⁻¹ (table 3.3.1(c)).

3.3.3 Reaction of bromoform with Degussa 'C' γ -alumina.

Bromoform was allowed to heat at 523K in the presence of γ -alumina for 5 days, after which time it was allowed to cool to room temperature. An infrared spectrum was obtained of the reaction product mixture in the vapour phase and the results are tabulated below (table 3.3.3).

Table 3.3.3. Peak assignments for the volatile reaction products from the interaction of bromoform with calcined γ -alumina.

Band (cm ⁻¹)	Assignment	Compound
3130-2880	C-H(str)	CH ₄
2240-2040	CO(str)	CO
1200	C-H(def)	CH ₂ Br ₂
1148	C-H(def)	CHBr ₃ (*)
668	C-Br(str)	CHBr ₃ (*)
650	C-Br(str)	CH ₂ Br ₂

(* starting material)

Neutron activation analysis of the halogenated γ -alumina indicated the quantity of bromine present to be 0.5mg atom Br g⁻¹ (table 33.(c)).

3.3.4 Reaction of dibromomethane with Degussa 'C' γ -alumina treated with carbonyl chloride.

Dibromomethane was allowed to heat at 523K in the presence of chlorinated γ -alumina for 5 days, after which time it was allowed to cool to room temperature. An infrared spectrum was obtained of the reaction product mixture in the vapour phase and the results are tabulated below (table 3.3.4).

Table 3.3.4. Peak assignments for the volatile reaction products from the interaction of dibromomethane with chlorinated γ -alumina.

Band (cm^{-1})	Assignment	Compound
3100-2700	HCl(str)	HCl
2700-2400	HBr(str)	HBr
2240-2040	CO(str)	CO

Unlike the previous experiments, reaction of dibromomethane with chlorinated γ -alumina, showed no evidence for the presence of dibromomethane (the brominating reagent) or any other halomethanes in the reaction product vapour phase. Neutron activation analysis of the halogenated γ -alumina indicated the quantity of bromine present to be 1.0mg atom Br g^{-1} and of chlorine to be 1.5mg atom Cl g^{-1} (table 3.3.4).

3.3.5 Reaction of bromochloromethane with Degussa 'C' γ -alumina treated with carbonyl chloride.

The infrared analysis of the volatile products after a 120h exposure, at 523K, of bromochloromethane to a sample of calcined γ -alumina treated with carbonyl chloride at 523K for 12h, indicated absorbances due to the formation of hydrogen chloride, hydrogen bromide, carbon monoxide and dibromomethane (table 3.3.5). Neutron activation analysis, carried out on the γ -alumina after the reaction, indicated the quantity of bromine and chlorine present to be 0.4 and 0.7mg atom g^{-1} respectively (table 3.3.5(c)).

Table 3.3.5. Peak assignments for the volatile reaction products from the interaction of bromochloromethane with chlorinated γ -alumina.

Band (cm^{-1})	Assignment	Compound
3100-2700	HCl(str)	HCl
2700-2400	HBr(str)	HBr
2240-2040	CO(str)	CO
1239	C-H(def)	CH ₂ ClBr (*)
1225	C-H(def)	CH ₂ ClBr (*)
1200	C-H(def)	CH ₂ Br ₂
740	C-Cl(str)	CH ₂ ClBr (*)
650	C-Br(str)	CH ₂ Br ₂
610	C-Br(str)	CH ₂ ClBr (*)

(* starting material)

3.3.6 Reaction of bromoform with Degussa 'C' γ -alumina treated with carbonyl chloride.

The infrared analysis of the volatile products after a 120h exposure, at 523K, of bromoform to a sample of calcined γ -alumina treated with carbonyl chloride at 523K for 12h, indicated absorbances due to the formation of hydrogen chloride and carbon monoxide (table 3.3.6). Neutron activation analysis, carried out on the γ -alumina after the reaction, indicated that the bromine content (0.3mg atom Br g⁻¹) was significantly less than the chlorine content (4.1mg atom Cl g⁻¹), table 3.3.1(c).

Table 3.3.6. Peak assignments for the volatile reaction products from the interaction of bromoform with chlorinated γ -alumina.

Band (cm ⁻¹)	Assignment	Compound
3100-2700	HCl(str)	HCl
2240-2040	CO(str)	CO
1148	C-H(def)	CHBr ₃ (*)
668	C-Br(str)	CHBr ₃ (*)

(* starting material)

In the ²⁷Al-MAS NMR spectrum of the halogenated γ -alumina, figure 3.3.2, the two signals observed were due to an octahedral aluminium environment, 4.4 ppm, and a tetrahedral aluminium environment, 52.2 ppm. These chemical shifts were with reference to AlCl₃.

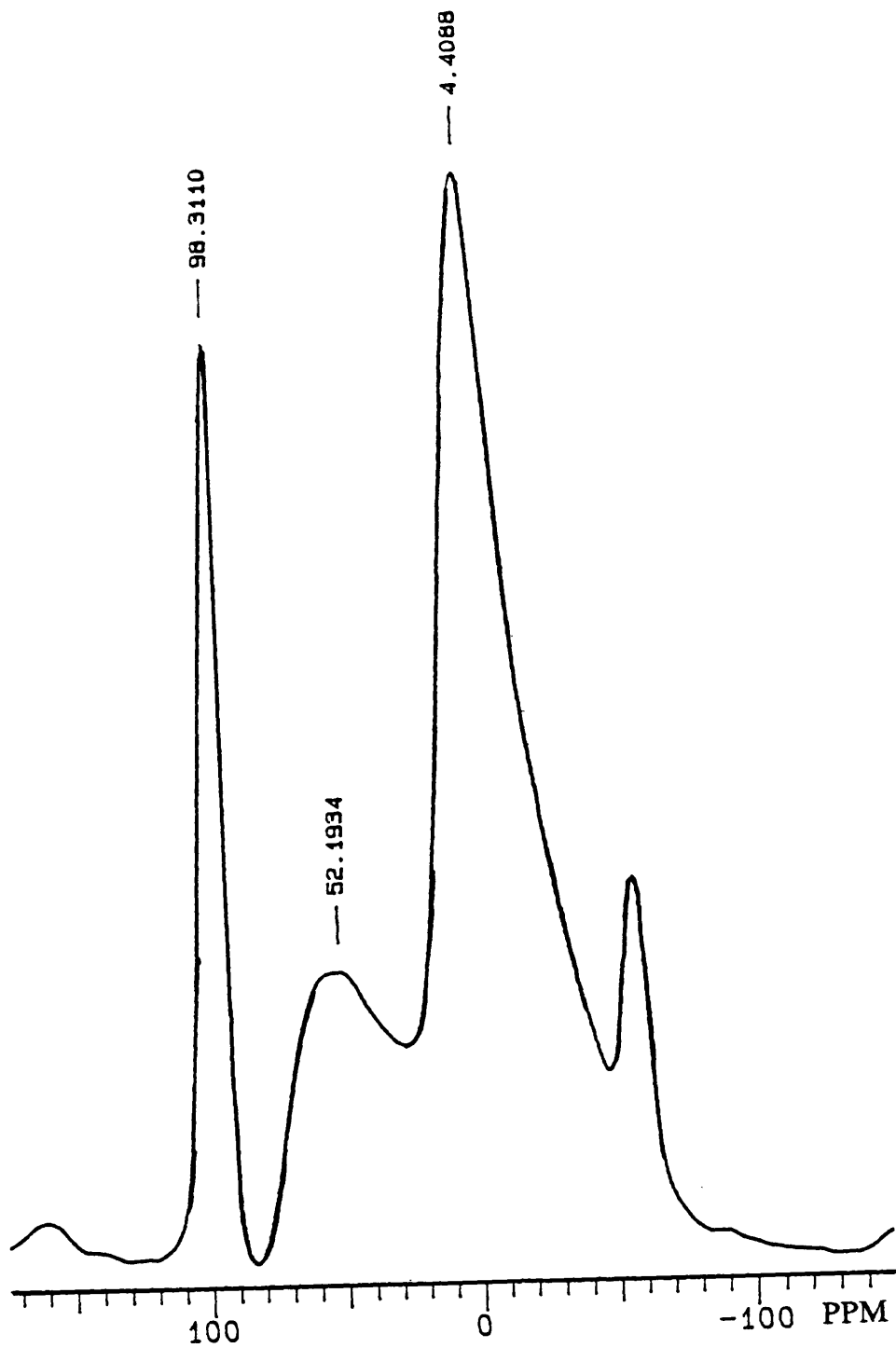


Figure 3.3.2. ^{27}Al MAS NMR spectrum of brominated/chlorinated γ -alumina

3.3.7 Reaction of dibromomethane with montmorillonite K10.

The infrared analysis of the volatile products after a 120h exposure, at 523K, of dibromomethane to a sample of calcined montmorillonite K10, indicated absorbances due to the formation of hydrogen bromide and carbon monoxide (table 3.3.7). Neutron activation analysis, carried out on the montmorillonite K10 after the reaction, indicated a bromine content (1.2mg atom Br g⁻¹), table 3.3.1(c), much greater than that observed in the dibromomethane/ γ -alumina experiment.

Table 3.3.7. Peak assignments for the volatile reaction products from the interaction of dibromomethane with calcined montmorillonite K10.

Band (cm ⁻¹)	Assignment	Compound
2700-2400	H-Br(str)	HBr
2240-2040	C-O(str)	CO
1200	C-H(def)	CH ₂ Br ₂ (*)
650	C-Br(str)	CH ₂ Br ₂ (*)

(* starting material)

3.3.8 Reaction of bromochloromethane with montmorillonite K10.

The infrared analysis of the volatile products after a 120h exposure, at 523K, of bromochloromethane to a sample of calcined montmorillonite K10, indicated absorbances due to formation of the dismutation products dibromomethane and dichloromethane and also due to the formation of hydrogen chloride, hydrogen bromide and carbon monoxide (table 3.3.8). Neutron activation analysis carried out on the montmorillonite K10 after the reaction, indicated similar bromine and chlorine contents (both 0.5mg atom g^{-1}), table 3.3.1(c). These results differ once again from the comparable γ -alumina experiment which resulted in preferential chlorination of the solid.

Table 3.3.8. Peak assignments for the volatile reaction products from the interaction of bromochloromethane with calcined montmorillonite K10.

Band (cm^{-1})	Assignment	Compound
3100-2700	HCl(str)	HCl
2700-2400	HBr(str)	HBr
2240-2040	CO(str)	CO
1275	C-H(def)	CH_2Cl_2
1261	C-H(def)	CH_2Cl_2
1239	C-H(def)	CH_2ClBr (*)
1225	C-H(def)	CH_2ClBr (*)
1200	C-H(def)	CH_2Br_2
740	C-Cl(str)	CH_2ClBr (*)
650	C-Br(str)	CH_2Br_2
610	C-Br(str)	CH_2ClBr (*)

(* starting material)

3.3.9 Reaction of bromoform with montmorillonite K10.

The infrared analysis of the volatile products after a 120h exposure, at 523K, of bromoform to a sample of calcined montmorillonite K10, indicated absorbances due to formation of hydrogen chloride, hydrogen bromide and carbon monoxide (table 3.3.9). There was no evidence for the presence of the brominating reagent bromoform, or any other halomethanes. Data obtained from neutron activation analysis of the montmorillonite after the reaction indicated the presence of only a small amount of bromine (0.3mg atom Br g⁻¹), table 3.3.1(c)

Table 3.3.9. Peak assignments for the volatile reaction products from the interaction of bromoform with calcined montmorillonite K10.

Band (cm ⁻¹)	Assignment	Compound
3100-2700	HCl(str)	HCl
2700-2400	HBr(str)	HBr
2240-2040	CO(str)	CO

3.3.10 Reaction of dibromomethane with montmorillonite K10 treated with carbonyl chloride.

The infrared analysis of the volatile products after a 120h exposure, at 523K, of dibromomethane to a sample of calcined montmorillonite K10 treated with carbonyl chloride at 523K for 12h, showed absorbances due to formation of bromochloromethane, hydrogen chloride, hydrogen bromide and carbon monoxide (table 3.3.10). Data obtained

from neutron activation analysis of the montmorillonite K10, after the reaction, indicated a bromine content ($1.25\text{mg atom Br g}^{-1}$) almost twice that of the chlorine ($0.7\text{mg atom Br g}^{-1}$), table 3.3.1(c).

Table 3.3.10. Peak assignments for the volatile reaction products from the interaction of dibromomethane with chlorinated montmorillonite K10.

Band (cm^{-1})	Assignment	Compound
3100-2700	HCl(str)	HCl
2700-2400	HBr(str)	HBr
2240-2040	CO(str)	CO
1239	C-H(def)	CH_2ClBr
1225	C-H(def)	CH_2ClBr
1200	C-H(def)	CH_2Br_2 (*)
740	C-Cl(str)	CH_2ClBr
650	C-Br(str)	CH_2Br_2 (*)
610	C-Br(str)	CH_2ClBr

(* starting material)

3.3.11 Reaction of bromochloromethane with montmorillonite K10 treated with carbonyl chloride.

The infrared analysis of the volatile products after a 120h exposure, at 523K, of bromochloromethane to a sample of calcined montmorillonite K10 treated with carbonyl chloride at 523K for 12h, showed absorbances due to formation of dichloromethane, hydrogen chloride, hydrogen bromide and carbon monoxide (table 3.3.11). Neutron activation analysis, carried out on the montmorillonite K10 after the reaction, indicated a bromine content of $0.6\text{mg atom Br g}^{-1}$ and a chlorine content of $2.45\text{mg atom Cl g}^{-1}$, table 3.3.1(c).

Table 3.3.11. Peak assignments for the volatile reaction products from the interaction of bromoform with chlorinated montmorillonite K10.

Band (cm ⁻¹)	Assignment	Compound
3100-2700	HCl(str)	HCl
2700-2400	HBr(str)	HBr
2240-2040	CO(str)	CO
1275	C-H(def)	CH ₂ Cl ₂
1261	C-H(def)	CH ₂ Cl ₂
1239	C-H(def)	CH ₂ ClBr (*)
1225	C-H(def)	CH ₂ ClBr (*)
740	C-Cl(str)	CH ₂ ClBr (*)
610	C-Br(str)	CH ₂ ClBr (*)

(* starting material)

3.3.12 Reaction of bromoform with montmorillonite K10 treated with carbonyl chloride.

The infrared analysis of the volatile products after a 120h exposure, at 523K, of bromoform to a sample of calcined montmorillonite K10 treated with carbonyl chloride at 523K for 12h, showed absorbances due to formation of hydrogen chloride, hydrogen bromide, carbon dioxide and carbon monoxide (table 3.3.12). The results of neutron activation analysis, carried out on the montmorillonite K10 after the reaction, indicated much greater bromine (1.4mg atom Br g⁻¹) and chlorine (4.8mg atom Cl g⁻¹) contents than observed in previous experiments in this section. In the ²⁷Al-MAS NMR spectrum of the halogenated montmorillonite, figure 3.4.1, the two signals observed were due to an octahedral aluminium environment at -1.7 ppm, and a tetrahedral aluminium environment at 67.8 ppm. These chemical shifts were with reference to AlCl₃.

Table 3.3.12. Peak assignments for the volatile reaction products from the interaction of bromoform with chlorinated montmorillonite K10.

Band (cm ⁻¹)	Assignment	Compound
3100-2700	HCl(str)	HCl
2700-2400	HBr(str)	HBr
2400-2300	CO(str)	CO ₂
2240-2040	CO(str)	CO
668	CO(str)	CO ₂

3.4 Discussion.

3.4.1 Bromination of γ -alumina.

Dibromomethane does not react with γ -alumina to an appreciable extent below 523K and even at this temperature the reaction is slow. The products identified by IR spectroscopy after 48h reaction time at 523K were methyl bromide, hydrogen bromide and carbon monoxide. The spectroscopic features used for identification purposes are given in table 3.3.1(c). The components in the reaction mixture were identified by comparison with those of authentic samples and library spectra [72]. These products were always obtained irrespective of the reaction time used. Even after 120h the gas phase infrared spectrum of the product mixture indicated that a substantial quantity of CH₂Br₂ was still present. In view of the very slow reaction no attempt has been made to analyse quantitatively the composition of reaction product mixture but relative intensities (expressed as %

transmittance) for reactions of 48, 96 and 120h duration are given in Table 3.3.1(b). Neutron activation analysis of the solid for the 120h reaction indicated that its bromine content was 0.8mg atom g⁻¹. For comparison, chlorination of γ -alumina with Cl₂CO for 6h at 523K led to chlorine contents in the range 3–4mg atom g⁻¹[73].

The formation of CH₃Br suggested that the dismutation, equation 3.4.1, is a possibility, provided that CHBr₃ reacted further with γ -alumina. As dismutation reactions involving chlorofluorocarbons have been observed on γ -alumina [74].

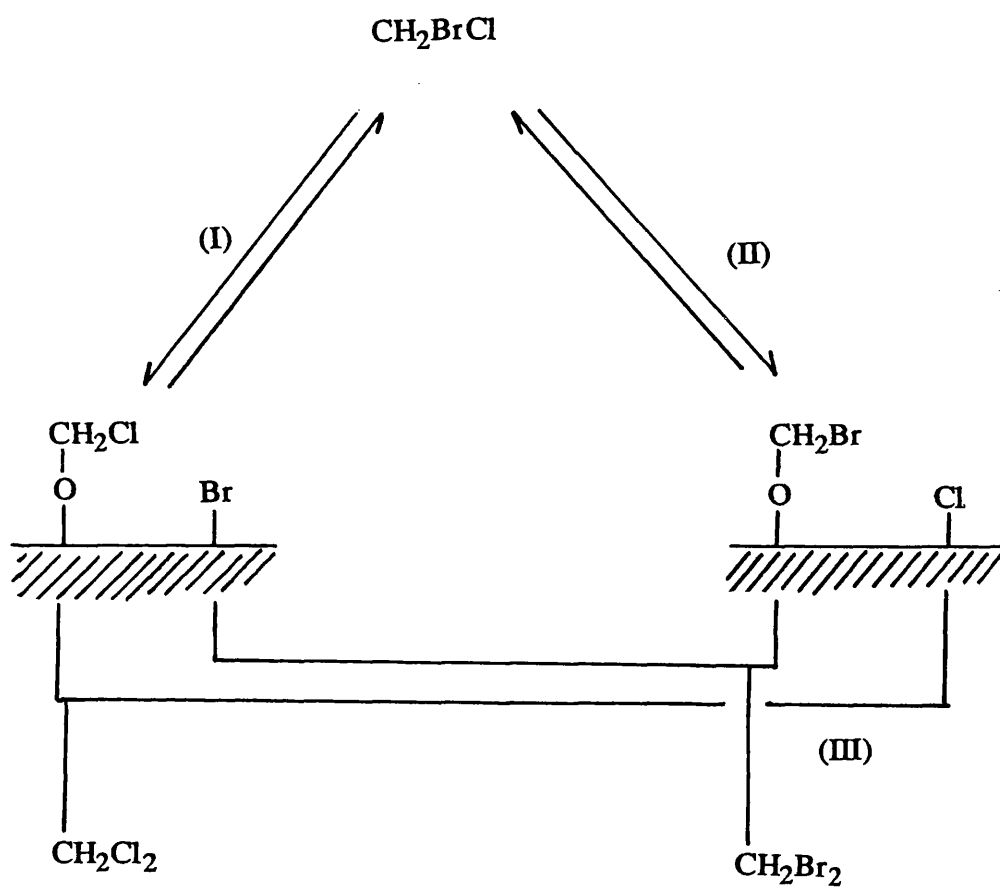


However the reaction between CHBr₃ and γ -alumina, at 523K, leads to the formation of CH₄, CO, CH₂Br₂ and unchanged CHBr₃ (table 3.3.3). Consequently, if bromination of γ -alumina with dibromomethane involves the dismutation product bromoform, equation 3.4.1, it would be expected that bromine uptake onto the γ -alumina should be greater in the bromoform reaction. The experimental results, table 3.3.(c), demonstrate that this is not the case.

A more detailed insight into the relationship between the bromination and dismutation processes is revealed by the behaviour of bromochloromethane as the brominating reagent (experiment 3.2.2). The formation of CH₂Br₂ is consistent with a dismutation reaction occurring, equation 3.4.2, but only if CH₂Cl₂ reacts further, presumably with the γ -alumina, as it is not observed in the volatile phase.



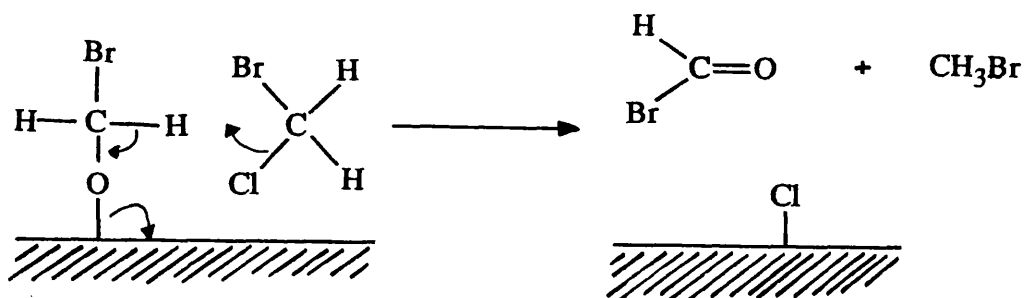
This dismutation process would occur on the surface of the γ -alumina as shown in scheme 3.4.1. In this reaction scheme bromochloromethane interacts with calcined γ -alumina to give either I) brominated γ -alumina with a CH₂Cl adsorbed species, or II) chlorinated γ -alumina with a CH₂Br adsorbed species. The interactions I) and II), as indicated, are most likely to be reversible steps. These initial type of interactions could also give rise to



Scheme 3.4.1. Interaction of bromochloromethane and solid support, with the formation of dismutation products.

the dismutation products, dichloromethane (III) and dibromomethane (IV), if the adsorbed CH_2Cl interacted with the adsorbed Cl species, and the adsorbed CH_2Br interacted with the adsorbed Br. Neutron activation analysis carried out on the γ -alumina after the interaction of bromochloromethane indicated, table 3.3.1(c), that the chlorine content is eight times that of the bromine. This contrast between the bromine and chlorine contents coincides with the lack of evidence for the presence of the chloromethanes CH_2Cl_2 and CH_3Cl in the volatile reaction product mixture, suggesting the reaction pathway for the chlorination of the γ -alumina is favoured over that for the formation of the chloromethanes.

The formation of methyl bromide implies that CH_2Br_2 and/or CH_2ClBr , which require the substitution of a halogen by a hydrogen, react with the surface of the solid, as this is the most likely source of hydrogen. A possible reaction scheme which results in the formation of methyl bromide and an increased chlorination of the surface is given in scheme 3.4.2.



Scheme 3.4.2. Possible mechanism for the formation of methyl bromide.

This interaction of bromochloromethane with $\text{CH}_2\text{Cl}_{(\text{ads})}$ or $\text{CH}_2\text{Br}_{(\text{ads})}$ leads to the formation of the reaction product methyl halide and also a HXCO species (where $\text{X} = \text{Cl}$ or Br), scheme 3.4.2. The reaction of halomethanes on γ -alumina, leading to the oxidation of the halomethane to carbon monoxide, requires the removal of an oxygen species from the γ -alumina. Recent work [75] has shown that the reaction of CH_3Cl with γ -alumina

produces CO and HCl; in the present work CH_2ClBr also forms CO and HX (where X is Cl or Br). The formation of these species appears concomitant and may be due to the decomposition of HXCO species, as work published recently [76] has shown these types of species (where X is F or Cl) are unstable.

The lack of dehydrochlorination when 1,1,1-trichloroethane is added to brominated γ -alumina, experiment 3.3.1, suggests that, unlike its chlorine analogue, brominated γ -alumina does not have sufficiently strong Lewis acid sites to perform this reaction. However, this does not mean that there is no Lewis acidity present on the brominated γ -alumina.

3.4.2 Bromination of chlorinated γ -alumina.

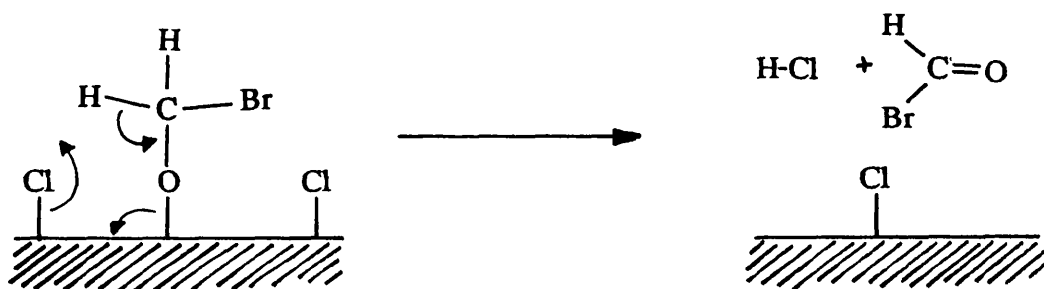
As discussed in section 3.4.1, the chlorine content of chlorinated γ -alumina is much greater than the bromine content of brominated γ -alumina. In chapter 5 it was noted that chlorine present at the impurity level in Degussa 'C' γ -alumina was displaced when dibromine was allowed to interact. A similar exchange process when a bromine containing species is reacted with chlorinated γ -alumina was investigated, as a possible route to increasing the bromine content in γ -alumina.

The reaction products from the chlorination process, described in chapter 1, include CO_2 and HCl. Since the chlorinating agent, Cl_2CO , does not contain protons itself, the formation of hydrogen chloride must involve the removal of a hydrogen species from the γ -alumina. Hence, although the chlorination process enhances Brønsted acidity, the extent of hydroxylation on the surface of the chlorinated γ -alumina must be less than that for calcined γ -alumina. The chlorination process provides several different chlorine species on the surface of alumina (figures 1.9.1-1.9.2). Radiotracer experiments [49] have shown that the dissociative adsorption of hydrogen chloride on to γ -alumina produces a labile chlorine species which can undergo exchange reactions with HCl. It is this chlorine

species that is most likely to be involved in exchange with the bromine.

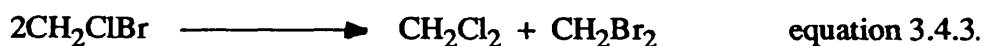
The products for the interaction of dibromomethane with chlorinated γ -alumina (experiment 3.3.4), identified by FTIR spectroscopy, were hydrogen chloride, hydrogen bromide and carbon monoxide. The formation of these hydrogen halides together with the neutron activation analysis data (bromine content 1.0mg atom g^{-1} and chlorine content 1.5mg atom g^{-1}), table 33.1(c), are indicative of bromine/chlorine exchange processes occurring on the surface of the chlorinated γ -alumina. The products identified from the reaction of bromoform with chlorinated γ -alumina were; hydrogen chloride, carbon monoxide and bromoform. Surprisingly no hydrogen bromide was identified. This deficiency of hydrogen bromide in the product vapour phase can be explained if the bromoform mechanism is different from dibromomethane mechanism. A possible mechanism for this interaction is alpha elimination, discussed in section 3.4.4, which results in the formation of CO without the production of hydrogen bromide. The hydrogen chloride observed in the product vapour phase is therefore probably evolved from the surface of the γ -alumina and not from a HClCO species. Neutron activation analysis of the γ -alumina after this experiment indicated only a small uptake of bromine onto the γ -alumina (0.3mg atom g^{-1}), with no significant reduction in chlorine content (4.1mg atom g^{-1}).

In the bromination reaction involving bromochloromethane (experiment 3.3.5) dibromomethane is observed along with hydrogen bromide, hydrogen chloride and bromochloromethane. Using scheme 3.4.2 the expected reaction products for the interaction of bromochloromethane with chlorinated γ -alumina would be dichloromethane, methyl bromide and methyl chloride. The lack of evidence for the formation of these postulated reaction products indicates that the adsorbed species on chlorinated γ -alumina reacts differently from those on calcined γ -alumina. The postulated mechanism for the formation of HXCO, scheme 3.4.2, therefore has to be modified to account for the lack of formation of methyl halides. A possible mechanism is shown in scheme 3.4.3.

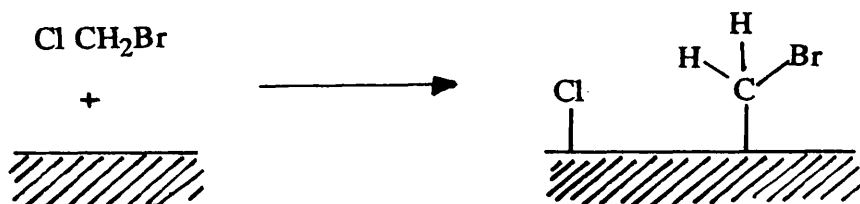


Scheme 3.4.3. Interaction of adsorbed CH_2Br species with chlorinated γ -alumina.

In this reaction scheme for the formation of HXCO on chlorinated γ -alumina, it is postulated that $\text{CH}_2\text{X}_{(\text{ads})}$ reacts with the chlorine present on the surface of the chlorinated γ -alumina. This is opposed to the reaction postulated in scheme 3.4.1, resulting in the formation of hydrogen chloride as opposed to methyl chloride. There are two possible routes for the formation of dibromomethane :- I) the chlorinated γ -alumina catalyses the dismutation process, equation 3.4.3, to give dibromomethane and dichloromethane, this route is flawed however as there is no evidence for the formation of dichloromethane,



or II) the dechlorination of bromochloromethane to give a CH_2Br intermediate, scheme 3.4.4. This intermediate then undergoes either :- a) a chlorination reaction to form the starting reagent bromochloromethane, or b) a bromination reaction to form dibromomethane. The second scheme is considered to be the most likely reaction pathway.



Scheme 3.4.4. Dechlorination of bromochloromethane on γ -alumina resulting in the formation of a CH_2Br intermediate.

The ^{27}Al MAS-NMR spectrum of brominated/chlorinated γ -alumina (experiment 3.2.2) is presented in figure 3.3.2. Two resonances were observed in the spectrum, a main broad peak at 4.4ppm, attributed to octahedral aluminium environments and a smaller resonance at 52.2ppm, with reference to AlCl_3 , attributed to tetrahedral aluminium environments. Chlorination of γ -alumina with CCl_4 [47], resulted in two resonances which are assigned to octahedral aluminium, chemical shift of 5.2ppm with reference to AlCl_3 , and tetrahedral aluminium 69.8ppm. In this work the main factor for determining nuclear shielding and hence chemical shift of the ^{27}Al was ligand substitution [77]. Ligands high in the nephelauxetic series cause greater shielding than those that have a lower nephelauxetic effect (nephelauxetic effect being the ability of a ligand to expand the valence cloud of a metal). In the nephelauxetic series shielding of the aluminium(III) increases down the halogen group. With the brominated/chlorinated γ -alumina both the octahedral and tetrahedral aluminium resonances have chemical shifts upfield from the comparable signals obtained from the chlorinated material. This movement in the chemical shift is indicative of increased shielding which the nephelauxetic series predicts if the aluminium is brominated.

3.4.3 Halogenation of montmorillonite K10.

The vapour phase reaction products from chlorination of montmorillonite K10, using carbonyl chloride, were the same, when analysed by FTIR, as those identified from the chlorination of γ -alumina, namely carbon monoxide, carbon dioxide, hydrogen chloride and unreacted carbonyl chloride. There was however an extra absorption band observed at 621cm^{-1} (figure 3.4.4), which was not observed in the chlorination of γ -alumina and has been assigned to V_3 (F_2 fundamental) of SiCl_4 [78]. NAA data from the chlorinated montmorillonite K10 indicated (table 33.1(c)) a chlorine content of 7.1mg atom g^{-1} , double that of chlorinated γ -alumina [73]. Studies using pyridine as a probe molecule, chapter 6, and [^{82}Br] radiotracer studies, chapter 4, have indicated an increase in the acidity of montmorillonite K10 after chlorination.

The ^{27}Al MAS-NMR spectrum of calcined montmorillonite K10 is presented in figure 3.4.2. Two resonances are observed in this spectrum, a main peak at -1.2ppm , attributed to octahedral aluminium environments and a smaller broad resonance at 67.2ppm , with reference to AlCl_3 , attributed to tetrahedral aluminium environments [79-81]. On chlorination of montmorillonite K10, the aluminium_(tet) resonance shifts 0.6ppm downfield with reference to calcined montmorillonite K10, figure 3.4.3, whereas the aluminium_(oct) resonance remains unchanged. The small movement in the chemical shift is not of great significance as the aluminium_(oct) has a broad resonance signal covering several ppm, limiting the precision with which the chemical shift may be measured. The ^{27}Al MAS NMR spectrum of brominated/chlorinated montmorillonite K10, experiment 3.2.12, is presented in figure 3.4.1. This spectrum indicates a movement upfield in the chemical shift in the aluminium_(oct) resonance signal of 0.5ppm . This movement in chemical shift is of greater significance than that of the aluminium_(tet) resonance, as this resonance has a stronger sharper signal resulting in greater precision with which the chemical shift may be measured. The movement in chemical shift of the aluminium_(oct) resonance signal is due to increased shielding of the aluminium which the nephelauxetic series predicts if the chlorinated aluminium in the montmorillonite K10 is then brominated.

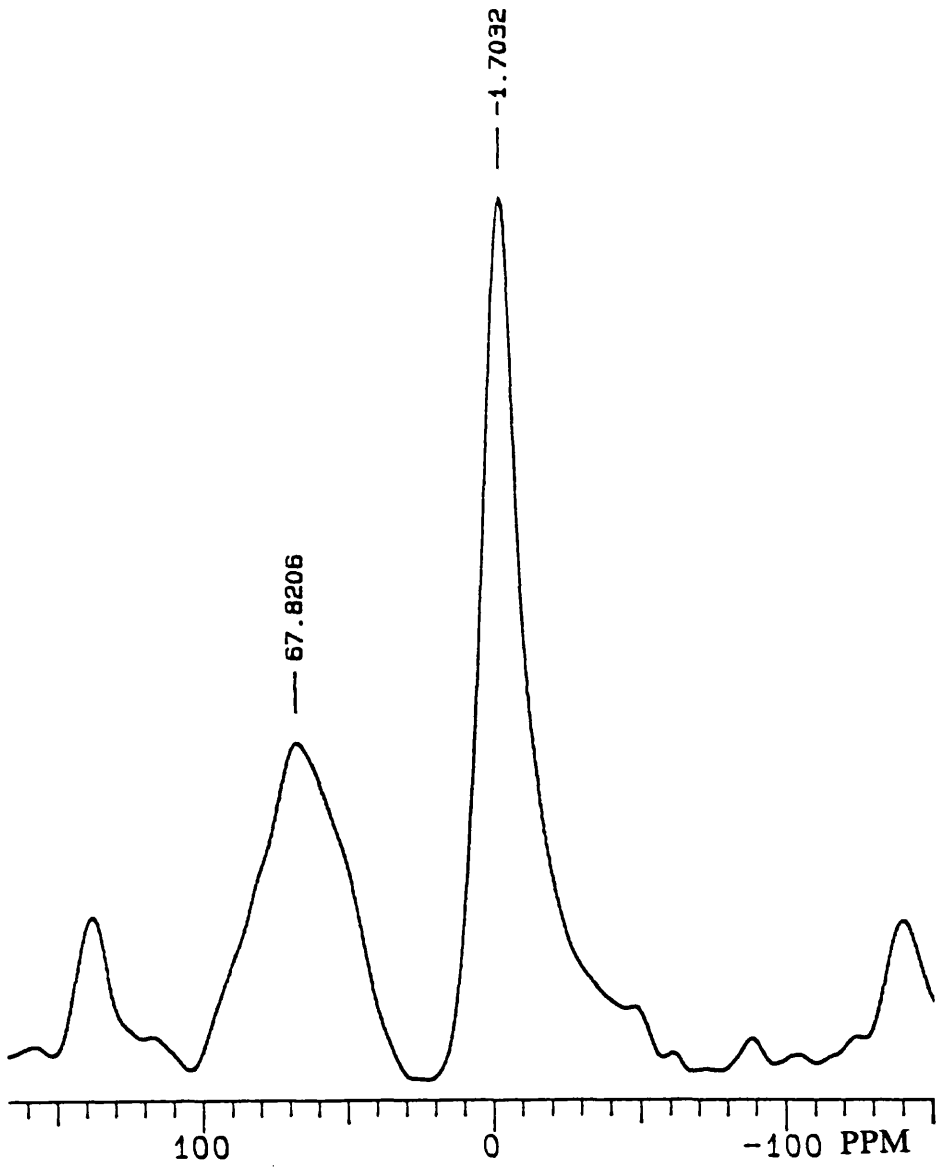


Figure 3.4.1. ^{27}Al MAS NMR spectrum of chlorinated montmorillonite K10 treated with bromoform.

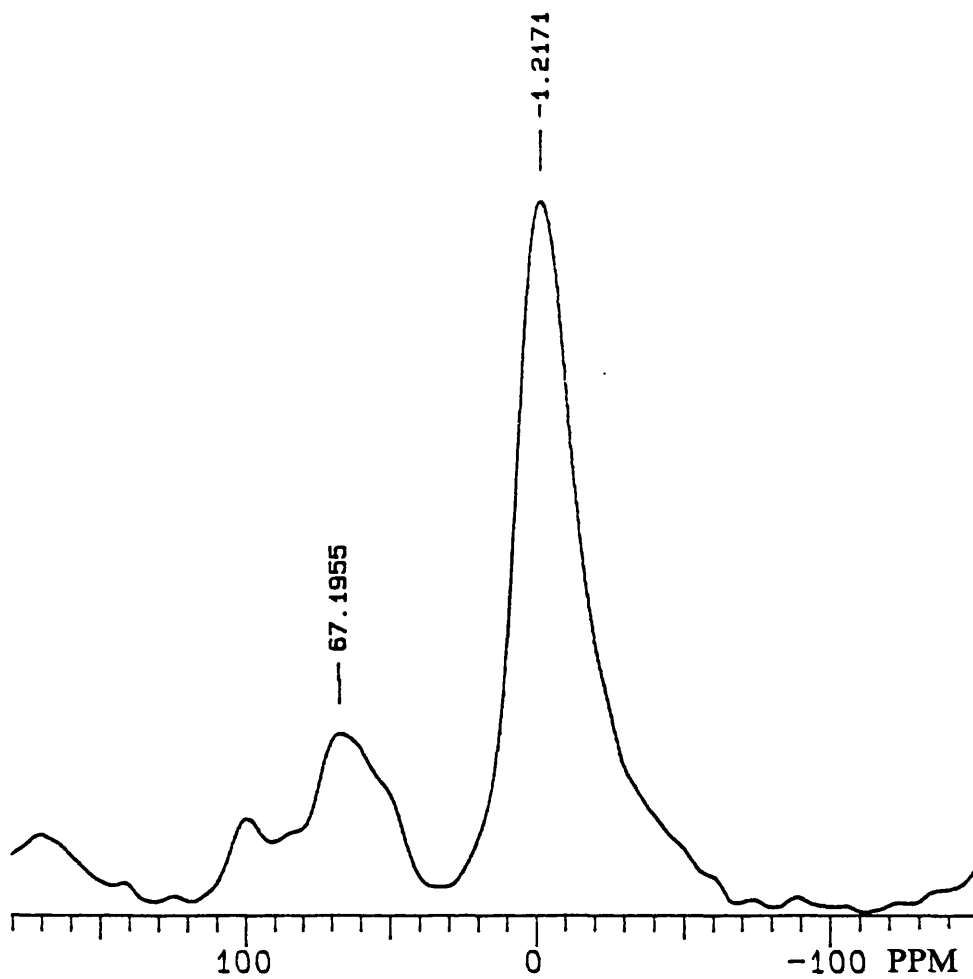


Figure 3.4.2. ^{27}Al MAS NMR spectrum of calcined montmorillonite K10.

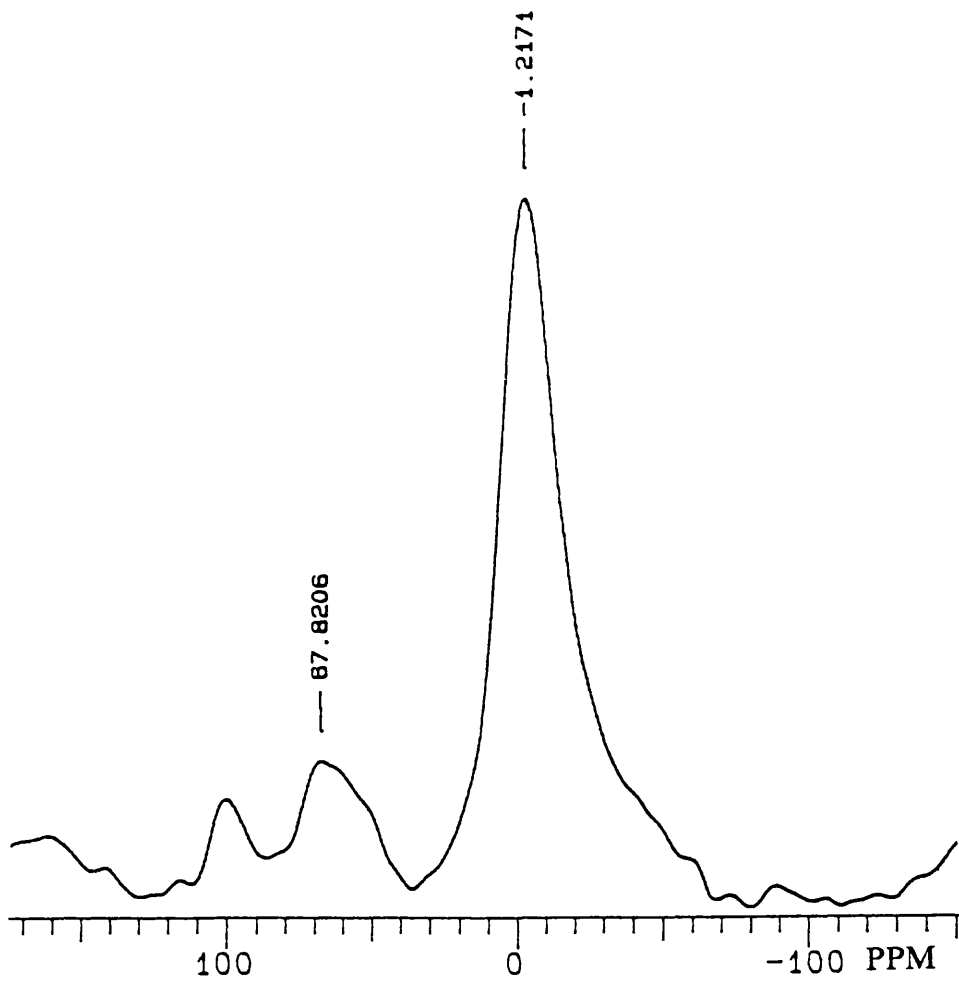


Figure 3.4.3. ^{27}Al MAS NMR spectrum of calcined montmorillonite K10 treated with carbonyl chloride.

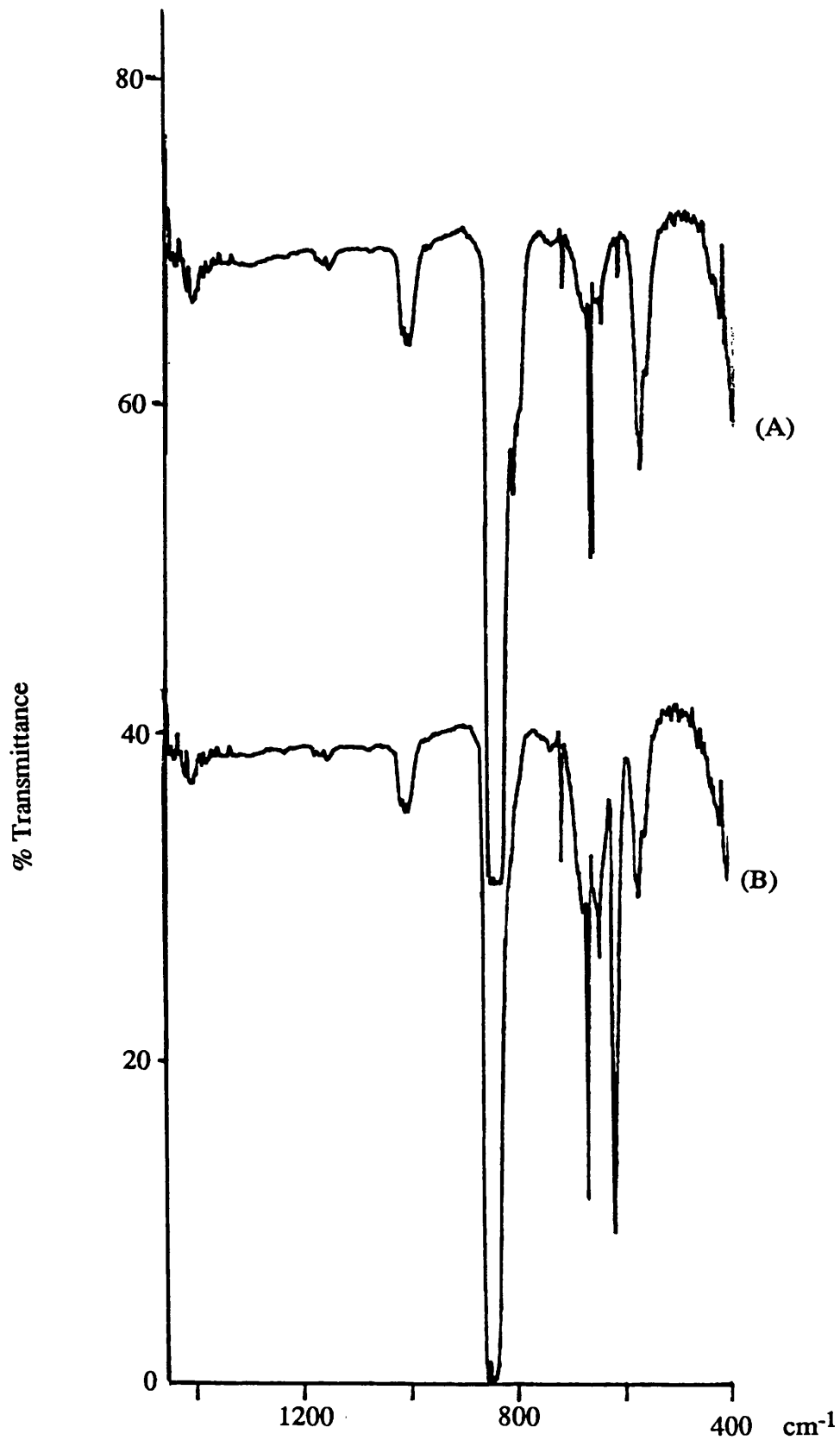
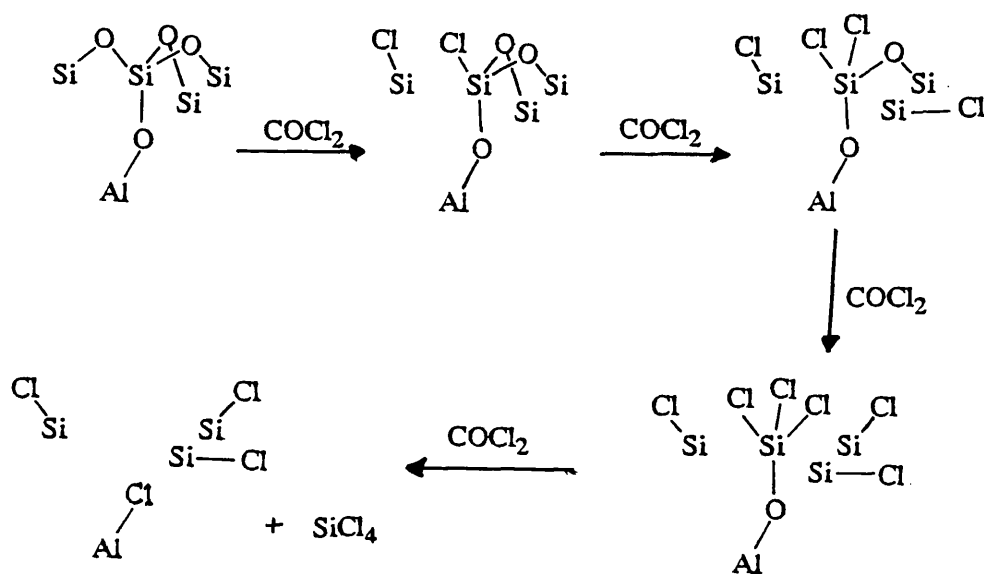


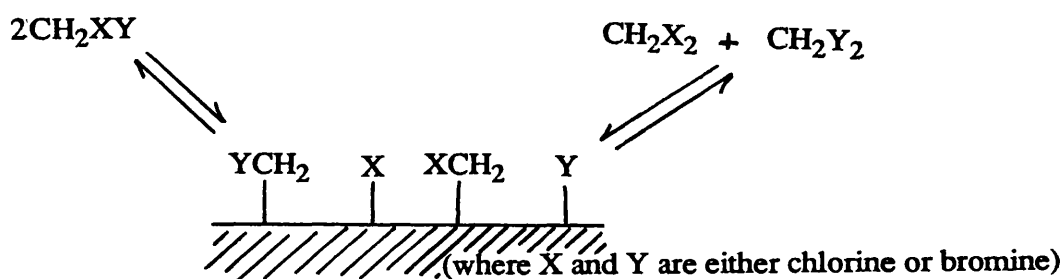
Figure 3.4.4. FTIR spectrum of the vapour phase after the 523K interaction of carbonyl chloride with γ -alumina (spectrum A) and montmorillonite K10 (spectrum B).

The idealised model of montmorillonite, figure 1.7.6 top structure, contains only octahedral aluminium environments, but as can be seen in the ^{27}Al MAS-NMR, the montmorillonite K10 and halogenated montmorillonite K10 contain both tetrahedral and octahedral aluminium environments. The tetrahedral aluminium environments in montmorillonite K10 are probably formed due to the collapsed nature of the montmorillonite K10 structure, figure 1.7.6, and aluminium environments at the edge of the basal planes. FTIR data obtained from the reaction product vapour phase of the chlorination of montmorillonite K10 allied with the ^{27}Al MAS-NMR data, indicates that the structure of chlorinated montmorillonite K10 differs from that of calcined montmorillonite K10. A possible reason for this difference in structure may be due to the formation of silicon tetrachloride during the chlorination process. A postulated mechanism for the formation of silicon tetrachloride is given in scheme 3.4.5. In this mechanism the reaction occurs at the edge of the basal plane, as this site will be less sterically hindered than sites located away from the edge of the basal plane. In the reaction scheme four carbonyl chloride molecules are required to form one silicon tetrachloride molecule. A consequence of the formation of silicon tetrachloride is the formation of Si-Cl and Al-Cl groups at the edge of the basal plane.



Scheme 3.4.5. The formation of SiCl_4 during the chlorination of montmorillonite K10 with carbonyl chloride.

Data from neutron activation analysis carried out on montmorillonite K10 after the halogenation reactions, indicate that bromination with dibromomethane (experiment 3.3.7), as in γ -alumina experiments, results in a bromine content (1.2mg atom g^{-1}) much lower than the comparable chlorine content (7.1mg atom g^{-1}) after chlorination with Cl_2CO for 6h at 523K. The data also indicates similar bromine and chlorine contents (0.5mg atom g^{-1}) result from the interaction of bromochloromethane with calcined montmorillonite K10 (total halogen content of 1.0mg atom g^{-1}), table 33.1(c). This impartial halogenation of the montmorillonite K10 affords the formation of the dismutation products dichloromethane and dibromomethane, shown in scheme 3.4.6.



Scheme 3.4.6. Formation of dismutation products on calcined montmorillonite K10.

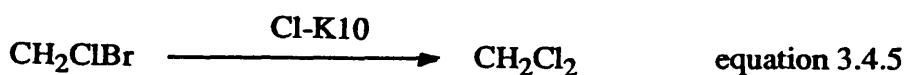
Calcined montmorillonite K10 treated with bromoform results in a bromine content of 0.3mg atom g^{-1} , a value much smaller than those obtained by either the dibromomethane or bromochloromethane reactions.

The interaction of dibromomethane with chlorinated montmorillonite K10 (experiment 3.3.10) leads to the formation of bromochloromethane. Neutron activation analysis of the clay indicates a bromine content of $1.25\text{mg atom g}^{-1}$ and a much reduced chlorine content, in comparison with chlorinated montmorillonite K10, of 0.7mg atom g^{-1} . This lack of chlorine on the montmorillonite K10 may be attributed to the formation of the chlorine containing species bromochloromethane and hydrogen chloride, equation 3.4.4.



Chlorinated montmorillonite K10 treated with bromoform (experiment 3.3.12) results in the formation of hydrogen chloride, hydrogen bromide, carbon monoxide and carbon dioxide, with no evidence for the presence of bromoform or the formation of any dismutation products. The lack of bromoform in the reaction product vapour phase and neutron activation analysis indicating a high bromine content (1.4mg atom g⁻¹), suggest that the reaction has gone to completion.

The interaction with bromochloromethane leads to the formation of dichloromethane, equation 3.4.5.



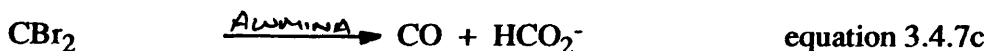
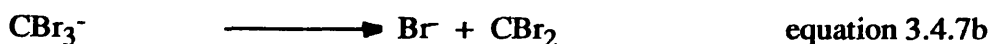
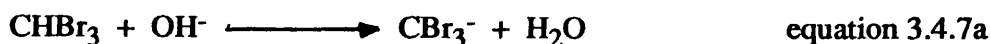
Neutron activation analysis of the montmorillonite K10 indicates a bromine content, approximately half that of the dibromomethane reaction, at 0.6mg atom g⁻¹ and the formation of reaction products follows a similar trend to that of the dibromomethane interaction, equation 3.4.6.



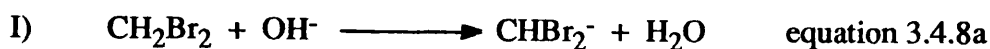
Thus interactions of dibromomethane and bromochloromethane with chlorinated montmorillonite K10 appear to be very similar.

3.4.4 Comparisons among the Halogenating Reagents.

The halogenation of γ -alumina and montmorillonite K10 indicates many similarities between the dibromomethane and bromochloromethane reagents. These include halogen uptake values (chlorine + bromine) on γ -alumina (0.8-0.9mg atom g^{-1}) and montmorillonite K10 (1.0-1.2mg atom g^{-1}), and formation of reaction products with the same number of halogens incorporated. The work in this section does however indicate that bromination of these supports with bromoform occurs via a different mechanism to that employed by dibromomethane and bromochloromethane. Possible reasons for this difference include; I) the formation of a $CHBr_2$ intermediate as opposed to the CH_2Br intermediate postulated in scheme 3.4.1, or II) an alpha elimination [82,83] which requires alkaline hydrolysis (equations 3.4.7a-3.4.7d).



Although this work concentrates on the acidic nature of γ -alumina, there is dissociative adsorption of hydrogen chloride [49] and hydrogen bromide (section 4.2.1) onto the surface. The nature of this adsorption necessitates basic sites, although whether or not the basic sites are strong enough for alkaline hydrolysis is not known. Alpha elimination involving dibromomethane or bromochloromethane is extremely unlikely however, as the formation of the carbene, equations 3.4.8a- 3.4.8b, would require the formation of an H^- ion.



3.4.5 Comparisons among the Halogenated Solids.

The work in this chapter has shown that the bromination of γ -alumina with dibromomethane is not, as was postulated at the outset of this work, similar to that of the chlorination of γ -alumina with carbonyl chloride. Halogen content data obtained by N.A.A consistently indicates chlorine contents 2-3 times greater than those observed for bromine. Whereas chlorination of γ -alumina with carbonyl chloride leads to the enhancement of both Brønsted and Lewis acidity, there is no evidence for any enhancement of Lewis acidity via the interaction with dibromomethane. The interaction of carbonyl chloride with γ -alumina leads to the formation of hydrogen chloride. This interacts with the γ -alumina by dissociative adsorption enhancing Brønsted acidity. In most of the reactions investigated in this chapter hydrogen halides (chlorides and bromides) are produced. It is therefore probable that the bromination of γ -alumina with bromomethanes enhances the Brønsted acidity, to some degree, through the dissociative adsorption of hydrogen bromide.

From this work it is postulated that these bromination reactions are not just due to the ability of the supports to undergo -OH/halogen exchange but also occur by organic mechanisms. The differing abilities for -OH/halogen exchange are highlighted by the fact that the reaction products observed differ for each individual support. The difference in organic mechanisms employed by halomethanes is discussed earlier, in section 3.4.4. The results from the reactions of bromochloromethane with the γ -alumina and montmorillonite K10 give an insight not only into the dismutation processes involved, but also into the competitive nature of the halogenation of these solids by bromine and chlorine. In the reactions involving γ -alumina, N.A.A. data indicates γ -alumina is more readily chlorinated than brominated (table 3.3.(c)), whilst montmorillonite K10 appears to have similar bromine and chlorine contents after the reaction. The results from this chapter also indicate that the halogen content of halogenated montmorillonite K10 is usually greater than those of halogenated γ -alumina. The prior chlorination of either the γ -alumina or montmorillonite K10 does not result in increased bromine content after bromination.

The general trend of reaction products for γ -alumina can be summed up by equation 3.4.9.



In this equation the reaction product contains one more proton than the starting material. This is observed in all the reactions carried out over calcined γ -alumina. Previous work [84] has shown what appears to be the opposite reaction occurring, by converting methyl chloride into bromochloromethane, equation 3.4.10.



It was expected that γ -alumina treated with carbonyl chloride, with its enhanced Brønsted acidity in comparison with calcined γ -alumina, would follow equation 3.4.9 and convert dibromomethane and chlorobromomethane to methyl bromide and methyl chloride. The fact that this does not occur suggests that the enhanced Brønsted acid sites on the chlorinated γ -alumina are not involved with the interaction of the halomethane. This would be similar to the interaction of carbonyl chloride with γ -alumina (section 1.9) which, it is postulated, results first in the removal of terminal hydroxyl groups. The preferential formation of dibromomethane over its chlorine analogue dichloromethane, after the treatment of chlorinated γ -alumina with bromochloromethane, is a major surprise and cannot be readily explained.

The halogenation of montmorillonite K10 with bromochloromethane leads to an equal bromine/chlorine content on the clay. A consequence of this impartial halogenation is that the reaction products contain the dismutation products dichloromethane, which was not observed in any of the alumina reactions, and dibromomethane. The neutron activation analysis results combined with the dismutation products observed indicate that the γ -alumina and montmorillonite K 10 react in different manners with the brominating reagents. The γ -alumina is more readily chlorinated than brominated whilst the

montmorillonite K10 tended to be more impartially halogenated, resulting in similar bromine and chlorine contents.

CHAPTER 4

Interaction of Hydrogen Bromide with Solid Supports and Their Effects on Hydrobromination Reactions.

4.1 Introduction.

Contrary to the impression often given in introductory organic text books [85-87], the electrophilic addition of hydrogen halides across olefinic bonds is fraught with a number of experimental difficulties. In the case of hydrogen chloride, addition does not occur at a preparatively useful rate unless the olefin is I) highly substituted [88-90] or II) strained [91-97]. The addition of hydrogen bromide, to an olefin, results in both Markovnikov and anti-Markovnikov reaction products. Formation of anti-Markovnikov reaction products is due to free radical addition [98], in which the main regioselective factor appears to be steric: $\text{CH}_2=\text{CHR}$ is preferentially attacked at CH_2 regardless of the identity of R [99]. The observed orientation in both kinds of hydrogen bromide addition, Markovnikov (electrophilic) and anti-Markovnikov (radical) is, therefore, determined by the formation of the secondary intermediate, which in the electrophilic case is more stable than the primary intermediate and in the radical case is sterically preferred. These dual reaction products are rarely observed in hydrogen chloride additions and never observed in hydrogen fluoride or hydrogen iodide additions.

In recent years there has been considerable interest in catalytic reactions by inorganic reagents supported on high surface area inorganic materials. Kodomari [100]

has shown enhanced selectivity in the bromination of methylbenzenes with CuBr_2 when the CuBr_2 is supported on alumina. Recent studies into the hydrohalogenation of alkenes and alkynes [101,102], have shown that the presence of inorganic supports can both enhance the rate of reaction and alter the regiochemistry of the reaction. These reactions often proceed with greater selectivity and under milder conditions than analogous homogeneous reactions. The work in this section investigates the interaction of anhydrous hydrogen bromide with modified high surface area γ -aluminas and clays, using neutron activation analysis and radiotracer techniques. The potential of these clays and γ -aluminas as catalysts for the hydrobromination of olefins, using both 48% hydrobromic acid and anhydrous hydrogen bromide as the brominating agent, were investigated in this work. The olefins selected for these reactions were isomers of butene and 1,9-decadiene. Butene was chosen as it has a low boiling point/high vapour pressure (at stp) resulting in a gas phase interaction with the inorganic support, and 1,9-decadiene was chosen as it has a high boiling point/low vapour pressure (at stp), which results in a liquid phase interaction with the inorganic support. The double bonds in 1,9-decadiene are sufficiently far apart to eliminate any conjugate effect.

4.2 Experimental.

4.2.1 Interaction of hydrogen bromide with calcined Degussa 'C' γ -alumina at 523K.

Calcined γ -alumina (0.8g) was loaded into a Monel bomb, 75cm³ capacity, in the inert atmosphere glove box. The vessel was then transferred to a vacuum line and the contents degassed. The bomb was cooled to 77K using liquid nitrogen, before a measured aliquot of hydrogen bromide (approx 60mmol) was condensed into it. The bomb was then placed in an electrical furnace and the contents heated to 523K for 120h, before being allowed to cool to room temperature. Gaseous material from the bomb was expanded into a manifold with a gas cell attached, to give a pressure of 50 Torr, and a gas phase FTIR spectrum obtained.

A sample of the brominated alumina (0.054g) was loaded, in the dry box, into a polythene ampoule which was then sealed. The ampoule was then transferred to the SURRC at East Kilbride for neutron activation analysis (section 2.5.7).

4.2.2 Interaction of [⁸²Br]-bromine labelled hydrogen bromide with calcined Degussa 'C' γ -alumina at room temperature.

Calcined γ -alumina (approximately 0.1g) was transferred into a double limbed counting vessel (figure 4.2.1) and accurately weighed; this process was undertaken in an inert atmosphere glove box. The counting vessel was then transferred to a vacuum line manifold and the contents degassed.

A known quantity of [⁸²Br]-bromine labelled hydrogen bromide, measured using a Heiss pressure gauge, was condensed into the limb of the double limbed counting vessel, that did not contain alumina. The [⁸²Br]-bromine labelled hydrogen bromide was allowed

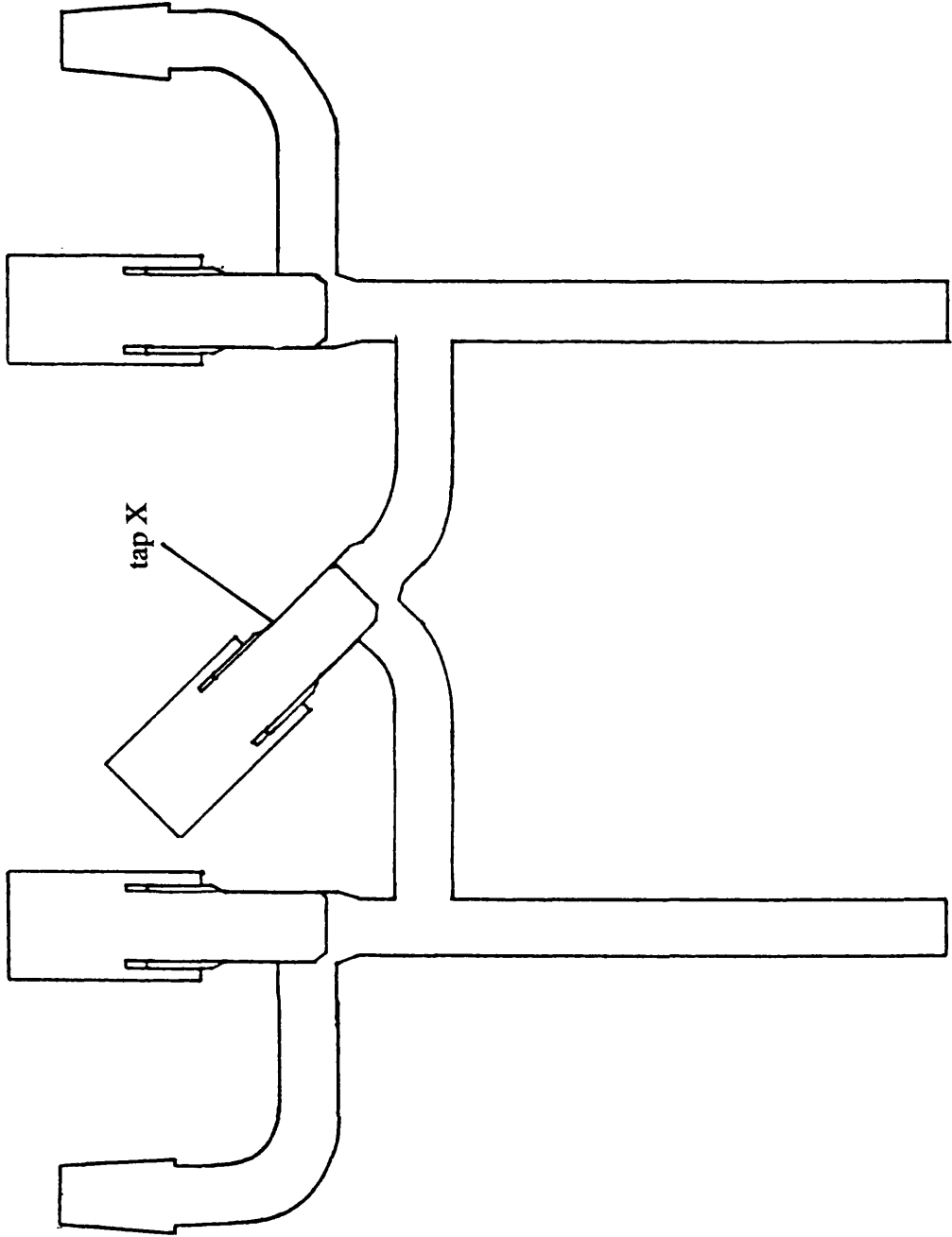


Figure 4.2.1. Double limbed counting vessel.

to warm to room temperature and the count rate determined using a time period sufficient to accumulate approximately 10000 counts. Tap X was then opened, allowing the [^{82}Br]-bromine labelled hydrogen bromide to interact with the γ -alumina, and the γ -alumina was counted immediately. The contents of both limbs were counted alternately until the uptake of [^{82}Br] on to the alumina had ceased, at which point tap X was closed and the vessel transferred to the vacuum line where another measured aliquot of [^{82}Br]-bromine labelled hydrogen bromide was condensed into the vessel and the process repeated. The reaction was halted when further additions of [^{82}Br]-bromine labelled hydrogen bromide did not lead to any further uptake of radioactivity.

These count rates were compared with the specific count rate of a known quantity of [^{82}Br]-bromine labelled hydrogen bromide which had been reacted with solid sodium hydroxide, section 2.5.5. The [^{82}Br]-bromine labelled hydrogen bromide was from the same bulk stock in each case.

4.2.3 Interaction of [^{82}Br]-bromine labelled hydrogen bromide with brominated Degussa 'C' γ -alumina at room temperature.

The procedure to investigate the interaction, at 293K, of anhydrous gaseous [^{82}Br]-bromine labelled hydrogen bromide with calcined γ -alumina treated with anhydrous gaseous hydrogen bromide and but-1-ene at 373K, was the same as described in section 4.2.2.

4.2.4 Interaction of [⁸²Br]-bromine labelled hydrogen bromide with chlorinated Degussa 'C' γ -alumina at room temperature.

The procedure to investigate the interaction, at 293K, of anhydrous gaseous [⁸²Br]-bromine labelled hydrogen bromide with calcined γ -alumina treated with anhydrous gaseous carbonyl chloride at 523K for 12h, was the same as described in section 4.2.2.

4.2.5 Interaction of [⁸²Br]-bromine labelled hydrogen bromide with uncalcined montmorillonite K10 at room temperature.

The experimental procedure for the room temperature interaction of [⁸²Br]-bromine labelled hydrogen bromide with uncalcined montmorillonite K10 was the same as that described for the interaction of [⁸²Br]-bromine labelled hydrogen bromide with calcined γ -alumina, section 4.2.2.

4.2.6 Interaction of [⁸²Br]-bromine labelled hydrogen bromide with calcined montmorillonite K10 at room temperature.

The experimental procedure for the room temperature interaction of [⁸²Br]-bromine labelled hydrogen bromide with montmorillonite K10 heated to 523K for 12h, was the same as that described for the interaction of [⁸²Br]-bromine labelled hydrogen bromide with calcined γ -alumina, section 4.2.2.

4.2.7 Interaction of [⁸²Br]-bromine labelled hydrogen bromide with chlorinated montmorillonite K10 at room temperature.

The procedure to investigate the interaction, at 293K, of anhydrous gaseous [⁸²Br]-bromine labelled hydrogen bromide with calcined montmorillonite K10 treated with anhydrous gaseous carbonyl chloride at 523K for 12h, was the same as that described in section 4.2.2.

4.2.8 Reaction of [⁸²Br]-bromine labelled hydrogen bromide with but-1-ene in the presence of calcined Degussa 'C' γ -alumina at 373K

Calcined γ -alumina (approximately 0.1g) was transferred into the counting limb of the counting vessel, figure 4.2.2, and accurately weighed; this process was undertaken in an inert atmosphere glove box. The counting vessel was then transferred to a vacuum line manifold and the contents degassed.

A known quantity of [⁸²Br]-bromine labelled hydrogen bromide was condensed into the bulb of the counting vessel. A similar quantity of but-1-ene was also condensed into the bulb, before allowing the bulb to warm to room temperature. Tap X was then opened, to allow the reaction mixture to interact with the γ -alumina, and the limb containing the γ -alumina was counted. The limb containing γ -alumina was counted until the uptake of bromine had ceased. The limb was then placed in an electrical furnace, heated to 373K for 12h, then counted as it cooled. Counting continued until the uptake of bromine ceased.

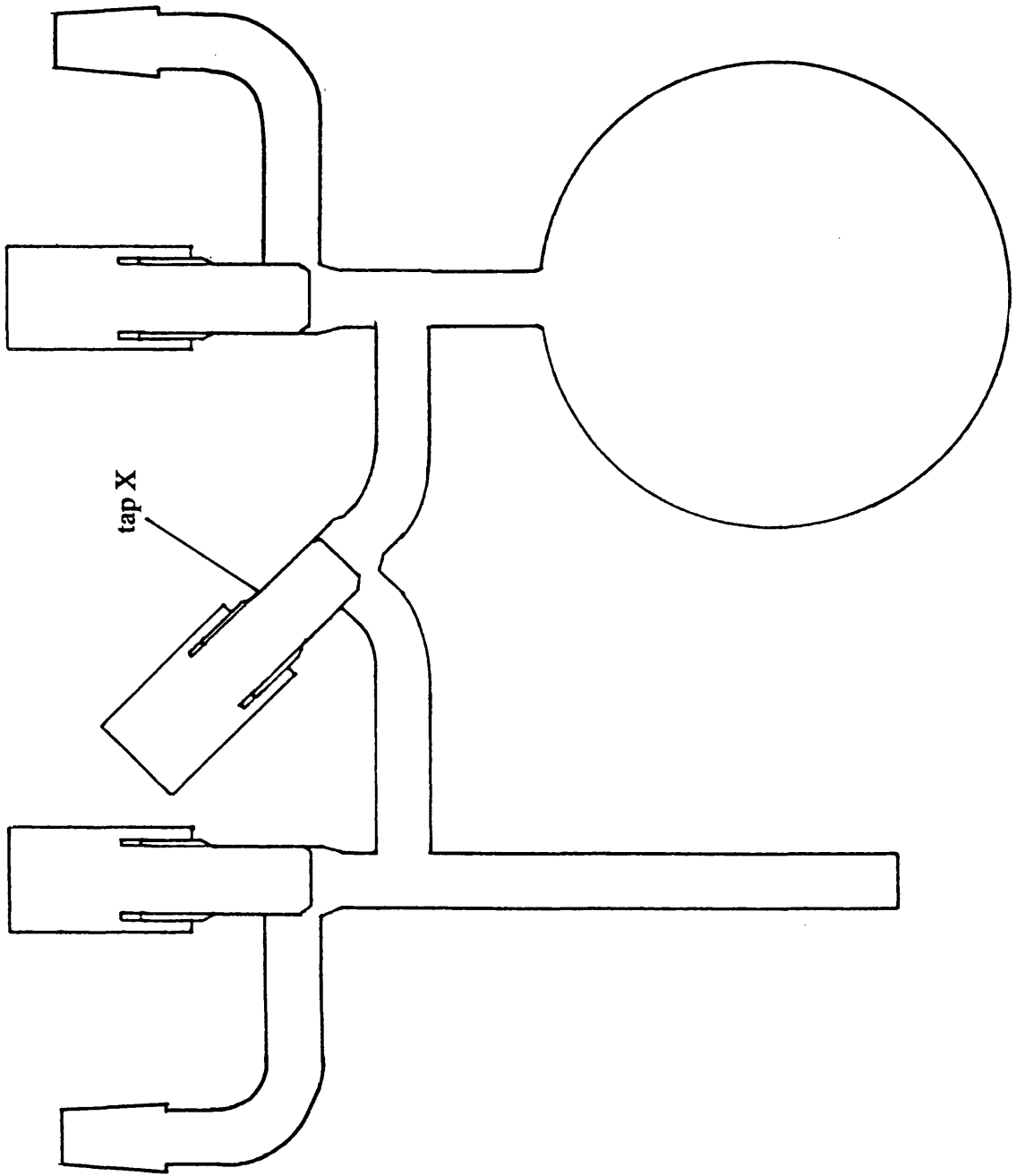


Figure 4.2.2. Counting vessel with reservoir bulb.

4.2.9 Reaction of [^{82}Br]-bromine labelled hydrogen bromide with but-1-ene in the presence of calcined montmorillonite K10 at 373K.

The experimental procedure for the investigation of the reaction involving [^{82}Br]-bromine labelled hydrogen bromide with but-1-ene, at 373K, in the presence of montmorillonite K10, pretreated by heating to 523K, under *vacuo*, for 12h is described in section 4.2.8.

4.2.10 Interaction of [^{82}Br]-bromine labelled hydrogen bromide with montmorillonite K10, treated with pyridine, at room temperature.

The experimental procedure for the investigation of the interaction of [^{82}Br]-bromine labelled hydrogen bromide with montmorillonite K10, pretreated with anhydrous pyridine vapour at room temperature (section 6.2.5), was the same as that described for the interaction of [^{82}Br]-bromine labelled hydrogen bromide with γ -alumina, section 4.2.2.

4.2.11 Interaction of [^{82}Br]-bromine labelled hydrogen bromide with chlorinated montmorillonite K10, treated with pyridine, at room temperature.

The experimental procedure for the investigation of the interaction of [^{82}Br]-bromine labelled hydrogen bromide with montmorillonite K10, pretreated with anhydrous gaseous carbonyl chloride at 523K for 12h and then anhydrous pyridine vapour at room temperature (section 6.2.6), was the same as that described for the interaction of [^{82}Br]-bromine labelled hydrogen bromide with γ -alumina, section 4.2.2.

4.2.12 Reaction of hydrogen bromide with but-1-ene at 373K.

The reaction vessel, a Monel bomb, was attached to a vacuum line manifold and evacuated. The bomb was cooled to 77K, using liquid nitrogen, before condensing into it a measured aliquot of hydrogen bromide (approx 60mmol), then a similar quantity of but-1-ene. The bomb was then placed in an electrical furnace and heated at 373K for 12h, before being allowed to cool to room temperature. The gaseous material from the bomb was expanded into a manifold with a gas cell attached, to give a pressure of 50 Torr, and a gas phase FTIR spectrum obtained.

4.2.13 Reaction of hydrogen bromide with but-1-ene (mol ratio 3:2) in the presence of calcined Degussa 'C' γ -alumina at 373K.

Calcined γ -alumina (approximately 0.8g) was loaded into a Monel bomb, in the inert atmosphere glove box. The vessel was then transferred to a vacuum line and the contents degassed. The bomb was cooled to 77K, using liquid nitrogen, before condensing into it a measured aliquot of hydrogen bromide (approx 60mmol), then a similar quantity of but-1-ene. The bomb was placed in an electrical furnace and heated at 373K for 12h, before being allowed to cool to room temperature. The gaseous material from the bomb was expanded into a manifold with a gas cell attached, to give a pressure of 50 Torr, and a gas phase FTIR spectrum obtained. The volatile materials from the bomb were then condensed into a collection vessel, which was sealed and sent to Associated Octel for G.C. analysis.

4.2.14 Reaction of hydrogen bromide with but-1-ene (mol ratio 1:1) in the presence of calcined Degussa 'C' γ -alumina at 373K.

The experimental procedure for the above investigation is described in section 4.2.13. A DRIFT spectrum of the halogenated alumina was obtained after the reaction (see section 2.3.2).

4.2.15 Reaction of hydrogen bromide with but-1-ene (mol ratio 1:1) in the presence of dibromomethane brominated γ -alumina at 373K.

The experimental procedure for the reaction of hydrogen bromide with but-1-ene (mol ratio 1:1), at 373K, in the presence of γ -alumina treated with dibromomethane at 523K for 120h (section 3.2.1), is the same as that described in section 4.2.13. No GC analysis was carried out on the volatile reaction products.

4.2.16 Reaction of hydrogen bromide with but-2-ene (mol ratio 3:2) in the presence of calcined Degussa 'C' γ -alumina at 373K.

The experimental procedure for the above investigation is described in section 4.2.13.

4.2.17 Reaction of hydrogen bromide with but-2-ene (mol ratio 1:1) in the presence of calcined Degussa 'C' γ -alumina at 373K.

The experimental procedure for the above investigation is described in section 4.2.13.

4.2.18 Reaction of hydrogen bromide with but-2-ene (mol ratio 2:3) in the presence of calcined Degussa 'C' γ -alumina at 373K.

The experimental procedure for the above investigation is described in section 4.2.13.

4.2.19 Reaction of hydrogen bromide with but-2-ene (mol ratio 1:1) in the presence of chlorinated γ -alumina at 373K.

The experimental procedure for the reaction of hydrogen bromide with but-2-ene (mol ratio 1:1) in the presence of calcined γ -alumina, treated with carbonyl chloride at 523K for 12h, is the same as described in section 4.2.13. No GC analysis was carried out on the volatile reaction products.

4.2.20 Reaction of 1,9-decadiene with 48% hydrobromic acid in the presence of uncalcined Degussa 'C' γ -alumina.

1,9-Decadiene (0.48mol) was transferred into reaction vessel A, shown in figure 4.2.3, containing uncalcined Degussa 'C' γ -alumina (2.37g). 48% Hydrobromic acid (2.06mol) was added to the reaction mixture, which was then warmed to 363K, and stirred for 70 minutes. A sample of the organic phase of the final reaction mixture was taken and a gas chromatogram obtained.

4.2.21 Reaction of 1,9-decadiene with 48% hydrobromic acid in the presence of calcined Degussa 'C' γ -alumina.

1,9-Decadiene (0.47mol) was transferred into reaction vessel A, shown in figure 4.2.3, containing calcined Degussa 'C' γ -alumina (2.75g). 48% Hydrobromic acid (1.95mol) was added to the reaction mixture, which was then warmed to 363K, and stirred for 330 minutes. Samples of the organic phase of the reaction mixture were taken at set times and gas chromatograms obtained.

4.2.22 Reaction of 1,9-decadiene with 48% hydrobromic acid in the presence of calcined acidic, Brockmann 1 standard grade alumina.

1,9-Decadiene (0.49mol) was transferred into reaction vessel A, figure 4.2.3, containing calcined acidic, Brockmann 1 standard grade alumina (13.0g). 48% Hydrobromic acid (1.95mol) was added to the reaction mixture, which was then warmed to 363K, and stirred for 330 minutes. Samples of the organic phase of the reaction mixture

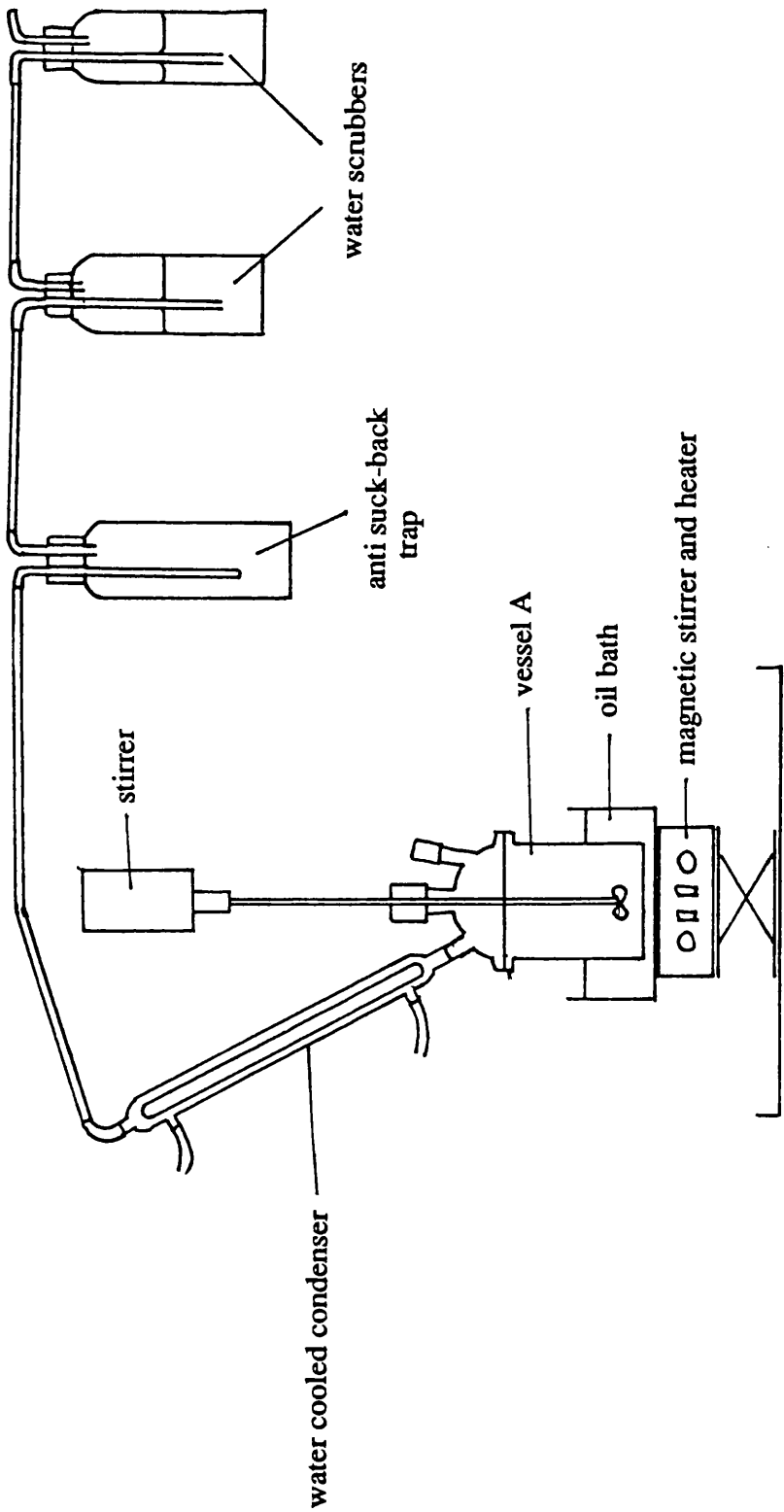


Figure 4.2.3. Apparatus for the hydrobromination of 1,9-decadiene using 48% aqueous hydrobromic acid.

were taken at set times and gas chromatograms obtained.

4.2.23 Reaction of 1,9-decadiene with 48% hydrobromic acid in the presence of calcined montmorillonite K10.

1,9-Decadiene (0.48mol) was transferred into reaction vessel A, figure 4.2.3, containing calcined montmorillonite K10 (10.6g). 48% Hydrobromic acid (1.93mol) was added to the reaction mixture, which was then warmed to 363K, and stirred for 330 minutes. Samples of the organic phase of the reaction mixture were taken at set times and gas chromatograms obtained.

4.2.24 Reaction of 1,9-decadiene with hydrogen bromide gas, at 318K, in the presence of calcined Degussa 'C' γ -alumina.

1,9-Decadiene (0.24mol) was transferred into reaction vessel A, figure 4.2.4, containing calcined Degussa 'C' γ -alumina (2.6g) and a solvent, carbon tetrachloride (300cm³). The reaction mixture was warmed to 318K and stirred for 40 minutes, whilst hydrogen bromide was sparged into the vessel at a rate of 0.167 l min⁻¹, measured using a gas flow meter. A sample of the final reaction mixture was taken and a gas chromatogram obtained.

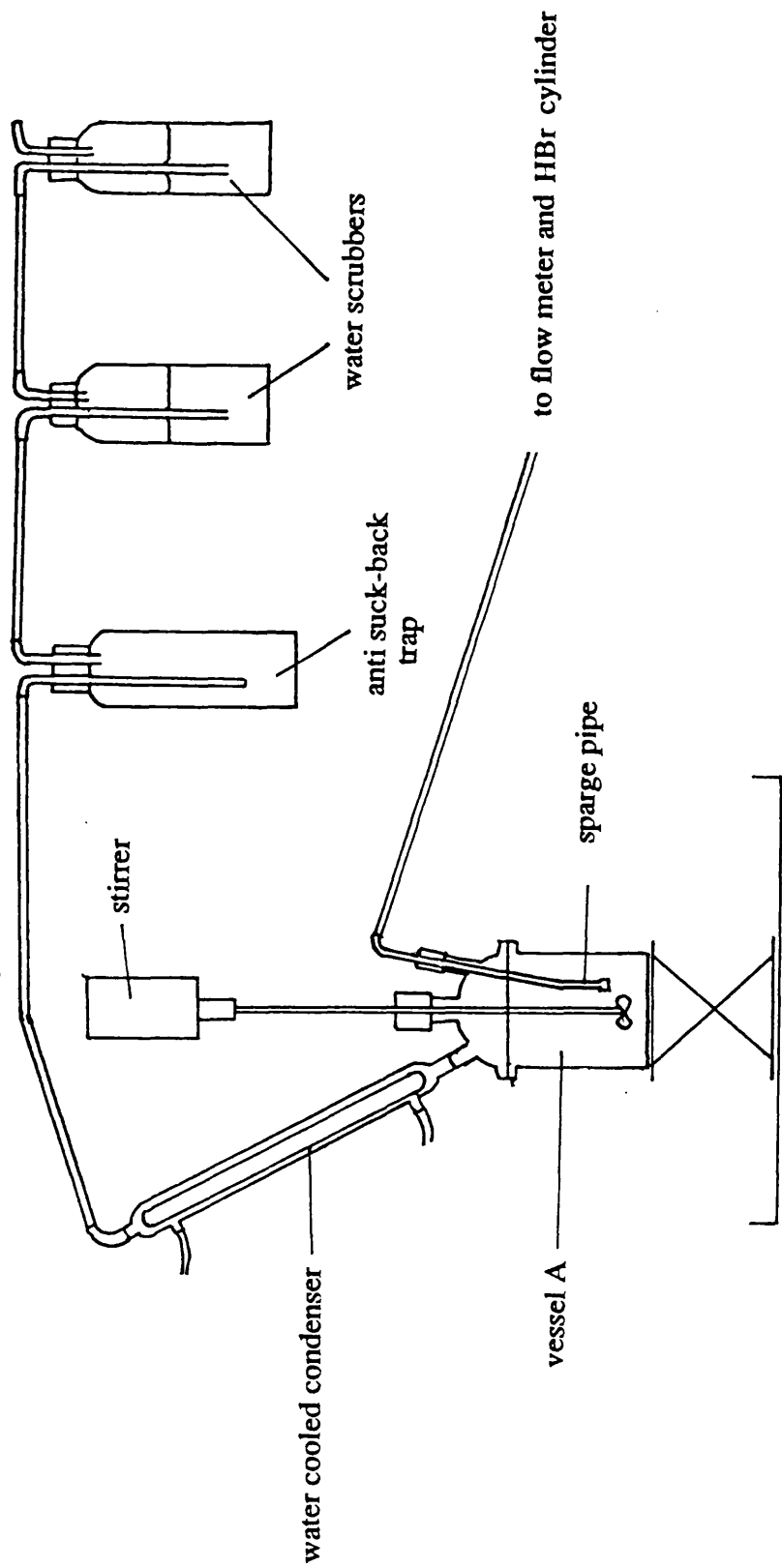


Figure 4.2.4. Apparatus for the hydrobromination of 1,9-decadiene using hydrogen bromide gas.

4.2.25 Reaction of 1,9-decadiene with hydrogen bromide gas in the presence of calcined Degussa 'C' γ -alumina.

1,9-Decadiene (0.26mol) was transferred into reaction vessel A, figure 4.2.4, containing calcined Degussa 'C' γ -alumina (2.72g) and a solvent, carbon tetrachloride (250cm³). The reaction mixture was stirred for 165 minutes, whilst hydrogen bromide was sparged into the vessel at a rate of 0.167 l min⁻¹. Samples of the organic phase of the reaction mixture were taken at set times and gas chromatograms obtained.

4.2.26 Reaction of 1,9-decadiene with hydrogen bromide gas in the presence of calcined montmorillonite K10.

1,9-Decadiene (0.29mol) was transferred into reaction vessel A, figure 4.2.4, containing calcined montmorillonite K10 (11.2g) and a solvent, carbon tetrachloride (250cm³). The reaction mixture was stirred for 120 minutes, whilst hydrogen bromide was sparged into the vessel at a rate of 0.167 l min⁻¹. Samples of the organic phase of the reaction mixture were taken at set times and gas chromatograms obtained.

4.2.27 Reaction of 1,9-decadiene with hydrogen bromide gas.

1,9-Decadiene (30mmol) was transferred into a round bottomed, 100cm³, glass reaction vessel (figure 4.2.5). The vessel was transferred to a vacuum line and the contents degassed, before condensing in hydrogen bromide (1mmol) at 77K. The vessel was allowed to warm to room temperature before being attached to a shaker and shaken for 12h. The vapour phase of the reaction products was analysed by FTIR, while the liquid

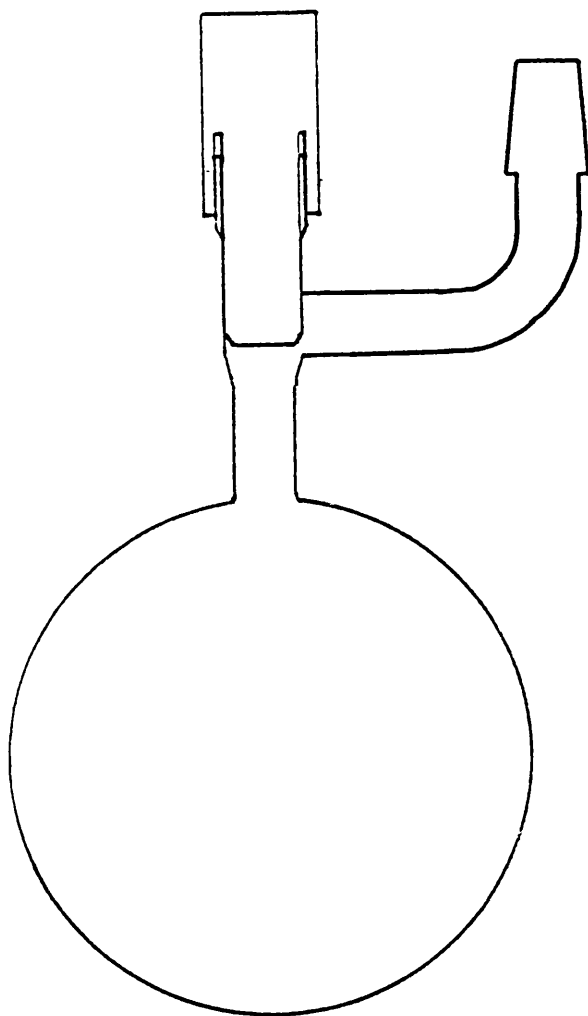


Figure 4.2.5. Round bottomed reaction vessel.

phase was sent to the Associated Octel Company for GCMS analysis.

4.2.28 Reaction of 1,9-decadiene with hydrogen bromide gas in the presence of chlorinated γ -alumina.

γ -Alumina (0.23g), treated with carbonyl chloride at 523K for 12h, was placed into the reaction vessel (figure 4.2.5). 1,9-Decadiene (30mmol) was then decanted into the reaction vessel. The vessel was transferred to a vacuum line and the contents degassed, before hydrogen bromide (1mmol) was condensed in, at 77K. The vessel was allowed to warm to room temperature before being attached to a shaker and shaken for 12h. The vapour phase of the reaction products was analysed by FTIR, while the liquid phase was sent to the Associated Octel Company for GCMS analysis.

4.2.29 Reaction of 1,9-decadiene with hydrogen bromide gas in the presence of brominated γ -alumina.

The experimental procedure for the reaction of 1,9-decadiene with hydrogen bromide gas in the presence of calcined γ -alumina treated with dibromine at 523K for 120h, was the same as that described in section 4.2.28.

4.2.30 Reaction of 1,9-decadiene with hydrogen bromide gas in the presence of chlorinated montmorillonite K10.

The experimental procedure for the reaction of 1,9-decadiene with hydrogen bromide gas in the presence of montmorillonite K10, treated with carbonyl chloride at 523K for 12h, was the same as that described in section 4.2.28.

4.2.31 Reaction of 1,9-decadiene with hydrogen bromide gas in the presence of uncalcined bentonite.

The experimental procedure for the above investigation is described in section 4.2.28.

4.2.32 Interaction of [⁸²Br]-bromine labelled hydrogen bromide and decadiene solution with montmorillonite K10 and decadiene at room temperature.

Montmorillonite K10 (0.1g) was loaded into one limb of a double limbed counting vessel. Equal quantities of 1,9-decadiene (2.0g) were decanted into each limb of the double limbed counting vessel, which was then transferred to a vacuum line and the contents degassed. Tap X was closed and a measured amount of [⁸²Br]-bromine labelled hydrogen bromide condensed, at 77K, into the limb not containing montmorillonite K10. On warming to room temperature, the count rate of the limb containing [⁸²Br]-bromine labelled hydrogen bromide was determined, using a time period sufficient to accommodate approximately 10000 counts, before tap X was opened. The contents of both limbs were counted alternately for 36h.

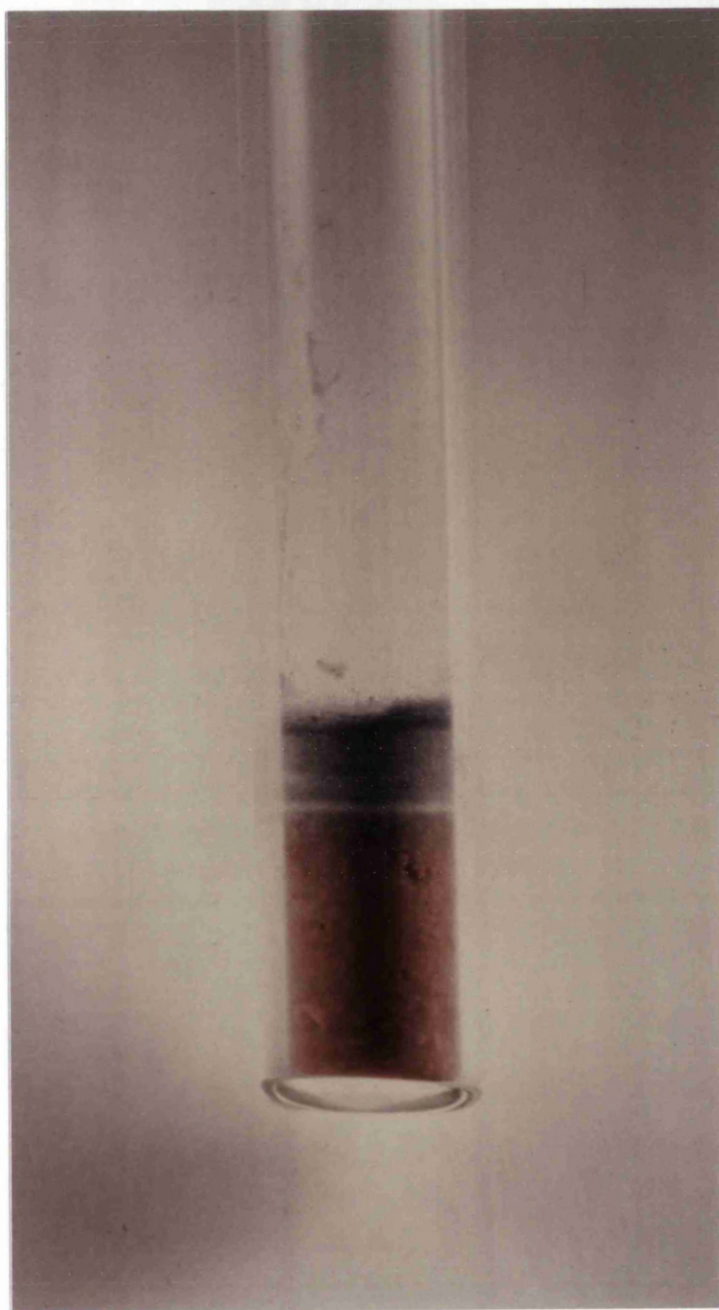


Figure 4.3.3. Coloured rings observed on the addition of [^{82}Br]-bromine labelled hydrogen bromide to γ -alumina treated with carbonyl chloride.

4.3 Results.

4.3.1 Interaction of hydrogen bromide with calcined Degussa 'C' γ -alumina at 523K.

The infrared analysis of the volatile products after a 12h exposure, at 523K, of hydrogen bromide to a sample of Degussa 'C' γ -alumina calcined at 523K, indicated absorbances at 2700-2400 cm^{-1} due to hydrogen bromide. Neutron activation analysis carried out on the alumina, after the reaction, indicated a bromide content of 0.3 mg atom g^{-1} . The ^{27}Al -MAS NMR spectrum of the γ -alumina after the interaction with hydrogen bromide, figure 4.3.1, indicated two resonance signals due to $\text{Al}_{(\text{oct})}$ at 5.0ppm and $\text{Al}_{(\text{tet})}$ at 51.9ppm, with reference to AlCl_3 .

4.3.2 Interaction of [^{82}Br]-bromine labelled hydrogen bromide with calcined Degussa 'C' γ -alumina at room temperature.

The results of this experiment indicated an immediate interaction between hydrogen bromide and γ -alumina, at room temperature. There was an initial rapid increase in the count rate of the solid, followed by a more gradual increase levelling to a plateau after 0.5h. Three aliquots of [^{82}Br]-bromine labelled hydrogen bromide, 0.46mmol, 0.61mmol and 0.81mmol [each with a specific count rate of $201.8 \pm 0.7 \text{ count s}^{-1} (\text{mg atom Br})^{-1}$, ascertained by the reaction of a measured quantity of [^{82}Br]-bromine labelled hydrogen bromide with solid sodium hydroxide, section 2.5.5], were allowed to interact successively with the calcined γ -alumina (0.13g). The second aliquot of [^{82}Br]-bromine labelled hydrogen bromide was added only after the count rate of the γ -alumina showed no further increase. The count rate of the γ -alumina, after the final addition of [^{82}Br]-bromine labelled hydrogen bromide, was measured at $33.1 \text{ count s}^{-1}$; this figure was corrected for

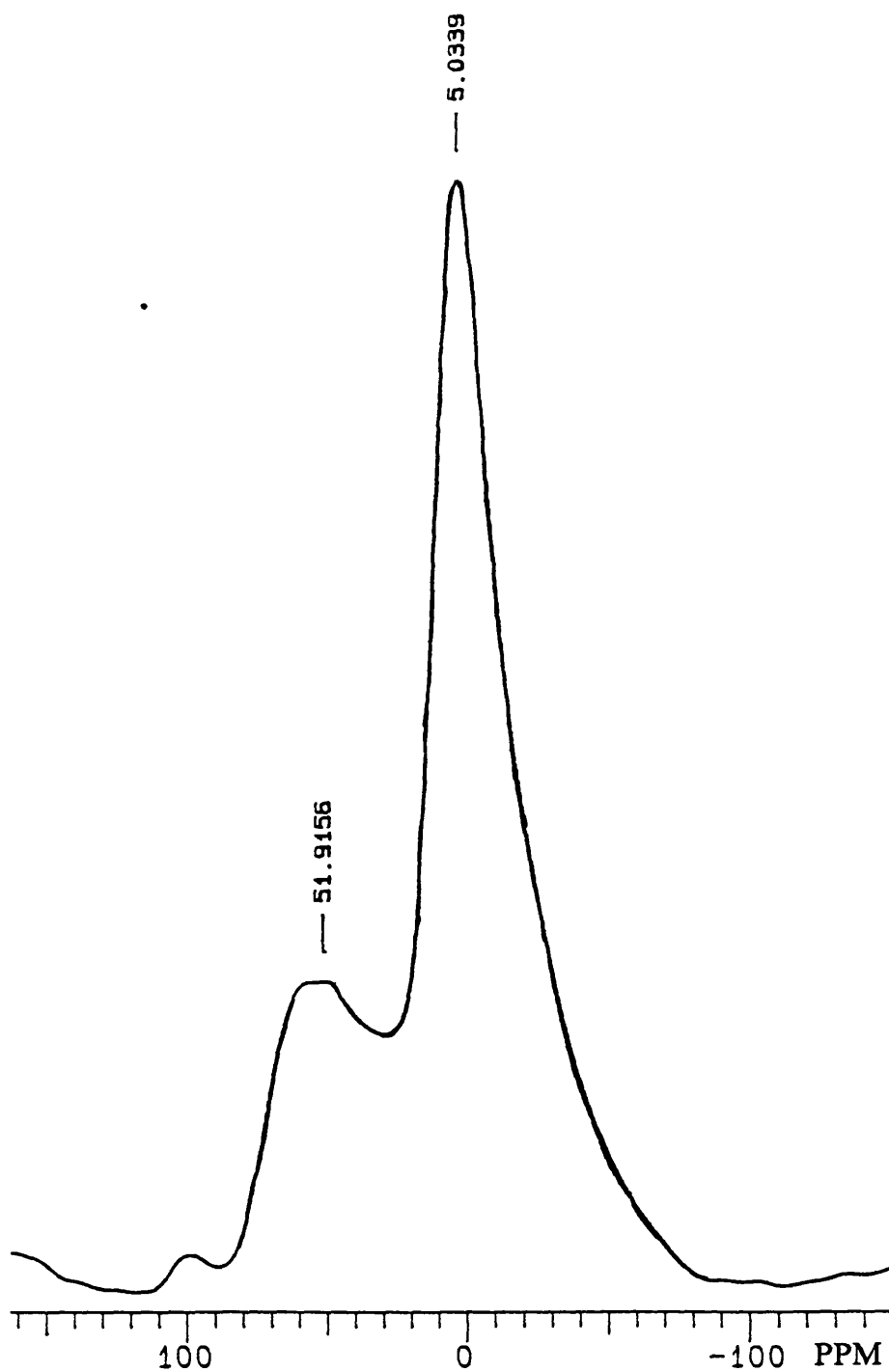


Figure 4.3.1. ^{27}Al MAS NMR Spectrum of γ -alumina after the interaction of hydrogen bromide at room temperature.

decay to $57.6 \pm 0.6 \text{ count s}^{-1}$, table 4.3.1. To ascertain the bromide content of the γ -alumina the gas phase count must be subtracted. This was measured at $15.1 \text{ count s}^{-1}$, corrected for decay to $27.2 \pm 0.4 \text{ count s}^{-1}$. The bromide content of the γ -alumina therefore corresponded to $30.2 \pm 0.6 \text{ count s}^{-1}$ (corrected for decay), indicating a bromide uptake of $1.1 \text{ mg atom g}^{-1}$. The γ -alumina was then degassed under *vacuo* for 5min, after which a count rate of $23.6 \pm 0.3 \text{ count s}^{-1}$ (corrected for decay) was obtained, indicating bromide retention of $0.9 \text{ mg atom g}^{-1}$. Typical data obtained from this type of reaction and their treatment for determination of specific count rates and bromide uptakes are given in section 4.3.6.

4.3.3 Interaction of [^{82}Br]-bromine labelled hydrogen bromide with brominated Degussa 'C' γ -alumina at room temperature.

The results of the interaction of [^{82}Br]-bromine labelled hydrogen bromide with γ -alumina pretreated with hydrogen bromide and but-1-ene (section 4.2.14), at room temperature, indicated an immediate interaction with a rapid increase in the count rate of the solid, followed by a more gradual increase, levelling to a plateau after 1h (figure 4.3.2). The [^{82}Br]-bromine labelled hydrogen bromide, 1.21 mmol [specific count rate of $811.0 \pm 2.7 \text{ count s}^{-1} (\text{mg atom Br})^{-1}$], interacted with the γ -alumina (0.11 g) resulting in a count rate, for the solid, of $323.0 \pm 2.9 \text{ count s}^{-1}$ (corrected for decay) after 46.7h. The count rate for the gas phase of $207.1 \pm 2.1 \text{ count s}^{-1}$ (corrected for decay), was subtracted from this solid count rate. This indicated a bromine uptake of $1.3 \text{ mg atom g}^{-1}$ (table 4.3.1). The brominated γ -alumina was pumped on a vacuum line for 5min, after which time a count of $109.6 \pm 1.1 \text{ count s}^{-1}$ (corrected for decay) was obtained, indicating bromide retention of $1.2 \text{ mg atom g}^{-1}$.

Table 4.3.1. Uptake of [⁸²Br]-bromine labelled hydrogen bromide onto various solid supports

Support	Bromine content	Bromine retention after pumping the solid.
calcined γ -alumina	1.1	0.9
brominated γ -alumina	1.3	1.2
γ -alumina treated with carbonyl chloride	0.7	0.7
uncalcined montmorillonite K10	1.8	0.7
calcined montmorillonite K10	2.2	0.7
montmorillonite K10 treated with carbonyl chloride	1.6	1.1

all values in mg atom Br g⁻¹

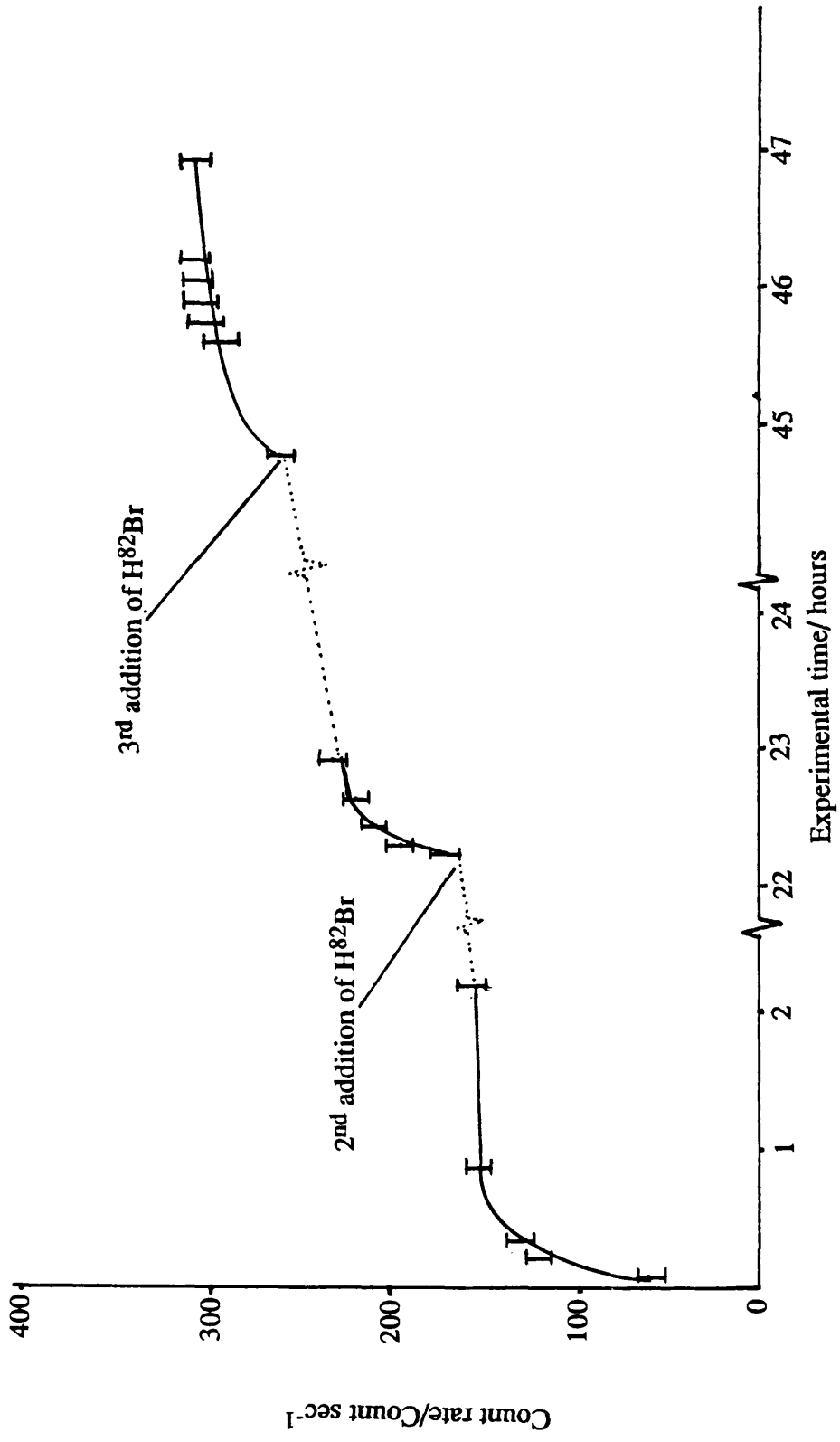


Figure 4.3.2. Surface count rate from the room temperature interaction of [⁸²Br]-bromine labelled hydrogen bromide with γ -alumina pretreated with hydrogen bromide and but-1-ene.

4.3.4 Interaction of [⁸²Br]-bromine labelled hydrogen bromide with chlorinated Degussa 'C' γ -alumina at room temperature.

The results of the interaction of [⁸²Br]-bromine labelled hydrogen bromide with calcined γ -alumina pretreated with carbonyl chloride at 523K for 12h, were a rapid increase in the count rate of the solid, followed by a more gradual increase levelling to a plateau after 2h. Two aliquots of [⁸²Br]-bromine labelled hydrogen bromide, 1.19mmol and 1.08mmol [specific count rate of 260.8 count s⁻¹ (mg atom Br)⁻¹], were allowed to interact with chlorinated γ -alumina (0.15g). The count rate from the γ -alumina, after 24.1h, was measured at 89.9 \pm 0.9 count s⁻¹ (corrected for decay), whilst the the count rate of the gas phase was measured at 63.4 \pm 0.6 count s⁻¹ (corrected for decay), giving a count for the solid of 26.5 \pm 0.9 count s⁻¹, indicating a bromide uptake of 0.7mg atom g⁻¹, table 4.3.1. The γ -alumina was then degassed on a vacuum line for 5min after which a count of 27.0 \pm 0.3 count s⁻¹ (corrected for decay) was obtained indicating bromide retention of 0.7mg atom g⁻¹. Further experiments indicated that there was no significant increase in the bromide uptake onto chlorinated γ -alumina by increasing the reaction time from 23h to 98h. One peculiarity in this reaction was the formation of multi-coloured rings in the alumina, figure 4.3.3, probably due to different surface species.

4.3.5 Interaction of [⁸²Br]-bromine labelled hydrogen bromide with uncalcined montmorillonite K10 at room temperature.

The results of this experiment indicated an immediate interaction between the hydrogen bromide and the uncalcined montmorillonite K10 (figure 4.3.4), involving an initial rapid increase in the count rate of the solid, followed by a more gradual increase reaching a plateau after 6min. Two aliquots of [⁸²Br]-bromine labelled hydrogen bromide, 1.02mmol and 1.02mmol [specific count rate of 675.1 \pm 1.5 count s⁻¹ (mg atom Br)⁻¹],

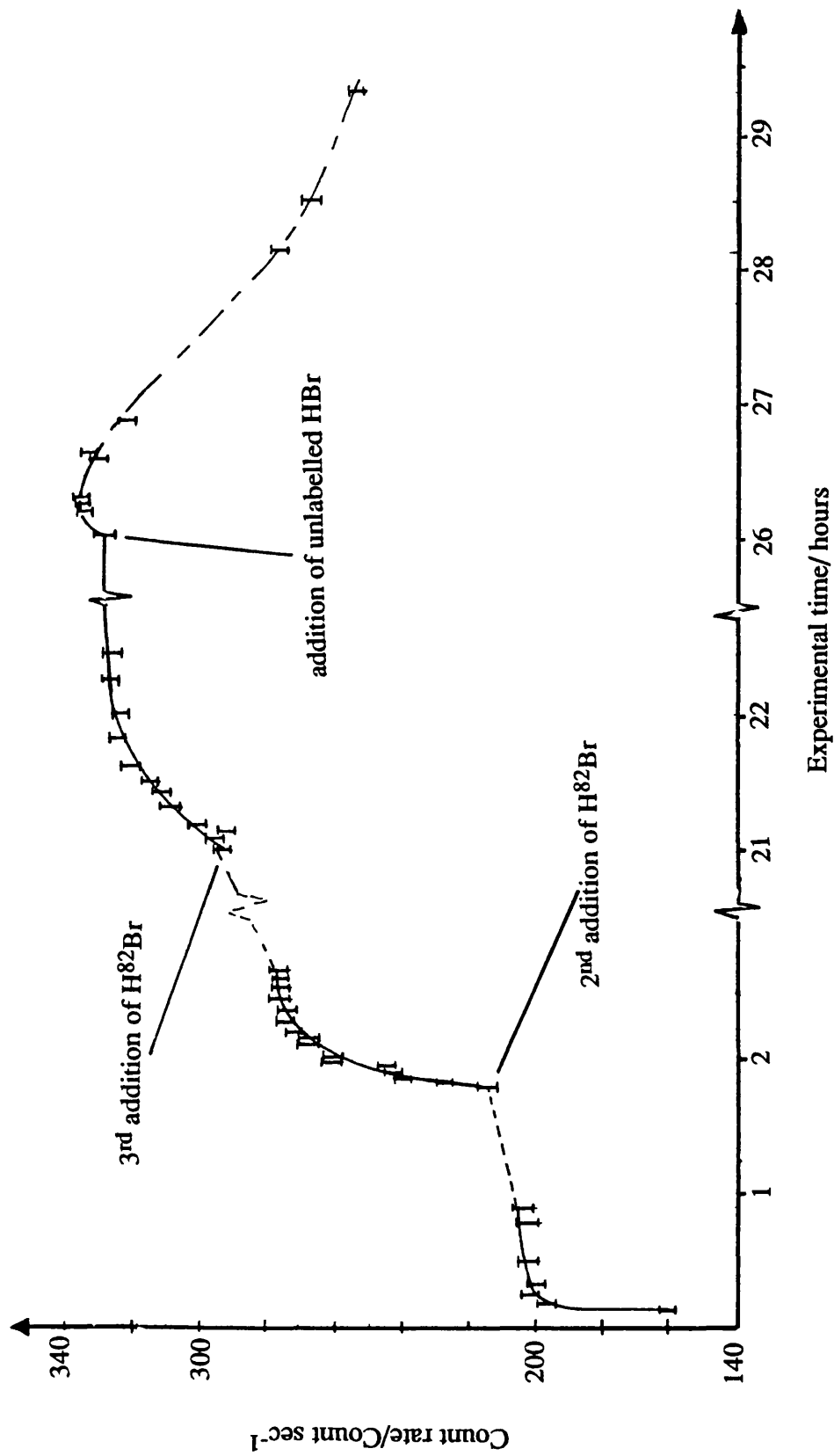


Figure 4.3.4. Surface count rate from the room temperature interaction of [⁸²Br]-bromine labelled hydrogen bromide with uncalcined montmorillonite K10.

were allowed to interact with uncalcined montmorillonite K10 (0.31g). The count rate of the montmorillonite after 23.0h was 126.3 count s⁻¹ corrected for decay to 326.7 ± 3.1 count s⁻¹, indicating a bromine uptake of 1.8mg atom g⁻¹. An aliquot of unlabelled hydrogen bromide (1.02mmol), was then condensed into the gas phase limb and allowed to interact with the halogenated montmorillonite K10. After 26h the count rate from the montmorillonite had dropped from 334.0 ± 3.4 count s⁻¹ (corrected for decay) to 196.4 ± 2.0 count s⁻¹ (corrected for decay), whilst the gas limb had increased from 1.5 ± 0.1 count s⁻¹ (corrected for decay) to 52.2 ± 1.4 count s⁻¹ (corrected for decay). For this exchange reaction the initial and final count rates (A₀ and A_t) were converted into specific count rates (S₀ and S_t), equations 4.3.1 and 4.3.2.

$$S_0 = \frac{A_0 \text{ count s}^{-1}}{\text{mg atom } ^{82}\text{Br}} = \frac{334}{0.496} = 673.39 \text{ count s}^{-1} (\text{mg atom Br})^{-1}$$

equation 4.3.1

$$S_t = \frac{A_t \text{ count s}^{-1}}{\text{mg atom } ^{82}\text{Br}} = \frac{196.4}{0.496} = 395.97 \text{ count s}^{-1} (\text{mg atom Br})^{-1}$$

equation 4.3.2.

The exchange factor (f) was then calculated using these specific count rates, equation 4.3.3.

$$f = \frac{S_0 - S_t}{S_0 - S}$$

equation 4.3.3.

S = calculated specific count rate assuming complete exchange.

$$S = \frac{\text{initial count rate}}{\text{mg atom } ^{82}\text{Br on surface} + \text{mg atom Br added to system}}$$

$$S = \frac{A_0 \text{ count s}^{-1}}{\text{mg atom } ^{82}\text{Br} + \text{mg atom Br}}$$

therefore:

$$f = \frac{673.39 - 395.97}{673.39 - 334/(0.496 + 1.02)}$$

$$f = 0.61 \pm 0.05$$

The montmorillonite was then pumped on a vacuum line for 20 min, the count rate falling from $218.0 \pm 2.1 \text{ count s}^{-1}$ (corrected for decay) to $84.2 \pm 0.9 \text{ count s}^{-1}$ (corrected for decay), a drop of 61.4%, indicating a bromine loss, after pumping, of $1.1 \text{ mg atom g}^{-1}$.

4.3.6 Interaction of [^{82}Br]-bromine labelled hydrogen bromide with calcined montmorillonite K10 at room temperature.

The results of this experiment indicated an immediate interaction between the hydrogen bromide and the montmorillonite K10 (figure 4.3.5), involving an initial rapid increase in the count rate of the solid, followed by a more gradual increase reaching a plateau after 4h. Three aliquots of [^{82}Br]-bromine labelled hydrogen bromide, 0.85mmol, 1.02mmol and 1.02mmol [specific count rate of $675.1 \pm 1.6 \text{ count s}^{-1} (\text{mg atom Br})^{-1}$], were allowed to interact with calcined montmorillonite (0.25g). The specific count rate was determined using the data in table 4.3.2a, where a known pressure of H^{82}Br (41 Torr) was reacted with excess NaOH. The molar quantity of hydrogen bromide was then

Table 4.3.2a. Count rates determined from the interaction of [⁸²Br]-bromine labelled hydrogen bromide with solid sodium hydroxide.

Time/h	Count	Count rate s ⁻¹	Phase	Corrected Count rates ⁻¹
4.05	10451	361.6	NaOH	391.0 ± 3.8
4.07	20113	364.4	NaOH	394.0 ± 2.8
4.08	20354	362.8	NaOH	392.5 ± 2.8
4.12	22645	365.8	NaOH	396.0 ± 2.6
4.15	20580	370.8	NaOH	401.7 ± 2.8
4.17	20134	368.8	NaOH	399.6 ± 2.8
4.93	20209	369.4	NaOH	406.3 ± 2.9
4.97	25461	370.6	NaOH	407.8 ± 2.6
5.45	21626	359.8	NaOH	399.6 ± 2.7
5.48	23599	365.9	NaOH	406.6 ± 2.6
12.27	20562	340.4	NaOH	431.1 ± 3.0
12.30	21350	335.2	NaOH	424.7 ± 2.9
12.33	20968	336.6	NaOH	426.5 ± 2.9
22.08	20082	298.4	NaOH	456.5 ± 3.2
22.18	100079	297.3	NaOH	455.7 ± 1.4
24.60	100125	286.1	NaOH	459.4 ± 1.5
24.72	100094	283.8	NaOH	456.8 ± 1.4
25.57	265181	277.8	NaOH	454.6 ± 0.9
27.35	131465	250.8	NaOH	424.6 ± 1.2
45.92	100030	193.5	NaOH	468.4 ± 1.5
46.07	101289	194.1	NaOH	471.2 ± 1.5
49.42	158773	180.9	NaOH	468.3 ± 1.2
52.72	100229	170.7	NaOH	471.1 ± 1.5
53.95	100031	165.3	NaOH	467.0 ± 1.5

calculated using equation 4.3.4.

$$\begin{aligned}
 PV &= nRT && \text{equation 4.3.4.} \\
 n &= \frac{PV}{RT} = \frac{41 * 310}{6.26 * 10^4 * 293} \\
 n &= 0.695\text{mmol}
 \end{aligned}$$

The average of the corrected count rates was then determined. As the count rate continued to increase for at least 27.5h only the last 5 count rates (a total of 560352 counts with 0.13% error) were used, equation 4.3.5.

$$\text{Average count rate} = \frac{468.4 + 471.2 + 468.3 + 471.1 + 467.0}{5}$$

equation 4.3.5.

$$\begin{aligned}
 \text{therefore} &= 469.2 \text{ count rate s}^{-1} \\
 0.695\text{mmol} &= 469.2 \text{ count rate s}^{-1} \\
 \text{so } 1.000\text{mmol} &= 675.1 \text{ count rate s}^{-1}
 \end{aligned}$$

All count rates determined from the interaction of montmorillonite K10 with [⁸²Br]-bromine labelled hydrogen bromide are given in table 4.3.2b. The count rate of the montmorillonite after 51.3h was measured at 140.4 count s⁻¹, corrected for decay to 379.0 ± 3.6 count s⁻¹. From this the bromine uptake was calculated, equations 4.3.6 & 4.3.7, at 2.2mg atom g⁻¹.

$$\frac{\text{count rate of solid}}{\text{weight of solid}} = \frac{379}{0.25\text{g}} = 1516 \text{ count rate g}^{-1}$$

equation 4.3.6.

$$\frac{\text{count rate g}^{-1}}{\text{specific count rate}} = \frac{1516}{675.1} = 2.2 \text{ mg atom Br g}^{-1}$$

equation 4.3.7.

An aliquot of unlabelled hydrogen bromide (1.02mmol), was then condensed into the gas phase limb and allowed to interact with the halogenated montmorillonite K10. After 28h the count rate from the montmorillonite had dropped from $343.8 \pm 2.3 \text{ count s}^{-1}$ (corrected for decay) to $172.8 \pm 1.7 \text{ count s}^{-1}$ (corrected for decay), whilst the gas limb had increased from $3.6 \pm 0.1 \text{ count s}^{-1}$ (corrected for decay) to $61.9 \pm 1.4 \text{ count s}^{-1}$ (corrected for decay). For this exchange reaction the initial and final count rates (A_0 and A_t) were converted into specific count rates (S_0 and S_t), equations 4.3.8 and 4.3.9.

$$S_0 = \frac{A_0 \text{ count s}^{-1}}{\text{mg atom } ^{82}\text{Br}} = \frac{343.8}{0.55} = 625.09 \text{ counts}^{-1} (\text{mg atom Br})^{-1}$$

equation 4.3.8.

$$S_t = \frac{A_t \text{ count s}^{-1}}{\text{mg atom } ^{82}\text{Br}} = \frac{172.8}{0.55} = 314.18 \text{ counts}^{-1} (\text{mg atom Br})^{-1}$$

equation 4.3.9.

The exchange factor (f) was calculated using these specific count rates, equation 4.3.10.

$$f = \frac{S_0 - S_t}{S_0 - S}$$

equation 4.3.10.

therefore:

$$f = \frac{625.09 - 314.18}{625.09 - 343.8/(0.55 + 1.02)}$$

Table 4.3.2b. Count rates determined from the interaction of montmorillonite K10 with [⁸²Br]-bromine labelled hydrogen bromide

Time/h	Count	Count rate s ⁻¹	Phase	Corrected Count rate s ⁻¹
0.85mmol H ⁸² Br introduced into the system.				
0.00	10016	60.7	Gas	60.7 ± 0.6
0.04	10024	66.2	K10	66.3 ± 0.7
0.07	10311	85.6	K10	85.8 ± 0.8
0.09	10215	93.4	K10	93.6 ± 0.9
0.12	11282	98.7	K10	99.1 ± 0.9
0.14	10033	104.5	K10	105.0 ± 1.0
0.15	10023	105.4	K10	105.9 ± 1.1
0.17	10055	108.7	K10	109.3 ± 1.1
0.19	10027	110.9	K10	111.6 ± 1.1
0.21	10028	114.5	K10	115.3 ± 1.2
0.25	13923	116.7	K10	117.6 ± 1.0
0.35	10143	118.1	K10	119.4 ± 1.2
0.37	10031	116.6	K10	118.0 ± 1.2
0.39	6108	33.9	Gas	34.3 ± 0.4
0.55	10206	118.8	K10	120.9 ± 1.2
0.57	21906	121.7	K10	123.9 ± 0.8
1.01	72875	127.3	K10	129.9 ± 0.5
1.12	67675	131.8	K10	134.8 ± 0.5
1.21	10625	133.1	K10	136.7 ± 1.3
3.57	10351	147.2	K10	158.9 ± 1.6
3.59	16229	145.0	K10	156.6 ± 1.2
4.11	10272	151.9	K10	164.7 ± 1.6

Table 4.3.2b cont'd

Time/h	Count	Count rate s ⁻¹	Phase	Corrected Count rate s ⁻¹
4.13	10040	150.1	K10	162.8 ± 1.6
4.15	22045	37.1	Gas	40.3 ± 0.3
5.10	25807	58.5	K10	64.6 ± 0.4
1.02mmol H ⁸² Br introduced into the system.				
5.19	11049	185.1	Gas	205.3 ± 2.0
5.20	12546	181.0	Gas	200.9 ± 1.8
5.23	20065	230.1	K10	255.2 ± 1.8
5.25	20200	233.3	K10	258.9 ± 1.8
5.35	20132	248.2	K10	276.4 ± 1.9
5.37	20242	247.2	K10	275.4 ± 1.9
5.39	24049	104.3	Gas	116.5 ± 0.8
5.42	20081	244.6	K10	273.0 ± 1.9
11.33	87117	198.8	K10	248.3 ± 0.8
11.41	25443	202.9	K10	254.1 ± 1.6
11.43	20054	208.5	K10	261.2 ± 1.8
11.46	24660	211.5	K10	265.3 ± 1.7
11.49	27613	212.6	K10	266.9 ± 1.6
11.51	22688	214.0	K10	268.9 ± 1.8
12.00	20127	218.1	K10	274.8 ± 1.9
12.02	20067	77.2	Gas	97.6 ± 0.7
12.07	29704	218.1	K10	275.4 ± 1.6
12.10	20726	222.8	K10	281.7 ± 2.0
12.12	26294	220.6	K10	279.0 ± 1.7
12.14	20882	223.1	K10	282.3 ± 2.0
20.03	12907	144.7	K10	212.9 ± 1.9

Table 4.3.2b cont'd

Time /h	Count	Count rate s ⁻¹	Phase	Corrected Count rate s ⁻¹
20.05	10752	149.3	K10	219.8 ± 2.1
20.55	11836	182.4	K10	272.8 ± 2.5
20.57	46906	57.9	Gas	87.2 ± 0.4
21.11	10618	172.6	K10	259.6 ± 2.5
21.12	11288	175.8	K10	264.5 ± 2.5
21.14	10834	173.1	K10	260.5 ± 2.5
22.00	10872	181.8	K10	277.7 ± 2.7
22.02	13309	183.3	K10	280.2 ± 2.4
24.00	10044	143.3	K10	227.4 ± 2.3
24.02	10296	80.3	Gas	128.4 ± 1.3
1.02mmol H ⁸² Br introduced into the system.				
24.06	10849	177.3	K10	281.9 ± 2.7
24.07	39043	181.8	K10	289.2 ± 1.5
24.49	11695	206.3	K10	332.6 ± 3.1
24.50	22827	204.9	K10	330.5 ± 2.2
25.22	20335	203.1	K10	331.1 ± 2.3
25.31	20953	202.2	K10	330.6 ± 2.3
45.21	48765	143.6	K10	343.9 ± 1.6
45.27	27115	142.2	K10	341.0 ± 2.1
45.31	22930	143.1	K10	343.8 ± 2.3
51.28	30041	125.5	K10	338.2 ± 2.0
1.02mmol unlabelled HBr introduced into system.				
51.34	11080	140.4	K10	379.0 ± 3.6
51.36	10117	136.7	K10	369.2 ± 3.7
51.37	10429	137.2	K10	370.7 ± 3.6

Table 4.3.2b cont'd

Time /h	Count	Count rate s⁻¹	Phase	Corrected Count rate s⁻¹
51.39	10806	136.6	K10	369.3 ± 3.6
51.41	10937	135.9	K10	367.5 ± 3.5
51.47	10294	136.2	K10	369.0 ± 3.6
51.49	904	1.3	Gas	3.6 ± 0.1
52.00	10064	128.7	K10	350.2 ± 3.5
52.02	10147	127.5	K10	347.1 ± 3.4
52.18	10561	120.4	K10	329.6 ± 3.2
52.20	1050	3.5	Gas	9.7 ± 0.3
52.25	10100	117.9	K10	323.3 ± 3.2
52.40	10048	111.4	K10	307.1 ± 3.1
53.48	10022	92.7	K10	261.2 ± 2.6
53.50	3112	12.3	Gas	35.0 ± 0.6
53.55	10208	91.5	K10	258.5 ± 2.6
54.15	10092	87.8	K10	249.4 ± 2.5
79.15	10042	38.0	K10	174.6 ± 1.7
79.20	10759	37.5	K10	172.8 ± 1.7
79.25	2041	13.0	Gas	61.9 ± 1.4
103.14	10037	24.1	K10	176.1 ± 1.8
Sample degassed under vacuum for 15min.				
103.35	4167	6.9	K10	50.4 ± 0.8

$$f = 0.77 \pm 0.05$$

The montmorillonite K10 was pumped on a vacuum line for 20 mins, the count rate falling from 176.1 count s⁻¹ (corrected for decay) to 50.4 count s⁻¹ (corrected for decay), a drop of 71.4%, indicating a bromine loss, after pumping, of 1.5mg atom g⁻¹.

4.3.7 Interaction of [⁸²Br]-bromine labelled hydrogen bromide with chlorinated montmorillonite K10 at room temperature.

The results of this experiment indicated an immediate interaction between hydrogen bromide and montmorillonite K10 pretreated with carbonyl chloride at 523K for 12h, involving an initial rapid increase in the count rate of the solid, followed by a more gradual increase reaching a plateau after 2h. Two aliquots of [⁸²Br]-bromine labelled hydrogen bromide, 1.19mmol and 1.02mmol (specific count rate of 260.8 ± 0.9 count s⁻¹ (mg atom Br)⁻¹), were allowed to interact with the chlorinated montmorillonite K10 (0.17g). The count rate of the chlorinated montmorillonite K10, after 24.2h, was measured at 113.2 ± 1.2 count s⁻¹ (corrected for decay), whilst the count rate of the gas phase was measured at 41.2 ± 0.5 count s⁻¹ (corrected for decay), giving a count for the solid of 72.0 ± 1.2 count s⁻¹, indicating a bromide uptake of 1.6mg atom g⁻¹, table 4.3.1. The montmorillonite K10 was then degassed under *vacuo* for 10min after which a count of 48.4 ± 0.5 count s⁻¹ (corrected for decay) was obtained, indicating bromide retention of 1.1mg atom g⁻¹.

4.3.8 Reaction of [^{82}Br]-bromine labelled hydrogen bromide with but-1-ene in the presence of calcined Degussa 'C' γ -alumina at 373K.

The results of the interaction between [^{82}Br]-bromine labelled hydrogen bromide and but-1-ene, in the presence of calcined γ -alumina, (figure 4.3.6), involved an initial rapid increase in the count rate of the solid, followed by a more gradual increase. An aliquot of [^{82}Br]-bromine labelled hydrogen bromide, 2.0mmol [specific count rate of $584.1 \pm 1.5 \text{ count s}^{-1} (\text{mg atom Br})^{-1}$], and an aliquot of but-1-ene, 2.0mmol, were condensed into the reservoir bulb and warmed to room temperature. The reaction mixture was then allowed to interact with the calcined γ -alumina (0.10g) present in the counting limb. The count rate of the γ -alumina after 22h, at room temperature, was measured at $767.2 \pm 5.2 \text{ count s}^{-1}$ (corrected for decay), indicating a bromide uptake of $13.1 \text{ mg atom g}^{-1}$ (table 4.3.2). The counting limb of the reaction vessel was then heated at 373K for 7h. The count rate obtained from the γ -alumina, immediately after this treatment, was measured at $68.2 \pm 0.7 \text{ counts}^{-1}$ (corrected for decay), indicating a decrease in bromide content to $1.2 \text{ mg atom g}^{-1}$. The reaction mixture was left for a further 50h, at room temperature, after which time the count rate obtained from the γ -alumina was measured at $394.2 \pm 2.8 \text{ count s}^{-1}$ (corrected for decay), indicating that the bromide content had increased to $6.7 \text{ mg atom g}^{-1}$. The reaction vessel was transferred to a vacuum line and its contents degassed under *vacuo* for 60mins, resulting in a count rate of $35.3 \pm 0.5 \text{ count s}^{-1}$ (corrected for decay) for the γ -alumina, indicating a bromide retention of $0.6 \text{ mg atom g}^{-1}$.

During this reaction process the γ -alumina present in the counting limb went through a series of colour changes. Initially the γ -alumina was off-white, but after the room temperature interaction of hydrogen bromide and but-1-ene, for 22h, the γ -alumina had become brilliant white in colour. On heating the contents of the counting limb at 373K for 7h, the colour of the γ -alumina had changed from brilliant white to faint purple. The brilliant white colouration returned after the reaction mixture was allowed to stand, at room temperature, for 50h. After degassing the contents of the reaction vessel, the γ -alumina once again changed colour from brilliant white to faint purple. These colour

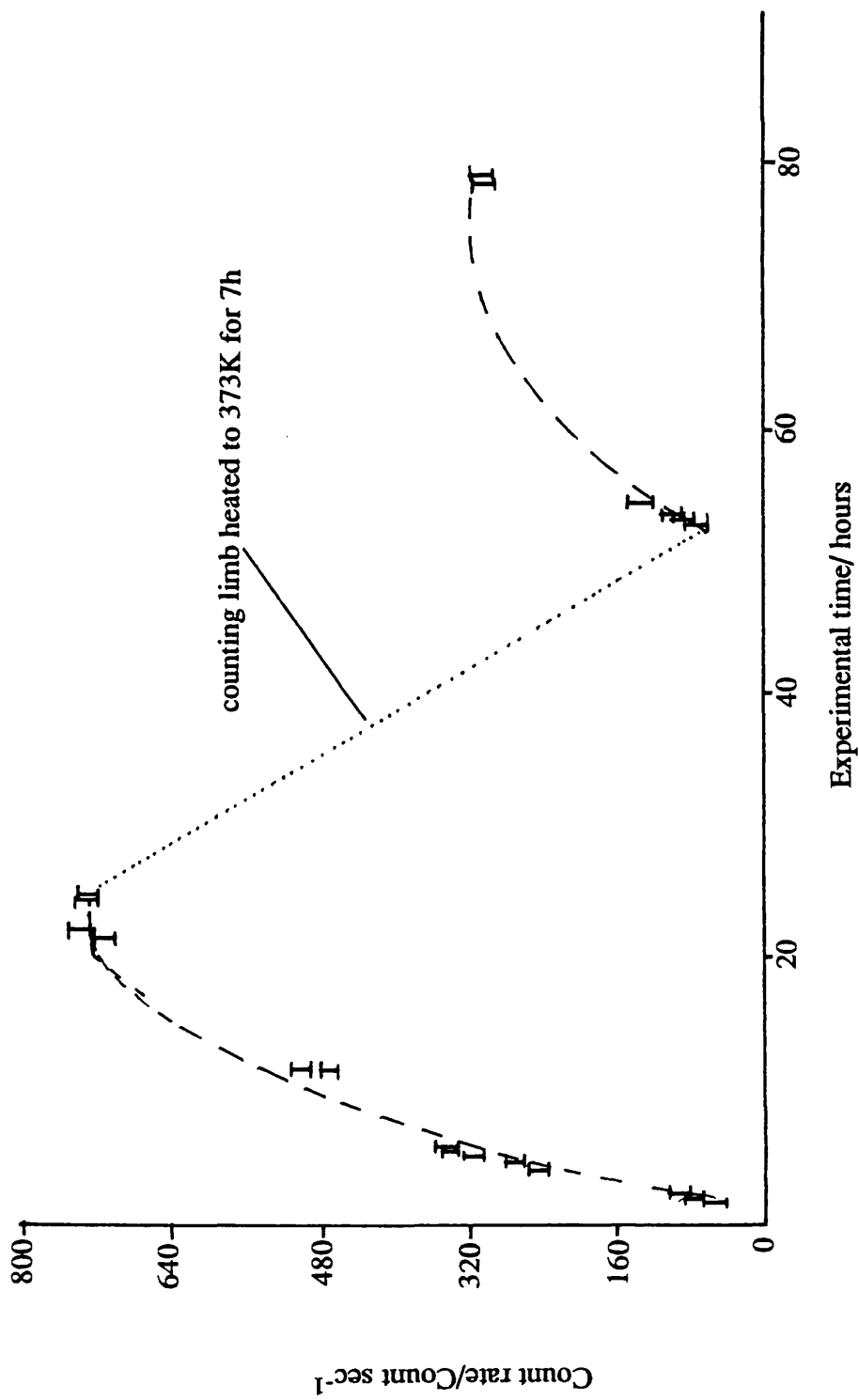


Figure 4.3.6. Surface count rate from the interaction of [⁸²Br]-bromine labelled hydrogen bromide with but-1-ene, in the presence of calcined γ -alumina.

changes could be correlated with the count rates observed; the highest count rates were observed when the γ -alumina was brilliant white and the lowest observed when the γ -alumina was faint purple.

4.3.9 Reaction of [^{82}Br]-bromine labelled hydrogen bromide with but-1-ene in the presence of calcined montmorillonite K10 at 373K.

The experimental procedure for the investigation was the same as for the interaction between [^{82}Br]-bromine labelled hydrogen bromide and but-1-ene, in the presence of γ -alumina. The results from this investigation have shown similar trends to those observed in the γ -alumina experiment, table 4.3.3. The initial bromine uptake value at $4.3 \text{ mg atom Br g}^{-1}$ was lower than that observed for γ -alumina, however after heating to 373K the bromine retention values were very similar. Unlike the γ -alumina experiment, no significant colour changes were observed in the montmorillonite K10 interaction.

4.3.10 Interaction of [^{82}Br]-bromine labelled hydrogen bromide with montmorillonite K10, treated with pyridine, at room temperature.

The results of this experiment indicated an immediate interaction between the hydrogen bromide and the montmorillonite, involving an initial rapid increase in the count rate of the solid, followed by a more gradual increase levelling to a plateau. Two aliquots of [^{82}Br]-bromine labelled hydrogen bromide, 1.22mmol and 1.36mmol [specific count rate of $199.6 \pm 0.7 \text{ count s}^{-1} (\text{mg atom Br})^{-1}$], were allowed to interact with montmorillonite K10 (0.13g) pretreated with pyridine. The count rate of the montmorillonite K10 was measured at $86.0 \pm 0.9 \text{ count s}^{-1}$ (corrected for decay), after

Table 4.3.3. Uptake of [^{82}Br]-bromine labelled hydrogen bromide onto solid supports, in the presence of organic compounds.

	Room temperature uptake	retention after heat treatment	further uptake	retention after pumping of solid
γ -alumina + butene	13.9	1.0	6.0	0.5
montmorillonite K10 + butene	4.3	1.1	3.5	
montmorillonite K10 + pyridine	4.3			2.2
montmorillonite K10 treated with carbonyl chloride + pyridine	4.8			3.1

all values in mg atom Br g⁻¹

60sec, whilst the gas phase count rate was measured at $14.2 \pm 0.2 \text{ count s}^{-1}$ (corrected for decay), indicating a hydrogen bromide uptake of $2.8 \text{ mg atom g}^{-1}$, table 4.3.3. After 1.8h the count rate of the montmorillonite K10 had risen to $103.2 \pm 1.0 \text{ count s}^{-1}$ (corrected for decay), whilst the gas phase count rate was measured at $15.4 \pm 0.2 \text{ count s}^{-1}$ (corrected for decay), indicating an increase in bromide content to $3.4 \text{ mg atom g}^{-1}$. The second aliquot of [^{82}Br]-bromine labelled hydrogen bromide was then introduced resulting in initial count rates for the montmorillonite K10 of $142.8 \pm 1.4 \text{ count s}^{-1}$ (corrected for decay), and $42.1 \pm 0.4 \text{ count s}^{-1}$ (corrected for decay) for the gas phase indicating a bromide content of $3.9 \text{ mg atom g}^{-1}$. The reaction mixture was then allowed to stand at room temperature, for 16h, after which time the count rates were measured at $149.7 \pm 1.5 \text{ count s}^{-1}$ (corrected for decay) for the montmorillonite K10 and $37.9 \pm 0.4 \text{ count s}^{-1}$ (corrected for decay) for the gas phase, indicating a bromide content of $4.3 \text{ mg atom g}^{-1}$. The counting vessel was then placed on a vacuum line and the contents degassed under *vacuo* for 10min, before the final count rate of the montmorillonite was measured, $56.2 \pm 0.6 \text{ count s}^{-1}$ (corrected for decay), indicating bromide retention of $2.2 \text{ mg atom g}^{-1}$.

4.3.11 Interaction of [^{82}Br]-bromine labelled hydrogen bromide with chlorinated montmorillonite K10, treated with pyridine, at room temperature.

The experimental procedure for this investigation of the was the same as for the interaction between [^{82}Br]-bromine labelled hydrogen bromide and calcined montmorillonite K10 pretreated with pyridine. The results from this investigation have indicated greater bromine uptake values at 4.8 and $3.1 \text{ mg atom Br g}^{-1}$, table 4.3.3, than those observed in experiment 4.3.10.

4.3.12 Reaction of hydrogen bromide with but-1-ene at 373K.

The vapour phase reaction products from the interaction between hydrogen bromide and but-1-ene, at 373K for 12h, were analysed using FTIR spectroscopy. The reaction product vapour phase included absorption bands due to 2-bromobutane, but-1-ene and hydrogen bromide, table 4.3.4.

4.3.13 Reaction of hydrogen bromide with but-1-ene (mol ratio 3:2) in the presence of calcined Degussa 'C' γ -alumina at 373K.

Infrared analysis of the reaction product vapour phase indicated absorption bands due to the presence of 2-bromobutane and but-2-ene, table 4.3.4. Gas chromatography mass spectroscopy carried out on these volatile products confirmed the FTIR data, showing peaks due to the presence of 2-bromobutane (93.0%) and butene (5.0%), table 4.3.5. It was not possible to resolve the different butene isomers by the GCMS technique.

4.3.14 Reaction of hydrogen bromide with but-1-ene (mol ratio 1:1) in the presence of calcined Degussa 'C' γ -alumina at 373K.

Infrared analysis of the reaction product vapour phase indicated absorption bands due to the presence of 2-bromobutane and but-2-ene (table 4.3.4), whilst GCMS analysis of the volatile products confirmed the FTIR data by indicating the presence of 2-bromobutane (92.2%) and butene (7.1%), table 4.3.5. Neutron activation analysis of the γ -alumina, after the reaction, indicated a bromide content of 0.8mg atom g⁻¹, table 3.2.1.

In the ²⁷Al-MAS NMR spectrum of the brominated γ -alumina, figure 4.3.7, two

Table 4.3.4. Vapour phase products identified, by FTIR analysis, from the interaction of hydrogen bromide with butene, in the presence of modified aluminas.

Reagent	Support	Bromobutane	But-1-ene	But-2-ene	Hydrogen bromide	Hydrogen chloride
But-1-ene		✓	✓	✓	✓	
But-1-ene	γ-alumina	✓		✓	✓	
But-1-ene	β-alumina	✓				
But-2-ene	Cl-alumina	✓		✓	✓	✓

Table 4.3.5. Reaction products from the interaction of hydrogen bromide with butene, in the presence of calcined γ -alumina.

Reagent	Ratio		Products			
	Butene : HBr	Butene	2-bromobutane	Octene	2-chlorobutane	
But-1-ene	2:3	5	93	0	0	
But-1-ene	1:1	7	92	0	0	
But-2-ene	2:3	0	95.5	0	0	
But-2-ene	1:1	16	72	10	2	
But-2-ene	3:2	6	79	13	1	

all results are in mol %

resonance signals were observed due to an aluminium_(oct) environment, at 4.69ppm, and an aluminium_(tet) environment, at 52.8ppm with reference to AlCl₃. DRIFTS analysis of the brominated γ -alumina (figure 4.3.8) indicated bands at 1647cm⁻¹ and 1550cm⁻¹, due to the presence of organic species adsorbed on the surface.

4.3.15 Reaction of hydrogen bromide with but-1-ene (mol ratio 1:1) in the presence of dibromomethane brominated γ -alumina at 373K.

The vapour phase reaction products from the interaction between hydrogen bromide and but-1-ene in the presence γ -alumina, treated with dibromomethane at 523K for 120h, at 373K, were analysed using FTIR spectroscopy. This analysis of the reaction product vapour phase indicated absorption bands due to 2-bromobutane, table 4.3.4. There was however no evidence for the presence of any butenes.

4.3.16 Reaction of hydrogen bromide with but-2-ene (mol ratio 3:2) in the presence of calcined Degussa 'C' γ -alumina at 373K.

Infrared analysis of the reaction product vapour phase indicated absorption bands due to the presence of 2-bromobutane (table 4.3.4), whilst GCMS analysis of the volatile products also indicated the presence of 2-bromobutane (95.5%), table 4.3.5. There was no evidence for the presence of any unreacted but-2-ene.

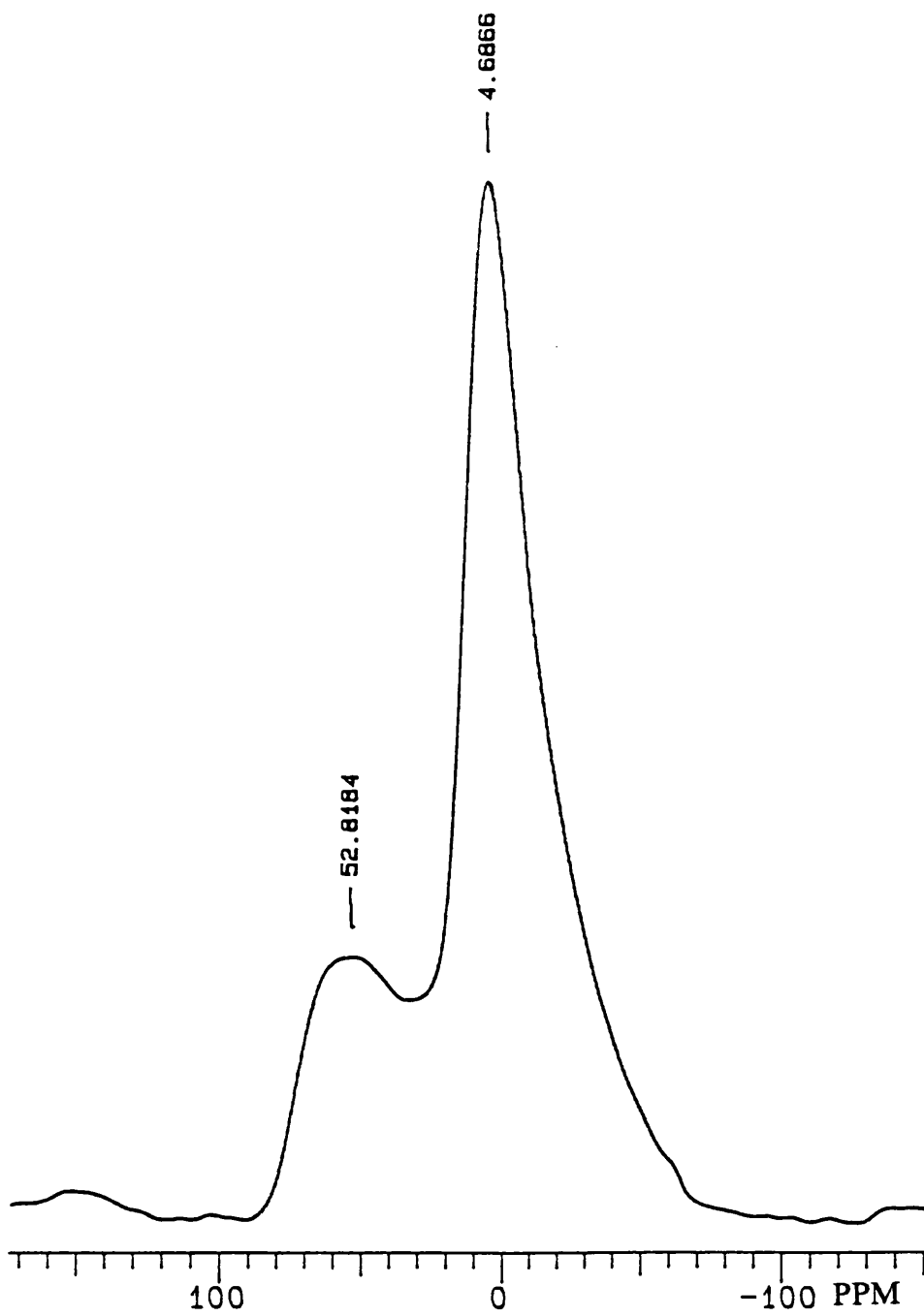


Figure 4.3.7. ^{27}Al MAS NMR Spectrum of γ -alumina after the interaction of hydrogen bromide and but-1-ene at 373K.

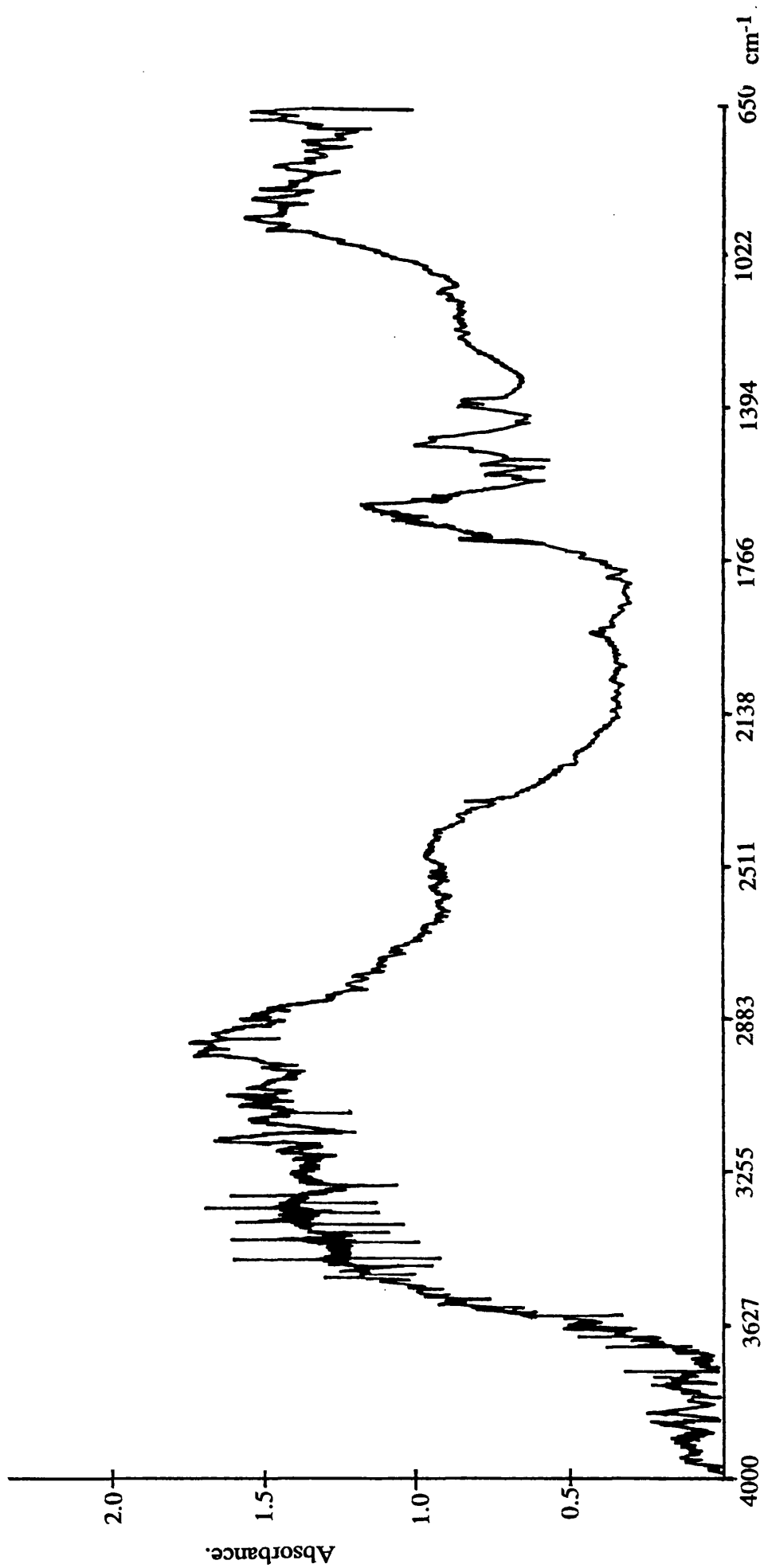


Figure 4.3.8. DRIFT spectrum of γ -alumina after the interaction of hydrogen bromide and but-1-ene.

4.3.17 Reaction of hydrogen bromide with but-2-ene (mol ratio 1:1) in the presence of calcined Degussa 'C' γ -alumina at 373K.

Infrared analysis of the reaction product vapour phase for the interaction of hydrogen bromide with but-2-ene, in the presence of calcined Degussa 'C' γ -alumina, at 373K showed absorption bands due to the presence of 2-bromobutane and but-2-ene, table 4.3.4. GCMS analysis of these volatile products indicated the presence of 2-bromobutane (72%), butene (16%), C_8H_{16} isomers (10%) and chloromethane (2%), table 4.3.5. This formation of C_8H_{16} oligomers suggests more than a simple hydrobromination reaction was occurring in the presence of γ -alumina.

4.3.18 Reaction of hydrogen bromide with but-2-ene (mol ratio 2:3) in the presence of calcined Degussa 'C' γ -alumina at 373K.

The procedure and results for the interaction of hydrogen bromide with but-2-ene (mol ratio 2:3), in the presence of calcined Degussa 'C' γ -alumina, at 373K are similar to those described in section 4.3.17. The results from the gas phase infrared analysis are given in table 4.3.4 and the GCMS analysis in table 4.3.5.

4.3.19 Reaction of hydrogen bromide with but-2-ene (mol ratio 1:1) in the presence of chlorinated γ -alumina at 373K.

Infrared analysis of the reaction product vapour phase for the interaction of hydrogen bromide with but-2-ene (mol ratio 1:1) in the presence of γ -alumina treated with carbonyl chloride at 523K for 12h, at 373K, showed absorption bands due to the presence

of 2-bromobutane, hydrogen chloride, hydrogen bromide and but-2-ene, table 4.3.4.

4.3.20 Reaction of 1,9-decadiene with 48% hydrobromic acid in the presence of uncalcined Degussa 'C' γ -alumina.

The results from this experiment indicate, from GC analysis (table 4.3.6), a large amount of unreacted 1,9-decadiene (76.1 mol%) still present in the reaction mixture after 70min. The reaction products from the hydrobromination of 1,9-decadiene with 48% hydrobromic acid, in the presence of uncalcined γ -alumina, included the formation of the 2,9-dibromodecane (3.3 mol%) and 2,8-dibromodecane (3.4 mol%) isomers, in an approximate 1:1 ratio. Several bromodecene isomers (2.0 mol%) were also detected.

4.3.21 Reaction of 1,9-decadiene with 48% hydrobromic acid in the presence of calcined Degussa 'C' γ -alumina.

The results from the interaction of 1,9-decadiene with 48% hydrobromic acid in the presence of calcined Degussa 'C' γ -alumina indicated, from GC analysis (table 4.3.6), a large quantity of unreacted 1,9-decadiene (75.1 mol%) present in the reaction mixture after 330 mins. The reaction products included the 2,9-dibromodecane (12.6 mol%) and 2,8-dibromodecane (7.1 mol%) isomers, in the approximate ratio of 2:1, and also several bromodecene isomers (5.3 mol%).

Table 4.3.6. Reaction products from the interaction of aqueous hydrogen bromide (48%) and/or hydrogen bromide gas with 1,9-decadiene.

	1,9-C ₁₀	BrC ₁₀	1,10-Br ₂ C ₁₀	1,9-Br ₂ C ₁₀	2,8-Br ₂ C ₁₀	2,9-Br ₂ C ₁₀
48% hydrobromic acid plus hydrogen bromide sparge 333K/5hours	0.2	18.7	45.2	17.8	-	-
48% hydrobromic acid plus hydrogen bromide sparge 333K/5hours (Teepol)	-	7.2	-	-	22.8	66.6
48% hydrobromic acid 363K/1hour (montmorillonite)	39.6	19.1	-	-	14.8	26.5
48% hydrobromic acid 363K/5hours (γ-alumina)	75.1	5.3	-	-	7.1	12.6
48% hydrobromic acid 363K/5hours (Brockmann alumina)	88.7	2.2	-	-	2.8	5.6
hydrogen bromide sparge 293K/1hour (montmorillonite)	-	0.4	-	-	27.3	64.9
hydrogen bromide sparge 293K/2.75hours (γ-alumina)	24.7	38.4	-	-	2.4	20.9

All values are in mol%.

Key for table 4.3.6 on next page.

Key for table 4.3.6.

$1,9-C_{10}$	→	1,9-decadiene
BrC_{10}	→	bromodecene
$1,10-Br_2C_{10}$	→	1,10-dibromodecane
$1,9-Br_2C_{10}$	→	1,9-dibromodecane
$2,8-Br_2C_{10}$	→	2,8-dibromodecane
$2,9-Br_2C_{10}$	→	2,9-dibromodecane

4.3.22 Reaction of 1,9-decadiene with 48% hydrobromic acid in the presence of calcined acidic, Brockmann 1 standard grade alumina.

The procedure for the interaction of 1,9-decadiene with 48% hydrobromic acid in the presence of calcined acidic, Brockmann 1 standard grade alumina was similar to that for the reaction of 1,9-decadiene with 48% hydrobromic acid in the presence of calcined Degussa 'C' γ -alumina, section 4.3.21. The results of the GC analysis from the reaction product are given in table 4.3.6.

4.3.23 Reaction of 1,9-decadiene with 48% hydrobromic acid in the presence of calcined montmorillonite K10.

The procedure for the interaction of 1,9-decadiene with 48% hydrobromic acid in the presence of calcined montmorillonite K10 was similar to that for the reaction of 1,9-decadiene with 48% hydrobromic acid in the presence of calcined Degussa 'C' γ -alumina, section 4.3.21. The results of the GC analysis from the reaction product, given in table 4.3.6, indicate that montmorillonite K10 was the most efficient of the solid supports in catalysing the hydrobromination of 1,9-decadiene.

4.3.24 Reaction of 1,9-decadiene with hydrogen bromide gas, at 318K, in the presence of calcined Degussa 'C' γ -alumina.

The results from the interaction of 1,9-decadiene with sparged hydrogen bromide gas, at 318K, in the presence of calcined Degussa 'C' γ -alumina indicated, from GC analysis (table 4.3.6), that a large quantity of unreacted 1,9-decadiene (76 mol%)

remained in the reaction mixture after 70min.

4.3.25 Reaction of 1,9-decadiene with hydrogen bromide gas in the presence of calcined Degussa 'C' γ -alumina, at room temperature.

The results from the interaction of 1,9-decadiene with sparged hydrogen bromide gas, in the presence of calcined Degussa 'C' γ -alumina, at room temperature show from GC analysis (table 4.3.6), that only a small quantity of unreacted 1,9-decadiene (24.7 mol%) was present in the reaction mixture after 165min. This hydrobromination of 1,9-decadiene resulted in the formation of 2,9-dibromodecane (20.9 mol%) and 2,8-dibromodecane (2.4 mol%) isomers, in the approximate ratio of 8:1, and also a quantity of bromodecene isomers (38.4 mol%).

4.3.26 Reaction of 1,9-decadiene with hydrogen bromide gas in the presence of calcined montmorillonite K10.

The results from the interaction of 1,9-decadiene with hydrogen bromide gas in the presence of calcined montmorillonite K10, indicated, from GC analysis (table 4.3.6), that none of the 1,9-decadiene remained after 45mins of sparging with hydrogen bromide. The results of the GC analysis from the reaction product after 120min indicated only a trace amount of bromodecene (0.4 mol%) present. The major constituents were the 2,9-dibromodecane (62.1 mol%) and 2,8-dibromodecane (27.9 mol%) isomers. These results suggest that under dry conditions montmorillonite K10 was the most effective solid support in catalysing the hydrobromination of 2,9-decadiene.

4.3.27 Reaction of 1,9-decadiene with hydrogen bromide gas in the presence of calcined montmorillonite K10.

The results of the interaction of 1,9-decadiene with hydrogen bromide gas in the presence of calcined montmorillonite K10, indicated, from GCMS analysis (table 4.3.7), that a large quantity of unreacted 1,9-decadiene (73.2 mol%) and several isomers of decadiene (6.6 mol%) were present in the final reaction mixture. This was expected as there was a large excess of 1,9-decadiene in the initial reaction mixture. The main hydrobromination products were 9-bromodec-1-ene (10.1 mol%), with several other isomers of bromodecene (4.6 mol%), the 2,9-decadiene (1.3 mol%) and 2,8-dibromodecane (0.2 mol%) isomers along with a small quantity of tribromodecane isomers (2.95 mol%).

4.3.28 Reaction of 1,9-decadiene with hydrogen bromide gas in the presence of chlorinated γ -alumina.

The experimental procedure for the interaction of 1,9-decadiene with hydrogen bromide gas in the presence of calcined γ -alumina, treated with carbonyl chloride at 523K for 12h, is similar to those for the interaction of 1,9-decadiene with hydrogen bromide gas in the presence of calcined montmorillonite K10. The results from the GCMS analysis of the reaction products, given in table 4.3.7, show the product composition to be similar to that from the calcined montmorillonite K10 experiment (expt 4.3.27)

Table 4.3.7. Reaction products from the room temperature interaction of hydrogen bromide gas with excess 1,9-decadiene, under static conditions.

	K10 treated with carbonyl chloride	γ -Alumina treated with carbonyl chloride	Brominated γ -alumina	Montmorillonite K10	Bentonite
1,9-decadiene	40.2	73.3	73.1	55.0	92.5
other decadiene isomers	34.0	5.6	4.2	19.7	2.7
8-bromodecene	1.8	2.6	0.5	0.8	0.1
9-bromodecene	10.9	10.0	12.5	10.1	2.3
other bromodecene isomers	4.8	1.5	2.7	3.8	0.4
2,9-bromochlorodecane	0.1	0.1	0.1	0	0.0
2,8-dibromodecane	0.6	0.8	0.4	0.2	0.1
2,9-dibromodecane	1.8	1.1	3.4	1.3	1.0
tribromodecane	3.0	0.2	1.8	3.0	0.1

All results are in mol %

4.3.29 Reaction of 1,9-decadiene with hydrogen bromide gas in the presence of brominated γ -alumina.

The experimental procedure for the interaction of 1,9-decadiene with hydrogen bromide gas in the presence of calcined γ -alumina treated with dibromine at 523K for 120h, was the same as for the interaction of 1,9-decadiene with hydrogen bromide gas in the presence of calcined montmorillonite K10. The results from the GCMS analysis of the reaction products, given in table 4.3.7, show the product composition to be similar to that from the calcined montmorillonite K10 and chlorinated γ -alumina experiments.

4.3.30 Reaction of 1,9-decadiene with hydrogen bromide gas in the presence of chlorinated montmorillonite K10.

The experimental procedure for the interaction of 1,9-decadiene with hydrogen bromide gas in the presence of calcined montmorillonite K10, treated with carbonyl chloride at 523K for 12h, was the same as for the interaction of 1,9-decadiene with hydrogen bromide gas in the presence of calcined montmorillonite K10. Although the results from the GCMS analysis of the reaction products, given in table 4.3.7, show the product composition to be similar to the previous reactions (expt 4.3.27-29), the composition of the decadiene in the reaction product was significantly different. Only 46.9 mol% was 1,9-decadiene and 28.3 mol% isomers of decadiene other than 1,9-decadiene. This increased quantity of decadiene isomers suggests that although the chlorinated montmorillonite K10 does not increase the hydrobromination process it does catalyse the isomerisation process.

4.3.31 Reaction of 1,9-decadiene with hydrogen bromide gas in the presence of bentonite.

The experimental procedure for the interaction of 1,9-decadiene with hydrogen bromide gas in the presence of bentonite, was the same as for the interaction of 1,9-decadiene with hydrogen bromide gas in the presence of calcined montmorillonite K10. The results from the GCMS analysis, given in table 4.3.7, indicate that bentonite was the least successful solid support for catalysing the hydrobromination reaction, with 91.5 mol% 1,9-decadiene remaining in the reaction product. It was noted in this experiment that on opening the reaction vessel a white vapour was evolved (hydrogen bromide); this did not occur with any of the previous experiments (expt 4.3.27-30) in which a greater degree of hydrobromination occurred.

4.3.32 Interaction of [⁸²Br]-bromine labelled hydrogen bromide and decadiene solution with montmorillonite K10 and decadiene at room temperature.

The results from this experiment (figure 4.3.9) indicated a gradual transfer of the [⁸²Br]-bromine labelled hydrogen bromide from the limb containing [⁸²Br]-bromine labelled hydrogen bromide and 1,9-decadiene to the limb containing 1,9-decadiene and calcined montmorillonite K10. The limb containing [⁸²Br]-bromine labelled hydrogen bromide and 1,9-decadiene was opened to the limb containing 1,9-decadiene and montmorillonite K10; after 20mins the surface of the montmorillonite had an orange colour. The count rate from the montmorillonite limb was measured at $338.2 \pm 1.8 \text{ count s}^{-1}$ (corrected for decay), whilst the count rate for the 1,9-decadiene limb was measured at $605.5 \pm 2.8 \text{ count s}^{-1}$ (corrected for decay). After 2.1h the count rates had almost converged at $430.4 \pm 2.2 \text{ count s}^{-1}$ (corrected for decay) for the montmorillonite and $464.2 \pm 2.1 \text{ count s}^{-1}$ (corrected for decay) for the 1,9-decadiene. After a further 14h the count

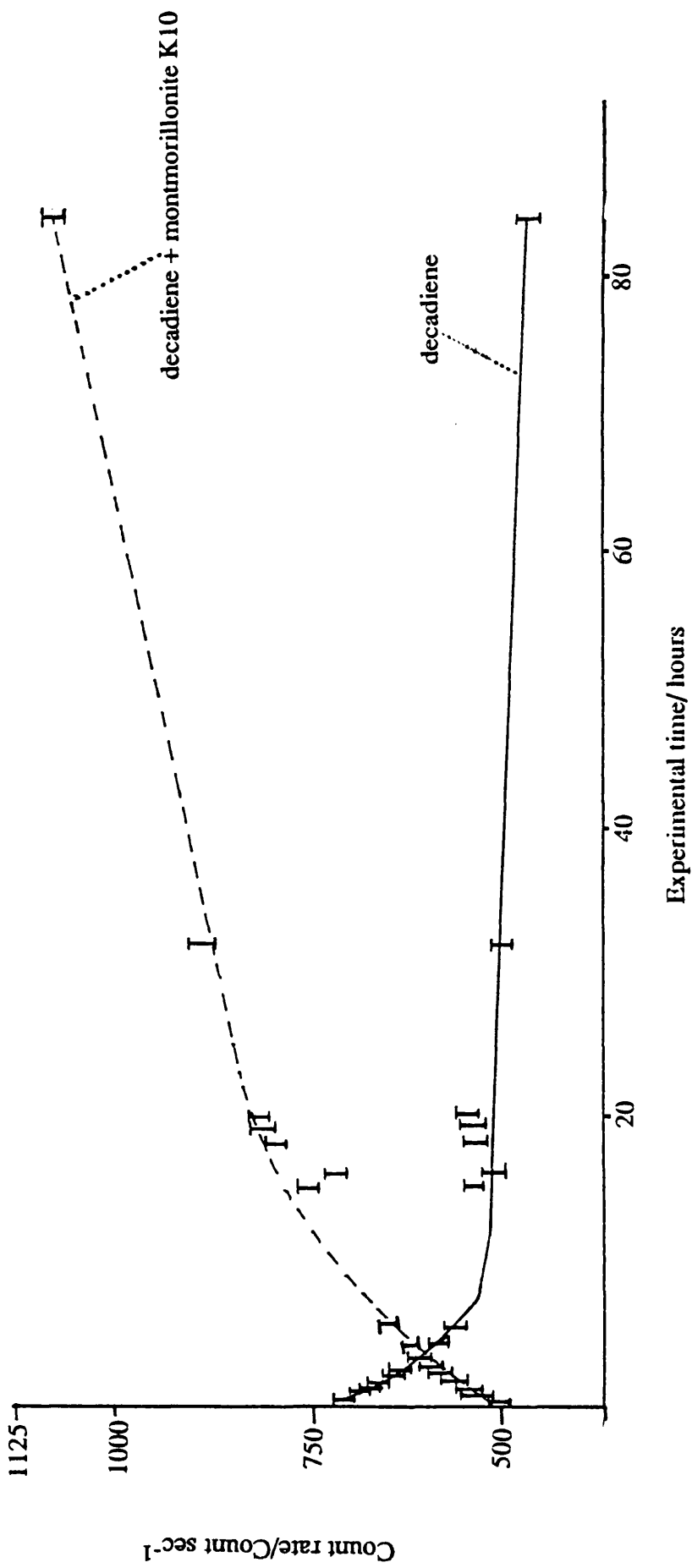


Figure 4.3.9. Count rate obtained from the interaction of [⁸²Br]-bromine labelled hydrogen bromide and decadiene solution with montmorillonite K10 and decadiene.

rate for the montmorillonite had increased to 671.0 ± 3.1 count s^{-1} (corrected for decay), whilst the count rate for the 1,9-decadiene had fallen to 381.7 ± 2.4 count s^{-1} (corrected for decay). The final count rates, 1202.2 ± 3.8 count s^{-1} (corrected for decay) for the montmorillonite and 302.4 ± 1.2 count s^{-1} (corrected for decay) for the 1,9-decadiene, were measured 116h after the experiment began, indicative of the slow but continues uptake of bromine by the montmorillonite K10 through the 1,9-decadiene.

4.4 Discussion

4.4.1 Interaction of [^{82}Br]-Bromine Labelled Hydrogen Bromide with Solid Supports.

The [^{82}Br]-bromine labelled hydrogen bromide tracer experiments have shown that hydrogen bromide, unlike dibromomethane, interacts readily with clays and γ -aluminas at room temperature. This mirrors the chlorine analogue experiments [49] where chlorination via hydrogen chloride is by dissociative adsorption whereas chlorination using carbonyl chloride requires removal of an oxygen from the solid. The fact that hydrobromination, like hydrochlorination, occurs at room temperature suggests that dissociative adsorption is occurring, figure 4.4.1.

The [^{82}Br]-bromine labelled hydrogen bromide tracer experiments usually involved the addition of [^{82}Br]-bromine labelled hydrogen bromide in three separate aliquots. In all cases the first aliquot leads to a rapid initial uptake of bromine onto the solid, followed by a more gradual uptake, in the case of γ -alumina (expt 4.3.2) for approximately 1h, after

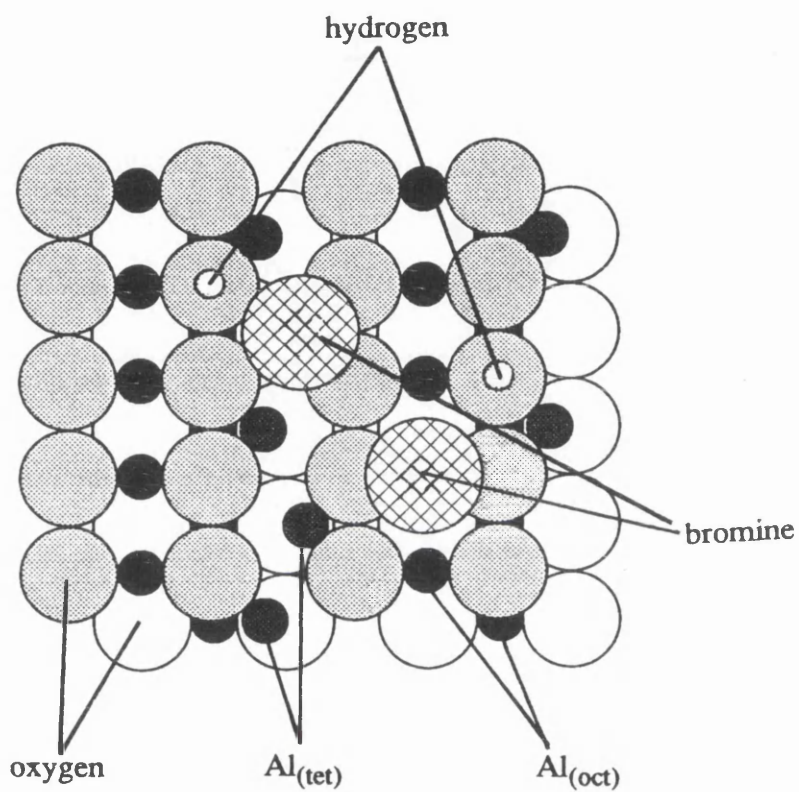


Figure 4.4.1. Postulated bromine environments present on the surface of γ -alumina after the room temperature interaction of hydrogen bromide.

which time the count rate of the solid remains static. With the second aliquot of [^{82}Br]-bromine labelled hydrogen bromide the initial uptake is not as rapid as for the first aliquot, but the count rate of the solid increases gradually for a further 5h. The addition of the third aliquot made no significant difference to the count rate of the solid, suggesting the surface of the solid had been saturated with hydrogen bromide. Degassing the brominated solid on a vacuum line leads to a decrease in the count rate of approximately 10%. These radiotracer experiments have shown that although calcined montmorillonite K10 (2.5mg atom g^{-1}) and uncalcined montmorillonite K10 (1.8mg atom g^{-1}) have greater [^{82}Br]-bromine contents than γ -alumina (1.1mg atom g^{-1}) before degassing; after the samples are degassed the bromine contents in all the samples appear to be very similar, with no real significant difference. NAA data for the interaction of hydrogen bromide with γ -alumina at 523K, expt 4.2.1, indicated a bromine content, after degassing, of 0.3mg atom g^{-1} . Half the figure observed from the room temperature interactions.

The lability of this bromine species adsorbed, at room temperature, on the surface of both calcined and uncalcined montmorillonite K10, with respect to exchange with gaseous hydrogen bromide, was investigated in experiments 4.3.5 & 4.3.6. These studies indicated that there was a slight difference in behaviour between the 'hydrogen bromide' brominated calcined montmorillonite K10 and the 'hydrogen bromide' brominated uncalcined montmorillonite K10. The exchange factor for the calcined material was measured at 0.77, whereas the uncalcined material gave a value of 0.61. These results suggest that although the calcination process increases the number of available sites for the adsorption of hydrogen bromide, the process must increase, to a greater extent, the number of labile sites in comparison to inert bromide sites. These results differ from those in the 'hydrogen chloride' chlorinated γ -alumina which has a 100% exchange rate with gaseous H^{36}Cl [49].

Prior chlorination of γ -alumina made no significant difference to the [^{82}Br]-bromide uptake in comparison with γ -alumina, but prior chlorination of montmorillonite K10 led to an increase in the bromine content obtained after degassing, from 0.7mg atom g^{-1} to 1.1mg atom g^{-1} . This difference between the chlorinated γ -alumina and

montmorillonite K10 is consistent with the results in chapter 3, where it was shown that montmorillonite K10 has no preference between chlorination and bromination, whilst γ -alumina is preferentially chlorinated. For this reason, exchange reactions between hydrogen bromide and the chloride species on the solid are more likely to occur on montmorillonite K10 than on γ -alumina.

The interaction of [^{82}Br]-bromine labelled hydrogen bromide with γ -alumina treated with but-1-ene and hydrogen bromide, experiment 4.2.3, leads to a large uptake of [^{82}Br] onto the surface of the γ -alumina, 1.3mg atom g^{-1} . This increase in bromide content of the γ -alumina, in comparison with calcined γ -alumina, may be explained by two reasons, I) this method of bromination gives rise to organics on the surface of γ -alumina (discussed later in this chapter), which may be brominated, or II) NAA data of the brominated γ -alumina indicates a bromine content of 0.8mg atom g^{-1} . The increase of [^{82}Br]-bromide species on the γ -alumina may be due therefore to a bromine exchange reaction occurring.

The results of the interaction of [^{82}Br]-bromine labelled hydrogen bromide with montmorillonite K10 treated with pyridine (table 4.3.3), indicated a rapid uptake of hydrogen bromide onto the clay, resulting in an immediate colour change from blue to orange. This rapid uptake is probably due to the formation of pyridinium bromide species, discussed in chapter 6, as many of the characteristic infrared absorption bands for pyridine were shifted during the hydrobromination process. The final uptake figure of [^{82}Br]-bromine labelled hydrogen bromide on pyridine treated montmorillonite K10 was 4.3mg atom g^{-1} reducing to 2.2mg atom g^{-1} after degassing, a significantly larger bromine content than that for calcined montmorillonite K10. The results of the interaction of [^{82}Br]-bromine labelled hydrogen bromide with chlorinated montmorillonite K10 treated with pyridine (experiment 4.2.11), indicated, like the montmorillonite K10 treated with pyridine, a rapid uptake of hydrogen bromide onto the clay. The bromine uptake figures for the chlorinated montmorillonite K10 treated with pyridine, 4.9mg atom g^{-1} dropping to 3.1mg atom g^{-1} after degassing, are significantly greater than those for the montmorillonite K10 treated with pyridine. A possible reason for this could be the chlorination process,

which enhances both Brønsted and Lewis acidity. If the chlorination of montmorillonite K10 enhances both the Brønsted and Lewis acidity of the clay, then the number of pyridine probe molecules adsorbed on the surface should increase. This increased pyridine content causes the [^{82}Br]-bromine labelled hydrogen bromide uptake onto the montmorillonite to increase. If this supposition is correct then this may be a route for comparative quantitative measurement of the acidity of solid supports.

4.4.2. Reaction of hydrogen bromide with butenes in the presence of acidic solid supports.

π -Electrons in alkene systems are polarisable and therefore subject to attack from electron seeking species called electrophiles. Although this addition can be both regioselective and stereospecific this work will investigate the regioselectivity of these reactions. The regioselectivity of the hydrobromination of alkenes is not just governed by Markovnikov's rule which states that 'the reaction pathway with the most stable carbonium intermediate is the reaction pathway most likely to be followed', figure 4.4.2. The regioselectivity is also governed by free radical mechanisms.

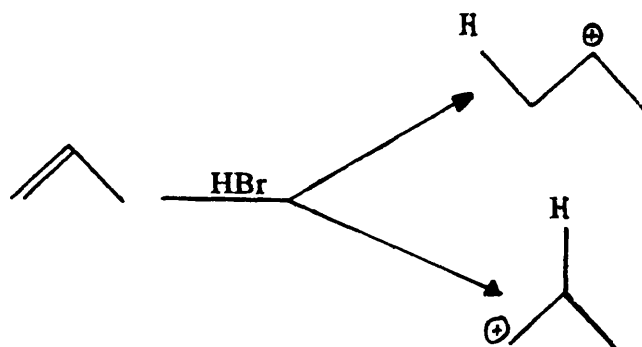


Figure 4.4.2. Possible reaction intermediates in the hydrohalogenation of asymmetric alkenes.

There are two possible hydrobromination products for but-1-ene, 2-bromobutane (Markovnikov addition) and 1-bromobutane (anti-Markovnikov addition), figure 4.4.3,

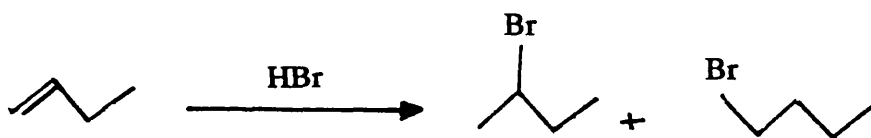


Figure 4.4.3. Possible reaction products from the hydrobromination of but-1-ene.

but only one possible reaction product for but-2-ene, 2-bromobutane, figure 4.4.4.

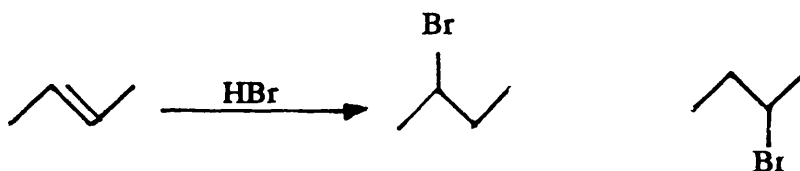


Figure 4.4.4. Possible reaction products from the hydrobromination of but-2-ene.

The impression often given in introductory organic text books is that the hydrohalogenation of alkenes should be a fast and efficient reaction. Without the presence of a promoter or enhancer, however, the reaction proceeds very slowly. The interaction of hydrogen bromide with but-1-ene, at 373K for 8h, results in the formation of 2-bromobutane, and various products detected by FTIR. The main spectral features however are due to unreacted but-1-ene. The addition of calcined γ -alumina to the system results in the formation of but-2-ene and the hydrobromination product 2-bromobutane. In this interaction there is no evidence for the presence of but-1-ene. The use of excess hydrogen bromide made no significant difference to the reaction products, table 4.4.1, compared with those from the 1:1 mol ratio reaction. The most interesting result arises from the use

of calcined γ -alumina treated with dibromomethane (section 3.2.1) as a support. As with previous reactions 2-bromobutane is observed but unlike these reactions no butene isomers are detected in the reaction products. It is concluded from these investigations that i) due to the formation of Markovnikov addition products, the reaction mechanism must be ionic, and ii) due to the isomerisation of but-1-ene to but-2-ene in the presence of the supports, the but-1-ene may adsorb and desorb from the surface without hydrobromination occurring. However, this is not the case when the γ -alumina is treated with dibromomethane. As only hydrobromination products are observed it is postulated that the adsorption of but-1-ene onto the treated γ -alumina results in the hydrobromination process.

The interaction of hydrogen bromide with but-2-ene (1:1 mol ratio) in the presence of calcined γ -alumina affords the formation of a C_8H_{16} oligomer product (10.0mol%) and the expected hydrobromination product 2-bromobutane (72.0mol%). This oligomer product and 2-bromobutane are observed again when an excess of but-2-ene is used in the reaction. However, when an excess of hydrogen bromide is used, the only reaction product detected by GCMS is 2-bromobutane (95.5mol%). This interaction when carried out in the presence of γ -alumina treated with carbonyl chloride results in the formation of both 2-bromobutane and 2-chlorobutane. As this process of chlorination results in the adsorption of hydrogen chloride onto the surface of the support, the formation of 2-chlorobutane is not unexpected. The presence of hydrogen chloride in the reaction product vapour phase is surprising and indicates that a halogen exchange process is occurring.

DRIFTS analysis of γ -alumina after the hydrobromination reaction, figure 4.3.8, indicated that there are organic species present on the surface of the γ -alumina. The ^{27}Al MAS NMR spectrum of γ -alumina after the treatment with hydrogen bromide and but-1-ene, figure 4.3.7, shows two resonances. A main broad resonance at 4.7ppm, attributed to $Al_{(oct)}$ and a smaller resonance at 52.8ppm attributed to $Al_{(tet)}$ environments, with reference to $AlCl_3$. These chemical shifts are similar to those observed previously in this work (section 3.4.2), in which bromination of γ -alumina has occurred. Neutron activation analysis of this sample indicates a bromine content of 0.8mg atom g^{-1} . This figure is greater than that observed for the room temperature adsorption of hydrogen bromide onto

γ -alumina (experiment 4.2.1), which resulted in a bromine content of 0.3mg atom g^{-1} . The increase in bromine content is probably due to bromo-organic species (R-Br) present on the surface of the γ -alumina, figure 4.4.5.

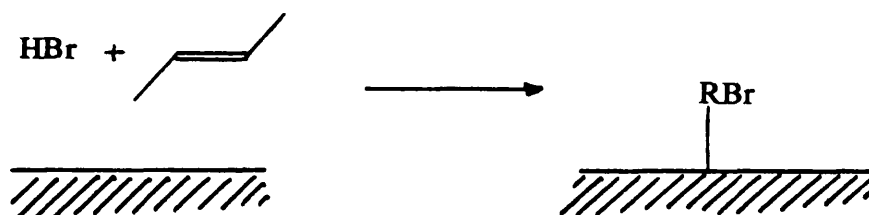


Figure 4.4.5. Interaction of hydrogen bromide with butene on a solid support.

$[^{82}\text{Br}]$ -Bromine labelled hydrogen bromide tracer studies (experiment 4.2.8) indicate that the uptake of bromine onto the γ -alumina, in the presence of but-1-ene, increases gradually for 24h. This results in a bromine content of $13.1\text{mg atom g}^{-1}$ and the γ -alumina takes on a brilliant white appearance. After heating at 353K for 7h, the γ -alumina acquired a faint purple hue with a decrease in bromine content to 1.2mg atom g^{-1} . On allowing the reaction mixture to stand at room temperature for a further 50h the brilliant white appearance of γ -alumina returned and the bromine content rose to 6.7mg atom g^{-1} . After degassing on a vacuum line for 60min, the faint purple hue of the γ -alumina returned. It is postulated that the faint purple colour is an initial organic bromide layer attached to the surface of the alumina. The brilliant white appearance of the γ -alumina is due to the interaction of hydrogen bromide and but-2-ene, to form 2-bromobutane, on the original 'faint purple' organic bromide layer. At room temperature 2-bromobutane builds up gradually on the γ -alumina, over a period of 24h, which results in the brilliant white appearance. On heating, at 373K for 7h, 2-bromobutane desorbs leaving the original 'faint purple' organic bromide layer exposed, figure 4.4.6.

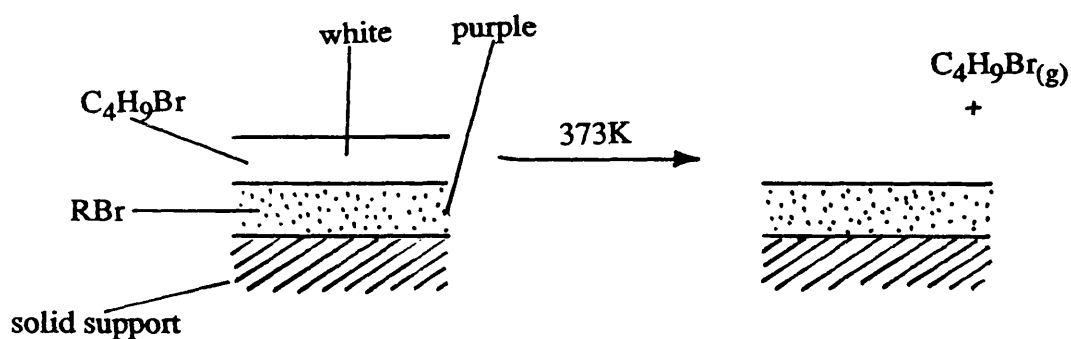


Figure 4.4.6. Desorption of 2-bromobutane from the surface of γ -alumina.

On allowing the mixture to stand for a further 50h at room temperature, the unreacted hydrogen bromide and but-2-ene interact on the γ -alumina, turning it brilliant white. The γ -alumina is finally pumped under *vacuo*, which removes the volatile 2-bromobutane, figure 4.4.7.

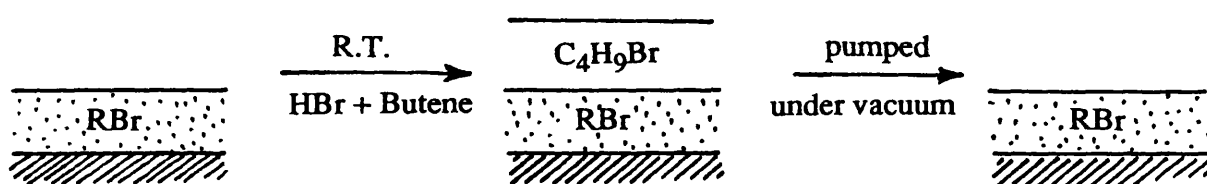


Figure 4.4.7. Build up and desorption of 2-bromobutane from the surface of γ -alumina.

4.4.3. Reaction of hydrogen bromide with 1,9-decadiene in the presence of acidic solid supports.

There are several possible reaction pathways for the interaction of hydrogen bromide with 1,9-decadiene, each of which result in different reaction products. If

hydrobromination proceeds via Markovnikov addition the product will be the 2,9-dibromodecane isomer, figure 4.4.8. The reaction could also proceed via anti-Markovnikov addition resulting in formation of the 1,10-dibromodecane isomer. If, however, the reaction mechanism is a mixture of Markovnikov and anti-Markovnikov additions, then the products formed will be the two dibromodecane isomers mentioned previously, along with the 1,9-dibromodecane isomer. The interaction is further complicated by the ability of acidic supports used in this work to isomerise alkenes [103,104], as illustrated in the previous section with but-1-ene.

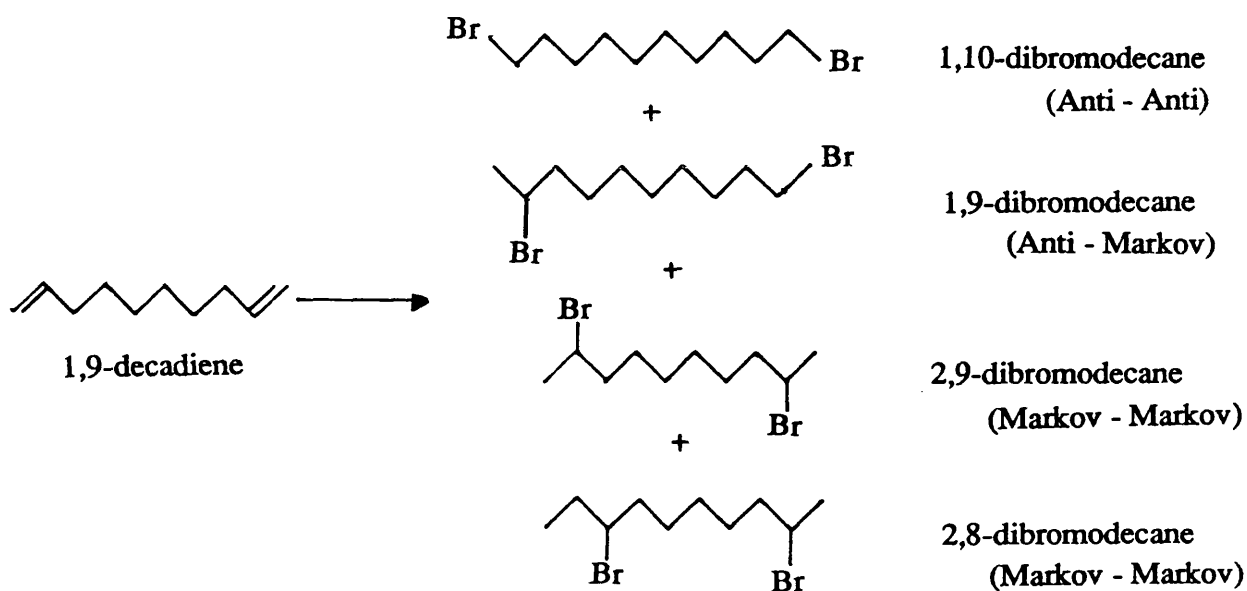


Figure 4.4.8. Possible hydrobromination products of 1,9-decadiene.

The hydrobromination reactions examined in this work can be divided into three categories: I) those using 48% aqueous hydrobromic acid as the hydrobrominating reagent, II) those using hydrogen bromide gas as the hydrobrominating reagent and III) those using hydrogen bromide gas with excess 1,9-decadiene. The standard experiments for the hydrobromination of 1,9-decadiene, table 4.4.2, were carried out by Dr C. Tattershall at the Associated Octel Company Ltd. These experiments were conducted under similar conditions to those described in experiment 4.2.18, with the exception that hydrogen bromide was also sparged into the reaction mixture. Hydrobromination of 1,9-decadiene was complete after 5h. The addition of Teepol as a surfactant makes a significant

difference to the reaction products formed. Without Teepol the hydrobromination occurs via an anti-Markovnikov addition to give 1,10-dibromodecane, but with Teepol present hydrobromination occurs almost exclusively via Markovnikov addition.

Hydrobromination reactions involving 48% aqueous hydrobromic acid, in the presence of acidic solid supports (experiments 4.2.20-23), lead to the formation of 2,9-dibromodecane and 2,8-dibromodecane, indicating that the reactions proceed via Markovnikov addition. These reactions are slow; in the case of Brockmann alumina, after 5h at 363K, 88.7mol% 1,9-decadiene remains unchanged, and with γ -alumina 75.1mol% remains unchanged. The most efficient of the solids examined is montmorillonite K10. In this reaction only 39.6mol% 1,9-decadiene remained after 1h at 363K. The least efficient solid support, Brockmann alumina, is slightly more selective towards the formation of 2,9-dibromodecane over 2,8-dibromodecane. The product ratio is 2:1, compared with montmorillonite K10 and γ -alumina where the product ratios are both 1.8:1.

Hydrobromination reactions in which hydrogen bromide was sparged into the reaction mixture (experiments 4.2.24-26) proved to be much faster than the hydrobromination reactions involving aqueous hydrobromic acid. Using γ -alumina, after 2.75h at room temperature, only 24.7mol% 1,9-decadiene remained unreacted, but using montmorillonite K10 there is no evidence for the presence of 1,9-decadiene after 1h at room temperature.

The ability of montmorillonite K10 to adsorb hydrogen bromide rapidly is illustrated in the [^{82}Br]-bromine labelled hydrogen bromide tracer experiments. This ability is illustrated again in experiment 4.2.26. In this experiment, under sparging conditions, the addition of hydrogen bromide gas into the reaction mixture would be expected to displace air already in the system, unless the reaction between hydrogen bromide and the decadiene is very rapid. As the reaction of hydrogen bromide with decadiene does not occur readily without the presence of an acidic support (experiment 4.3.27), the hydrogen bromide must adsorb onto the surface before reacting with the decadiene. When montmorillonite K10 is used as the support, for the initial 10min of sparging no air is displaced, therefore the hydrogen bromide must rapidly adsorb onto the

surface. This ability for the montmorillonite K10 to adsorb hydrogen bromide is also demonstrated under static conditions. In this reaction a double limbed vessel, figure 4.2.1, is charged with decadiene in one limb and decadiene/montmorillonite K10 in the other. [^{82}Br]-Bromine labelled hydrogen bromide is condensed into the limb containing decadiene. Within 3h of allowing the the vapour phases to interact, the count rates in each limb are equivalent. Within 20h the [^{82}Br]-bromine species is almost exclusively in the limb containing montmorillonite K10. This experiment indicates that the montmorillonite K10 is drawing the hydrogen bromide from the original decadiene solution into the decadiene/montmorillonite K10 solution.

The significant difference between the two types of hydrobromination reactions investigated is that the aqueous hydrobromic acid reactions involve aqueous and organic phases. These therefore require a medium to carry the hydrogen bromide from the aqueous phase to the organic phase. In the sparging experiments the hydrogen bromide is introduced straight into the decadiene solution. The solid supports may also be less efficient in an aqueous medium due to the blocking the Brønsted acid sites by water, via hydrogen bonding.

In the experiments 4.2.27-31, hydrogen bromide gas is introduced into an excess of 1,9-decadiene (3:1 mol ratio). These experiments were designed to determine whether, during the course of the reaction, both alkene groups were hydrobrominated on the surface at the same time, or whether a single hydrobromination occurred, followed by the desorption of the bromodecene, figure 4.4.9.

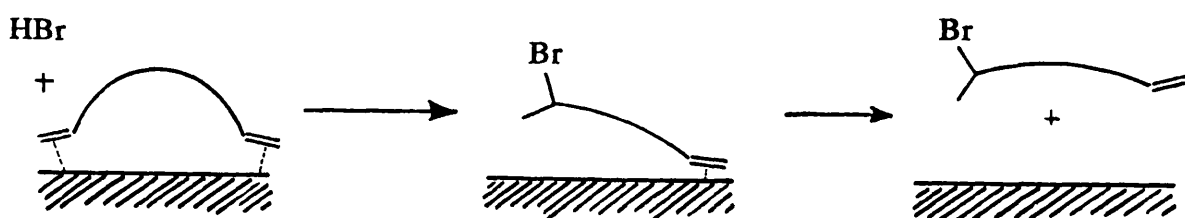


Figure 4.4.9. Proposed interaction of 2,9-decadiene with solid supports.

The results from these experiments indicate a correlation between the formation of the dibromodecanes and bromodecenes (table 4.4.2). This indicates that most of the γ -aluminas and montmorillonite K10s have a ratio of decadiene to bromodecene similar to that of bromodecene to dibromodecene. This is indicative of a single hydrobromination occurring followed by the desorption of the bromodecene. Bromodecene, in order to undergo further hydrobromination, has to compete with unreacted decadiene for the active sites on the acidic supports. Bentonite has proven to be the exception, with an approximate bromodecene to dibromodecene ratio of 2:1 but a decadiene to bromodecene ratio of 50:1. This suggests that the bentonite holds the bromodecene species tighter than the γ -alumina and montmorillonite K10, thus allowing further hydrobromination of the bromodecene, figure 4.4.10.

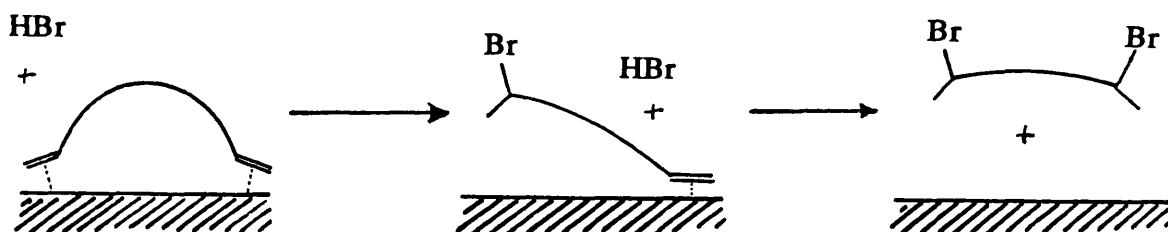


Figure 4.4.10. Proposed interaction of 2,9-decadiene with bentonite.

Montmorillonite K10 and chlorinated montmorillonite K10 produce the highest levels of isomerisation in decadiene. This does not necessarily lead to the expected higher levels of 2,8-dibromodecane isomer. Chlorinated γ -alumina, with a much lower level of decadiene isomerisation, has the highest percentage of 2,8-dibromodecane present. It is possible, therefore, that these acidic supports have different abilities to complex and add hydrogen bromide to internal double bonds. It would appear that chlorinated γ -alumina is effective at adding to internal double bonds, but not at isomerising the terminal double bonds, figure 4.4.11.

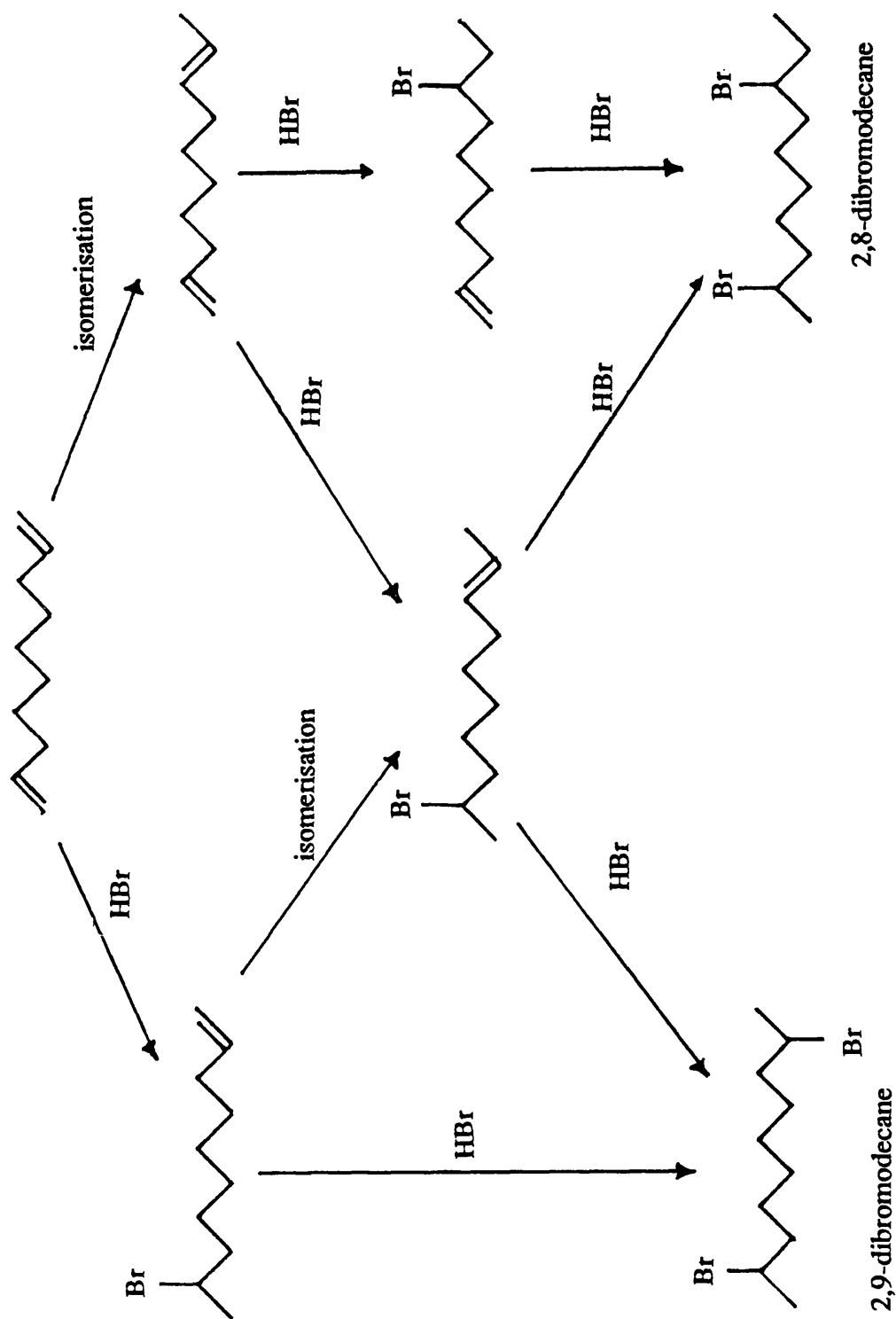


Figure 4.4.11. Proposed reaction pathways for the formation of 2,8-dibromodecane and 2,9-dibromodecane from 1,9-decadiene.

4.4.4. Alkene isomerisation in the presence of acidic solid supports.

The scarcity of but-1-ene, and evidence for the presence of but-2-ene, in the reaction product vapour phases after the hydrobromination of but-1-ene over γ -alumina, are indicative of isomerisation occurring. This isomerisation process does not occur in the absence of the solid support and is not reversible, as but-1-ene is not detected in the hydrobromination of but-2-ene. This process probably occurs on the γ -alumina due to the Brønsted acid nature of its surface, figure 4.4.12.

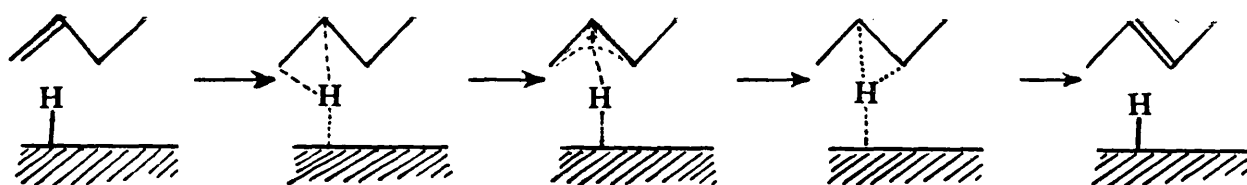


Figure 4.4.12. Isomerisation of alkenes on an acidic surface.

The isomerisation products in the 1,9-decadiene experiments varied with the nature of the solid supports used. Due to the excess of 1,9-decadiene in the experiments 4.2.27-31, the isomerisation process was not limited to the hydrobrominated species but included decadiene itself. This equates with the but-1-ene hydrobromination reactions where but-2-ene is observed. As a standard, a sample of 1,9-decadiene was analysed (table 4.4.2) and found to contain 1.7mol% of impurities in the form of decadiene isomers. The general trend for the isomerisation of decadiene is that the more active a solid support is at catalysing the hydrobromination reaction, the more active it will be at catalysing the isomerisation process. The least active of the solid supports is the clay bentonite. Decadiene analysed after this reaction contains 2.9% decadiene isomers (table 4.4.2) that are not 1,9-decadiene, an increase of 1.2% on the standard decadiene. In the case of

chlorinated montmorillonite K10, GCMS analysis of the decadiene after the reaction indicates that 45.8% is in the form of isomers other than 1,9-decadiene. Unfortunately this analysis could not identify the individual decadiene isomers present.

It is not surprising that, with so many decadiene isomers present in the reaction mixture, there are also many bromodecene and dibromodecane isomers present. There is, however, a significant quantity of tribromodecane isomers observed in some reaction products, notably in the reactions involving brominated alumina (1.8mol%), montmorillonite K10 (2.9mol%) and chlorinated montmorillonite K10 (3.0mol%). It is postulated that these species may be formed via I) the formation of a decatriene species, or II) the oxidation of HBr to Br₂ followed by addition of bromine to the alkene bonds. A pointer to which of these postulates may be correct is obtained from experiment 4.3.32, where after a short period of time the surface of montmorillonite K10 obtained an orange hue, the colour expected if a small amount of dibromine is present.

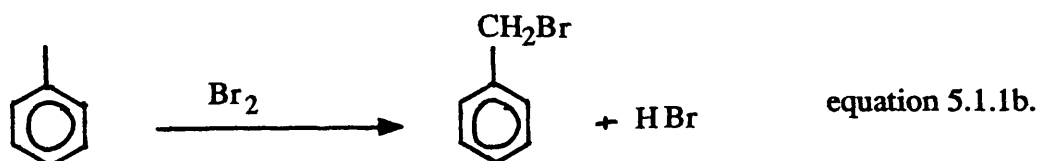
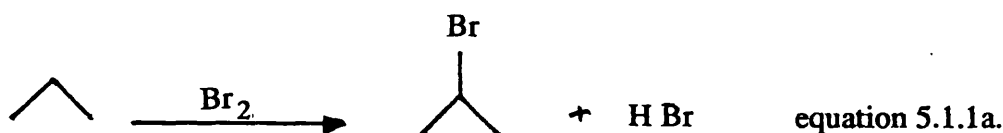
Recent publications [101,102] have shown that the use of appropriate alumina or silica gel surfaces facilitates hydrohalogenation of alkenes and alkynes. These surface-mediated additions afford selectivity unattainable in solution. The work undertaken in this chapter has investigated the surface interactions that afford these hydrobromination reactions. This work has shown, through gas phase interactions, that the most efficient supports are the ones which adsorb the hydrogen bromide most rapidly, as illustrated by montmorillonite K10. These interactions also indicate, by the isomerisation products observed, that not all alkenes that adsorb onto the surface undergo hydrobromination reactions before desorption occurs.

CHAPTER 5

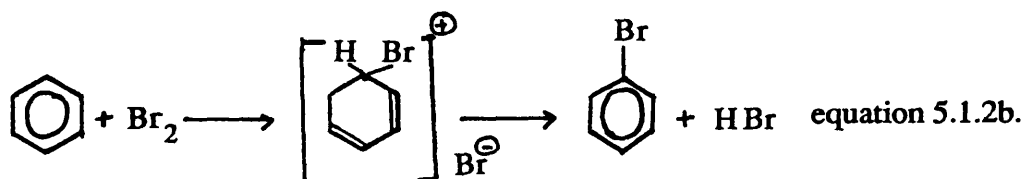
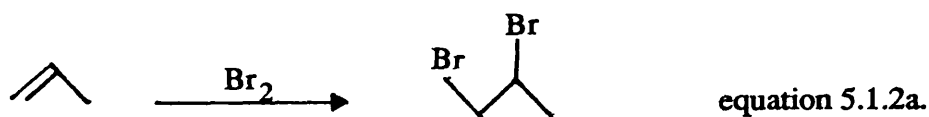
Interaction of Dibromine with Solid Supports and the Effects of Solid Supports in Bromination Reactions.

5.1 Introduction.

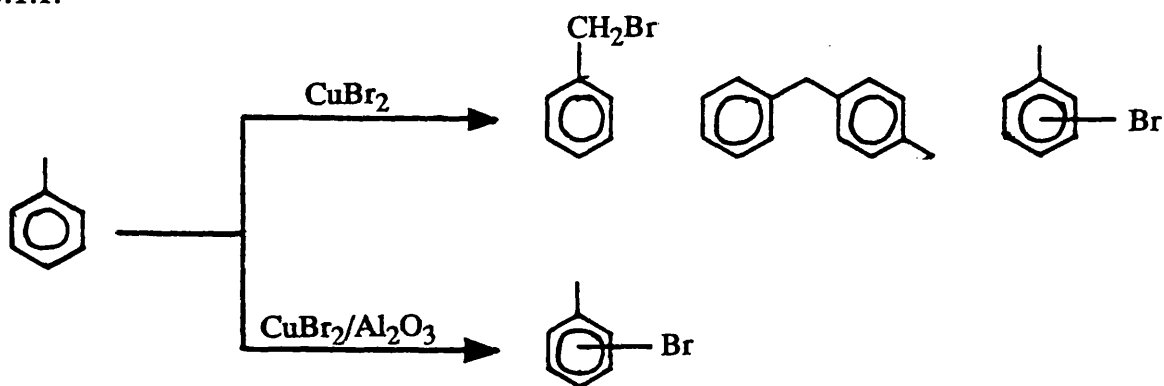
The bromination of organic compounds, using dibromine, has been well documented. These bromination reactions occur by either free radical or ionic mechanisms. Typical free radical brominations include the bromination of propane, equation 5.1.1a, resulting in the formation of 2-bromopropane and the bromination of toluene, equation 5.1.1b, resulting in the formation of benzyl bromide. Light must be present for all such free radical reactions.



Typical ionic brominations include the bromination of propene, equation 5.1.2a, resulting in the formation of 1,2-dibromopropane and the bromination of benzene, equation 5.1.2b, resulting in the formation of bromobenzene.



Recent work has shown [105-113] that the addition of a solid support to a reaction mixture changes the reaction products observed. Kodomari [100] has shown that the addition of alumina to a CuBr_2 /toluene system affords much greater selectivity, scheme 5.1.1.



Scheme 5.1.1. The enhancement of product selectivity by the incorporation of alumina into a reaction system.

A study by Vega and Sasson on the selective, liquid phase bromination of toluene catalysed by zeolites [114] has shown that different solid supports afford different product ratios.

The work in this section investigates the vapour phase interaction of anhydrous dibromine with modified high surface area clays and aluminas, using radiotracer techniques. It has been shown, in chapter 4, that these modified clays and aluminas have potential for hydrobromination reactions; their potential as possible catalysts for the

bromination of aromatic compounds and for the α -bromination of hexanoic acids is also investigated in this section.

5.2 Experimental.

5.2.1 Interaction of dibromine with Degussa 'C' γ -alumina.

Calcined γ -alumina (0.3g) was loaded into the reaction vessel shown in figure 2.1.2, in the inert atmosphere glove box. The vessel was transferred to a vacuum line and the contents degassed; care was taken to avoid carriage of alumina into the manifold. After degassing, an aliquot of dibromine was condensed onto the alumina and left at room temperature for 24 hours. The volatile materials were then condensed into a collection vessel leaving the alumina pale yellow in colour. A gas phase (15 Torr) FTIR spectrum was obtained of the volatile materials. The bromination process was repeated a further three times using the same alumina, but a fresh aliquot of bromine on each occasion.

5.2.2 Interaction of [^{82}Br]-bromine labelled dibromine with Degussa 'C' γ -alumina.

Calcined γ -alumina (0.1g) was transferred into a double limbed counting vessel (figure 4.2.1) and accurately weighed; this process was undertaken in an inert atmosphere glove box. The counting vessel was then transferred to a vacuum line manifold and the contents degassed.

A measured pressure, using a Heiss pressure gauge, of [^{82}Br]-bromine labelled dibromine vapour was introduced into the calibrated manifold. This dibromine was condensed, using liquid nitrogen, into the limb of the double limbed vessel that did not contain γ -alumina, and allowed to warm to room temperature. The [^{82}Br] count rate was determined over a time period sufficient to accumulate approximately 10000 counts. Tap X was then opened, allowing the [^{82}Br]-bromine labelled dibromine to interact with the γ -alumina, and the alumina counted immediately. The contents of both limbs were counted alternately until the uptake of [^{82}Br] on to the alumina had ceased. The vessel was transferred to a vacuum line and degassed, allowing the count rate for the [^{82}Br] retained on the alumina to be measured.

These count rates were compared with the specific count rate of a known quantity of [^{82}Br]-bromine labelled dibromine in chloroform solution, section 2.5.6.

5.2.3 Interaction of [^{82}Br]-bromine labelled dibromine with montmorillonite K10.

The procedure to investigate the interaction, at 293K, of anhydrous [^{82}Br]-bromine labelled dibromine with calcined montmorillonite K10, was the same as the procedure described in section 5.2.2.

5.2.4 Interaction of [^{82}Br]-bromine labelled dibromine with dibromomethane brominated Degussa 'C' γ -alumina.

The experimental procedure for the room temperature interaction of anhydrous [^{82}Br]-bromine labelled dibromine with calcined γ -alumina pretreated with dibromomethane at 523K, for 120h (section 3.2.1), was the same as that described for the

interaction of anhydrous [^{82}Br]-bromine labelled dibromine with calcined γ -alumina.

5.2.5 Interaction of [^{82}Br]-bromine labelled dibromine with hydrogen bromide brominated Degussa 'C' γ -alumina.

The procedure to investigate the interaction, at 293K, of anhydrous [^{82}Br]-bromine labelled dibromine with calcined γ -alumina treated with hydrogen bromide at 523K, for 120h (section 4.2.1), was the same as the procedure described in section 5.2.2.

5.2.6 Interaction of [^{82}Br]-bromine labelled dibromine with chlorinated Degussa 'C' γ -alumina.

The procedure to investigate the interaction, at 293K, of anhydrous [^{82}Br]-bromine labelled dibromine with calcined γ -alumina treated with anhydrous carbonyl chloride at 523K for 12h, was the same as the procedure described in section 5.2.2.

5.2.7 Interaction of [^{82}Br]-bromine labelled dibromine with chlorinated montmorillonite K10.

The experimental procedure for the room temperature interaction of anhydrous [^{82}Br]-bromine labelled dibromine with calcined montmorillonite K10 pretreated with anhydrous carbonyl chloride at 523K for 12h, was the same as that described for the interaction of anhydrous [^{82}Br]-bromine labelled dibromine with calcined γ -alumina

(section 5.2.2).

5.2.8 Interaction of [⁸²Br]-bromine labelled dibromine with fluorinated Degussa 'C' γ -alumina.

The experimental procedure for the room temperature interaction of anhydrous [⁸²Br]-bromine labelled dibromine with calcined γ -alumina treated at room temperature with several aliquots of SF₄ (section 2.2.11), was the same as the procedure described in section 5.2.2.

5.2.9 Interaction of [⁸²Br]-bromine labelled dibromine with Kel-F.

The experimental procedure for the above investigation was the same as that described for the interaction of anhydrous [⁸²Br]-bromine labelled dibromine with calcined γ -alumina.

5.2.10 Reaction of anisole with bromine supported on Degussa 'C' γ -alumina.

Calcined γ -alumina (0.28g) was loaded into the reaction vessel shown in figure 2.1.2, in the inert atmosphere glove box. The vessel was transferred to a vacuum line and the contents degassed. An aliquot of dibromine (1.07g) was condensed onto the alumina and allowed to react at room temperature for 24h.

Anisole (0.77g) was vacuum distilled onto the brominated alumina (77K) and allowed to react at room temperature for 24h. It was noted, after this time, that a purple

solid had formed. The purple solid was washed with dichloromethane to separate any organics from the γ -alumina. The resulting purple solution was filtered into a round bottomed flask and the dichloromethane removed by bubbling nitrogen gas into the solution via a pipette. The volatile purple material was analysed by ^1H NMR spectroscopy.

5.2.11 Reaction of hexanoic acid with dibromine using phosphorus trichloride as a promoter.

Dibromine (0.47mol) was transferred to reaction vessel A, figure 5.2.1, containing hexanoic acid (0.44mol) and stirred. Phosphorus trichloride (0.01mol) was added slowly and the reaction mixture warmed gradually to 363K. After 180min the reaction mixture had changed in colour from a dark red bromine colouration to orange, and the evolution of HBr had ceased. The orange reaction mixture, on cooling to room temperature, was washed with distilled water, the organic layer removed, and the aqueous layer washed with dichloromethane. The combined organic fractions were shaken with an aqueous potassium metabisulphite solution, the organic layer removed, and the aqueous fraction washed with dichloromethane. Sodium sulphate was added to the combined organic fractions and the mixture stirred vigorously for 30 minutes then allowed to stand. After several hours the sodium sulphate was filtered off, leaving a clear yellow solution. The solvent, dichloromethane, was removed by Rotavapor leaving a golden yellow solution, which was distilled into three colourless fractions. Samples of the three fractions were taken for G.C. analysis.

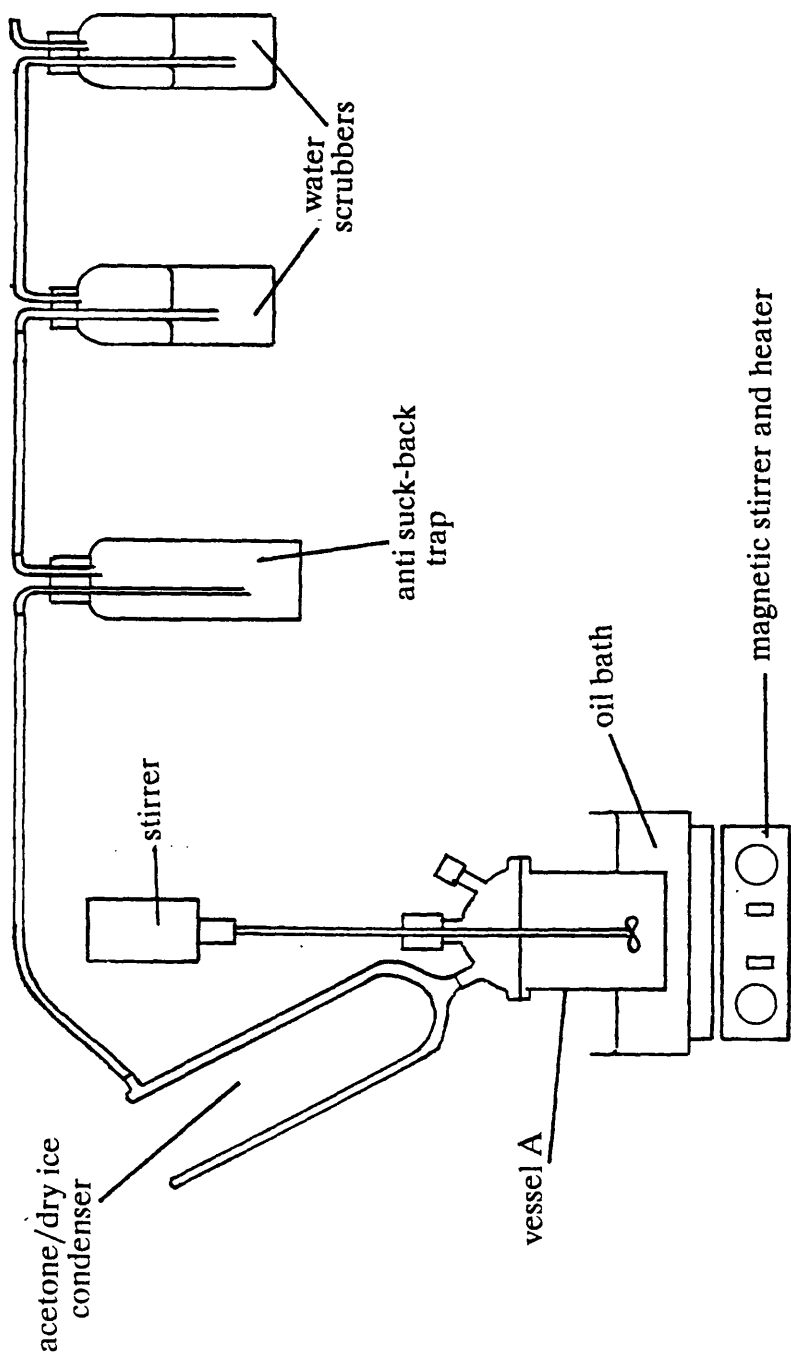


Figure 5.2.1. Apparatus for the bromination of hexanoic acid.

5.2.12 Reaction of hexanoic acid with dibromine in the presence of calcined Degussa 'C' γ -alumina.

Dibromine (0.39mol) was transferred to reaction vessel A, figure 5.2.1, containing hexanoic acid (0.18mol), calcined γ -alumina (3.36g) and dichloromethane (30cm³). The reaction mixture was warmed to 363K and stirred for 150min, after which time the reaction mixture was allowed to cool to room temperature and a sample taken for G.C. analysis.

5.2.13 Reaction of hexanoic acid with dibromine in the presence of uncalcined montmorillonite K10.

Dibromine (0.39mol) was transferred to reaction vessel A, figure 5.2.1, containing hexanoic acid (0.16mol), uncalcined montmorillonite K10 (14.25g) and dichloromethane (30cm³). The reaction mixture was warmed to 363K and stirred for 150min, after which time the reaction mixture was allowed to cool to room temperature and a sample taken for G.C. analysis.

5.2.14 Interaction of hexanoic acid with chlorinated Degussa 'C' γ -alumina at 293K.

Calcined γ -alumina (0.10g), treated at 523K for 12h with anhydrous carbonyl chloride, was loaded into a Monel bomb in the inert atmosphere glove box. An aliquot of hexanoic acid (2cm³) was added to the bomb, which was then transferred to a vacuum line manifold. The bomb was allowed to stand for 30min, at room temperature, before gaseous material from the bomb was expanded into the manifold containing a gas cell to give a

pressure of 50 Torr, and a gas phase FTIR spectrum obtained.

5.2.15 Interaction of hexanoic acid with chlorinated montmorillonite K10 at 293K.

The experimental procedure for the room temperature interaction of hexanoic acid with calcined montmorillonite K10 treated with carbonyl chloride at 523K for 12h, was the same as the procedure described in section 5.2.14

5.2.16 Reaction of hexanoic acid with dibromine in the presence of chlorinated Degussa 'C' γ -alumina at 363K.

Calcined γ -alumina (0.10g), treated with carbonyl chloride at 523K for 12h, was loaded into a Monel bomb in the inert atmosphere glove box. The bomb was then transferred to the vacuum line manifold and the contents degassed.

Bromine (15g, 0.094mol) was transferred into the mixing vessel, figure 5.2.2, in a fume hood. Hexanoic acid (10g, 0.086mol) was added to the mixing vessel and the vessel closed then shaken vigorously for 60sec. The vessel was transferred to the vacuum line manifold and degassed several times. The bromine/hexanoic acid mixture was allowed to warm to room temperature before the mixing vessel was attached to the valve on the Monel bomb, using PTFE Swagelok fittings. The bromine/hexanoic acid mixture was decanted into the Monel bomb, which was then placed in an electrical furnace and the contents heated at 363K for 8h. The bomb was allowed to cool to room temperature before gaseous material from the bomb was expanded into a manifold containing a gas cell to give a pressure of 50 Torr, and a gas phase FTIR spectrum obtained. The volatile contents of the bomb were collected in a storage vessel and the non-volatile products

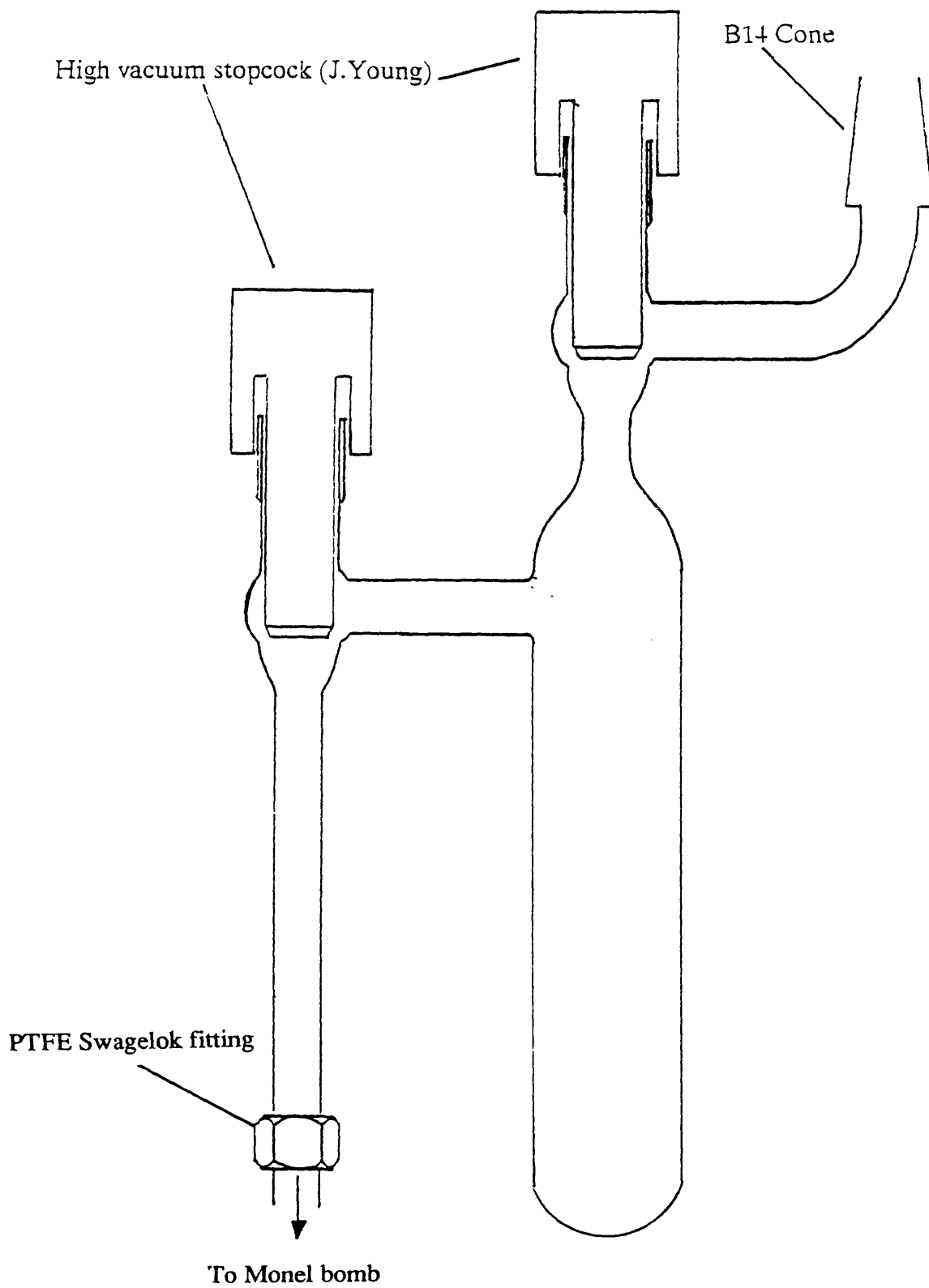


Figure 5.2.2. Hexanoic acid/dibromine mixing and degassing vessel.

transferred to the dry box and placed in a sample bottle.

5.2.17 Reaction of hexanoic acid with dibromine in the presence of chlorinated Degussa 'C' γ -alumina at 293K.

The experimental procedure for the room temperature interaction of hexanoic acid with dibromine in the presence of calcined γ -alumina treated with carbonyl chloride at 523K for 12h, was the same as that described in section 5.2.16, with the exception that the reaction vessel was not heated.

5.2.18 Reaction of hexanoic acid with dibromine in the presence of chlorinated montmorillonite K10 at 273K.

The experimental procedure for the room temperature interaction of hexanoic acid with dibromine in the presence of calcined montmorillonite K10 treated with carbonyl chloride at 523K for 12h, was the same as that described in section 5.2.17.

5.3 Results.

5.3.1 Interaction of dibromine with Degussa 'C' γ -alumina.

The infrared analysis of the volatile products after a 24h exposure, at room temperature, of dibromine to a sample of Degussa 'C' γ -alumina calcined at 523K, indicated that reduction of dibromine to hydrogen bromide had occurred. Absorbances at 3100-2700 cm^{-1} due to hydrogen chloride and 2700-2400 cm^{-1} due to hydrogen bromide were observed. Infrared analysis of the volatile products from the further additions of dibromine to the calcined γ -alumina indicated the continuing formation of hydrogen bromide, whilst the formation of hydrogen chloride diminished with each exposure of dibromine. Infrared spectra showed that only a trace amount of hydrogen chloride was present after the fourth addition, figures 5.3.1a-d.

5.3.2 Interaction of [^{82}Br]-bromine labelled dibromine with Degussa 'C' γ -alumina.

The results of this experiment indicated an immediate interaction between the dibromine and the γ -alumina (figure 5.3.2), characterised by a gradual increase in the count rate of the solid which reached a plateau after approximately 120h. The aliquot of [^{82}Br]-bromine labelled dibromine, 1.36mmol [specific count rate of 58.2 $\text{count s}^{-1} (\text{mg atom Br})^{-1}$], formed a liquid reservoir in the limb of the counting vessel, the vapour of which was then allowed to interact with calcined γ -alumina (0.065g). The count rate of the γ -alumina after 119h was 4.9 count s^{-1} corrected for decay to $47.7 \pm 0.7 \text{ count s}^{-1}$, indicating a dibromine uptake of 17.1mg atom Br g^{-1} .

The lability of dibromine adsorbed on γ -alumina was investigated by brominating a

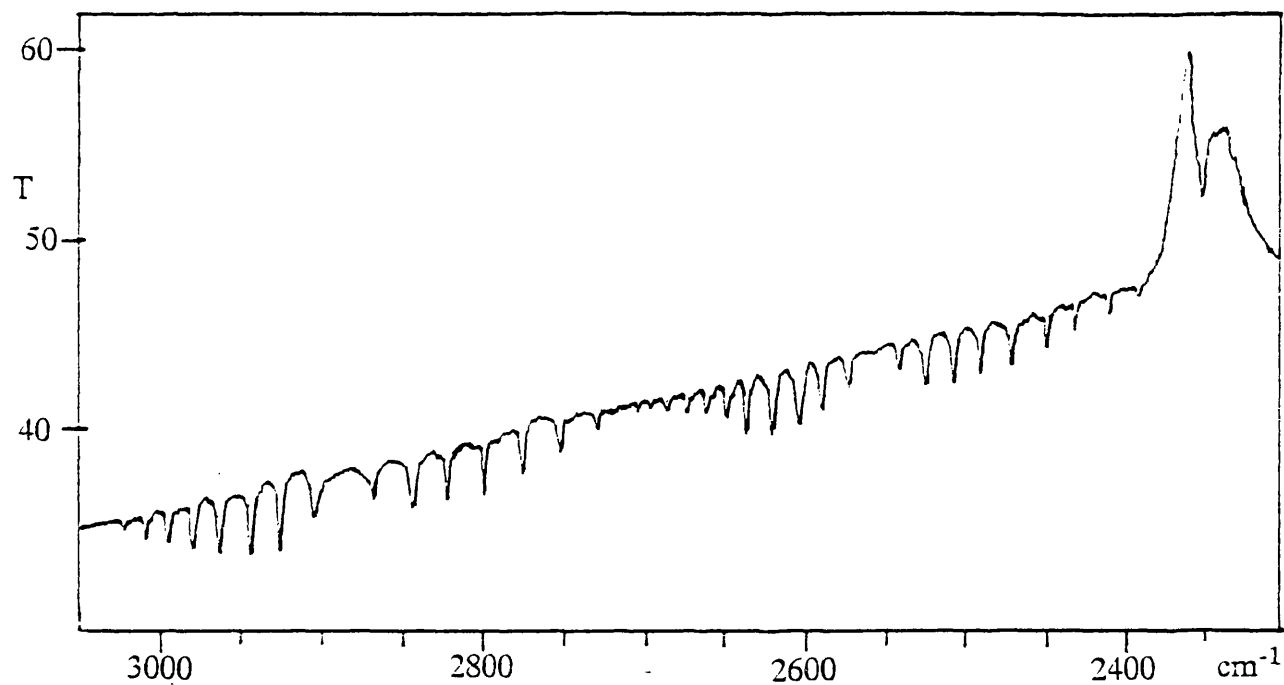


Figure 5.3.1(a). FTIR spectrum of the vapour phase after the room temperature interaction of dibromine with γ -alumina.

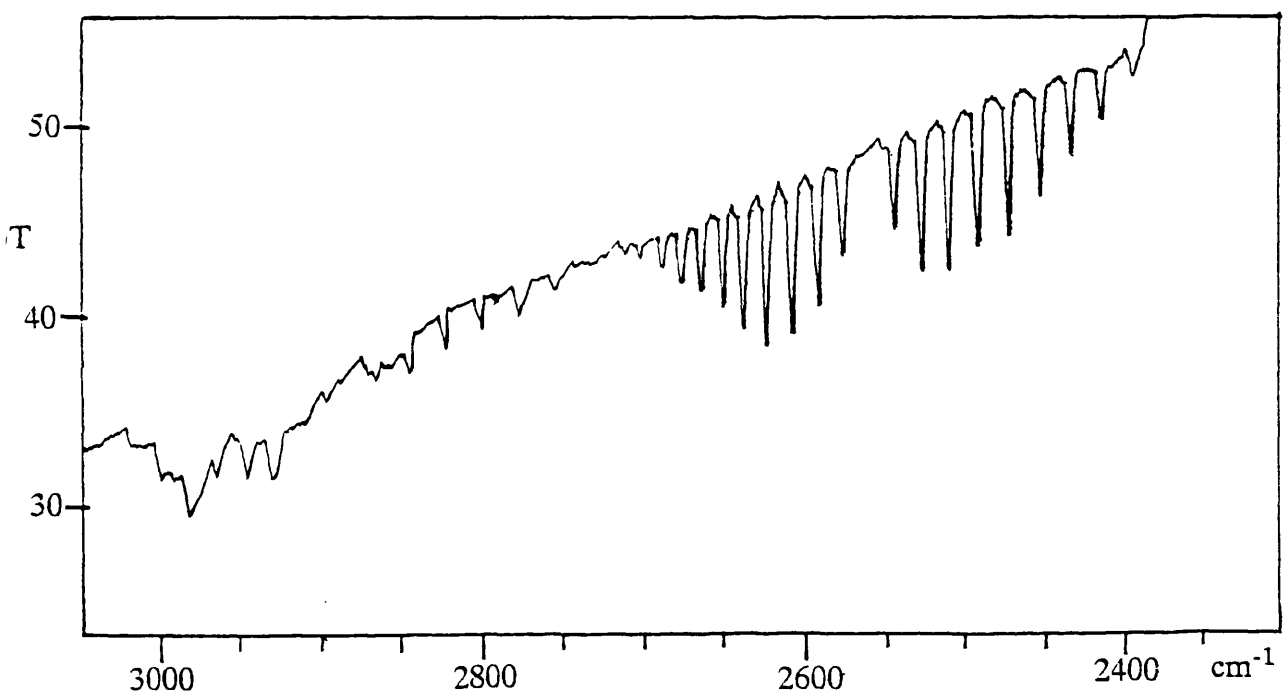


Figure 5.3.1(b). FTIR spectrum of the vapour phase after the room temperature interaction of the second aliquot of dibromine with γ -alumina.

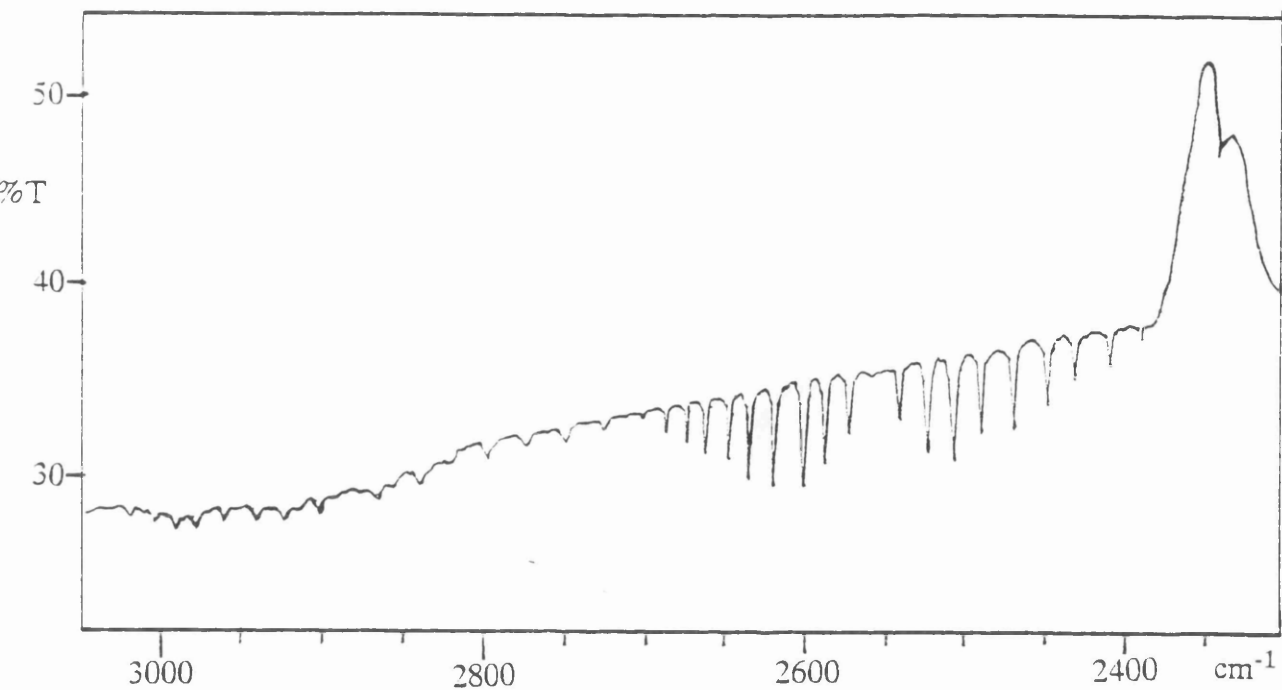


Figure 5.3.1(c). FTIR spectrum of the vapour phase after the room temperature interaction of the third aliquot of dibromine with γ -alumina.

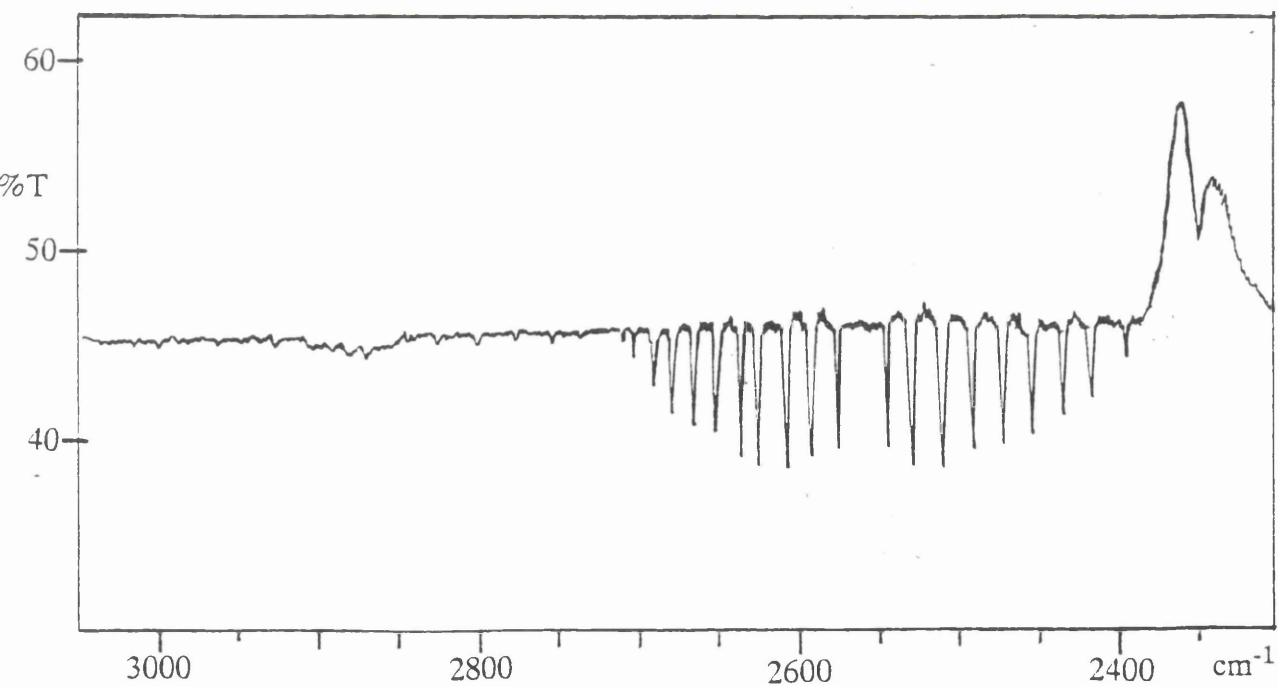
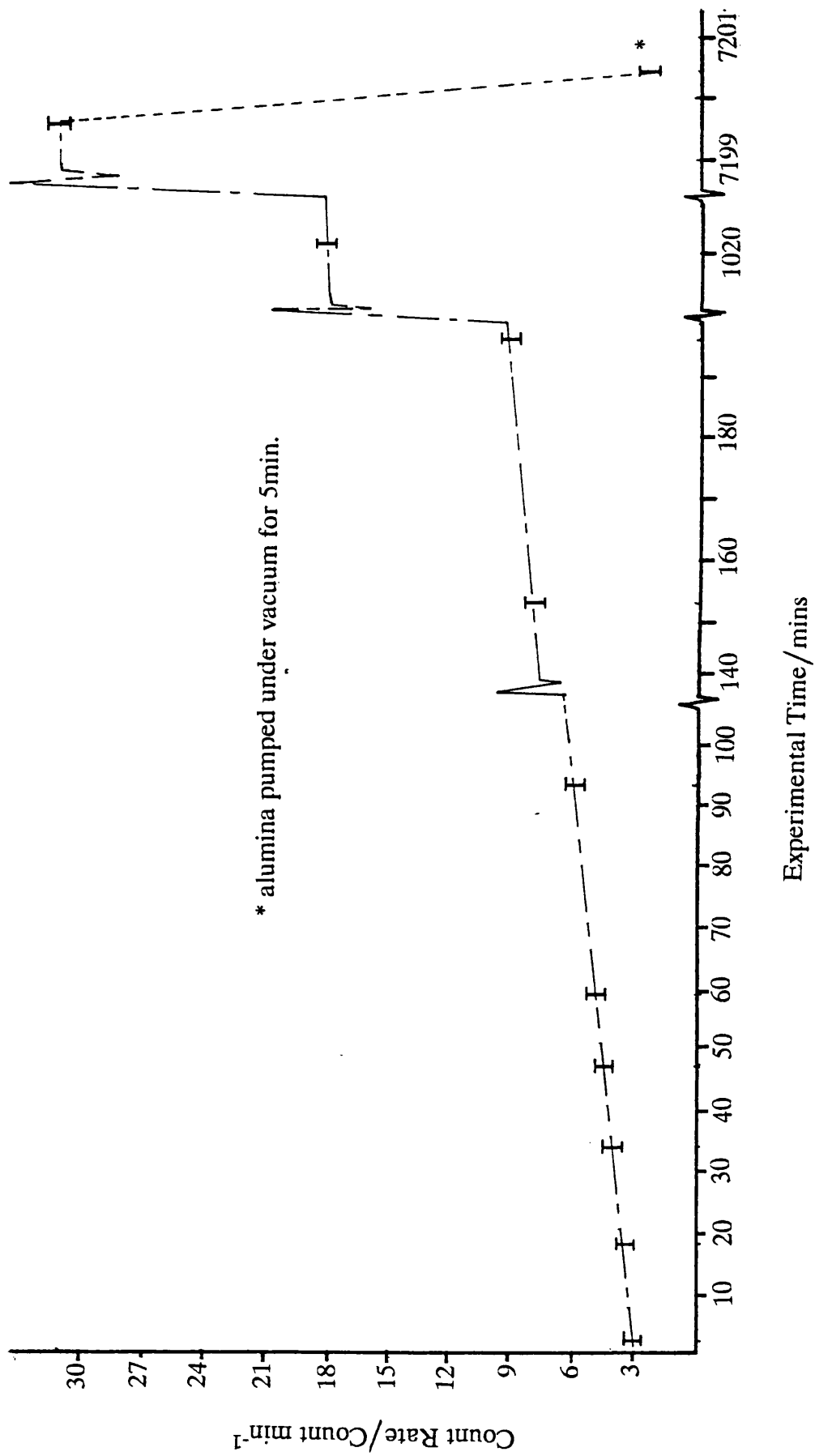


Figure 5.3.1(d). FTIR spectrum of the vapour phase after the room temperature interaction of the fourth aliquot of dibromine with γ -alumina.

Figure 5.3.2. Surface count rate from the interaction of [^{82}Br]-bromine labelled dibromine with calcined γ -alumina.



sample of γ -alumina with [^{82}Br]-bromine labelled dibromine for a period of 18h. It was not possible to investigate the lability of dibromine adsorbed after 100h as the activity of the [^{82}Br] on the γ -alumina was too weak for accurate analysis. After 18h, the count rate of the brominated alumina was measured at $326.9 \pm 0.6 \text{ count s}^{-1}$, corrected for decay, indicating a bromine content of $6.02 \text{ mg atom Br g}^{-1}$. The γ -alumina was then pumped under *vacuo* for 10min, resulting in a count rate for the solid of $79.9 \pm 0.6 \text{ count s}^{-1}$, indicating a bromine content of $1.47 \text{ mg atom Br g}^{-1}$. Unlabelled dibromine (1.34 mmol) was condensed onto the [^{82}Br]-brominated γ -alumina and allowed to react, at room temperature, for 20h. The γ -alumina was once again pumped under *vacuo* for 10min, resulting in a count rate of $12.7 \pm 0.1 \text{ count s}^{-1}$, corrected for decay.

For the calculation of the exchange factor the initial and final count rates (A_0 and A_t) were converted into specific count rates (S_0 and S_t), equations 5.3.1 and 5.3.2.

$$S_0 = \frac{A_0 \text{ count s}^{-1}}{\text{mg atom } ^{82}\text{Br}} = \frac{79.9}{0.147} = 543.54 \text{ count s}^{-1} (\text{mg atom } ^{82}\text{Br})^{-1}$$

equation 5.3.1

$$S_t = \frac{A_t \text{ count s}^{-1}}{\text{mg atom } ^{82}\text{Br}} = \frac{12.7}{0.147} = 86.39 \text{ count s}^{-1} (\text{mg atom } ^{82}\text{Br})^{-1}$$

equation 5.3.2.

The exchange factor (f) was then calculated using these specific count rates, equation 5.3.3.

$$f = \frac{S_0 - S_t}{S_0 - S}$$

equation 5.3.3.

S = calculated specific count rate assuming complete exchange.

$$= \frac{A_0 \text{ count s}^{-1}}{\text{mg atom } ^{82}\text{Br} + \text{mg atom Br}}$$

therefore:

$$f = \frac{543.54 - 86.39}{543.54 - 79.9/(0.15 + 2.72)}$$

$$f = 0.89 \pm 0.05$$

5.3.3 Interaction of [^{82}Br]-bromine labelled dibromine with montmorillonite K10.

The aliquot of [^{82}Br]-bromine labelled dibromine, 1.67mmol [specific count rate of 58.2 count s^{-1} (mg atom Br) $^{-1}$], formed a liquid reservoir in the limb of the counting vessel, the vapour of which was allowed to interact with calcined montmorillonite K10 (0.10g). The count rate of the montmorillonite K10 after 17.1h was 26.1 count s^{-1} corrected for decay to 36.2 ± 0.4 count s^{-1} , indicating a dibromine uptake of 8.4mg atom Br g^{-1} . A further count was taken after 118.8h giving a count rate of 7.5 count s^{-1} corrected for decay to 73.4 ± 0.8 count s^{-1} , indicating a dibromine uptake of 17.0mg atom g^{-1} . The montmorillonite K10 was then pumped on a vacuum line for 30min, before a final count of 0.4 count s^{-1} corrected for decay to 3.9 ± 0.2 count s^{-1} was taken. This final count indicated a dibromine uptake of 0.9mg atom Br g^{-1} .

5.3.4 Interaction of [^{82}Br]-bromine labelled dibromine with dibromomethane brominated Degussa 'C' γ -alumina.

The aliquot of [^{82}Br]-bromine labelled dibromine, 1.36mmol [specific count rate of 53.4 count s^{-1} (mg atom Br) $^{-1}$], formed a liquid reservoir in the limb of the counting vessel, the vapour of which was allowed to interact with a sample of γ -alumina (0.10g), which had been treated with dibromomethane at 523K over a 120h period. The count rate of the brominated γ -alumina after 100h was 11.6 count s^{-1} corrected for decay to 85.2 ± 1.1 count s^{-1} , indicating a dibromine uptake of 15.8mg atom Br g^{-1} . On pumping the γ -alumina, in *vacuo*, for 5min the count rate dropped to 14.0 ± 0.5 count s^{-1} (corrected for decay) indicating bromine retention of 2.6mg atom g^{-1} .

5.3.5 Interaction of [^{82}Br]-bromine labelled dibromine with hydrogen bromide brominated Degussa 'C' γ -alumina.

The aliquot of [^{82}Br]-bromine labelled dibromine, 1.36mmol [specific count rate of 43.8 count s^{-1} (mg atom Br) $^{-1}$], formed a liquid reservoir in the limb of the counting vessel, the vapour of which was then allowed to interact with a sample of γ -alumina (0.10g), which had been treated with hydrogen bromide at 523K over a 120h period. The count rate of the brominated γ -alumina after 43.3h was 205.9 count s^{-1} corrected for decay to 486.3 ± 4.9 count s^{-1} , indicating a dibromine uptake of 17.1mg atom Br g^{-1} .

5.3.6 Interaction of [⁸²Br]-bromine labelled dibromine with chlorinated Degussa 'C' γ -alumina.

The aliquot of [⁸²Br]-bromine labelled dibromine, 1.02mmol [specific count rate of 52.25 count s⁻¹ (mg atom Br)⁻¹], formed a liquid reservoir in the limb of the counting vessel, the vapour of which was then allowed to interact with a sample of γ -alumina (0.10g), which had been treated with carbonyl chloride at 523K over a 12h period. The count rate of the chlorinated γ -alumina after 18.15h was 7.8 count s⁻¹ corrected for decay to 11.2 \pm 0.2 count s⁻¹, indicating a dibromine uptake of 4.2mg atom Br g⁻¹. The count rate of the chlorinated γ -alumina after 113.4h was 2.8 count s⁻¹ corrected for decay to 26.0 \pm 0.5 count s⁻¹, indicating an increase in dibromine uptake to 10.0mg atom Br g⁻¹.

FTIR analysis of the product vapour phase following the interaction of unlabelled dibromine with chlorinated alumina, indicated that neither hydrogen chloride nor hydrogen bromide were evolved.

5.3.7 Interaction of [⁸²Br]-bromine labelled dibromine with chlorinated montmorillonite K10.

The aliquot of [⁸²Br]-bromine labelled dibromine, 1.09mmol (specific count rate of 52.25 count s⁻¹ (mg atom Br)⁻¹), formed a liquid reservoir in the limb of the counting vessel, the vapour of which was then allowed to interact with a sample of montmorillonite K10 (0.10g), which had been treated with carbonyl chloride at 523K over a 12h period. The count rate of the chlorinated montmorillonite K10 after 16.8h was 25.9 count s⁻¹ corrected for decay to 36.0 \pm 0.4 count s⁻¹, indicating a dibromine uptake of 3.2mg atom Br g⁻¹. The count rate of the chlorinated montmorillonite K10 after 112.45h was 11.1 count s⁻¹ corrected for decay to 100.9 \pm 1.3 count s⁻¹, indicating an increase in the dibromine uptake to 9.2mg atom Br g⁻¹.

5.3.8 Interaction of [⁸²Br]-bromine labelled dibromine with fluorinated Degussa 'C' γ -alumina

The aliquot of [⁸²Br]-bromine labelled dibromine, 2.92mmol (specific count rate of 338.6 count s⁻¹ (mg atom Br)⁻¹), formed a liquid reservoir in the limb of the counting vessel, the vapour of which was then allowed to interact with a sample of γ -alumina (0.50g), which had been treated with SF₄ at room temperature. The count rate of the halogenated γ -alumina after 21h was 562.5 count s⁻¹ corrected for decay to 865.9 \pm 8.7 count s⁻¹, indicating a dibromine uptake of 5.1mg atom Br g⁻¹. On pumping the γ -alumina, under *vacuo*, for 10min the count rate dropped to 355.0 \pm 3.6 count s⁻¹ (corrected for decay) indicating bromine retention of 2.1mg atom g⁻¹.

5.3.9 Interaction of [⁸²Br]-bromine labelled dibromine with Kel-F

The interaction between [⁸²Br]-bromine labelled dibromine and Kel-F powder was studied as Kel-F powder is a high surface area inert material, affording no sites for the bromine to react with. The interaction should therefore involve only physisorbed dibromine species. The Kel-F powder was generously supplied by Dr J.Pola, Institute of chemical process fundamentals, Academy of Sciences of Czech Republic, Prague, Czech Republic.

The aliquot of [⁸²Br]-bromine labelled dibromine, 1.87mmol (specific count rate of 338.6 count s⁻¹ (mg atom Br)⁻¹), formed a liquid reservoir in the limb of the counting vessel, the vapour of which was then allowed to interact with a sample of Kel-F (0.198g). The count rate of the Kel-F after 96h was 21.2 count s⁻¹ corrected for decay to 139.6 \pm 1.4 count s⁻¹, indicating a dibromine uptake of 2.1mg atom Br g⁻¹. On pumping the Kel-F under *vacuo*, all the activity was removed from the solid.

5.3.10 Reaction of anisole with bromine supported on Degussa 'C' γ -alumina

^1H NMR analysis, figure 5.3.3, of volatile purple material deposited on the calcined γ -alumina, after the bromination of anisole, indicated that several reaction products were present. When the spectrum was compared to a reference ^1H NMR spectrum of anisole [115], figure 5.3.4, it was found that the signals at 3.74ppm, 6.9ppm and 7.3ppm were due to anisole. Evidence of an AA'BB' spin system was detected in the signal observed at 6.72ppm, the most likely candidate for this would be para-brominated anisole. The signal observed at 7.62ppm is a deshielded aromatic proton, this was assigned to the meta proton of an aromatic ring brominated in the ortho and para positions i.e. 2,4-dibromoanisole.

The product ratio was determined from the integral of the methyl signals. The product ratio 2,4 dibromoanisole, para bromoanisole and anisole was in the order of 50:30:20 respectively. The same reaction products were observed when dibromine was reacted with the anisole without the presence of γ -alumina.

The reaction was repeated but with anisole added to the alumina before the addition of dibromine. The results indicate, from ^1H NMR analysis, figure 5.3.5, different reaction products to those previously observed. Although anisole was present, several new signals were observed. The signal at 5.8ppm was identified as the proton from the hydroxyl group of phenol, with the aromatic protons evident at 6.8ppm and 7.3ppm. A further signal at 2.67ppm was identified as methyl bromide.

5.3.11 Reaction of hexanoic acid with dibromine using phosphorus trichloride as a catalyst.

The results from this experiment show, from GC analysis (table 5.3.2), that fractions two and three contained mainly 2-bromohexanoic acid (92.9mol% and 95.7mol%

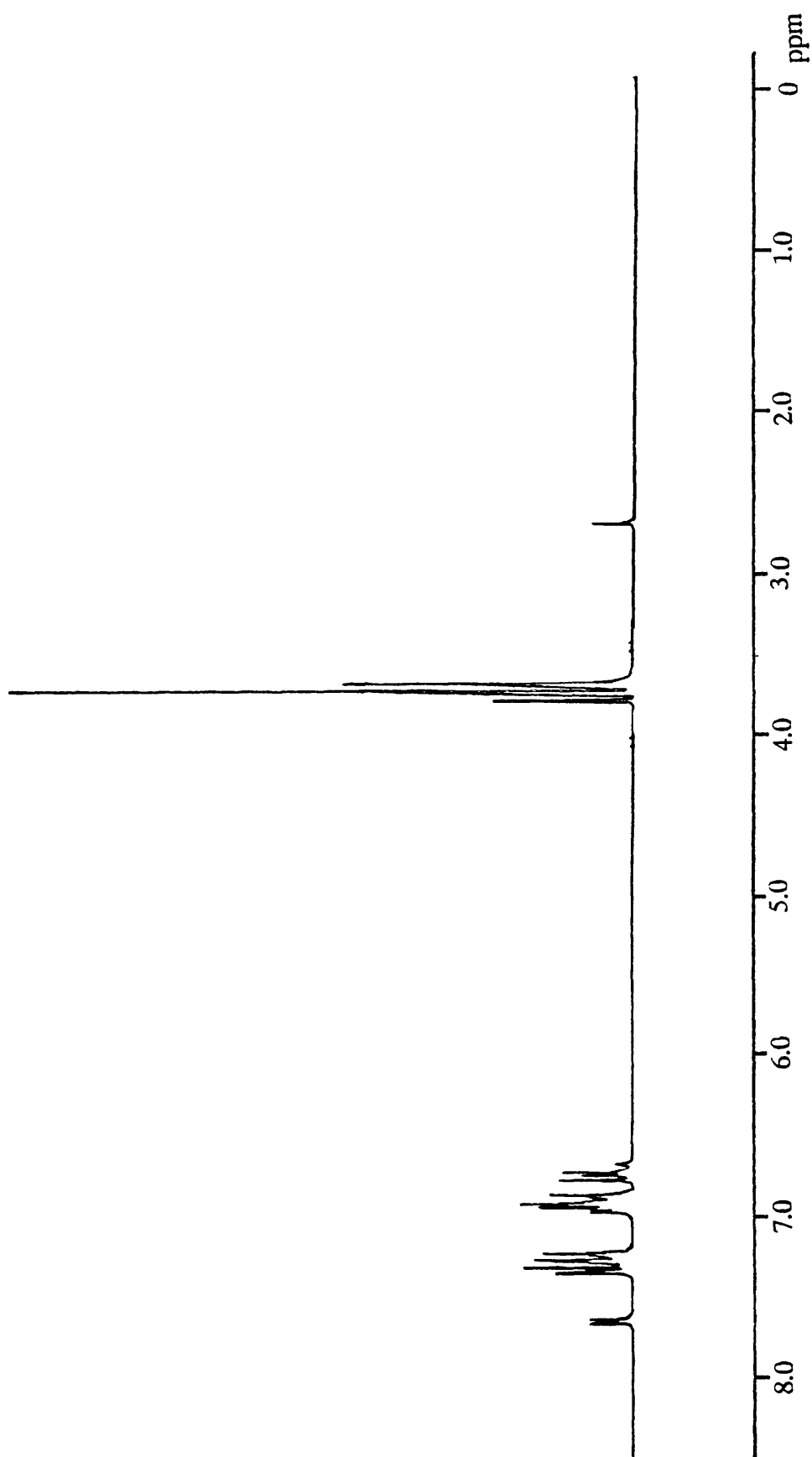


Figure 5.3.3. ^1H NMR spectrum of purple material formed after the interaction of anisole with brominated alumina.

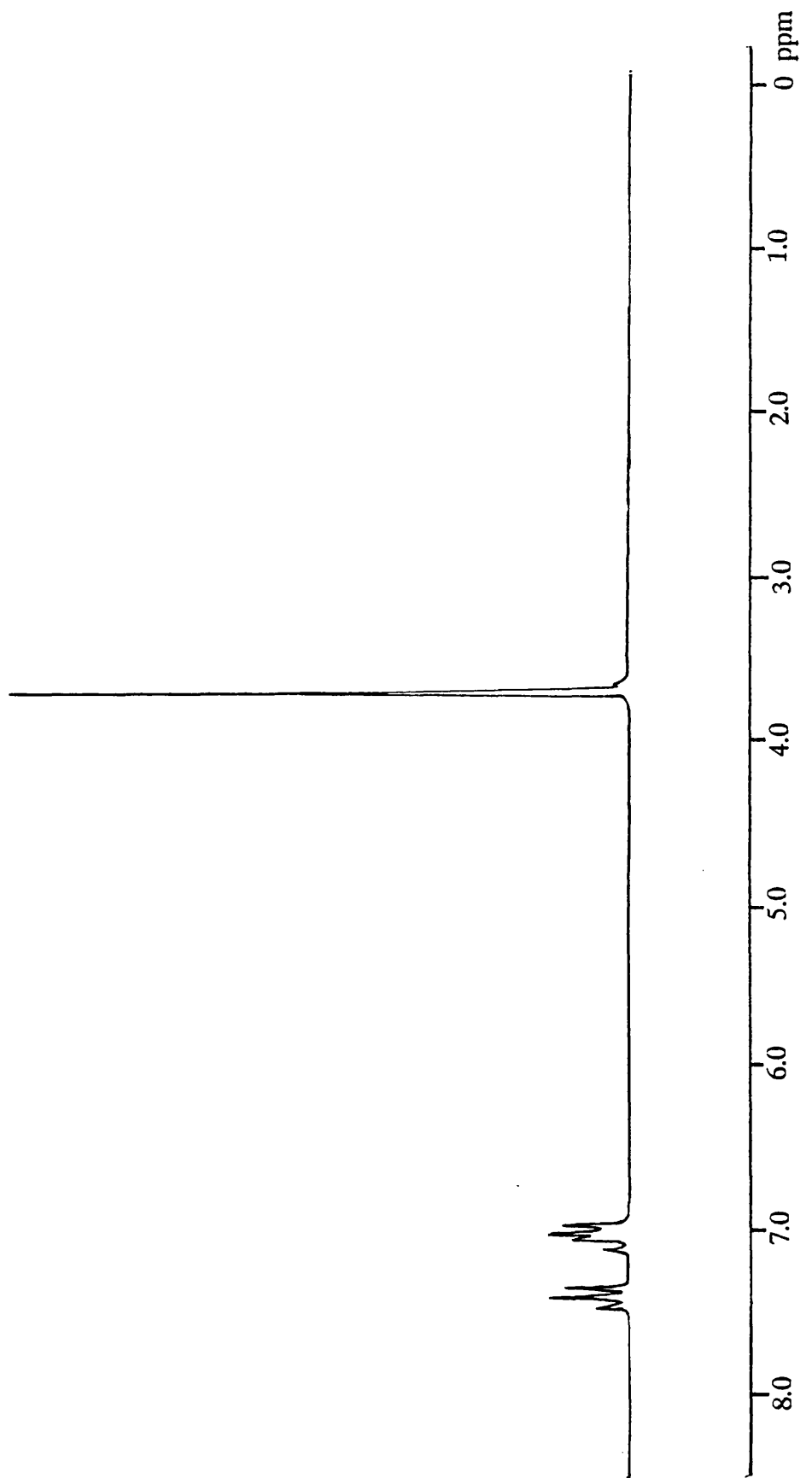


Figure 5.3.4. Reference ^1H NMR spectrum of anisole.

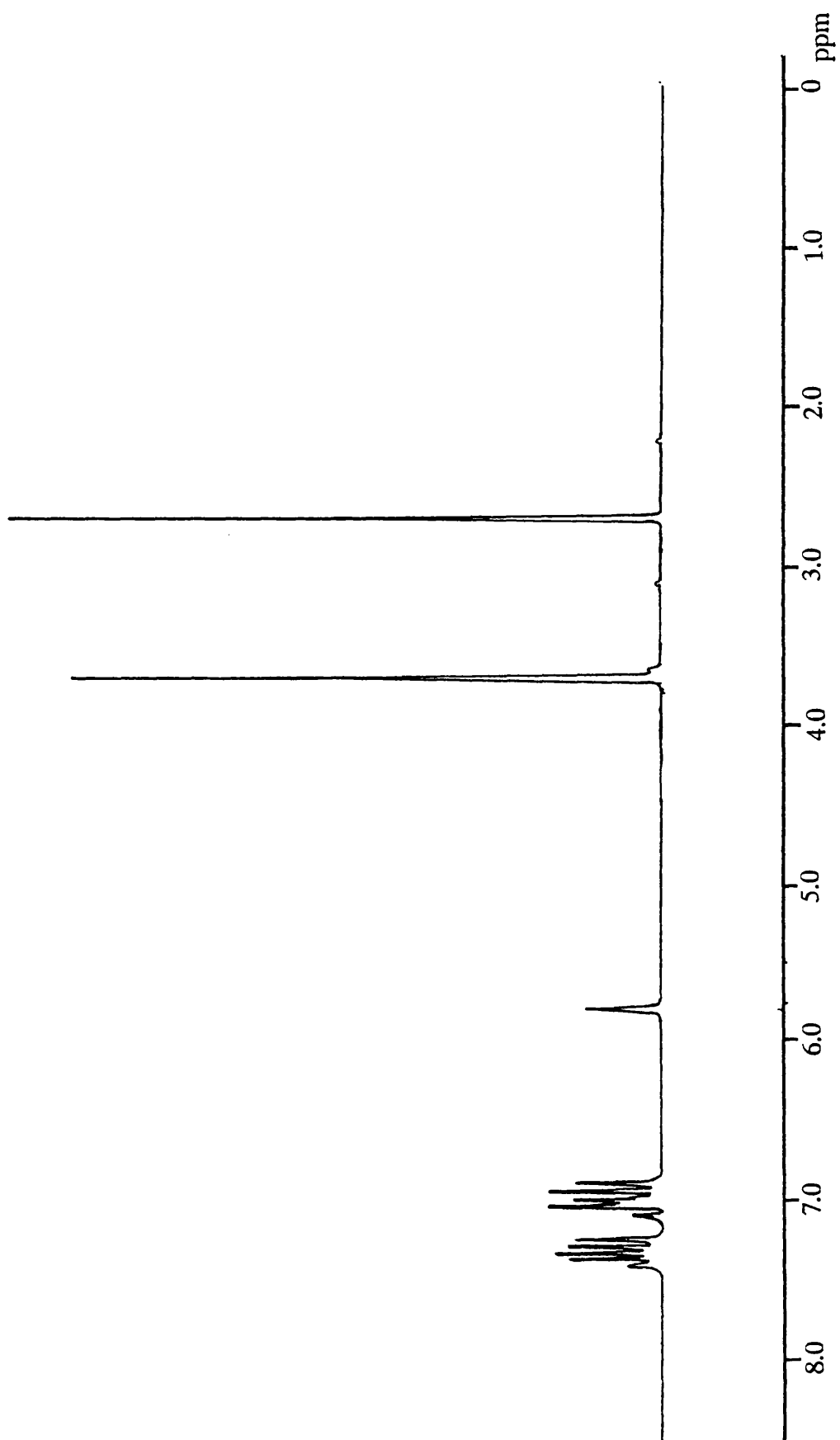


Figure 5.3.5. ^1H NMR spectrum of reaction products formed after the interaction of anisole/alumina with dibromine.

respectively). A gaseous material was evolved during the reaction but was soluble in the water scrubbers, to give an acidic solution. Although no spectroscopic information was available for the gaseous material, it was believed to be hydrogen bromide.

FTIR analysis of the vapour phase from the interaction of hexanoic acid with PCl_3 , figure 5.3.6, without the presence of dibromine, indicates absorbances in the region $3100\text{-}2700\text{cm}^{-1}$ due to the presence of hydrogen chloride.

5.3.12 Reaction of hexanoic acid with dibromine in the presence of calcined Degussa 'C' γ -alumina.

The results from this experiment show, from GC analysis, that no bromohexanoic acid was formed during the reaction, and that the final reaction mixture consisted of hexanoic acid and dibromine. There was no evidence for the formation of hydrogen bromide during the reaction.

5.3.13 Reaction of hexanoic acid with dibromine in the presence of uncalcined montmorillonite K10.

The results from this experiment showed, from GC analysis, that no bromohexanoic acid was formed during the reaction, and that the final reaction mixture consisted of hexanoic acid and dibromine. There was no evidence for the formation of

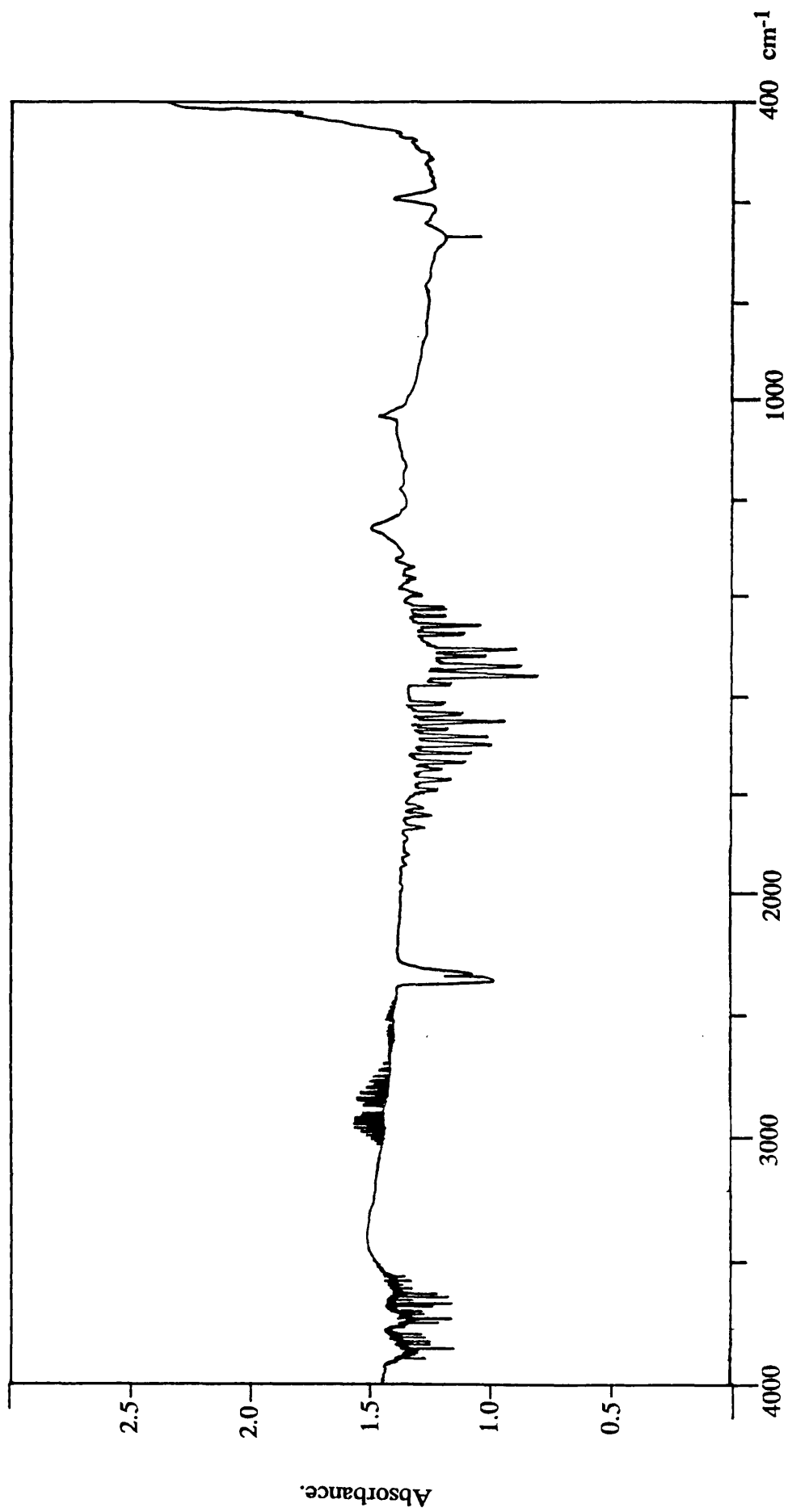


Figure 5.3.6. FTIR spectrum of the vapour phase after the room temperature interaction of PCl_3 and hexanoic acid.

hydrogen bromide during the reaction.

5.3.14 Interaction of hexanoic acid with chlorinated Degussa 'C' γ -alumina.

The infrared analysis of the volatile products after a 30min exposure, at room temperature, of hexanoic acid to a sample of chlorinated γ -alumina indicated the presence of hydrogen chloride, with absorbances in the region 3100-2700 cm^{-1} .

5.3.15 Interaction of hexanoic acid with chlorinated montmorillonite K10.

The infrared analysis of the volatile products after a 10min exposure, at room temperature, of hexanoic acid to a sample of chlorinated montmorillonite K10 indicated the presence of hydrogen chloride. The hydrogen chloride was detected despite the fact that on addition of hexanoic acid to the chlorinated montmorillonite K10, in the dry box, white fumes were observed.

5.3.16 Reaction of hexanoic acid with dibromine in the presence of chlorinated Degussa 'C' γ -alumina at 363K.

The infrared analysis of the volatile products after a 8h exposure, at 363K, of hexanoic acid to a sample of chlorinated γ -alumina indicated a reduction of some dibromine to hydrogen bromide. Absorbances at 3100-2700 cm^{-1} due to hydrogen chloride, 2700-2400 cm^{-1} due to hydrogen bromide, 2400-2300 cm^{-1} due to carbon dioxide

and $2240\text{-}2040\text{cm}^{-1}$ due to carbon monoxide were observed. Several weak absorbances were also detected between $1200\text{-}600\text{cm}^{-1}$. On removal of the volatile products from the reaction vessel a black sludge remained.

5.3.17 Reaction of hexanoic acid with dibromine in the presence of chlorinated Degussa 'C' γ -alumina at 293K.

The infrared analysis of the volatile products after a 8h exposure, at room temperature, of hexanoic acid to a sample of chlorinated γ -alumina indicated a reduction of some dibromine to hydrogen bromide. Absorbances at $3100\text{-}2700\text{cm}^{-1}$ due to hydrogen chloride and $2400\text{-}2300\text{cm}^{-1}$ due to carbon dioxide were observed. Several weak absorbances were detected between $1200\text{-}800\text{cm}^{-1}$ which were similar, but not identical, to the corresponding region in the reference spectrum of hexonyl chloride [72].

5.3.18 Reaction of hexanoic acid with dibromine in the presence of chlorinated montmorillonite K10 at 293K.

The infrared analysis of the volatile products after a 8h exposure at room temperature, of hexanoic acid and dibromine to a sample of chlorinated montmorillonite K10 indicated a reduction of some dibromine to hydrogen bromide. Absorbances at $3100\text{-}2700\text{cm}^{-1}$ due to hydrogen chloride and $2700\text{-}2400\text{cm}^{-1}$ due to hydrogen bromide were observed. The absorbances observed at $1820\text{-}1810\text{cm}^{-1}$ and $857\text{-}850\text{cm}^{-1}$ were assigned to the chlorinating agent carbonyl chloride. Several weak absorbances were detected between $1200\text{-}800\text{cm}^{-1}$ which, as in the analogous chlorinated alumina experiment, were similar but not identical to the corresponding region in the reference spectrum of hexonyl

chloride [72].

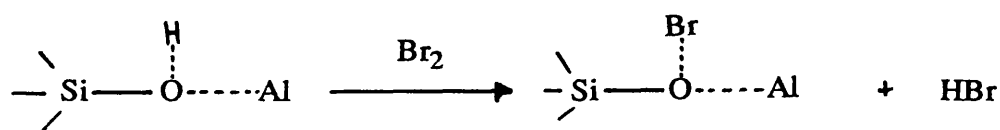
5.4 Discussion.

5.4.1 Interaction of [^{82}Br]-Bromine Labelled Dibromine with Solid Supports.

The [^{82}Br]-bromine labelled dibromine tracer experiments have shown that dibromine interacts with both aluminas and clays at room temperature. These radiotracer experiments usually involved the addition of a [^{82}Br]-bromine labelled dibromine reservoir to one limb of the double limb counting vessel and allowing the dibromine vapour phase to interact with the solid. As a result of using this reservoir method it is not possible, as it is in the [^{82}Br]-bromine labelled hydrogen bromide experiments (chapter 4), to measure and subtract the gas phase count rate. The error by not subtracting the gas phase in this case is small as the vapour phase of dibromine in the system (approx 200Torr) accounts for approx 0.02mmol dibromine, < 2% of the dibromine present in the system.

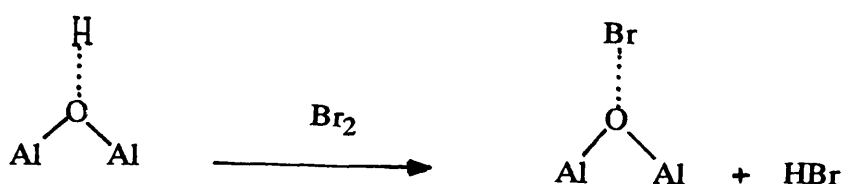
The uptake of [^{82}Br]-bromine labelled dibromine onto the solid supports is a slow reaction. This is partly due to the process of bromination which requires the dibromine to condense from the counting limb, containing the dibromine reservoir, to the solid support held in the second counting limb. These dibromine uptake times, over 100h in some cases, are very much slower than the times observed for the uptake of [^{82}Br]-bromine labelled hydrogen bromide (section 4.3.1 - 4.3.7) onto similar supports. This contrast in uptake times is due mainly to the fact that hydrogen bromide is completely in the vapour phase, unlike the dibromine liquid reservoir, hence the reaction time does not depend on the evaporation and condensation of a hydrogen bromide reservoir.

The addition of unlabelled dibromine to γ -alumina affords the formation of hydrogen bromide. In recent work involving the bromination of zeolites [116] a model for the formation of hydrogen bromide in this type of reaction is given, scheme 5.4.1.



Scheme 5.4.1. The formation of hydrogen bromide from dibromine on a zeolite structure.

This model for the formation of hydrogen bromide can be applied to γ -alumina, as the surface of γ -alumina possesses bridging hydroxyl groups, scheme 5.4.2.



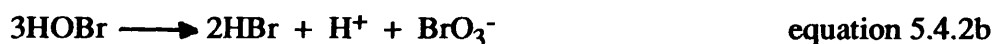
Scheme 5.4.2. A possible route for the formation of hydrogen bromide from dibromine on the surface of γ -alumina.

This speculative model for the formation of HBr is debatable as the brominated species is effectively an hypobromite, and hypobromites (including hypobromous acid) are known to be unstable and decompose [117]. A possible route for the formation of hydrogen bromide is the interaction of dibromine with water present on the surface of alumina as OH^- and H^+ groups, for although the alumina is calcined, the calcination process does not lead to the complete removal of all the surface hydroxyl groups [118,119]. Dibromine is stored over

the drying agent P_2O_5 , in this work to avoid the formation of hydrogen bromide. A more likely route for the formation of hydrogen bromide is the bromination of terminal Al-OH groups by dibromine, equation 5.4.1.



Hypobromous acid is unstable, with two main competing modes of decomposition both of which result in the formation of hydrogen bromide, equations 5.4.2a & b.



Hydrogen chloride is an unexpected reaction product identified from the interaction of γ -alumina and dibromine. With each successive addition of dibromine to the γ -alumina the evolution of hydrogen chloride decreases. It is postulated that trace amounts of chloride are present in the γ -alumina, due to its formation by flame hydrolysis of AlCl_3 . The chloride is displaced on addition of dibromine, by bromide, resulting in the evolution of hydrogen chloride. The fact that hydrogen chloride formation decreases over several additions of dibromine indicates that its formation is not rapid, and may be similar to that of hydrogen bromide, equations 5.4.3a and 5.4.3b.



The hypochlorous acid may then undergo similar interactions to those expressed in equations 5.4.2a and 5.4.2b, to form hydrogen chloride. Similar interactions between dibromine and γ -alumina chlorinated with carbonyl chloride do not result in the formation

of hydrogen chloride, suggesting that chloride present originally at the impurity level is more labile, in exchange with bromide, than the chloride present after chlorination with carbonyl chloride.

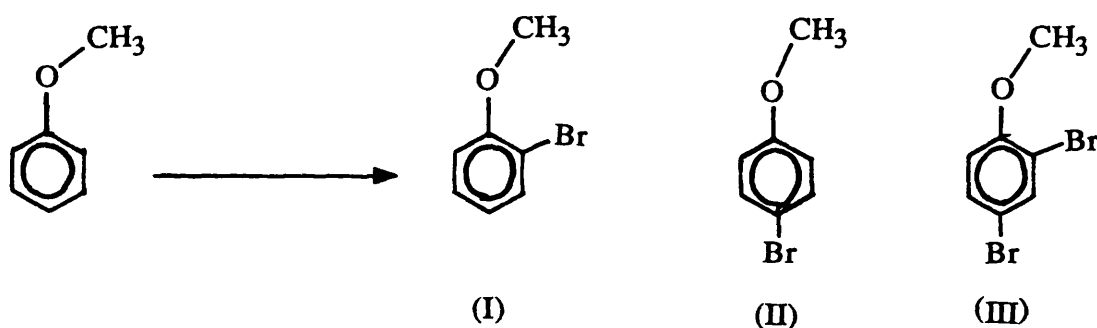
The results from the interaction of [^{82}Br]-bromine labelled dibromine with various modified clays and aluminas, table 5.3.1, show that bromine uptakes for these interactions are much greater than the uptake values observed from similar hydrogen bromide experiments (section 4.3.1 - 4.3.7). Although after pumping under *vacuo* the bromine retention values are similar for both types of interaction. Lability studies carried out on brominated γ -alumina, where the γ -alumina is firstly brominated with [^{82}Br]-bromine labelled dibromine before an aliquot of unlabelled dibromine is introduced, indicate an exchange factor of 0.89. It is postulated from this exchange factor value that there are two types of bromine species present on the support; I) a Br species chemisorbed on the surface of the support that is inert to Br exchange, and II) dibromine physisorbed onto the support which is labile towards Br exchange. The physisorbed dibromine would make up 90% of the bromine on the surface of the γ -alumina. This would explain the high bromine uptake onto the supports and also the sizeable reduction in bromine content on pumping under *vacuo*. Similar interactions with the chemically inert Kel-F powder indicated a slow bromine uptake, but on pumping under *vacuo*, and hence removing the physisorbed dibromine, the [^{82}Br] count rate is reduced to zero.

The prior bromination of the supports, with HBr and CH_2Br_2 , makes no significant difference to the bromine uptake, when compared to the calcined material. The prior chlorination however, results in a decrease in bromine uptake, onto both the γ -alumina and montmorillonite K10, by a factor of 1/2. This decrease in bromine uptake onto chlorinated γ -alumina is due to the chlorination process reducing the surface area of the γ -alumina [73], thus reducing the amount of dibromine able to physisorb onto the surface. In the case of montmorillonite K10 there have been no studies into surface area determination after the chlorination process, but the reduction in bromine uptake from calcined montmorillonite K10 to chlorinated montmorillonite K10 is indicative of a reduced surface area, similar to that found between calcined and chlorinated γ -alumina. This work has

shown that the bromine uptake onto solid supports, using dibromine, is much greater than was anticipated.

5.4.2 Interaction of dibromine with anisole in the presence calcined Degussa 'c' γ -alumina.

The activated ring system of anisole, resulting in δ^- charges at the ortho and para positions, allows for bromination via electrophilic substitution of the ring system [120], scheme 5.4.3.



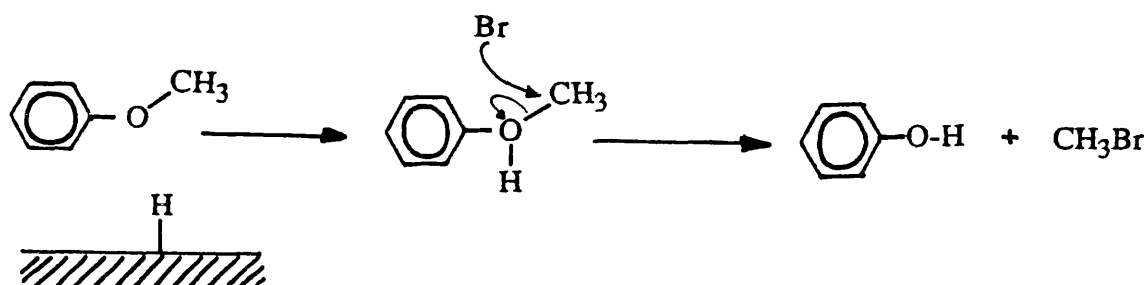
Scheme 5.4.3. The electrophilic bromination products from the bromination of anisole.

The interaction of anisole with dibromine, in the presence of calcined γ -alumina, indicates that the order in which the reagents are added to the γ -alumina affects the reaction products obtained. When anisole is added to a mixture of dibromine and γ -alumina, the reaction products (I) & (III) are similar to those obtained for the interaction of anisole with dibromine without the presence of alumina. However, when dibromine is added to a mixture of anisole and γ -alumina, the reaction products are no longer brominated anisoles but phenol and methyl bromide.

The addition of dibromine to calcined γ -alumina, as discussed in section 5.4.1, results not only in the formation of chemisorbed bromine species on the surface but also

physisorbed dibromine. It is this physisorbed dibromine species, coating the γ -alumina, that hinders any interaction between the anisole and solid, thus allowing only the interaction between dibromine and anisole which is probably responsible for the different reaction products observed.

A mechanism for the formation of phenol and methyl bromide from anisole is given in scheme 5.4.4. In this reaction mechanism the oxygen of the anisole is protonated by a Brønsted acid site on the surface of the γ -alumina. The methyl is then cleaved from the anisole resulting in the formation of phenol and methyl bromide [121].

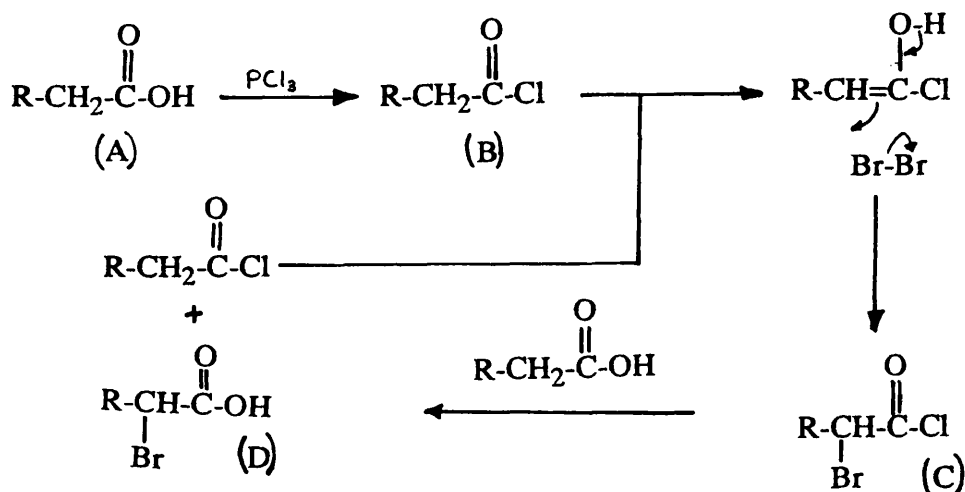


Scheme 5.4.4. Mechanism for the formation of methyl bromide and phenol from anisole.

5.4.3 Interaction of dibromine with hexanoic acid in the presence of modified solid supports.

In this section the Lewis acid properties of modified montmorillonite K10 and γ -alumina are investigated to ascertain whether they will promote the α -bromination of hexanoic acid (Hell Volhard Zelinsky reaction), scheme 5.4.5. The Hell Volhard Zelinsky method [122-126] uses a Lewis acid, in this case PCl_3 , to promote the reaction. The reaction mechanism, scheme 5.4.5, involves the formation of an acid chloride (B) from the carboxylic acid (A). It is this acid chloride which catalyses the reaction by undergoing α -

bromination.



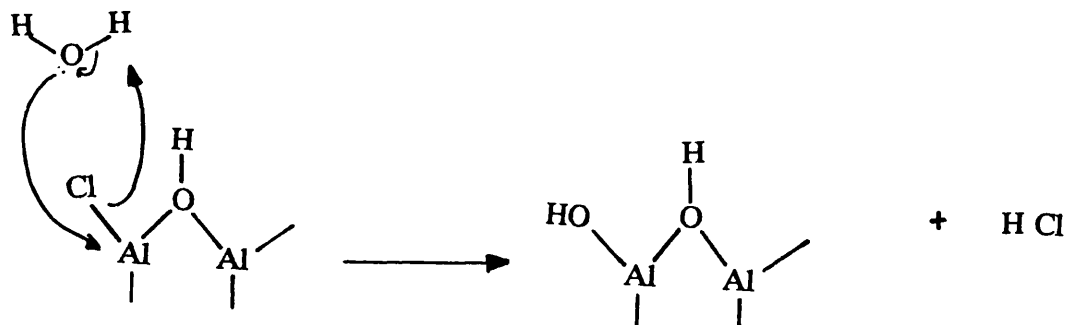
Scheme 5.4.5. The Hell Volhard Zelinsky reaction mechanism for the α -bromination of hexanoic acid.

The α -brominated acid chloride (C) undergoes a nucleophilic substitution reaction with hexanoic acid to form 2-bromohexanoic acid (D) and a further acid chloride, which will undergo an α -bromination thus continuing the reaction process. The evolution of hydrogen bromide gas from the reaction mixture, as a result of the reduction of dibromine, is a good indicator that α -bromination is proceeding.

The work in chapter 6 has shown that calcined γ -alumina and montmorillonite K10 both possess Brønsted and Lewis acid sites. The presence of Brønsted acid sites was not expected to promote the bromination reaction, as the reaction mechanism in scheme 5.4.5 uses PCl_3 (a Lewis acid) to promote the reaction. It was postulated however that Lewis acid sites on these supports may behave in an analogous fashion to scheme 5.4.5, thus promoting the reaction. Unfortunately all attempts to promote the reaction using these supports (expt 5.3.12 -5.3.13) failed to produce any evidence for the formation of 2-bromohexanoic acid. If calcined γ -alumina and montmorillonite K10 are to be used to promote the reaction, and the intermediate which catalyses the reaction is an acid chloride, then the most logical approach is to chlorinate the γ -alumina and montmorillonite K10, thus increasing the possibility of acid chloride formation on the surface.

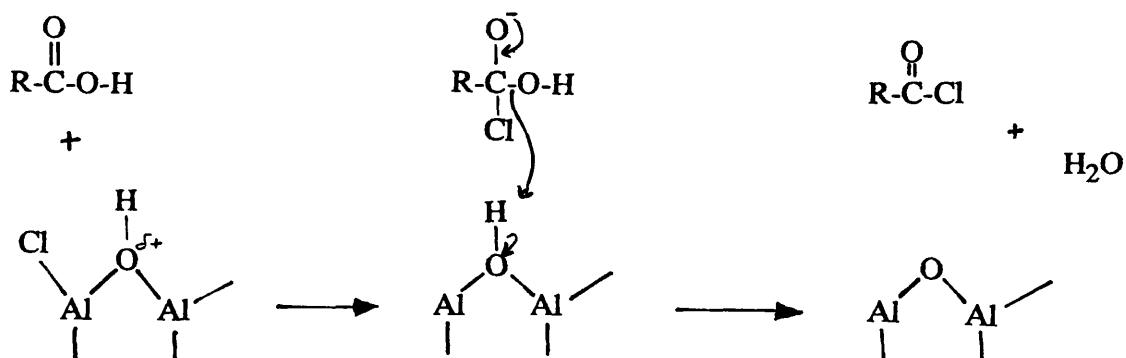
Treatment of both chlorinated γ -alumina and chlorinated montmorillonite K10 with

hexanoic acid, at room temperature, affords the formation of hydrogen chloride gas. This initial finding is surprising as hydrogen chloride is a stronger acid than hexanoic acid. This formation of hydrogen chloride is mostly likely due to surface rehydration of the chlorinated supports, scheme 5.4.6.



Scheme 5.4.6. The surface rehydration of chlorinated calcined γ -alumina.

There are two possible sources of this water, I) a small quantity present in the hexanoic acid and/or II) the interaction of hexanoic acid with the solid support resulting in the formation of an acid chloride and water, scheme 5.4.7.

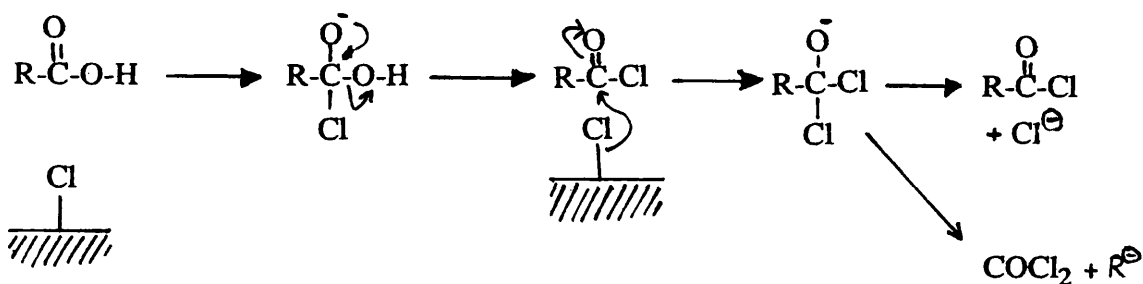


Scheme 5.4.7. The interaction of hexanoic acid with a chlorinated support resulting in the formation of an acid chloride and water.

Conditions for the treatment of hexanoic acid with dibromine in the presence of chlorinated γ -alumina, at 363K for 8h, are too harsh for the hexanoic acid resulting in its

decomposition. This decomposition is so complete that no liquid is observed in the reaction products, even when a substantial volume of reagent (15cm³) was used. Formation of carbon monoxide and carbon dioxide in the reaction products not only suggests that the hexanoic acid is oxidised under these conditions, but also that the alumina, which is recovered as a black sludge, has decomposed since it is the only source of oxygen in the reaction system. There is only indirect evidence for the occurrence of a bromination reaction and that is the formation of hydrogen bromide, as observed earlier in previous Hell Volhard Zelinsky reactions.

The treatment of hexanoic acid with dibromine in the presence of chlorinated γ -alumina and chlorinated montmorillonite K10, at room temperature, proved to be more successful than the 363K treatment. FTIR analysis of the vapour phase product from the interaction with chlorinated alumina suggests the formation of the Hell Volhard Zelinsky reaction intermediate hexonyl chloride and hydrogen bromide. Although the formation of the hexonyl chloride is a positive step towards promoting the reaction, the formation of CO and CO₂ indicates that the reaction conditions are still too harsh and decomposition of the hexanoic acid is still occurring. In the presence of chlorinated montmorillonite K10 there is again evidence for the formation of hexonyl chloride and hydrogen bromide, there is also evidence for the presence of the chlorinating agent carbonyl chloride. Since the chlorinated montmorillonite K10 is pumped for 10min after the chlorination process and no carbonyl chloride has been detected previously in any reaction involving chlorinated montmorillonite K10, the supposition must be that carbonyl chloride is formed during the reaction possibly as a decomposition product of hexonyl chloride, scheme 5.4.8.



Scheme 5.4.8. Postulated mechanism for the formation of carbonyl chloride.

Although the work in this section has given no conclusive proof that the chlorinated alumina and montmorillonite K10 will promote the Hell Volhard Zelinsky reaction to the same extent as PCl_3 , the work does indicate that these chlorinated supports have the potential to catalyse the Hell Volhard Zelinsky reaction at room temperature or below.

CHAPTER 6

Infrared Analysis of Pyridine and 2,6-Dimethylpyridine Adsorption on Solid Supports.

6.1 Introduction.

The important structural characteristic of acidic solid supports, such as γ -alumina and montmorillonite K10, in catalysis is the surface [127]. Spectroscopic techniques for analysis of these Brønsted and Lewis acid sites is fraught with difficulties. Solid state NMR is an ideal technique for the analysis of solid materials but unfortunately this technique analyses the bulk as well as the surface. This results in the swamping of the required surface resonances by those of the bulk. Although infrared techniques can identify hydroxyl groups on the surface of the supports (Brønsted acid sites) [118,119], IR cannot be used for the identification of Lewis acid sites as these possess no infrared active functional groups.

The characterisation of acidic sites therefore has to be determined via an indirect method involving the adsorption of basic probe molecules onto the acidic sites, followed by the analysis of these probe molecules. Since NMR and infrared spectroscopy are the techniques most frequently used to study these probe molecules, they must possess strong, easily defined infrared absorption bands and/or a basic functional group containing an atom with a nuclear spin, allowing NMR techniques to be employed. There is an extensive range of probe molecules which fit these criteria and are used in this type of work. For NMR studies the probe molecules usually contain nitrogen (^{15}N) or phosphorus (^{31}P); it is these atoms that interact with the different types of acidic surface species (figure 6.1.1),

resulting in several different environments for ^{15}N or ^{31}P , which can then be characterised by NMR.



Figure 6.1.1. Interaction of basic probe molecules with acidic surface groups.

Typical probe molecules for this type of NMR analysis are ammonia [128,129], pyridine [129-131], trimethylphosphine [132] and trimethylamine [128,129].

For infrared studies the most common probe used is pyridine [130,133-145], since its organic ring structure is ideal for infrared adsorption techniques. The infrared spectrum of pyridine coordinately bonded to the surface is markedly different from that of the pyridinium ion, permitting the differentiation of acid type on the surface, figure 6.1.2.

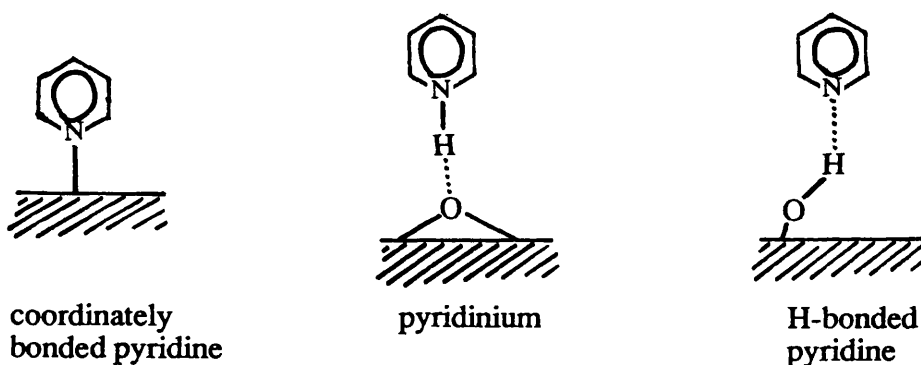


Figure 6.1.2. Adsorbed pyridine and pyridinium species.

In this work the pyridine derivative 2,6-dimethylpyridine is used as a probe molecule. With 2,6-dimethylpyridine the nitrogen is sterically hindered by the two

adjacent methyl groups, in comparison to the nitrogen in pyridine. As a result of this, 2,6-dimethylpyridine fails to react with the sterically hindered BMe_3 acid [146], whereas the less hindered, weaker base pyridine, does. The 2,6-dimethylpyridine should therefore interact with Brønsted acid sites more readily than pyridine but interact with the sterically hindered Lewis acid sites less readily than pyridine.

The work in this section involves infrared analysis, using DRIFTS and PAS techniques, of adsorbed pyridine and 2,6-dimethylpyridine on pretreated γ -alumina and montmorillonite K10. The pyridine and 2,6-dimethylpyridine vapour were adsorbed at room temperature under their own vapour pressures.

6.2 Experimental.

6.2.1. Infrared analysis of the adsorption of pyridine onto calcined Degussa 'C' γ -alumina.

Calcined γ -alumina (0.2g) was loaded in the dry box into a reaction vessel, figure 2.1.2. The vessel was transferred to a vacuum line manifold with an ampoule of dried pyridine, and the contents degassed. The ampoule was then opened to the manifold allowing the pyridine vapour to interact with the γ -alumina. After 10min the reaction vessel was closed to the manifold and left at room temperature for 24h. The vessel was then opened to the vacuum pump and the γ -alumina degassed for 10min. The contents of the reaction vessel were transferred, in a dry box, to a storage vessel. A sample of γ -alumina/pyridine (approx 0.05g) was analysed by the DRIFTS technique (section 2.3.2).

6.2.2. Infrared analysis of the adsorption of pyridine onto dibromine brominated Degussa 'C' γ -alumina.

The procedure to investigate the adsorption of pyridine onto calcined γ -alumina pretreated with anhydrous dibromine at 523K for 120h, was the same as that described in section 6.2.1. Two samples of brominated γ -alumina/pyridine (both approx 0.05g) were taken and analysed by DRIFTS and PAS (section 2.3.3) techniques.

6.2.3. Infrared analysis of the adsorption of pyridine onto calcined montmorillonite K10.

The experimental procedure for the investigation of the adsorption of pyridine onto calcined montmorillonite K10 was the same as that described for the adsorption of pyridine onto calcined γ -alumina. A sample of montmorillonite K10/pyridine (approx 0.05g) was analysed by the DRIFTS technique.

6.2.4. Infrared analysis of the adsorption of pyridine onto chlorinated montmorillonite K10.

The experimental procedure for the investigation is described in section 6.2.1. The calcined montmorillonite K10 sample was pretreated with anhydrous carbonyl chloride at 523K for 12h. Two samples of chlorinated montmorillonite/pyridine (both approx 0.05g) were taken and analysed by DRIFTS and PAS techniques.

6.2.5. Infrared analysis of the interaction of hydrogen bromide gas with pyridine adsorbed onto montmorillonite K10.

Calcined montmorillonite K10 (0.1g) was loaded into the reaction vessel, figure 2.1.2. The vessel was transferred to a vacuum line manifold with an ampoule of dried pyridine, and the contents degassed. The pyridine ampoule was opened to the manifold allowing the pyridine vapour to interact with the montmorillonite. After approx 10min the reaction vessel was closed to the manifold and left, at room temperature, for 24h. The vessel was then opened to the vacuum pump and the montmorillonite degassed for 10min. A Dewar flask, containing liquid nitrogen, was placed around the reaction vessel and hydrogen bromide (2.5mmol) condensed into the vessel, which was then allowed to warm to room temperature. The hydrogen bromide was left to interact with the montmorillonite/pyridine for 24h. A sample of the brominated montmorillonite/pyridine (0.05g) was taken to be analysed using DRIFTS.

6.2.6. Infrared analysis of the interaction of hydrogen bromide gas with pyridine adsorbed onto chlorinated montmorillonite K10.

The experimental procedure for the interaction of hydrogen bromide with calcined montmorillonite K10 treated with carbonyl chloride at 523K for 12h and pyridine vapour at room temperature for 24h, was the same as that described in section 6.2.5. A sample of chlorinated montmorillonite/pyridine (approx 0.05g) was analysed by the DRIFTS technique.

6.2.7. Infrared analysis of the adsorption of 2,6-dimethylpyridine onto chlorinated Degussa 'C' γ -alumina.

The calcined γ -alumina sample was pretreated with anhydrous carbonyl chloride at 523K for 12h. The chlorinated γ -alumina (0.2g) was loaded in the dry box into a reaction vessel, figure 2.1.2. The vessel was transferred to a vacuum line manifold with an ampoule of dried 2,6-dimethylpyridine, and the contents degassed. The ampoule was then opened to the manifold allowing the 2,6-dimethylpyridine vapour (3-4 Torr) to interact with the chlorinated γ -alumina. After 20min the reaction vessel was closed to the manifold and left at room temperature for 24h. The manifold was then opened to the vacuum pump and the chlorinated γ -alumina degassed for 10min. The contents of the reaction vessel were transferred, in a dry box, to a storage vessel. Two samples of chlorinated γ -alumina/2,6-dimethylpyridine (approx 0.05g) were taken and analysed by DRIFTS and PAS techniques.

6.2.8. Infrared analysis of the adsorption of 2,6-dimethylpyridine onto calcined montmorillonite K10.

The experimental procedure for the above investigation is described in section 6.2.7. Two samples of montmorillonite/dimethylpyridine (both approx 0.05g) were taken and analysed by DRIFTS and PAS techniques.

6.2.9. Infrared analysis of the adsorption of 2,6-dimethylpyridine onto chlorinated montmorillonite K10.

The procedure to investigate the interaction, at 293K, of 2,6-dimethylpyridine with calcined montmorillonite treated with anhydrous carbonyl chloride at 523K for 12h is described in section 6.2.7. Two samples of chlorinated montmorillonite/2,6-dimethylpyridine (both approx 0.05g) were analysed by DRIFTS and PAS techniques.

6.3 Results.

6.3.1. Infrared analysis of the adsorption of pyridine onto calcined Degussa 'C' γ -alumina.

DRIFTS analysis of the γ -alumina after the room temperature vapour phase interaction, indicated the presence of characteristic pyridine absorption bands in the 1700-1400 cm^{-1} region, figure 6.3.1, which are listed in table 6.3.1.

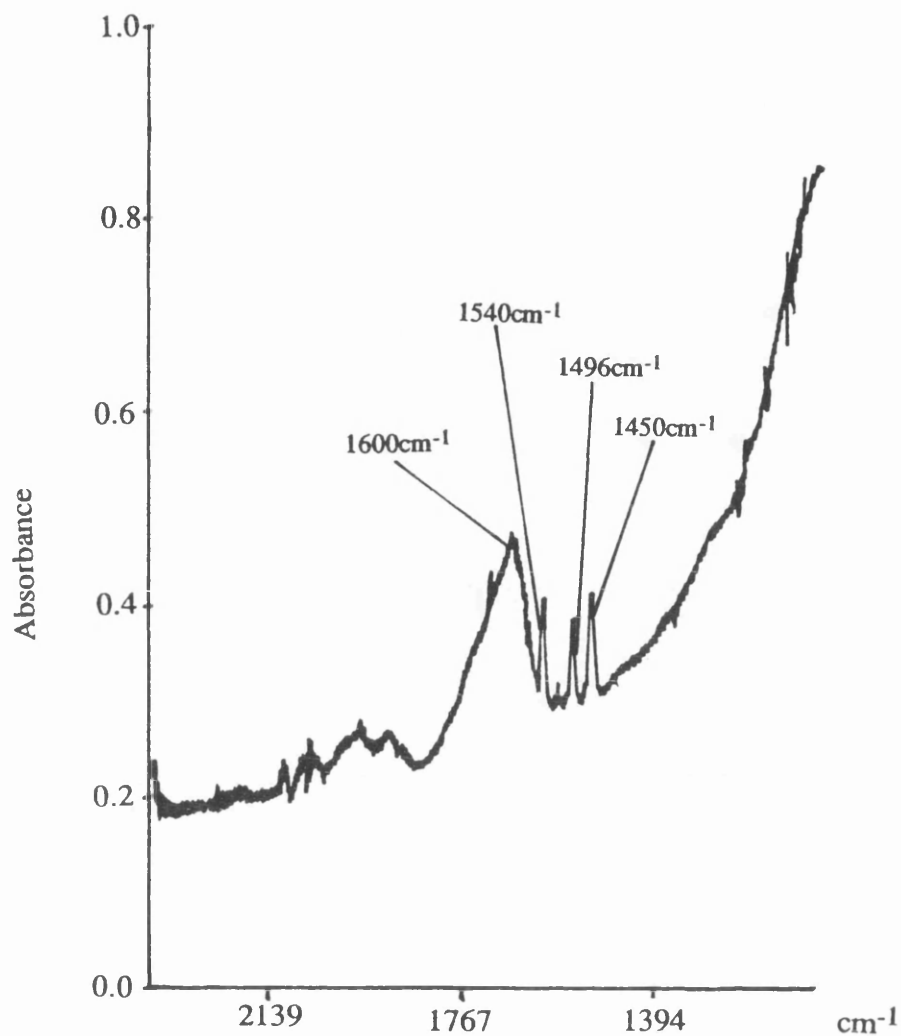


Figure 6.3.1. DRIFT spectrum of pyridine adsorbed on calcined γ -alumina.

6.3.2. Infrared analysis of the adsorption of pyridine onto dibromine brominated Degussa 'C' γ -alumina.

The interaction of pyridine vapour with calcined γ -alumina, pretreated with dibromine at 523K for 120h, was followed using both DRIFTS, figure 6.3.2a, and PAS, figure 6.3.2b, techniques. The results of these analyses, table 6.3.1, show I) the presence of both Brønsted and Lewis acid sites (the IR criteria for these sites, table 6.4.1, is discussed later in this section) and II) that absorption bands determined photoacoustically differ only marginally from those determined by diffuse reflectance spectroscopy.

6.3.3. Infrared analysis of the adsorption of pyridine onto calcined montmorillonite K10.

DRIFTS analysis of the calcined montmorillonite after room temperature interaction of pyridine vapour, figure 6.3.3a, indicated the presence of adsorbed pyridine species on the surface of the clay, when compared with the spectrum of calcined montmorillonite K10, figure 6.3.3b. Four main absorption bands were identified in the 1400-1700 cm^{-1} pyridine finger print region, table 6.3.2, and correspond to Lewis (1443 and 1490 cm^{-1}) and Brønsted (1490, 1598 and 1639 cm^{-1}) acid sites.

Table 6.3.1. Assignments for the spectral features observed from the adsorption of pyridine onto calcined and brominated γ -aluminas.

Assignment	<i>calcined γ-alumina</i>		<i>brominated γ-alumina</i>	
	DRIFTS		DRIFTS	PAS
Coordinately bonded Py	1450		1443	1450
Coordinately bonded Py + PyH	1496		1490	1495
PyH	1540		1530	1530
H-Bonded Py	1600		1603	1600

(Py = pyridine, PyH = pyridinium) all values in cm^{-1}

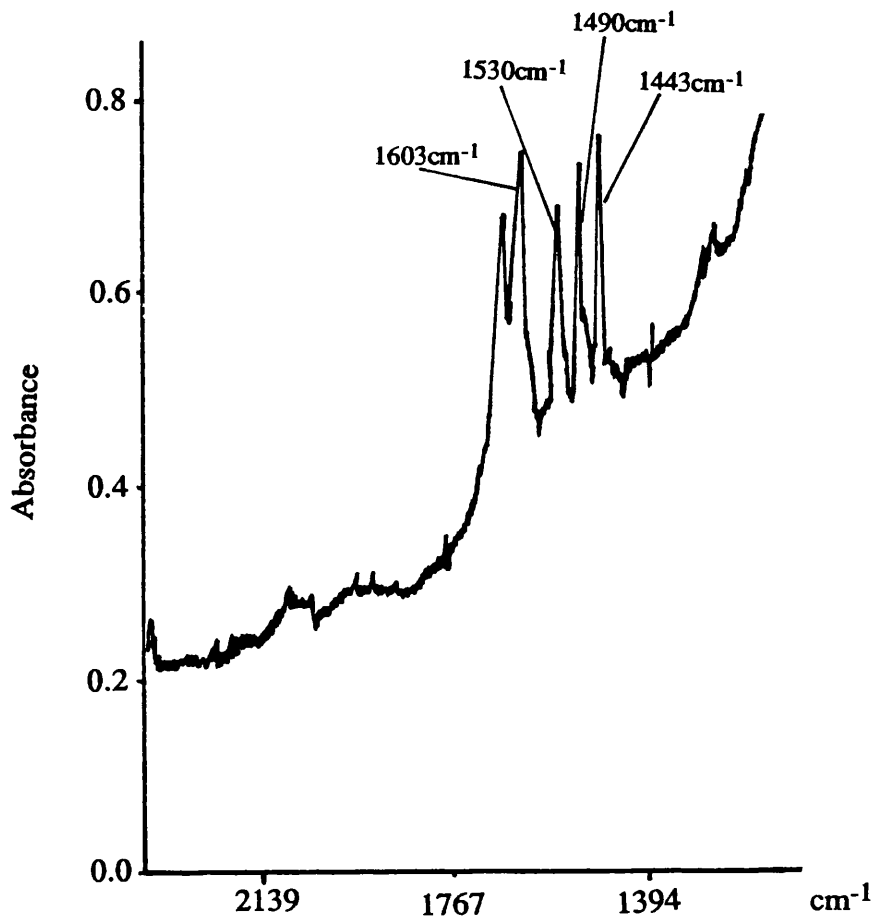


Figure 6.3.2a. DRIFT spectrum of pyridine adsorbed on brominated γ -alumina.

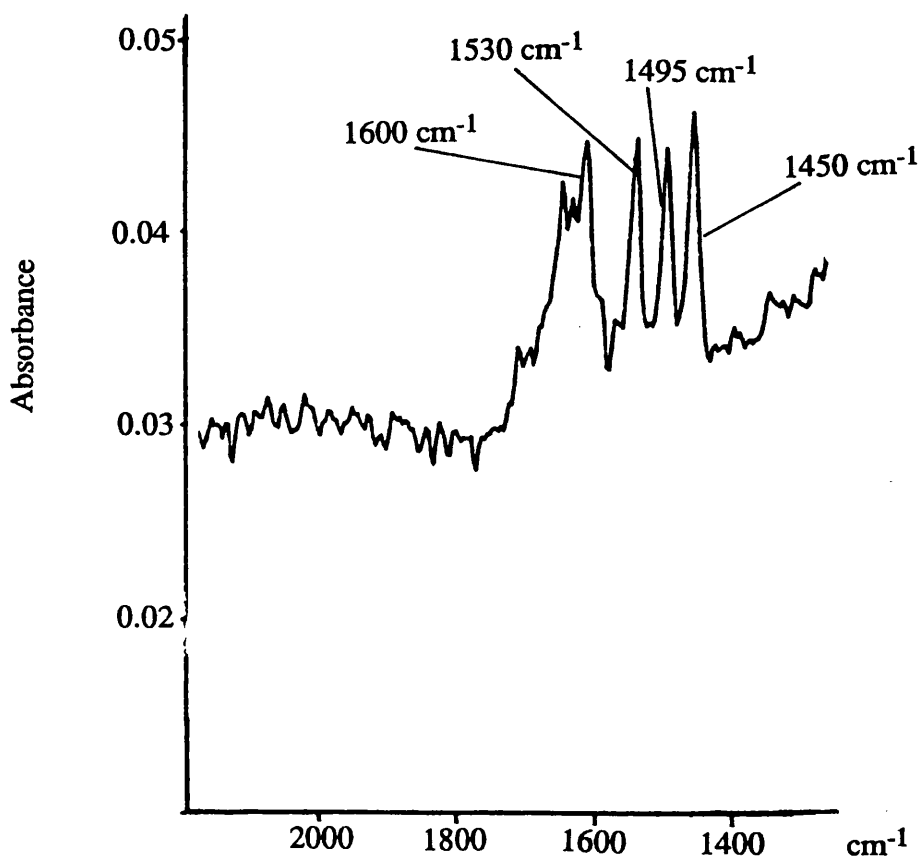


Figure 6.3.2b. PA spectrum of pyridine adsorbed on brominated γ -alumina.

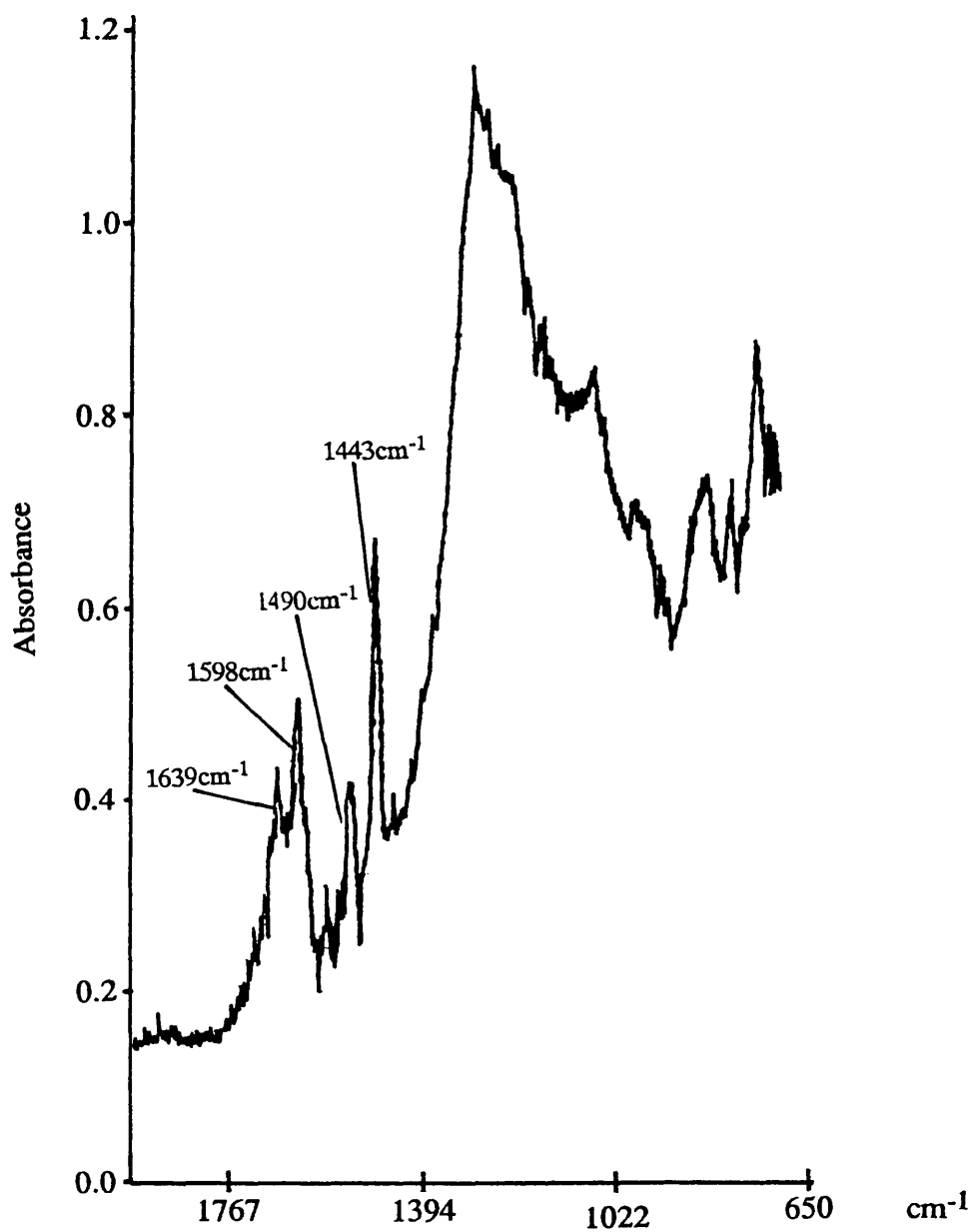


Figure 6.3.3a. DRIFT spectrum of pyridine adsorbed on calcined montmorillonite K10.

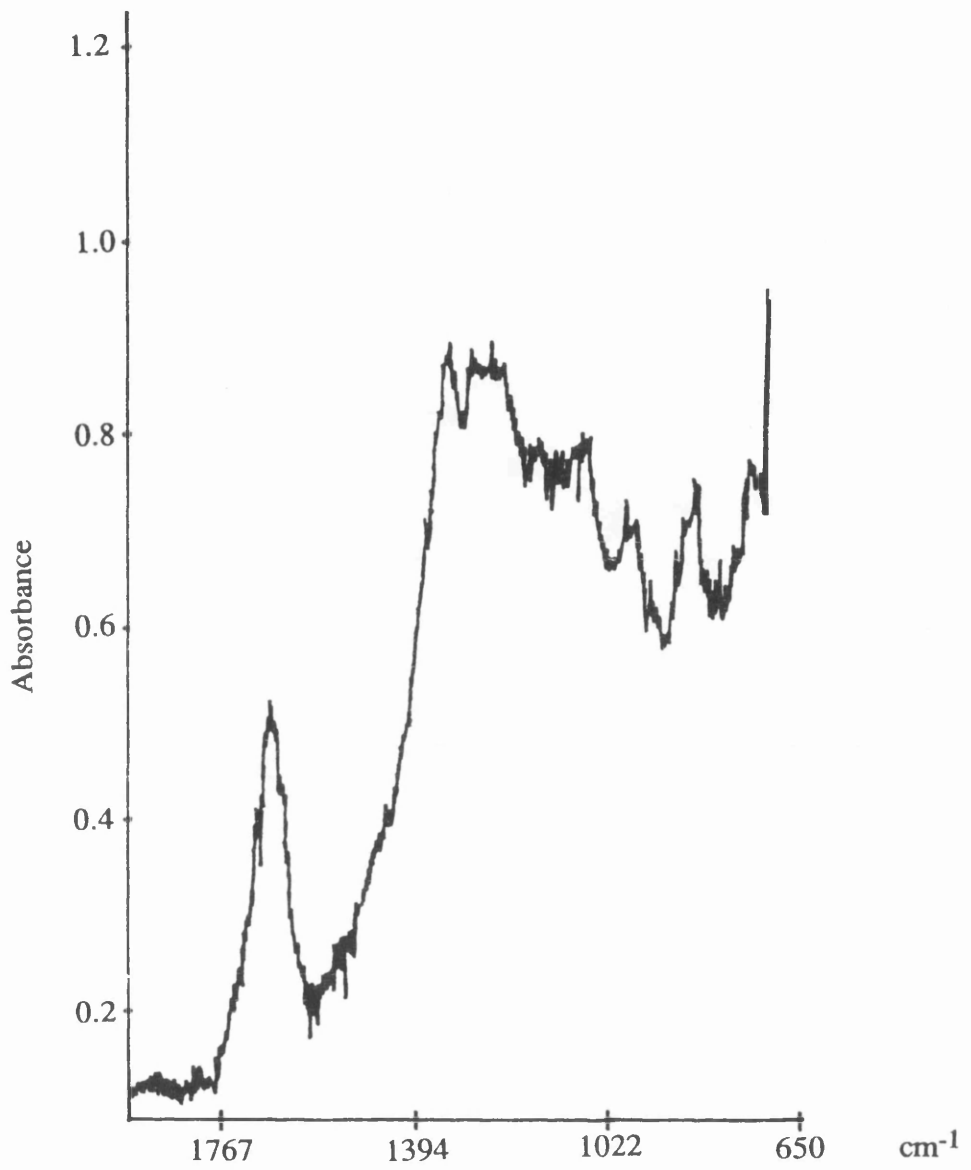


Figure 6.3.3b. DRIFT spectrum of calcined montmorillonite K10.

Table 6.3.2. Assignments for the spectral features observed from the adsorption of pyridine onto modified montmorillonite K10s.

Assignment	<i>K10</i>	<i>K10 + HBr</i>	<i>Cl-K10</i>	<i>Cl-K10 + HBr</i>
Py (C.B.)	1443			
Py (C.B.)		1457		1457
Py (C.B.) + PyH		1483	1483	1483
Py (C.B.) + PyH	1490			
PyH		1523		
PyH				1530
PyH		1536	1536	1536
PyH		1550		
PyH				1556
Py (C.B.)				1576
Py (H.B.)	1598			
Py (H.B.)			1609	
Py (H.B.)		1616		1616
PyH	1639	1640	1636	1636

(Py = pyridine, PyH = pyridinium, H.B. = hydrogen bonded, C.B. = coordinately bonded)

all values in cm^{-1}

6.3.4. Infrared analysis of the adsorption of pyridine onto chlorinated montmorillonite K10.

DRIFTS analysis of calcined chlorinated montmorillonite after room temperature interaction with pyridine vapour, figure 6.3.4a, like the calcined montmorillonite interaction, indicated the presence of pyridine species adsorbed on the chlorinated montmorillonite, when compared with the spectrum of chlorinated montmorillonite, figure 6.3.4b. Although, like the spectrum of pyridine adsorbed on calcined montmorillonite K10, four main absorption bands were identified in the 1400-1700 cm^{-1} region, table 6.3.2, none of these bands possessed the same wavenumbers as found in the calcined montmorillonite/pyridine spectrum. There were no absorption bands observed in the 1430-1456 cm^{-1} region, associated with chemisorbed pyridine (Lewis acid site).

6.3.5. Infrared analysis of the interaction of hydrogen bromide gas with pyridine adsorbed onto montmorillonite K10.

The results of the DRIFTS analysis, figure 6.3.5, are tabulated in table 6.3.2. They indicated that the acid hydrogen bromide interacted with the base pyridine on the surface of the clay, resulting in the shifted wavenumbers observed. Although none of the wavenumbers observed after this interaction correspond with wavenumbers observed from the interaction of pyridine with montmorillonite K10, some do match those observed in the interaction of pyridine with chlorinated montmorillonite K10 (1483 and 1536 cm^{-1}).

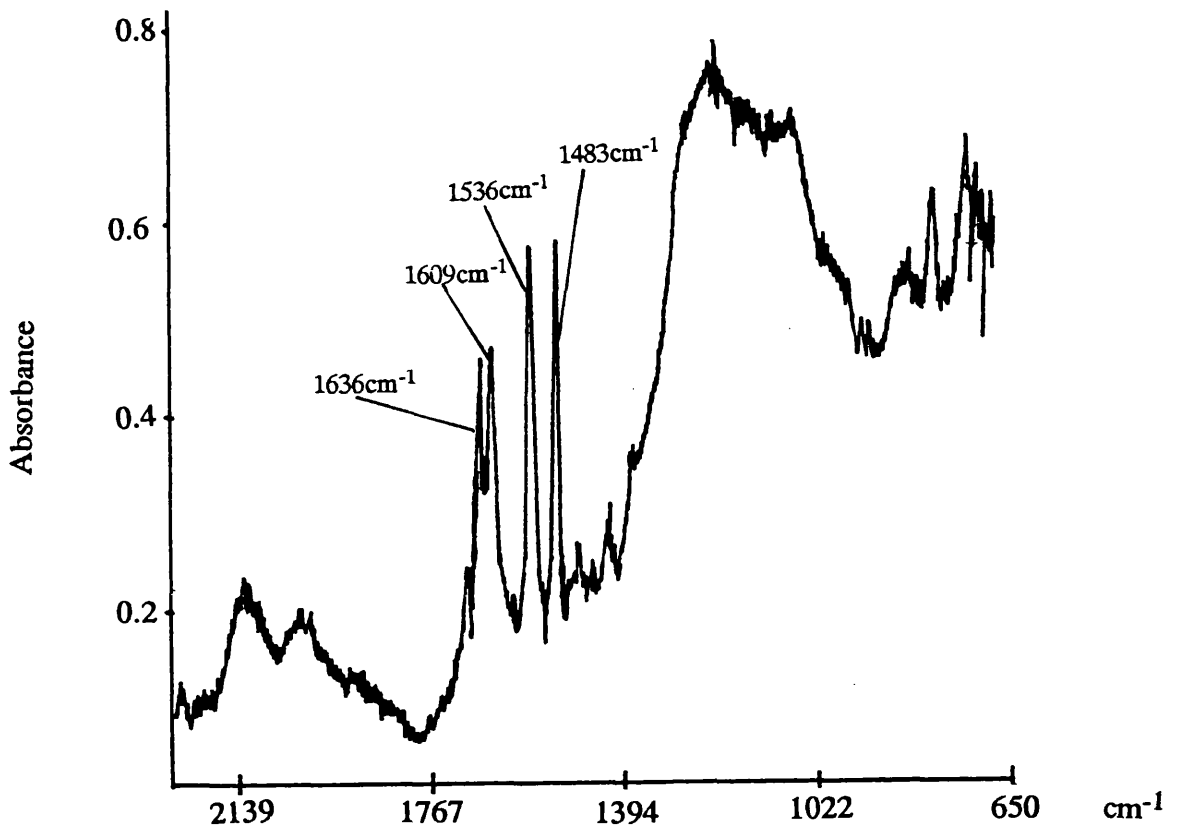


Figure 6.3.4a. DRIFT spectrum of pyridine adsorbed on calcined montmorillonite K10 treated with carbonyl chloride at 523K for 12h.

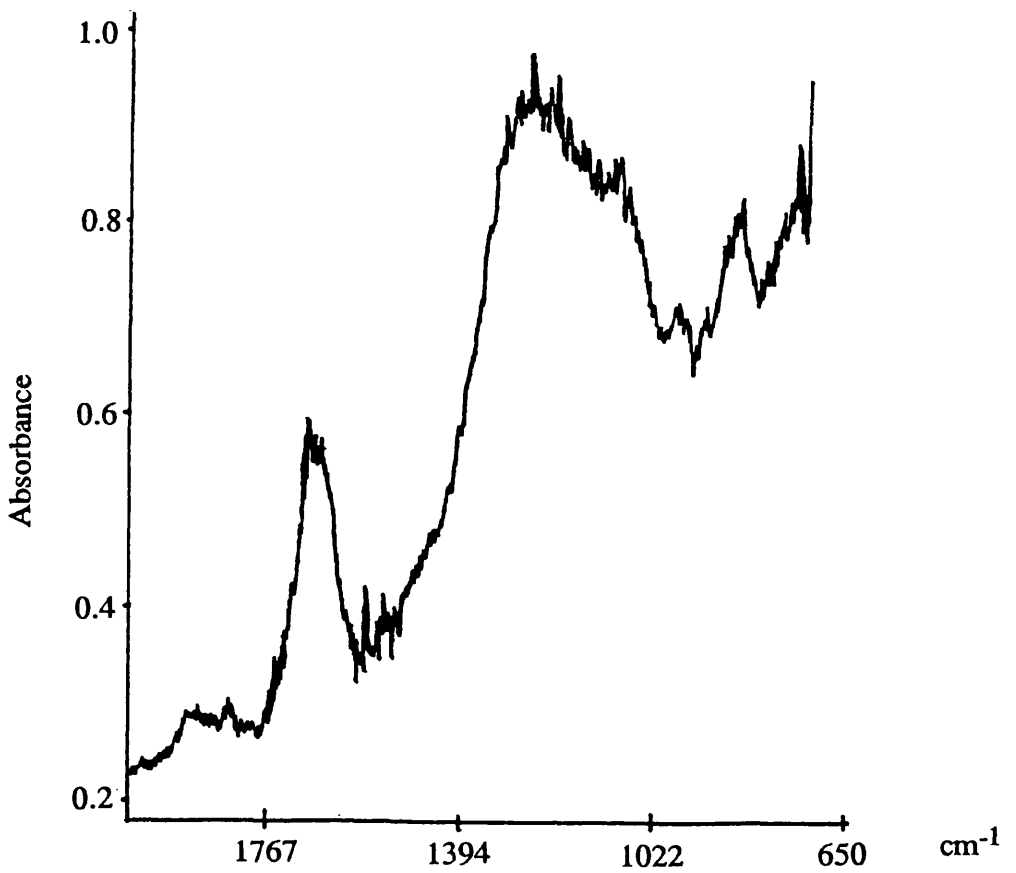


Figure 6.3.4b. DRIFT spectrum of calcined montmorillonite K10 treated with carbonyl chloride at 523K for 12h.

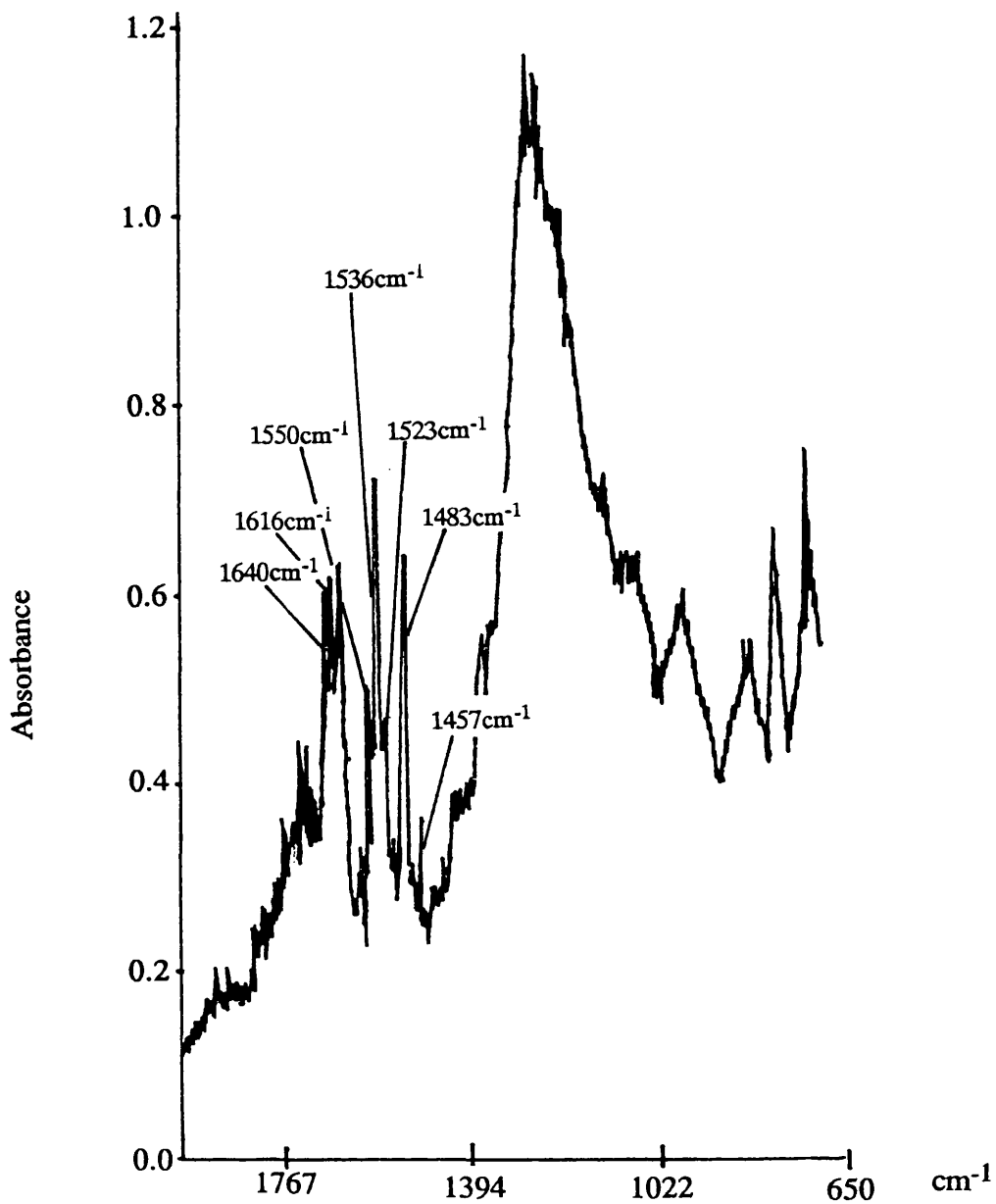


Figure 6.3.5. DRIFT spectrum of pyridine adsorbed on calcined montmorillonite K10, after the addition of hydrogen bromide.

6.3.6. Infrared analysis of the interaction of hydrogen bromide gas with pyridine adsorbed onto chlorinated montmorillonite K10.

The DRIFT spectrum obtained of the montmorillonite, after the interaction, is shown in figure 6.3.6. Eight main absorption bands were identified in the 1400-1700 cm^{-1} pyridine finger print region, table 6.3.2. Of these absorption bands, four were also observed in the montmorillonite K10 hydrogen bromide interaction (expt 6.3.5.) and three in the spectrum of pyridine adsorption on chlorinated montmorillonite K10 (expt 6.3.4).

6.3.7. Infrared analysis of the adsorption of 2,6-dimethylpyridine onto chlorinated Degussa 'C' γ -alumina.

The interaction of 2,6-dimethylpyridine with γ -alumina pretreated with anhydrous carbonyl chloride at 523K for 12h, was investigated using both DRIFTS, figure 6.3.7a, and PAS, figure 6.3.7b. The results of the DRIFTS analysis, table 6.3.3, indicated six absorption bands due to pyridinium species in Brønsted acid sites, but there were no absorption bands detected in the 1443-1490 cm^{-1} Lewis acid region. PAS analysis of the solid showed only one major absorption band at 1641 cm^{-1} .

6.3.8. Infrared analysis of the adsorption of 2,6-dimethylpyridine onto calcined montmorillonite K10.

The interaction of 2,6-Dimethylpyridine with calcined montmorillonite K10, was investigated using both DRIFTS, figure 6.3.8a, and PAS, figure 6.3.8b. The DRIFT spectrum obtained of the clay after the interaction with 2,6-dimethylpyridine was very

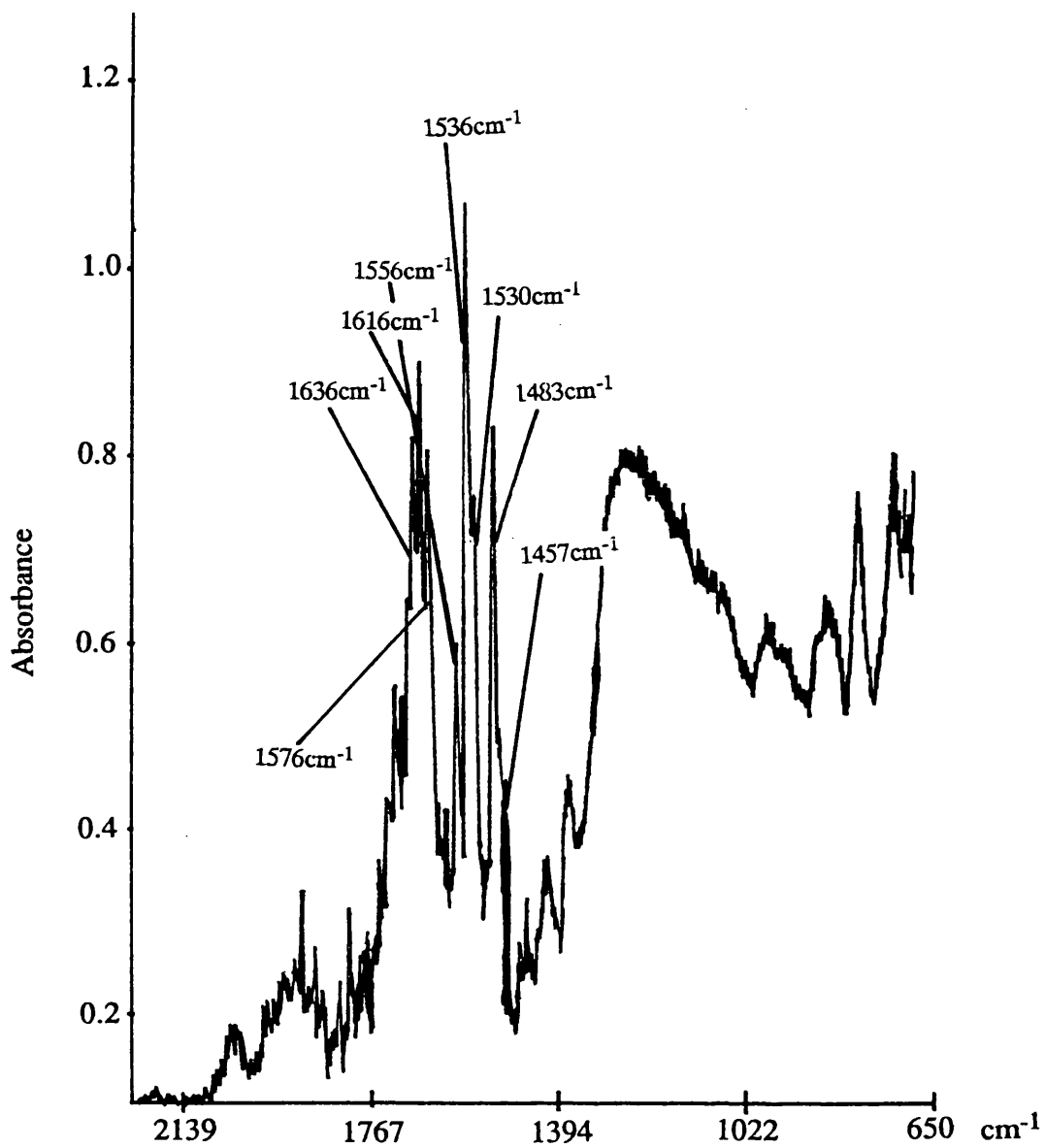


Figure 6.3.6. DRIFT spectrum of pyridine adsorbed on chlorinated montmorillonite K10, after the addition of hydrogen bromide.

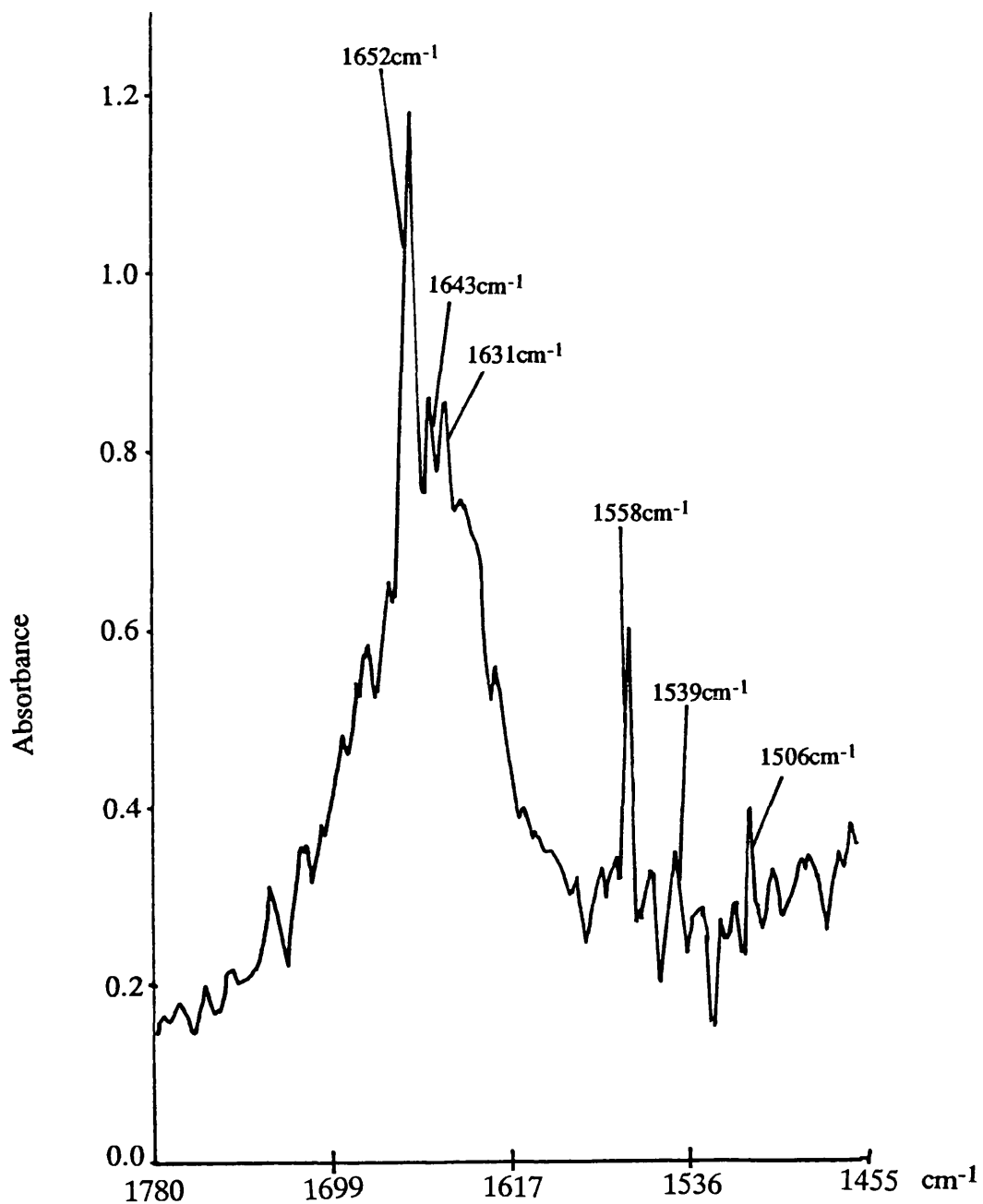


Figure 6.3.7a. DRIFT spectrum of 2,6-dimethylpyridine adsorbed on calcined γ -alumina treated with carbonyl chloride at 523K for 12h.

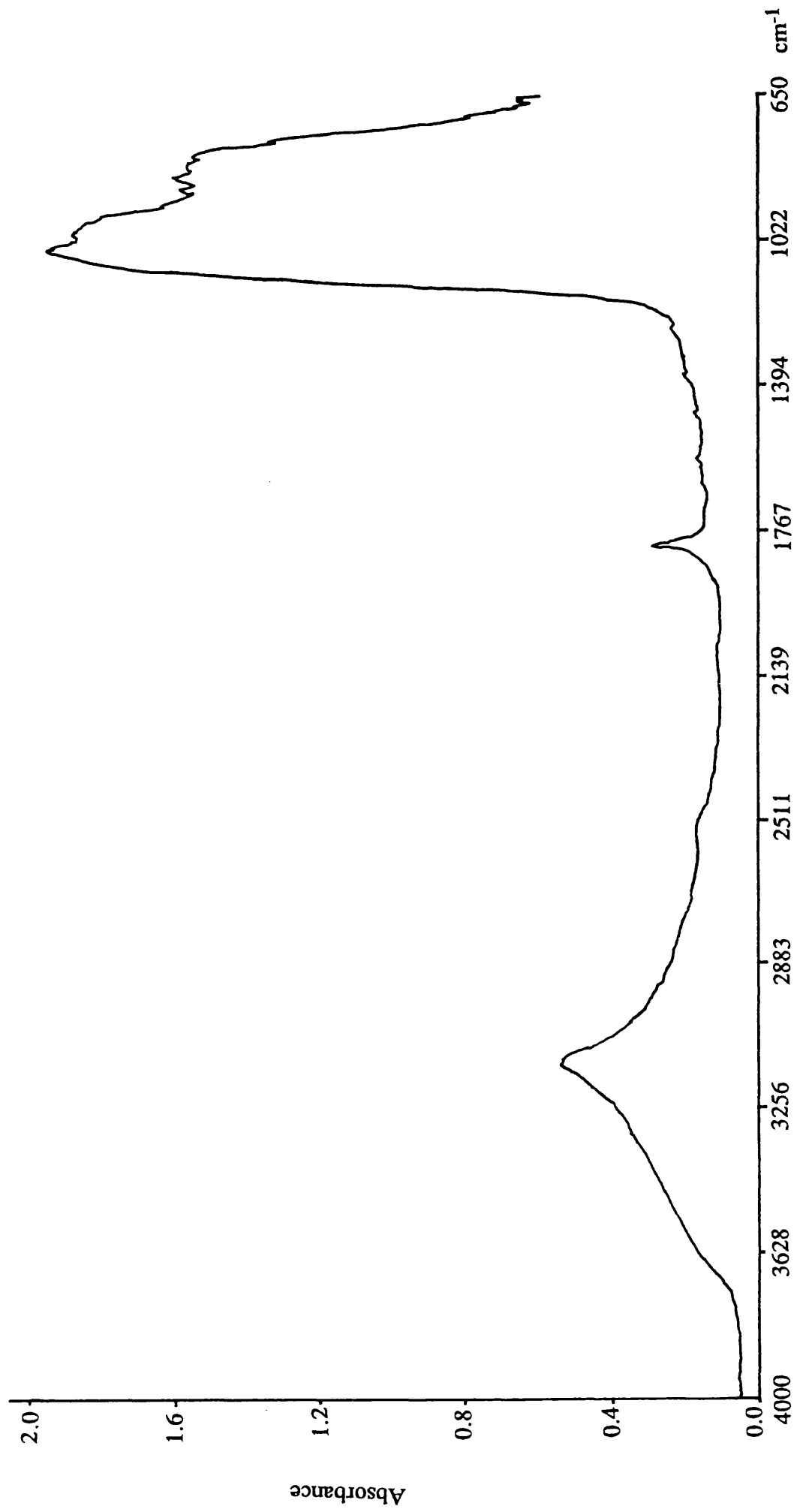


Figure 6.3.7b. PA spectrum of 2,6-dimethylpyridine adsorbed on calcined γ -alumina treated with carbonyl chloride at 523K for 12h.

Table 6.3.3. Assignments for the spectral features observed from the adsorption of 2,6-dimethylpyridine onto modified montmorillonite K10 and γ -alumina.

Assignment	<i>K10</i>	<i>Cl-K10</i>	<i>Cl-alumina</i>
PyH	1506	1506	1506
PyH	1540	1539	1539
PyH		1558	1558
PyH	1631 (1635)	1631	1631
PyH		1639 (1636)	
PyH	1647 (1649)	1646	1643 (1641)
PyH	1652	1652	1652

(figures in brackets denote PAS values.) all values in cm^{-1}

similar to that obtained from the 2,6-dimethylpyridine/chlorinated γ -alumina interaction, table 6.3.3, with the exception that no absorption band was observed at 1558cm^{-1} . The spectrum obtained by PAS analysis indicated two absorption bands (1635 and 1649cm^{-1}) in the pyridinium region.

6.3.9. Infrared analysis of the adsorption of 2,6-dimethylpyridine onto chlorinated montmorillonite K10.

DRIFTS analysis of calcined chlorinated montmorillonite after room temperature interaction with 2,6-dimethylpyridine vapour, figure 6.3.9a, like the calcined montmorillonite interaction, indicated the presence of 7 absorption bands, table 6.3.3. Two of these absorption bands (1558 and 1639cm^{-1}) did not correspond to bands observed in the calcined montmorillonite K10 interaction and must have been a result of the chlorination process. The spectrum obtained from PAS analysis, figure 6.3.9b, showed one absorption band at 1636cm^{-1} , in the 'pyridine ring region', table 6.3.3, and also indicated the presence of gaseous hydrogen chloride.

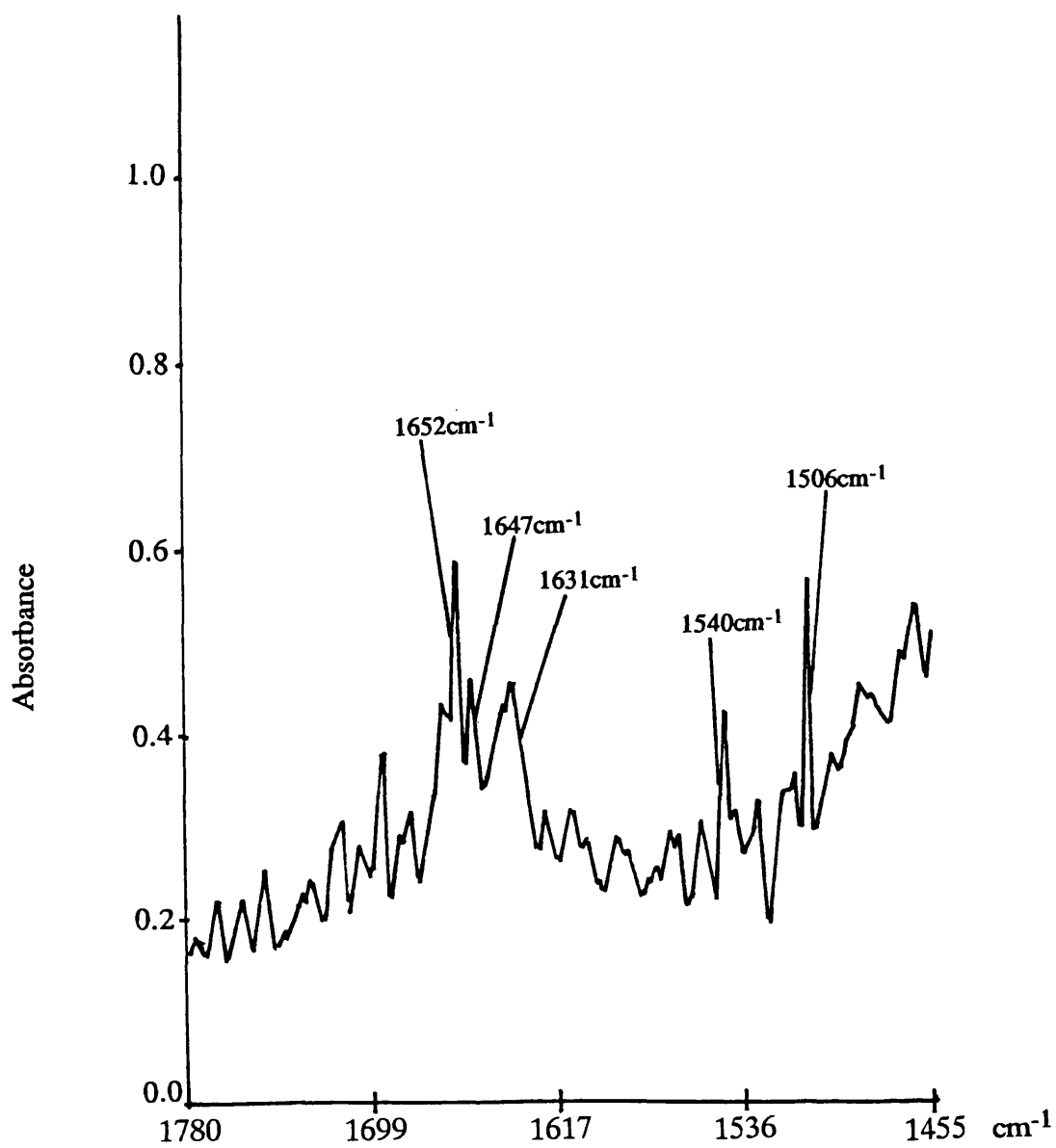


Figure 6.3.8a. DRIFT spectrum of 2,6-dimethylpyridine adsorbed on calcined montmorillonite K10.

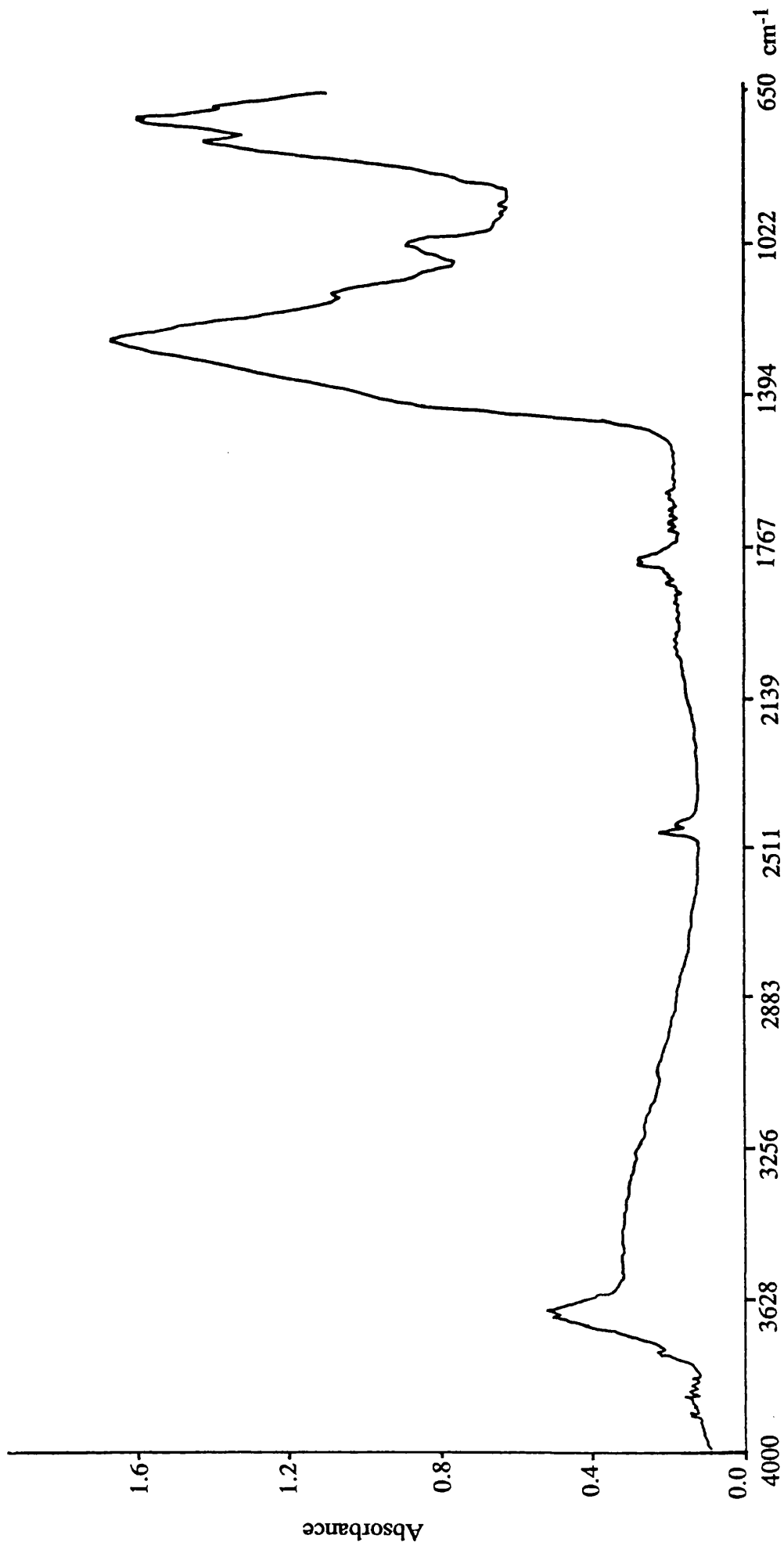


Figure 6.3.8b. IR spectrum of 2,6-dimethylpyridine adsorbed on calcined montmorillonite

K10.

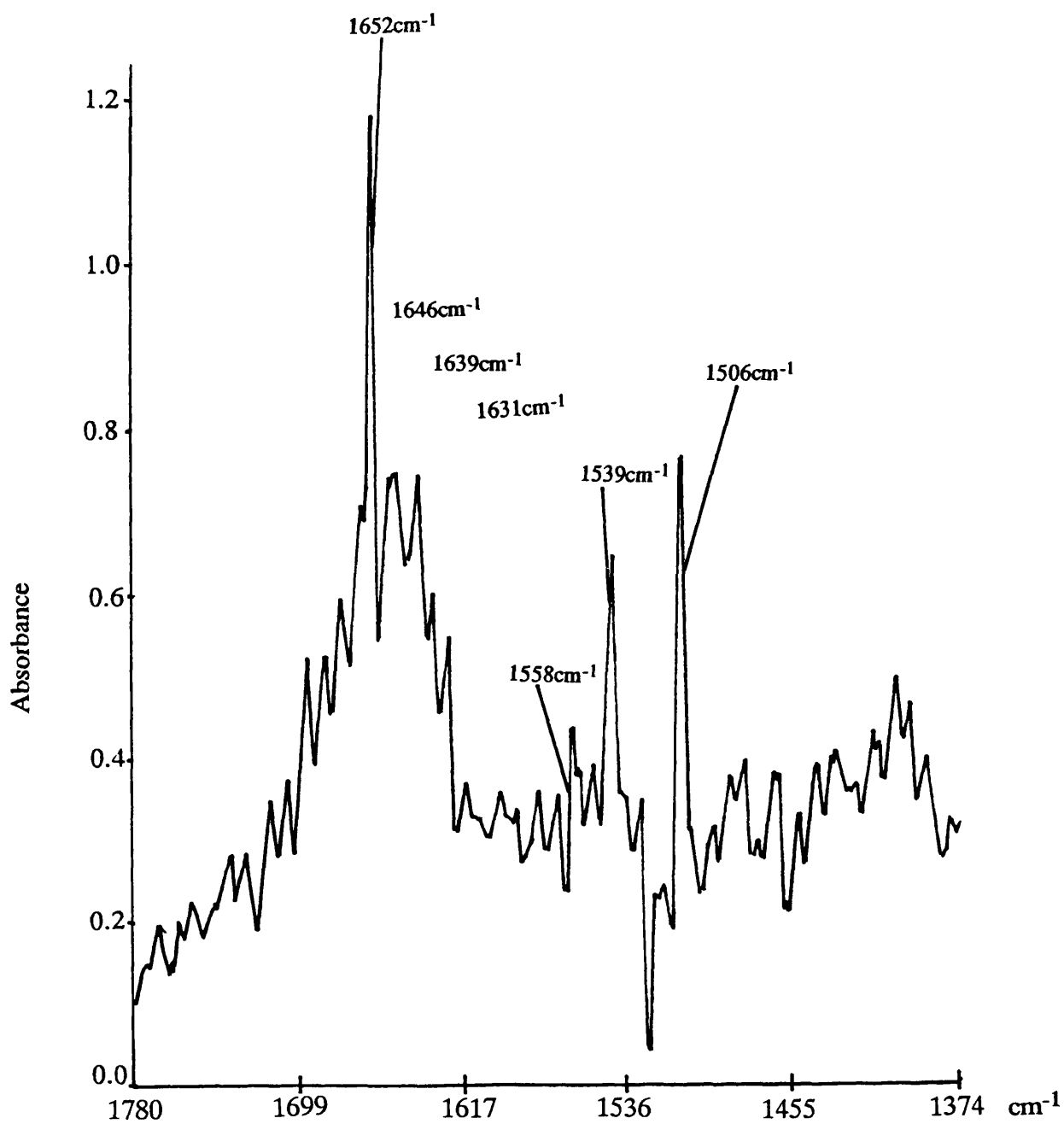


Figure 6.3.9a. DRIFT spectrum of 2,6-dimethylpyridine adsorbed on calcined montmorillonite K10 treated with carbonyl chloride at 523K for 12h.

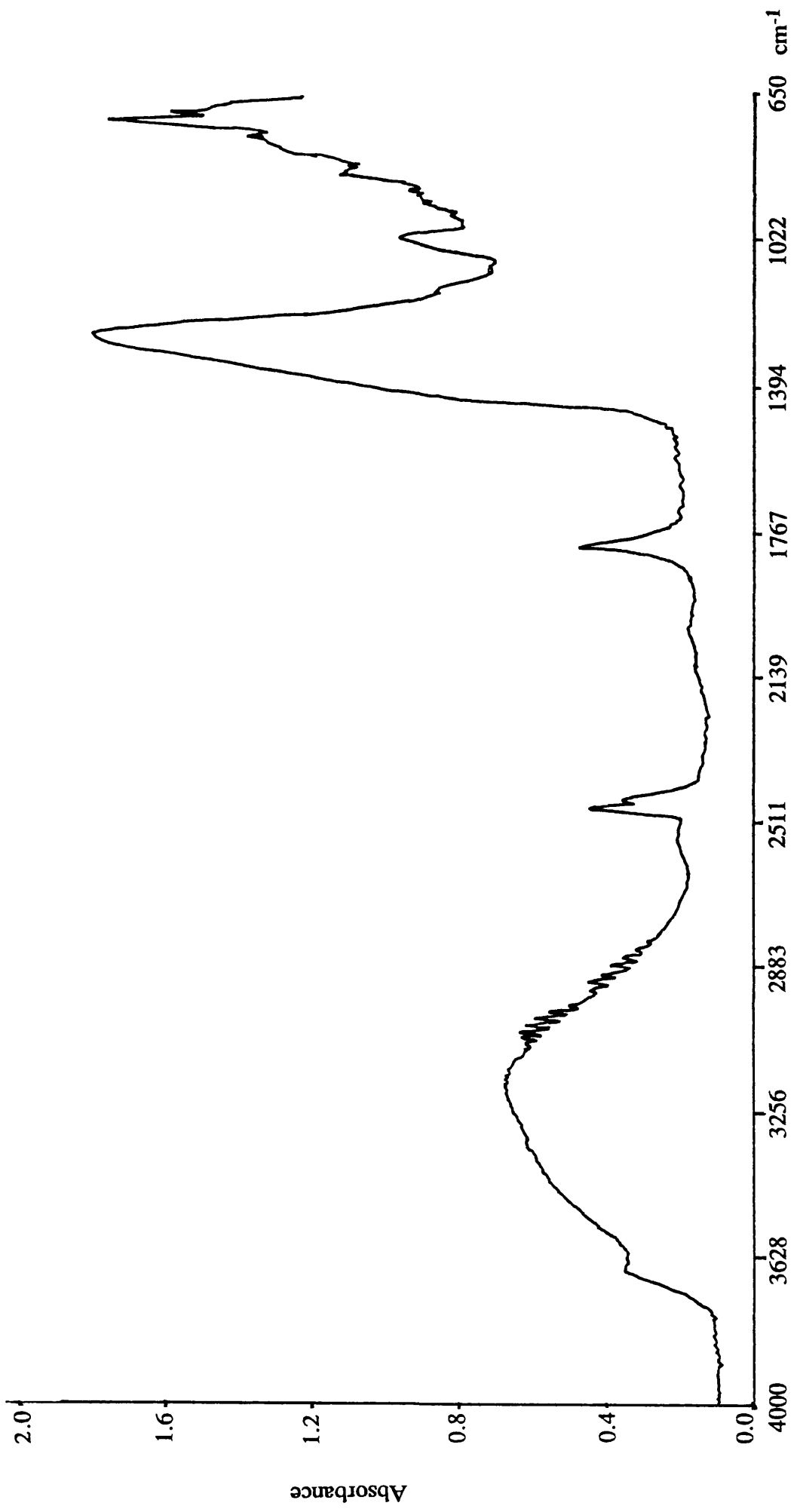


Figure 6.3.9b. PA spectrum of 2,6-dimethylpyridine adsorbed on calcined montmorillonite K10 treated with carbonyl chloride at 523K for 12h.

6.4 Discussion.

6.4.1. The adsorption of pyridine onto modified solid supports.

The use of the base pyridine as a probe molecule adsorbed onto catalytic surfaces, to determine the acidic nature of these surfaces, has been well established [129-131,133-145]. The room temperature introduction of pyridine vapour to acidic supports results in a surface coverage of approximately 17%-20% [143]. In this work the surface coverage is analysed using FTIR techniques (DRIFTS and PAS) to determine different pyridine-pyridinium species present on the surface. The spectroscopic region found to be most useful for this determination was the 'ring frequency region', 1700-1400 cm^{-1} . Although the assignments for the pyridine absorption bands in this region are well documented, there are a few discrepancies. The assignments most often used for these absorption bands are given in table 6.4.1, and were used as guide lines for the assignments of absorption bands observed in this work.

A comparison between the spectrum obtained for the pyridine adsorbed on calcined γ -alumina with that of pyridine adsorbed on brominated γ -alumina indicates that there is no substantial difference in adsorbed pyridine species. There is however a small shift in wavenumber, from 1530 cm^{-1} to 1540 cm^{-1} . This band, in a pyridinium absorption region, table 6.4.1, may be due to the formation of pyridinium bromide, $[\text{Py-H}]^+\text{Br}^-$ as opposed to pyridinium in the case of calcined γ -alumina. The fact that there are only minor differences between the pyridine absorption spectrum on calcined γ -alumina and brominated γ -alumina correlates with previous work (section 3.3.13) which found that brominating γ -alumina, unlike chlorinating, does not result in enhanced acidity.

Data for pyridine uptake onto calcined montmorillonite K10 shows coordinately bonded pyridine, hydrogen bonded and pyridinium species present, indicative of the presence of both Lewis and Brønsted acid sites. The coordinately bonded pyridine is associated with Lewis acid sites; as these sites are coordinately unsaturated they are most

Table 6.4.1. Assignments most often designated for pyridine absorption bands observed on the interaction of pyridine with solid supports.

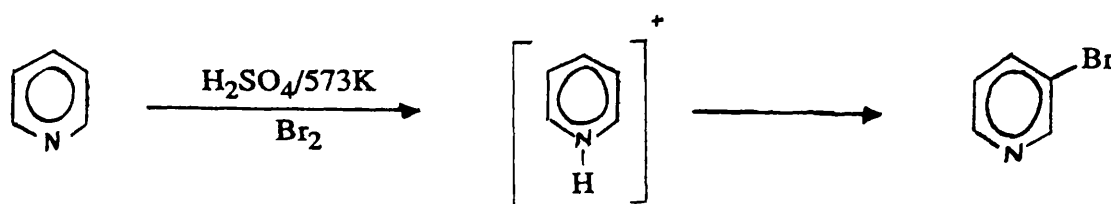
Bands (cm ⁻¹)	Coordinately	Pyridinium	H-Bonded
	Bonded Pyridine		Pyridine
1438			5
1440	1		
1445	4		2
1450	2,5		
1456	3		
1485	1	1	
1490	2,4,5	2,4,5	
1499	3	3	
1540		1,3	
1545	4	5	
1550		2	
1577	5		
1580		2	
1593			5,2
1614			5
1620	2,5	2,5	
1635		2	
1638		5	

Key to table 6.4.1.

Number	Author	Reference Number
1	E.Parry	133
2	D.W.A.Sharp	136
3	F.R.Cannings	141
4	R.S.Drago	144
5	M.R.Basila	140

likely found at the edges of the basal plane. The hydrogen bonded pyridine is associated with terminal hydroxyl groups, whereas the pyridinium species is associated with bridged hydroxyl groups, figure 6.1.2. Figure 6.4.1 shows an idealised model of the surface of montmorillonite, indicating possible Brønsted and Lewis acid sites with which pyridine may interact. The introduction of anhydrous hydrogen bromide gas to the system results in a doubling of absorption bands observed in the infrared spectrum, table 6.3.2. None of the new absorption bands correspond to those of pyridine adsorbed onto calcined montmorillonite K10, and radiotracer experiments (section 4.3.10) indicate an increase in bromine uptake in the presence of adsorbed pyridine. It is concluded, therefore, that hydrogen bromide interacts with all the different pyridine species adsorbed onto the surface. The hydrogen bromide could interact with the adsorbed pyridine by either I) brominating the pyridine ring (discussed later in this section) or II) formation of pyridinium bromide.

Bromination of the pyridine ring system is unlikely as the standard methods for the bromination of pyridine and its derivatives [147-151] usually involve acidic conditions and the heating of the reaction mixture, with dibromine as the brominating agent, scheme 6.4.1.



Scheme 6.4.1. Standard method for the bromination of a pyridine ring system.

A characteristic of these reactions is the insertion of bromine at the β -position. In this work, although acidic conditions are present on the surface of the solids, and pyridinium species are observed, bromine is only present as a nucleophile whereas the reaction mechanism requires bromine as an electrophile. It is therefore postulated that no ring bromination is occurring during the interaction of hydrogen bromide with the adsorbed pyridine and that all new absorption bands are due to the formation of pyridinium bromide

type species.

DRIFTS data for pyridine uptake onto chlorinated montmorillonite K10 indicate the presence of both hydrogen bonded pyridine and pyridinium. The evidence for the presence of coordinately bonded pyridine is inconclusive, as the band observed at 1483cm^{-1} lies in a region where both pyridinium and coordinately bonded pyridine absorptions occur. This band is also a spectral feature from the interaction of hydrogen bromide with pyridine adsorbed onto montmorillonite K10. As the addition of hydrogen bromide to supports does not afford Lewis acid sites it is unlikely that this band is due to coordinately bonded pyridine, but due to either hydrogen bonded pyridine or a pyridinium species. The lack of absorption bands due to coordinately bonded pyridine suggests that Lewis acid sites present in the calcined montmorillonite K10 have, during the chlorination process, been sterically hindered or neutralised, thus not allowing the pyridine to interact. If these proposed Lewis acid sites are at the edges of basal planes, figure 6.4.1, chlorination of these sites could affect the chemical environment of terminal hydroxyl groups also present at the edges of basal planes, figure 6.4.2. This would result in the observed change in wavenumber for hydrogen bonded pyridine from 1598cm^{-1} to 1609cm^{-1} . Evidence from ^{27}Al MAS NMR of montmorillonite K10 and chlorinated montmorillonite K10 (chapter 4) indicates that chlorination of montmorillonite K10 does not affect the tetrahedral aluminium environments. As the chlorination of γ -alumina with carbonyl chloride requires the removal of terminal hydroxyl groups [47], it is postulated that the tetrahedral aluminiums present either have no terminal hydroxyl groups or the chlorination process affects only terminal hydroxyl groups bonded to Si.

On introducing anhydrous hydrogen bromide to the pyridine/chlorinated montmorillonite K10, five new absorption bands were observed. Of these new absorption bands three (1530 , 1556 and 1576cm^{-1}) are observed in the pyridinium region, one (1616cm^{-1}) in the hydrogen bonded region and one (1457cm^{-1}) in the coordinately bonded pyridine region. It is postulated that this absorption band although in the coordinately bonded region is not due to this species. This absorption band occurs on the addition of hydrogen bromide to pyridine adsorbed on either calcined montmorillonite K10 or

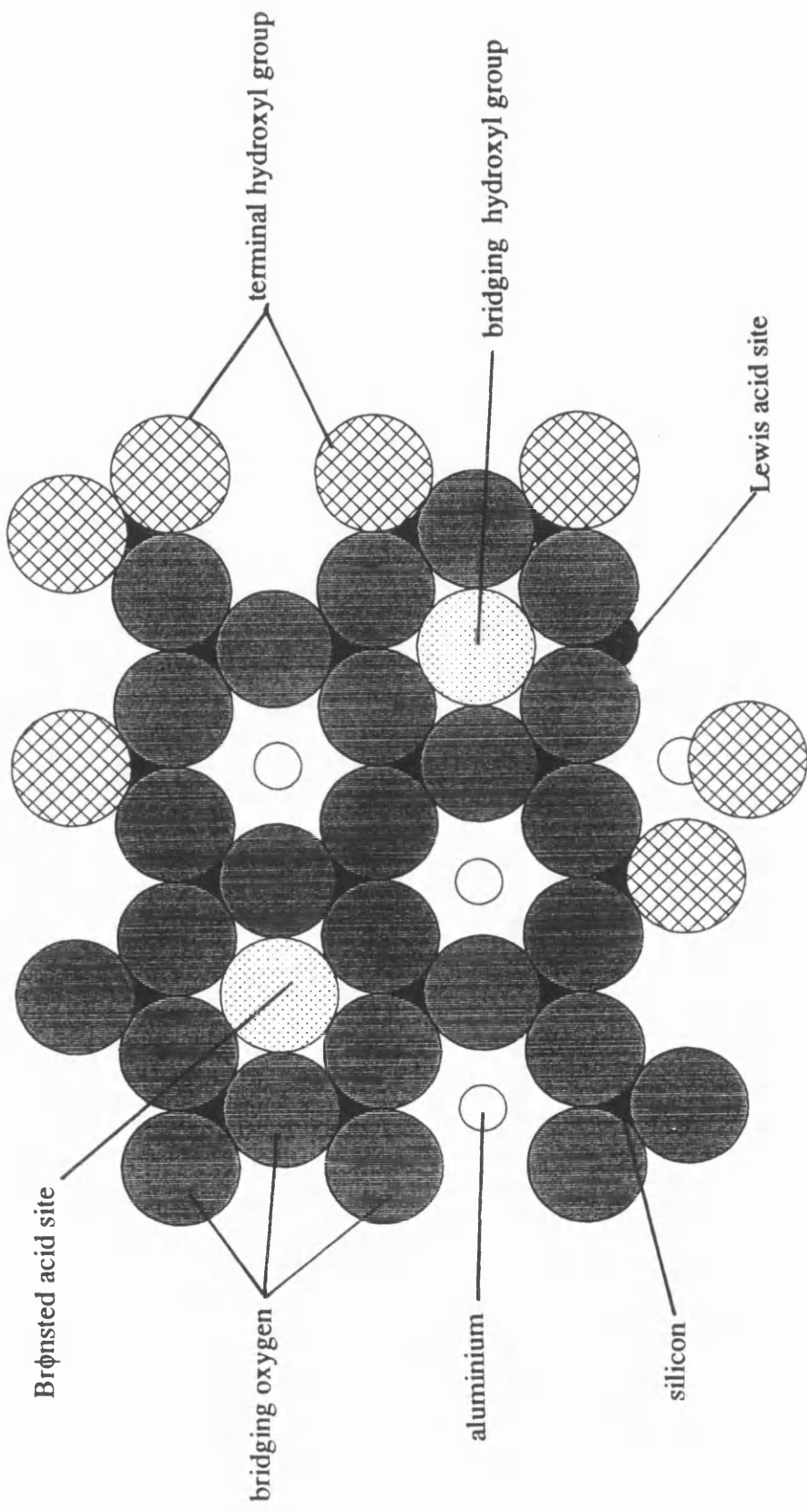


Figure 6.4.1. The idealised model of the surface of montmorillonite indicating possible Brønsted and Lewis acid sites.

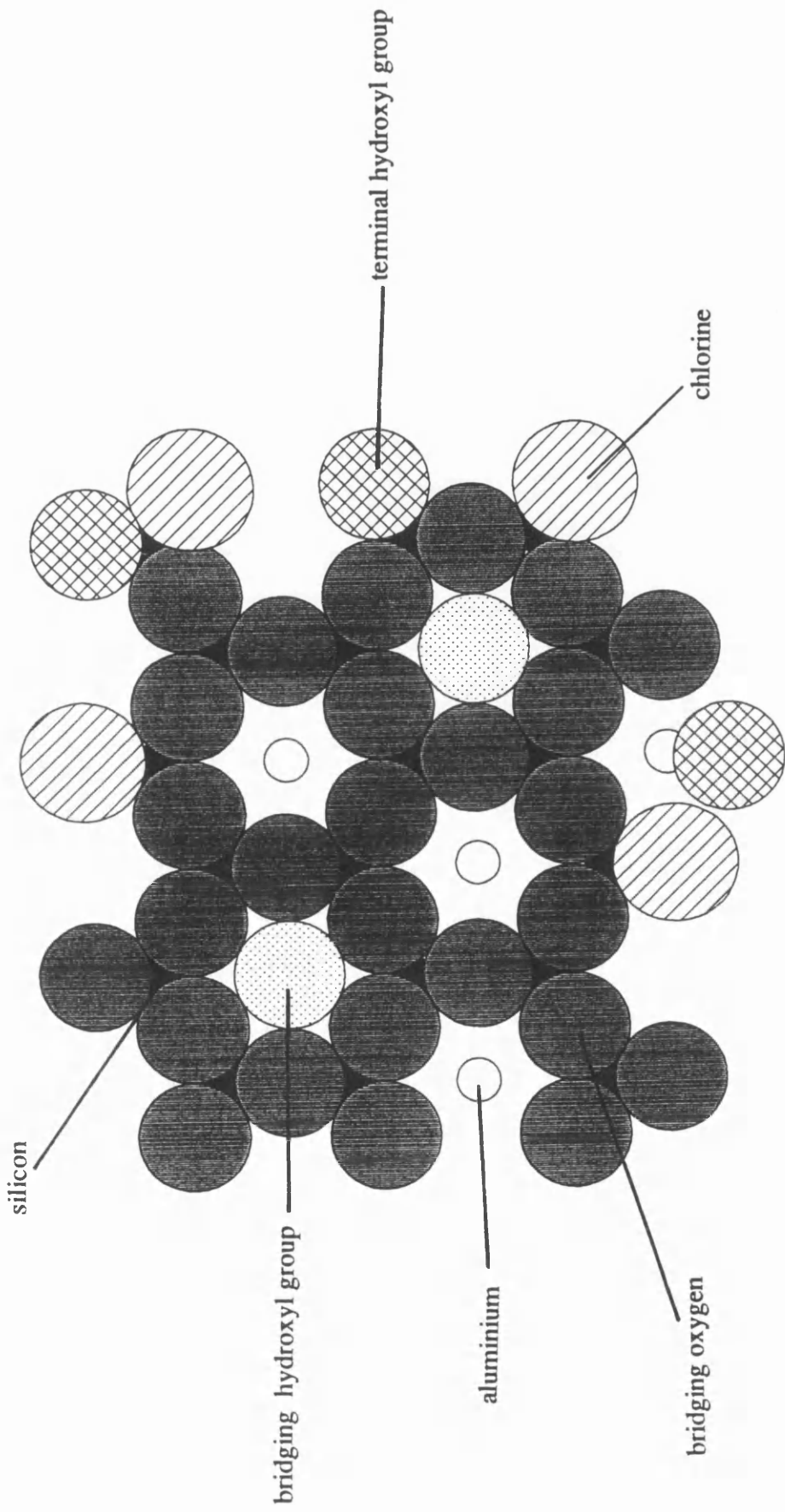


Figure 6.4.2. Postulated chlorine environments on the surface of montmorillonite, after the interaction of carbonyl chloride.

chlorinated montmorillonite K10 and is not observed under any other conditions. The band must therefore be a direct consequence of hydrogen bromide addition. For pyridine to coordinately bond to a Br species on the surface of montmorillonite K10, figure 6.4.3, an electrophilic bromine species is necessary. As the only source of bromine present is bromide, a nucleophile, it is very doubtful that this coordinately bonded species occurs. A more plausible postulate is that the hydrogen bromide interacts with pyridine adsorbed on the surface to form pyridinium bromide.

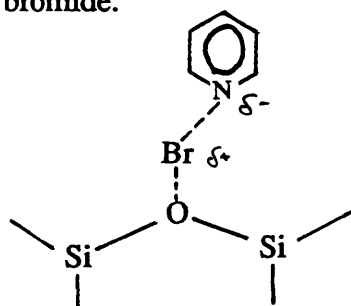
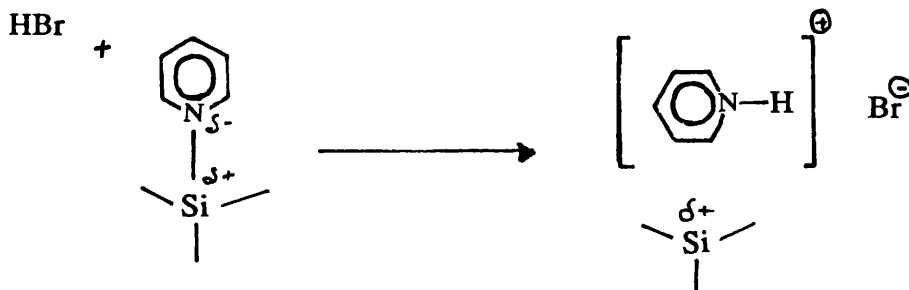


Figure 6.4.3. Pyridine coordinately bonded to Br species on the surface of montmorillonite K10

In the case of pyridine adsorbed onto calcined montmorillonite K10, the coordinately bonded pyridine (1457cm^{-1}) interacts with hydrogen bromide, scheme 6.4.2; this (1457cm^{-1}) absorption band does not appear after the interaction. The addition of hydrogen bromide also appears to facilitate the presence of a hydrogen bonded absorption band at 1616cm^{-1} for pyridine adsorbed on both calcined and chlorinated montmorillonite K10s.



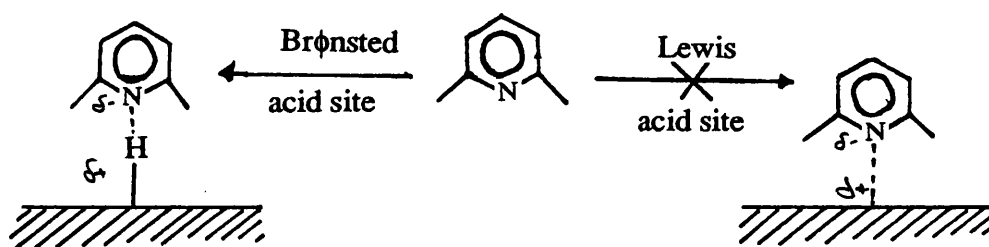
Scheme 6.4.2. The interaction of hydrogen bromide with coordinately bonded pyridine to form pyridinium bromide.

The work in this section has shown that the adsorbed pyridine species on brominated γ -alumina do not differ greatly from adsorbed species on calcined γ -alumina. This indicates that the bromination process does not alter the acidic surface properties significantly.

The pyridine adsorption experiments on calcined montmorillonite K10 and chlorinated montmorillonite K10 have led to a few unexpected results. None of the spectral features observed for pyridine adsorbed onto calcined montmorillonite K10 are observed for pyridine adsorbed on chlorinated montmorillonite K10. This suggests that the chlorination process affects all acidic sites present on calcined montmorillonite K10. Spectral features observed for pyridine adsorbed on chlorinated montmorillonite K10 give no indication for the presence of coordinately bonded pyridine, associated with Lewis acid sites. The interaction of hydrogen bromide with pyridine adsorbed on montmorillonite K10, scheme 6.4.2, gives an insight into why coordinately bonded pyridine is not observed on montmorillonite K10 treated with carbonyl chloride. In this reaction scheme the coordinately bonded pyridine is displaced, and the Lewis acid site brominated with hydrogen bromide. The pyridine then interacts with the adsorbed bromine to form pyridinium bromide. During the chlorination of montmorillonite K10, with carbonyl chloride, hydrogen chloride is evolved. If this interacts with the montmorillonite K10 in the same manner as hydrogen bromide, then pyridinium chloride would be observed on the surface and not coordinately bonded pyridinium. One final aspect of the addition of hydrogen bromide to pyridine adsorbed onto montmorillonite K10 is the increase in the number of absorption bands observed in the pyridinium region. This increase suggests that the addition of hydrogen bromide to the montmorillonite K10 results in the increase of acidic surface features present. This pattern is also observed on the addition of hydrogen bromide to pyridine adsorbed onto montmorillonite K10 treated with carbonyl chloride.

6.4.2. The adsorption of 2,6-dimethylpyridine onto modified solid supports.

The pyridine derivative 2,6-dimethylpyridine is used as a probe molecule because the sterically hindered nitrogen atom should interact with Brønsted acid sites present on the surface and not with the more sterically hindered Lewis acid sites, scheme 6.4.3.



Scheme 6.4.3. The interaction of 2,6-dimethylpyridine with Brønsted and Lewis acid sites.

In these comparative studies for the adsorption of 2,6-dimethylpyridine onto modified supports all the absorption bands observed, table 6.3.3, are in the pyridinium region, table 6.4.1. The DRIFTS analysis for the adsorption of 2,6-dimethylpyridine onto calcined montmorillonite K10 and chlorinated montmorillonite K10 show similar spectral features, but with differing relative intensities. The five absorption bands observed in the interaction with calcined montmorillonite K10, although very much less intense, are all observed in the interaction with chlorinated montmorillonite K10. The chlorinated montmorillonite K10 has two further absorption bands at 1558cm^{-1} and 1639cm^{-1} which, it is postulated, belong to dimethylpyridinium chloride species, figure 6.4.4.

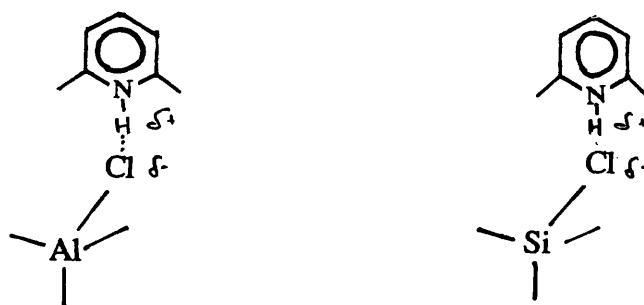


Figure 6.4.4. Proposed dimethylpyridinium chloride species on the surface of chlorinated montmorillonite K10.

DRIFTS analysis for the adsorption of 2,6-dimethylpyridine onto chlorinated γ -alumina, like that of chlorinated montmorillonite K10, show similar spectral features to those observed in the calcined montmorillonite interaction, table 6.3.3. Like the chlorinated montmorillonite K10, the chlorinated γ -alumina has an absorption band at 1558cm^{-1} relating to a dimethylpyridinium chloride species, figure 6.4.4, but unlike the chlorinated montmorillonite K10 there is no absorption band at 1639cm^{-1} . It is postulated therefore that the absorption band at 1558cm^{-1} corresponds to a dimethylpyridinium chloride species in which the chloride is adsorbed onto an aluminium atom and the absorption band at 1639cm^{-1} corresponds to a dimethylpyridinium chloride species in which the chloride is adsorbed onto a silicon atom, figure 6.4.4.

The photoacoustic analysis of the adsorption of 2,6-dimethylpyridine onto the solid supports has not conferred the same spectral definition as the DRIFTS analysis. Photoacoustic analysis has shown though the detection of hydrogen chloride gas, section 6.3.9, that this technique for analysing the surface of materials can also identify volatile materials above the surface. This evolution of hydrogen chloride suggests that exposure to a small amount of moisture results in the dechlorination of the surface. This observation is not surprising as the Si-Cl bond is readily hydrolysed in the presence of water [152], equation 6.4.1.



CHAPTER 7

Conclusions: The Nature of Brominated Oxides and their Catalytic Functions.

In this work the interactions of both calcined γ -alumina and calcined montmorillonite K10 with a variety of brominating agents have been investigated. These brominating reagents include dibromomethane, hydrogen bromide and dibromine. Results from these investigations indicate that each of the reagents used interacts with the supports in its own distinct manner. Consequently the nature of the bromine species adsorbed onto the supports differs for each reagent used. A common factor in all these cases is hydrogen bromide, as this species is formed as a result of both the dibromomethane and the dibromine interactions. It seems reasonable to assume therefore that dissociatively adsorbed hydrogen bromide, figure 7.1, by analogy with HCl [49], will be present on the surface of solid regardless of brominating agent employed.

The interaction of dibromomethane with calcined γ -alumina and calcined montmorillonite K10 (sections 3.3.1 & 3.3.7) appears on first inspection to be similar to that of carbonyl chloride with these oxides. The latter of these processes is believed to involve the replacement of inplane oxygens by chlorine atoms, figure 1.9.2. Similarities between the dibromomethane and carbonyl chloride interactions with γ -alumina include:- I) a reaction temperature of 523K, below which neither the chlorination nor bromination process occurs to any great extent, II) the formation of hydrogen chloride or bromide, and III) the formation of carbon dioxide or carbon monoxide, indicating the removal of oxygen from the surface of the support. One further similarity between the chlorination and bromination processes is that halomethanes with an odd number of halogens react

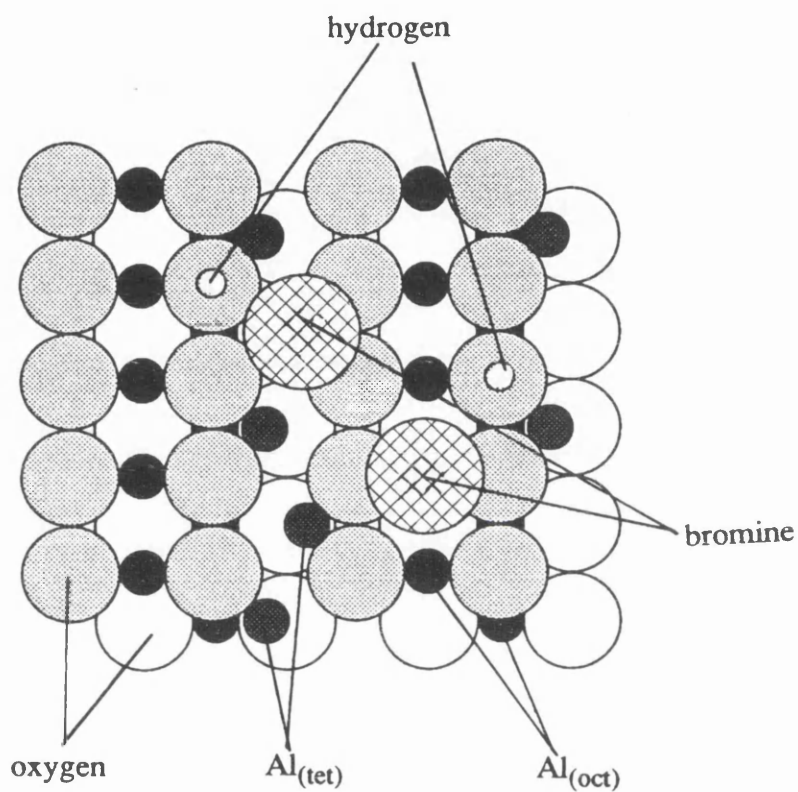


Figure 7.1. Postulated bromine environments present on the surface of γ -alumina after the room temperature interaction of hydrogen bromide.

differently than halomethanes with an even number of halogens. Although the reaction conditions and vapour phase products are similar in both reactions, the nature of the supports after the reactions are dissimilar. Whereas the interaction with carbonyl chloride increases the Lewis acidity of the support [47] the interaction with dibromomethane (page 67) does not. The chlorination process results in a halogen content 2-3 times greater than that of the bromination process even when greatly reduced reaction times are used. $^{82}\text{BrBr}$ Radiotracer studies (sections 5.3.2 - 5.3.9) have suggested that whilst the interaction of carbonyl chloride reduces the surface area of γ -alumina, the interaction of dibromomethane does not. DRIFTS analysis of the supports after the halogenation reactions show organics present after the reaction with dibromomethane; there are however no organics detected after the interaction of carbonyl chloride. It is postulated, from these observed similarities and dissimilarities, that the interaction of dibromomethane with γ -alumina is slower and less efficient than the carbonyl chloride due to the larger size of the bromine atom. On this basis γ -alumina is preferentially chlorinated as the smaller chlorine atom causes less disruption to the lattice structure than the larger bromine. With montmorillonite K10, it is postulated that the reaction with carbonyl chloride results mainly in the chlorination of species at the edge of the basal plane (page 171). When bromochloromethane reacts with montmorillonite K10 similar bromine and chlorine contents are observed. If, as postulated, the halogenation occurs at the edge of the basal plane then, unlike γ -alumina, the difference in size of the bromine and chlorine will not have such a marked affect on the halogenation process, as these sites are sterically less hindered. The fact that the surface Lewis acidity of γ -alumina after treatment with dibromomethane is not enhanced may be due also to the larger size of the bromine. Following the model used to account for strong Lewis acidity after chlorination with carbonyl chloride in which the formation of $-\text{AlCl}_2$ groups are postulated, leads to the suggestion that surface Al^{III} in $-\text{AlBr}_2$ groups is sterically too hindered to function as an effective Lewis acid, figure 7.2.

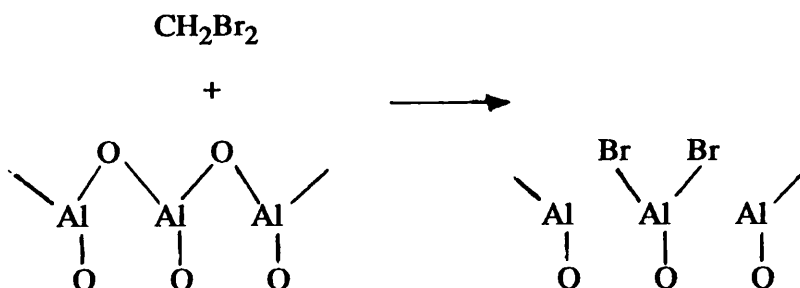


Figure 7.2. Postulated bromine species present on γ -alumina after the interaction of dibromomethane.

The interaction of hydrogen bromide with solid supports (sections 4.3.1-7), unlike that of dibromomethane, occurs readily and rapidly at room temperature. The resulting bromine content, approximately $1.0 \text{ mg atom g}^{-1}$, is similar to that of the dibromomethane interaction. The interaction of hydrogen bromide with montmorillonite K10 has proven to be the most interesting. Exchange reactions with radiolabelled hydrogen bromide indicate that there are several types of bromine species present on the support (page 115), one of which is labile to exchange with hydrogen bromide at room temperature, the other inert. These labile and inert species were detected on both uncalcined and calcined montmorillonite K10. The presence of at least two types of bromine species on the surface is supported by the pyridine adsorption experiments (chapter 6). In these investigations the addition of hydrogen bromide to pyridine adsorbed on calcined montmorillonite K10 resulted in the formation of seven absorption bands (section 6.3.5) not observed in pyridine adsorbed on calcined montmorillonite K10. Using the idealised model of montmorillonite K10 there are several possible sites for the dissociative adsorption of hydrogen bromide. One of these sites, figure 7.3(i), is on the surface plane of the clay, where the bromide is adsorbed onto a surface Si and the hydrogen to a neighbouring surface oxygen. Two other, sterically less hindered, sites are at the edge of the basal plane. Using these sites the

bromine can adsorb on either a Si atom, figure 7.3(ii), or on an Al atom, figure 7.3(iii), with the hydrogen being located on a neighbouring oxygen. One further possibility is the adsorption of bromide onto a tetrahedral aluminium. Although the idealised model of montmorillonite K10 does not contain tetrahedral aluminium environments, ^{27}Al MAS NMR (section 3.4.3) have shown this species to exist. There is no precise description for dissociative adsorption of hydrogen bromide onto montmorillonite K10 at the present time and therefore which of these sites results in labile bromine and which in inert bromine cannot be stated.

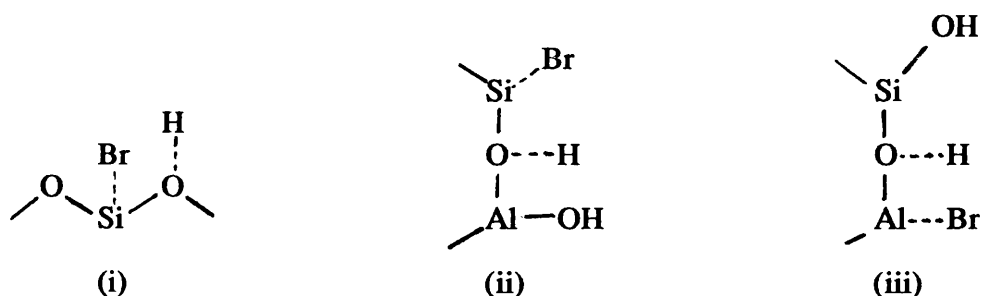


Figure 7.3. Postulated bromine species present on montmorillonite K10 after the interaction of hydrogen bromide.

Pyridine adsorption investigations (chapter 6) have shown the complex nature of the acidic surfaces of the supports after the interaction of hydrogen bromide and carbonyl chloride. The assignment of all the spectral features observed in these interactions to specific adsorbed species is difficult. The fallibility of these assignments is shown for the montmorillonite K10 treated with carbonyl chloride (table 6.3.5). This chlorinated montmorillonite K10 enhances a Lewis acid reaction, but the pyridine adsorption experiments indicated no coordinately bonded pyridine present (section 6.3.4). The Lewis acid sites on montmorillonite K10 must therefore be assigned a pyridinium species. Adsorption of pyridine onto montmorillonite K10 treated with carbonyl chloride results in

the formation of only 4 new absorption bands, when compared with pyridine adsorbed on calcined montmorillonite K10.

In contrast to the systems summarised above, the interaction of dibromine with the oxides results in substantial bromine uptake onto the supports (section 5.3.2-7). The room temperature interaction of dibromine with both calcined montmorillonite K10 and γ -alumina results in bromine contents 15 times greater than those observed for the other halogenating reagents. Most of the bromine is easily removed by pumping the solid under *vacuo*, resulting in bromine retention of approximately $1.0 \text{ mg atom g}^{-1}$, a value similar to the bromine uptake found in the dibromomethane and hydrogen bromide interactions. From this it is concluded that there are two bromine species on the surface; a physisorbed species, probably dibromine, and a chemisorbed species (section 5.4.1), figure 7.4. It is this chemisorbed species which is retained on the support after pumping under *vacuo*. The interaction of dibromine with powdered Kel-F polymer underlined this finding. As with montmorillonite K10 and γ -alumina dibromine adsorbs onto Kel-F powder. As Kel-F powder is inert to chemical attack the bromine present on the surface can be only physisorbed dibromine. On pumping all [^{82}Br] activity is removed from the powder, consistent with physisorbed dibromine.

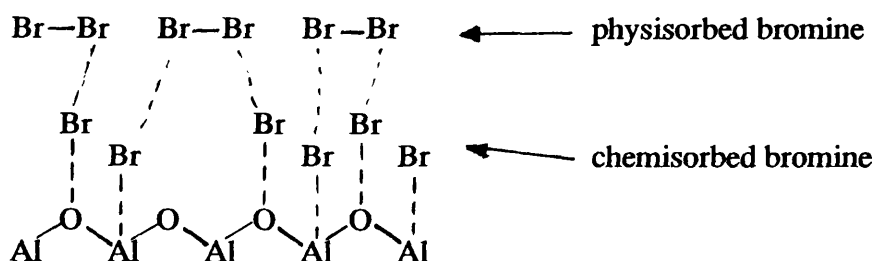


Figure 7.4. Postulated bromine species present on γ -alumina after the interaction of dibromine.

In summary, of the three brominating agents investigated in this work, the support with the least potential is that resulting from the interactions of dibromomethane. It had been hoped at the outset of this work that this bromination process would result in a support which possessed enhanced Lewis acidity, enabling the promotion of bromination reactions in situations when chlorinated supports could not be used, for example where cross contamination of the halogens might occur. This bromination process has however resulted in a brominated γ -alumina with properties closer to that of calcined γ -alumina than γ -alumina treated with carbonyl chloride. The rapid uptake of hydrogen bromide onto the solid supports, although small, has proved to be very useful in promoting hydrobromination reactions, as discussed below. The quantity of dibromine which can be adsorbed onto both calcined γ -alumina and montmorillonite K10 is surprising. Although this phenomenon may be a hindrance at times, such as in the anisole experiment (experiment 5.3.10), where the order of addition of reagents determines the products obtained, large dibromine contents may be beneficial if the dibromine can be leached slowly from the solid.

The use of calcined γ -alumina and montmorillonite K10 to enhance or promote reactions, in this work, has proved to be successful. Modifications to the supports have been required in some cases before promotion of the reaction occurs. In this work the supports were used to promote a Lewis acid catalysed reaction, Hell Volhart Zelinsky, and a Brønsted acid catalysed reaction, the hydrobromination of butenes and decadienes. The ability of γ -alumina and montmorillonite K10 to promote the Hell Volhart Zelinsky reaction was investigated initially. Although pyridine adsorption studies (sections 6.3.1 & 6.6.3) have indicated the presence of Lewis acid sites, there is no evidence that these sites enhance or promote this reaction. The Hell Volhart Zelinsky is promoted however by the use of γ -alumina and montmorillonite K10 treated with carbonyl chloride. This is an indication that these treated supports are a good source of Cl^- ions. While the reactions employing chlorinated supports are not as efficient as the original PCl_3 enhanced reaction, it must be pointed out that these reactions occurred at room temperature and under static conditions, whereas the original PCl_3 experiment was run under constant agitation at

373K.

Whereas the promotion of the Hell Volhart Zelinsky requires the modification of the supports, the promotion of the hydrobromination reactions merely required the calcined supports to be kept dry. This work has shown, using [^{82}Br]-bromine labelled hydrogen bromide, that the hydrobromination of the alkenes is a surface dependent reaction (chapter 4). The ability of the hydrogen bromide to rapidly adsorb onto the supports has therefore proved to be of great benefit in these reactions, as shown by a recent publication [101]. Even under aqueous conditions the supports enhance the hydrobromination reaction but with greatly reduced efficiency. Hydrobromination reactions may proceed via radical (anti-Markovnikov addition) or ionic (Markovnikov addition) mechanisms. These supports enhance the selectivity of the interactions as all hydrobromination reactions, involving the supports, occur via the ionic mechanism.

REFERENCES

- 1 Gmelins *Handbuch der Anorganischen Chemie*, Brom, Verlag Chemie, Berlin, 1931.
- 2 J. von Liebig, *Annal.*, 1838, 25, 29.
- 3 *Pharm. Zentralblatt*, 1833, 1, 2.
- 4 Z.E.Jolles, 'Bromine and its compounds', Ernest Benn Limited, London, 1966, 3-4.
- 5 N.N.Greenwood and A.Earnshaw, 'Chemistry of the elements', 1st Ed., 932.
- 6 Bromine Compounds, Chemistry and Applications, Price, Iddon and Wakefield., Elsevier, 1988, 12.
- 7 N.N.Greenwood and A.Earnshaw, 'Chemistry of the elements', 1st Ed., 933.
- 8 S.Rozen and M.Brand, *J. Chem. Soc., Chem Comm.*, 1987, 752.
- 9 M.Onaka and Y.Izumi, *Chem. Lett.*, 1984, 2007.
- 10 B.K.George and V.N.R.Pillai, *Macromolecules*, 1988, 21, 1867.
- 11 M.D.Kamen, 'Isotopic Tracers in Biology', 3rd Ed., Academic Press, New York, 1957.
- 12 G.E.Francis, W.Mulligan and A.Wormall, 'Isotopic Tracers', 2nd Ed., Athlone Press, London, 1959.
- 13 A.M.Kuzin, 'The application of Radioisotopes in Biology', International Atomic Energy Agency, Vienna Series, No. 7, 1960.
- 14 Z.B.Alfassi, *Radiochimica. Acta.*, 1990, 50, 41.
- 15 E.Browne and R.Firestone, 'Table of Radioactive Isotopes', A.Wiley-Interscience Publication, 1986, 82-1.
- 16 E.Browne and R.Firestone, 'Table of Radioactive Isotopes', A.Wiley-Interscience Publication, 1986, 80-2.
- 17 Z.E.Jolles, 'Bromine and its compounds', Ernest Benn Limited, London, 1966, 418-419.
- 18 M.Bodenstein, *Z. Physikal Chemie*, 1907, 57, 168.

- 19 D.H.Duncan, *Inorganic Synthesis*, 1939, 1, 151
- 20 E.Moles, *Compt. Rend.*, 1916, 162, 686.
- 21 E.Leger, *J. Chem. Soc.*, 1893, 64A, 11, 114.
- 22 J.N.Brønsted, *Rec. Trav. Chim.*, 1923, 42, 718.
- 23 T.M.Lowry, *Chem. Ind.*, 1923, 42, 43.
- 24 J.N.Brønsted, *Z. Phys. Chem.*, 1924, 108, 185.
- 25 J.N.Brønsted and R.P.Bell, *Proc. Roy. Soc.*, 1934, 143A, 377.
- 26 G.N.Lewis, *J. Franklin. Inst.*, 1938, 226, 293.
- 27 R.G.Pearson, *J. Chem. Educ.*, 1968, 45, 581, 643.
- 28 A.F.Wells, 'Structural Inorg. Chem., 5th Ed., Oxford Press, London, 1984, 1031.
- 29 S.B.Hendricks, R.A.Nelson and L.T.Alexander, *J. Am. Chem. Soc.*, 1940, 62, 1457.
- 30 R.W.Mooney and L.A.Wood, *J. Am. Chem. Soc.*, 1952, 74, 1367.
- 31 K.Norrish, *Disc. Faraday. Soc.*, 1954, 18, 120.
- 32 D.R.Collins, A.N.Fitch and R.A.Catlow, *J. Mater. Chem.*, 1992, 2, 865.
- 33 M.Onaka, Y.Hosokawa, K.Higuchi and Y.Izumi, *Tetrahedron Lett.*, 1993, 34, 1171.
- 34 F.A.Cotton and G.Wilkinson, 'Advanced Inorganic Chemistry', J.Wiley & Sons, 5th Ed., 1980, 211.
- 35 H.P.Rooksby, 'X-Ray Identification and Crystal Structure of Clays and Minerals', The Mineralogical socy., London, 1951.
- 36 B.C.Lippens, 'Structure and texture of Aluminas', Thesis, Delft University of Technology, The Netherlands, 1961.
- 37 H.Saalfeld, *Neues Jb. Miner Abh.*, 1960, 95, 1.
- 38 L.L. van Reijen, Thesis, Technical University of Eindhoven, The Netherlands, 1964.
- 39 A.F.Wells, 'Structural Inorg. Chem., 5th Ed., Oxford Press, London, 1984, 553.
- 40 H.Jagodszinski and H.Saalfeld, *Z. Kristallogr*, 1958, 110, 197.

- 41 J.M.Cowley and A.L.G.Rees, *Rep. Prog. Phys.*, 1958, 21, 165.
- 42 R.A. van Nordstrand, *Proc. Symp. Techniques Catalyst Prep.*, Dallas, Texas, 1956, 43.
- 43 H.Saalfeld and B.B.Mehrotra, *Ber. dt. keram. Ges.*, 1965, 42, 161.
- 44 J.Thomson, G.Webb and J.Winfield, *J. Chem. Soc., Chem. Commun.*, 1991, 323.
- 45 J.N.Miale and C.D.Chang, *US Pat.* 4, 427, 791, 1984.
- 46 M.Tanaka and S.Ogasawara, *J. Catal.*, 1970, 16, 157.
- 47 J.Thomson, G.Webb and J.M.Winfield, *Journal of Molecular Catal.*, 1991, 68, 347.
- 48 A.G.Goble and P.A.Lawrance, *Proc. Int. Congr.*, 3rd Amsterdam, 1964, 320.
- 49 J.Thomson, G.Webb and J.M.Winfield, *J. Mol. Catal.*, 1991, 67, 117.
- 50 J.Kelly, W.Schoen, C.N.Sechrist, *US Pat.* 3, 248, 343, 1966.
- 51 G. Friedlander, J.W. Kennedy and J.M. Miller, 'Nuclear and radiochemistry', 2nd Ed., J. Wiley and Sons Inc., N.Y., 171.
- 52 K.A. Brownlee 'Statistical Theory and Methodology in Science and Engineering', Wiley, N.Y., 1960.
- 53 C.A. Bennet and N.L. Franklin, 'Statistical Analysis in Chemistry and Chemical Industry', Wiley, N.Y., 1954.
- 54 E. Breitenberger, 'Scintillation-Spectrometer Statistics', *Progress in Nuclear Physics*, Vol. 4, (O.R. Frisch, Ed), Pergamon, London, 1955, 56-94.
- 55 C.R.C. Handbook of Chemistry and Physics, 73rd Ed., 11-44.
- 56 J.P.Damon, B.Delinon and J.M.Monnier, *J. Chem. Soc., Faraday Trans.*, 1, 1977, 73, 372.
- 57 A.Cornelis, L.Delaude, A.Gerstmans and P.Laszlo, *Tetrahedron Lett.*, 1988, 29, 5657.
- 58 A.Cornelis, A.Gerstmans and P.Laszlo, *Chem. Lett.*, 1988, 1839.
- 59 P.Laszlo and J.Vandormael, *Chem. Lett.*, 1988, 1843.
- 60 A.Cornelis, P.Y.Herze and P.Laszlo, *Tetrahedron Lett.*, 1982, 23, 5035.

- 61 A.Cornelis, P.Laszlo and P.Pennetreau, *J. Org. Chem.*, 1983, 48, 4771.
- 62 A.Cornelis and P.Laszlo, *Synthesis*, 1985, 909.
- 63 A.Cornelis and P.Laszlo, *Synthesis*, 1982, 162.
- 64 A.McKillop and D.W.Young, *Synthesis*, 1979, 401.
- 65 A.McKillop and D.W.Young, *Synthesis*, 1979, 481.
- 66 D.Villemin et al, *Synthesis*, 1989, 143.
- 67 D.Villemin et al, *J. Chem. Soc., Chem Commun.*, 1986, 386.
- 68 D.Villemin et al, *Synthetic Commun.*, 1990, 20, 3207.
- 69 J.H.Clark, A.P.Kybett, P.Landon, D.J.Macquarrie and J.J.Barlow, *J. Chem. Soc., Chem Commun.*, 1989, 1353.
- 70 M.L.Kantum, P.L.Santhi and M.F.Siddiqui, *Tetrahedron Lett.*, 1993, 34, 1185.
- 71 O.Sieskind and P.Albrecht, *Tetrahedron Lett.*, 1993, 34, 1197.
- 72 *The Aldrich Library of Infrared Spectra.*, 3rd Ed.
- 73 J.Thomson, Thesis, The University of Glasgow, 1988.
- 74 A.Hess and E.Kemnitz, *Applied Catalysis A*, 1992, 82, 247.
- 75 P.Fejes, I.Kiricsi, I.Hannus and G.Schobel, *Magyar Kemiai Folyoirat*, 1983, 89, 264.
- 76 Y.Zhao and J.S.Francisco, *Chem. Phys. Lett.*, 1990, 173, 551.
- 77 *The Multinuclear Approach to NMR Spectroscopy*, D.Reidel Publishing Company, Dordrecht, Holland, 330.
- 78 A.L.Smith, *J. Chem. Phys.*, 21, 1997.
- 79 D.Muller, W.Gessner, H.-J.Behrens, and G.Scheler, *Chem. Phys. Lett.*, 1981, 79, 59.
- 80 C.A.Fyfe, I.S.Gobbi, J.Hartman, J.Klinowski and J.M.Thomas, *J. Phys. Chem.*, 1982, 86, 1247.
- 81 E.Lippmaa, A.Samoson and M.Magi, *J. Am. Chem. Soc.*, 1986, 108, 1730.
- 82 J.Hine, *J. Am. Chem. Soc.*, 1950, 72, 2438.
- 83 J.Hine, *J. Am. Chem. Soc.*, 1954, 76, 2688.

- 84 W.A.Wynne and J.Chapman, BP. 759, 969, 1956.
- 85 J.McMurry, 'Organic Chemistry', 2nd Ed, Brooks/Cole Publishing Company, California, 1988, 175.
- 86 Fessenden and Fessenden, 'Organic Chemistry', 4th Ed, Brooks/Cole Publishing Company, California, 1990, 405.
- 87 F.A.Carey, 'Organic Chemistry', McGraw-Hill Book Company, London, 1987, 205.
- 88 J.D.Morrison, Asymmetric Synthesis, 15, 247.
- 89 S.P.Acharya and H.C.Brown, J. Chem. Soc., Chem Commun., 1968, 305.
- 90 R.C.Fahey and C.A.McPherson, J. Am. Chem. Soc., 1971, 93, 2445.
- 91 R.Goswami, J. Am. Chem. Soc., 1980, 102, 5974.
- 92 J.M.Tedder and J.C.Walton, Tetrahedron, 1980, 36, 701.
- 93 J.M.Tedder and J.C.Walton, Adv. Phys. Org. Chem., 1978, 16, 51.
- 94 L.Schmerling, J. Am. Chem. Soc., 1946, 68, 195.
- 95 H.Kwart and R.K.Miller, J. Am. Chem. Soc., 1956, 78, 5008.
- 96 F.M.Sonnenberg and T.H.Kinstle, J. Am. Chem. Soc., 1966, 88, 4922.
- 97 H.C.Brown and K.T.Liu, J. Am. Chem. Soc., 1975, 97, 600.
- 98 F.W.Stacey and J.F.Harris, Org. React., 1963, 13, 150-376.
- 99 J.March, 'Advanced Organic Chemistry', 3rd Ed., Wiley-Interscience, 1985, 679..
- 100 Kodomari, Bull. Chem. Soc. Jpn., 1988, 61, 4149.
- 101 P.J.Kropp, J. Am. Chem. Soc., 1990, 112, 7433.
- 102 P.Laszlo and L.Delaude, Tetrahedron Lett., 1991, 32, 3705.
- 103 J.P.Damon, B.Delionon and J.M.Monner, J. Chem. Soc., Faraday Trans., 1, 1977, 73, 372.
- 104 J.Herling, J.Shabtai and E.Gil-Av, J. Am. Chem. Soc., 1965, 87, 4107.
- 105 R.M.Pagni et al, J. Org. Chem., 1988, 53, 4477.
- 106 L.Delaude and P.Laszlo, Catalysis Letters, 1990, 5, 35.

- 107 V.K.Ahluwalia, Bhupinder Mehta and M.Rawat, *Synth. Commun.*, 1992, 22, 2697.
- 108 F.De la Vega and Y.Sasson, *J. Chem. Soc., Chem. Commun.*, 1989, 653.
- 109 B.C.Ranu, D.C.Sarkar and R.Chakraborty, *Synth. Commun.*, 1992, 22, 1095.
- 110 K.Smith and A.G.Mistry, *Tetrahedron Lett.*, 1986, 27, 1051.
- 111 K.Smith and M.Batters, *Synthesis.*, 1985, 1157.
- 112 J.C.Guillemin and J.M.Denis, *Synthesis.*, 1985, 1131.
- 113 M.Onaka and Y.Izumi, *Chem. Lett.*, 1984, 2007.
- 114 F.De la Vega and Y.Sasson, *Zeolites.*, 1989, 9, 418.
- 115 *The Aldrich Library of NMR Spectra*, 2nd Ed., vol 1, 833.
- 116 S.M.Nagy et al, *Mendeleev Commun.*, 1991, 94.
- 117 N.N.Greenwood and A.Earnshaw, 'Chemistry of the elements', 1st Ed., 1000-1012.
- 118 J.B.Peri, *J. Phys. Chem.*, 1965, 69, 211.
- 119 J.B.Peri, *J. Phys. Chem.*, 1965, 69, 220.
- 120 J.McMurry, 'Organic Chemistry'., 2nd Ed, Brooks/Cole Publishing Company, California, 1988, 526.
- 121 Fessenden and Fessenden, 'Organic Chemistry'., 4th Ed, Brooks/Cole Publishing Company, California, 1990, 308.
- 122 C.Hell, *Berichte Der Chemischem Gessellschaft*, 1881, 14, 891.
- 123 N.Zelinsky, *Berichte Der Chemischem Gessellschaft*, 1887, 20, 2026.
- 124 J.Volhard, *Ann. Der. Chem.*, 1887, 242, 141.
- 125 C.Hell, *Berichte Der Chemischem Gessellschaft*, 1889, 22, 1745.
- 126 C.Hell, *Berichte Der Chemischem Gessellschaft*, 1891, 24, 2388.
- 127 B.C.Gates, J.R.Katzer and G.C.A.Schmit, 'Chemistry of Catalytic Processes', McGraw-Hill Book Company, London, 1979, 256.
- 128 W.L.Earl, P.O.Fritz, A.A.V.Gibson and J.H.Lunsford, *J. Phys. Chem.*, 1987, 91, 2091.

- 129 D.Michel, A.Germanus and H.Pfeifer, *J. Chem. Soc., Faraday Trans.*, 1, 1982, 78, 237.
- 130 L.Petrakis and F.E.Kiviat, *J. Phys. Chem.*, 1976, 80, 606.
- 131 J.A.Ripmeester, *J. Am. Chem. Soc.*, 1983, 105, 2925.
- 132 J.H.Lunsford, W.P.Rothwell and W.Shen, *J. Am. Chem. Soc.*, 1985, 107, 1540.
- 133 E.P.Parry, *J. Catal.*, 1963, 2, 371.
- 134 M.Jia, H.Lechert and H.Foerster, *Zeolites*, 1992, 12, 32.
- 135 H.G.Karge and V.Dondur, *J. Phys. Chem.*, 1990, 94, 765.
- 136 N.S.Gill, R.H.Nuttall, D.E.Scaife and D.W.A.Sharp, *Journal of Inorganic and Nuclear Chemistry*, 1961, 18, 79.
- 137 C.Pesquera, F.Gonzalez, I.Benito, C.Blanco and S.Mendioroz, *Spectrosc. Lett.*, 1992, 25, 23.
- 138 C.H.Kline and J.Turkevich, *J. Chem. Phys.*, 1944, 12, 7.
- 139 M.Anderson, J.Klinowski and L.Xinsheng, *J. Chem. Soc., Chem. Commun.*, 1984, 1596.
- 140 M.R.Basila, T.R.Kantner and K.H.Rhee, *J. Phys. Chem.*, 1964, 68, 3197.
- 141 F.R.Cannings, *J. Phys. Chem.*, 1968, 72, 4691.
- 142 M.R.Basila and T.R.Kantner, *J. Phys. Chem.*, 1966, 70, 1681.
- 143 S.M.Riseman, F.E.Massoth, G.Murali Dhar and E.M.Eyring, *J. Phys. Chem.*, 1982, 86, 1760.
- 144 E.E.Getty and R.S.Drago, *Inorganic Chemistry.*, 1990, 29, 1186.
- 145 M.Primet and Y.B.Taarit, *J. Phys. Chem.*, 1977, 81, 1317.
- 146 H.C.Brown, *J. Chem. Soc.*, 1956, 1248.
- 147 B.A.Fox and T.L.Threlfall, *Org. Synth.*, 1964, 44, 34.
- 148 J.J.Eisch., *J. Org. Chem.*, 1962, 27, 1318.
- 149 E.E.Garcia, C.V.Greco, I.M.Hunsberger, *J. Am. Chem. Soc.*, 1960, 82, 4430.
- 150 G.B.Bachman and D.D.Micucci, *J. Am. Chem. Soc.*, 1948, 70, 2381.
- 151 T.R.Lewis, S.Archer et al, *J. Am. Chem. Soc.*, 1949, 71, 3749.

152 R.J.H. Voorhoeve, *Organohalosilanes: Precursors to Silicones.*, Elsevier Publishing Company, 1967, 302.

